University of Alberta

SEDIMENTOLOGY, ICHNOLOGY, AND STRATIGRAPHY OF MODERN CONGLOMERATIC DEPOSITIONAL ENVIRONMENTS

By
Shahin Exton Dashtgard

A thesis submitted to the faculty of graduate studies and research in partial fulfillment of the requirements for the degree of Doctor of Philosophy

Department of Earth and Atmospheric Sciences

Edmonton, Alberta
Fall 2006

Library and Archives Canada

Published Heritage Branch

395 Wellington Street
Ottawa ON K1A 0N4
Canada

Bibliothèque et Archives Canada

Direction du Patrimoine de l'édition

395, rue Wellington
Ottawa ON K1A 0N4
Canada

Your file Votre référence
ISBN: 978-0-494-23012-1
Our file Notre référence
ISBN: 978-0-494-23012-1

NOTICE:
The author has granted a non-exclusive license allowing Library and Archives Canada to reproduce, publish, archive, preserve, conserve, communicate to the public by telecommunication or on the Internet, loan, distribute and sell theses worldwide, for commercial or non-commercial purposes, in microform, paper, electronic and/or any other formats.

The author retains copyright ownership and moral rights in this thesis. Neither the thesis nor substantial extracts from it may be printed or otherwise reproduced without the author's permission.

AVIS:
L'auteur a accordé une licence non exclusive permettant à la Bibliothèque et Archives Canada de reproduire, publier, archiver, sauvegarder, conserver, transmettre au public par télécommunication ou par l'Internet, prêter, distribuer et vendre des thèses partout dans le monde, à des fins commerciales ou autres, sur support microforme, papier, électronique et/ou autres formats.

L'auteur conserve la propriété du droit d'auteur et des droits moraux qui protège cette thèse. Ni la thèse ni des extraits substantiels de celle-ci ne doivent être imprimés ou autrement reproduits sans son autorisation.

In compliance with the Canadian Privacy Act some supporting forms may have been removed from this thesis.

While these forms may be included in the document page count, their removal does not represent any loss of content from the thesis.

Conformément à la loi canadienne sur la protection de la vie privée, quelques formulaires secondaires ont été enlevés de cette thèse.

Bien que ces formulaires aient inclus dans la pagination, il n'y aura aucun contenu manquant.

Canada

ABSTRACT

Modern, conglomeratic depositional environments in the Bay of Fundy, Canada are studied to further understanding of the sedimentological, ichnological, and stratigraphic relations possible in ancient conglomeratic successions. Four main conclusions are derived. Firstly, the stratigraphic and sedimentological architecture of Waterside Marsh is assessed as a tool for predicting coastal geomorphology. Gravel is commonly transported into the marsh by ice and/or storm waves. The amount of gravel decreases away from the beach, such that the gravel content in a marsh deposit can be used to predict beach proximity. Secondly, facies modelling of the transgressive, gravel-dominated Waterside Beach suggests that depending on the rate of transgression, sedimentation, and tidal range, it is possible to preserve transgressive beach deposits up to 8 m thick. Increasing beach thickness correlates to slow transgression (partial aggradation) and/or increasing tidal range. Gravel systems are rarely tide dominated, yet tides influence both beach topography and the morphology of associated depositional environments. For Waterside Beach, the megatidal regime has resulted in large cross-sectional areas for the tidal creeks that drain the salt marsh. Overlying the tidal-creek scours, thick beach successions, oriented perpendicular to the depositional strike, are deposited.

Where possible, ichnological and sedimentological relationships are semi-quantified. Ichnologically, it is determined that to achieve 5% bioturbation in backshore sediments requires two consecutive seasons of colonization. Consequently, highly bioturbated backshore sediments are likely to occur in low wave-energy environments. Semi-quantification of sedimentological properties was done for average grain size (in phi values) versus the areal extent of the intertidal zone of Waterside Beach, Alma delta, and Big Salmon River delta. A log-linear relationship is derived suggesting that the areal extent of conglomeratic deposits is directly proportional to the average grain size.

Relative hydraulic influences on the geomorphology and sedimentology of the three systems is established and the systems classified. The Big Salmon River delta is considered river-dominated with low to moderate wave modification and the Alma delta river-dominated with high wave modification. Waterside is classified as a highly tide-modified, wave-dominated beach.

Acknowledgements

It is easy to assume that a PhD is an individual effort that culminates from the work of the author alone, but that simply isn't true. It's more of a team effort with many people making contributions of time, patience, support, and encouragement. So many people have helped me over the past 4 years that it is not possible to mention everyone here. So to those of you I have failed to mention - thank you! There are a few individuals though, who deserve special mention.

First and foremost, I want to thank my supervisor, Murray Gingras. Murray has been an amazing supervisor and a great friend! From giving me the opportunities to attend international conferences, to tearing apart my work because it's "good for me," he has continually challenged me to push myself further and see what I'm capable of. I can honestly say that Murray's supervision directly resulted in me developing the academic confidence that was lacking 4 years ago when I began the PhD program.

After Murray, George Pemberton has been the biggest influence on my academic career. George has been both a mentor and support for me over the years. He never lost faith in my abilities and never hesitated to offer whatever help he could. Selflessly, George wrote letters of support to help me earn my Professional Geologist designation and both NSERC scholarships, and to get into grad school. He's been one of the cornerstones upon which my scientific career has developed.

Where Murray was instrumental in developing my academic confidence and both George and Murray in developing my career, my parents, Jamshid and Janet Dashtgard, provided me with the skills to live life to the fullest and to strive to accomplish anything I set my mind too. Dad always expected the best of me and never settle for less. Mom taught me the values of hard work, honesty, and commitment even when I no longer felt like doing something. I am proud to be their son and love them both dearly.

The last two years I have also drawn support from an amazing woman who is soon to be my wife. Nerissa Harvey has been an emotional support for me and a calming influence when life's storms seem like they'll wash me away. With her by my side, I feel anything is possible. She has opened up whole new worlds of possibility for the future.

There have also been many close friends in the scientific community that I must mention. Ian Armitage, Jay French, and Paul Glombick have offered me friendship, good old-fashioned competition, and support through our undergrad together and in grad school. A special thanks is extended to Tyler Hauck, who assisted me in the field in 2004. Tyler had a knack for looking for things that completely escaped my attention. He added a dimension to my thesis that would never have existed otherwise. Thanks Ty!

Karl Butler and Richardo White at the University of New Brunswick are colleagues who have offered support and have made possible scientific ventures that otherwise would never have come to fruition. Karl organized seismic programs in both 2003 and 2004 and set up a grab sampling and drop-coring program in 2005. Richardo processed most of the seismic and has provided some stunning images within this thesis. It's was a real pleasure working with those two and I'm glad I had a chance to collaborate with them.

There are also several members of the scientific community not mentioned already who have contributed to this thesis. Duane Froese was a member of my supervisory committee and offered encouragement, advice, and constructive criticism when it was needed. Thanks Duane! Guy Plint was both the external examiner for my defense and a reviewer of one of the published chapters (chapter 4). His recommendations improved the idea presented herein and are greatly appreciated. Thanks is also extended to Doug Schmitt who sat on my defense committee, and to the various reviewers of the published chapters - Sanjeev Gupta, Urs Neumeier, Steve Hasiotis, Charles Savrda, Luis Buatois, and Guy Plint.

Finally, I wish to thank those who have had an impact on my life during my time in grad school. My sisters, Annahid and Fari Dashtgard. Bart Blakney, Christine Lodge, and Bill Harvey from Fredericton. Larry Amskold, Erin Walton, Alex MacNeil, Rachel Singer, and Nadine Pearson at the University of Alberta.

DEDICATION

I dedicate this thesis to my grandmother, Elsie Exton. She embodied the values of honesty, hard work, and compassion and was an amazing lady.

TABLE OF CONTENTS

CHAPTER 1: INTRODUCTION 1

Gravel-Dominated Coasts 1
Associated Depositional Environments 6
Thesis Organization 7

REFERENCES 10

CHAPTER 2: FACIES ARCHITECTURE AND ICHNOLOGY OF RECENT SALT-MARSH DEPOSITS: WATERSIDE MARSH, NEW BRUNSWICK, CANADA 18

INTRODUCTION 18
Study Area 20
Methods 22

FACIES ASSOCIATIONS: DESCRIPTIONS AND INTERPRETATION 24
Facies Association 1: Salt-Marsh Deposits 24
Facies 1 (F1) 27
Facies 2 (F2) 28
Facies 3 (F3) 29
Facies Association 2: Tidal-Creek Deposits 30
Facies 4 (F4) 30
Facies 5 (F5) 32
Facies 6 (F6) 34
Facies 7 (F7) 36
Facies Association 3: Beach-Related Deposits 38
Facies 8 (F8) 38
Facies 9 (F9) 39

DISCUSSION 40
Stratigraphy of Waterside Marsh 40
Application to the Rock Record 42

CONCLUSIONS 44

REFERENCES 46

CHAPTER 3: THE TEMPORAL SIGNIFICANCE OF BIOTURBATION IN BACKSHORE DEPOSITS: WATERSIDE BEACH, NEW BRUNSWICK, CANADA 50

INTRODUCTION 50
Degree of Bioturbation 50
Talitrid Distribution 51
Study Area 52
Methods 52

RESULTS 57
Sedimentology 57
Bioturbation 59

DISCUSSION 60
Application to the rock record 61

CONCLUSIONS 63

REFERENCES 64

CHAPTER 4: SEDIMENTOLOGY AND STRATIGRAPHY OF A TRANSGRESSIVE, MUDDY GRAVEL BEACH: WATERSIDE BEACH, BAY OF FUNDY, CANADA 68

INTRODUCTION 68
Study Area 70
Methods 70

RESULTS 75
Sediment Source 75
Beach Sedimentology 76
Deposits 1 through 5 77
Deposits 6 and 7 81
Deposits 8 through 11 82

DISCUSSION 86
Muddy Conglomerates and Mud Beds in Conglomerates 86
Transgressive, Muddy Gravel Beach Sequences 88
Strip logs 1A, 1B, and 1C 92
Strip logs 2A, 2B, and 2C 93
Application to the Rock Record 95

CONCLUSIONS 96

REFERENCES 98

CHAPTER 5: EFFECTS OF RELATIVE SEA LEVEL CHANGE ON THE DEPOSITIONAL ARCHITECTURE OF AN EMBAYED BEACH, BAY OF FUNDY, CANADA 104

INTRODUCTION 104
Tides and Relative Sea Level in the Bay of Fundy 106
Study Area 108
Methods 108
Seismic Acquisition and Processing 108
Sedimentological Methods 111

RESULTS AND DISCUSSION 113
Steeply Dipping Reflector Unit (SDRU) 113
Laminated Silty Sand Unit (LSSU) 121
Salt-Marsh Deposits 124
Beach Deposits 126
Implications for High-Resolution Sequence Stratigraphy 128

CONCLUSIONS 131

REFERENCES 132

CHAPTER 6: GRAVEL DELTAS TO SHOREFACES — LINKING HYDRAULIC PROCESS TO COASTAL GEOMORPHOLOGY AND SEDIMENTOLOGY IN THE BAY OF FUNDY, CANADA 139

INTRODUCTION 139
Study Area 142
Methods 143

RESULTS 146
Grain Size 146
Water Chemistry and Hydraulic-Energy Inputs 148
Geomorphology 151

DISCUSSION 159
Grain Size and Areal Extent of the Coastal Zone 159
Swash and Surf-Zone Bars 161
Hydraulic Controls on the Classification of Gravel-Dominated Coasts 164

CONCLUSIONS 167

REFERENCES 169

CHAPTER 7: CONCLUSIONS 177

REFERENCES 180

APPENDIX 182

APPENDIX A 182

Waterside Grain-Size Data 183

Alma Grain-Size Data 201

Big Salmon River Grain-Size Data 207

Wolman (Grid-Sampling) Grain-Size Data 213

APPENDIX B 218

Waterside Total Organic Carbon Data 219

Alma Total Organic Carbon Data 222

Big Salmon River Total Organic Carbon Data 223

LIST OF TABLES

TABLE 2.1 - Relative bioturbation levels observed in Waterside Marsh. 24
TABLE 2.2 - Summary of physical characteristics and ichnology of facies and facies associations of Waterside Marsh. 26

TABLE 3.1 - Distribution and dimensions of Talitrid amphipod burrows. 54
TABLE 3.2 - Grain-size distribution of backshore sediments. 55

TABLE 4.1 - Summary of sediment textures, structures, and distribution for Waterside Beach sediments - part 1. 78
TABLE 4.2 - Summary of sediment textures, structures, and distribution for Waterside Beach sediments - part 2. 79

TABLE 6.1 - River drainage, precipitation and flow rates. 150

LIST OF FIGURES

FIGURE 1.1 - Map of Bay of Fundy and location of study sites. 2
FIGURE 1.2 - Air photo of the Big Salmon River delta taken in 1993. 3
FIGURE 1.3 - Air photo of the Alma delta taken in 1993. 4
FIGURE 1.4 - Air photo of the Waterside Beach taken in 1996. 5

FIGURE 2.1 - Location map of Waterside Marsh, New Brunswick. 21
FIGURE 2.2 - Burrow morphology and incipient traces developed by infauna encountered in Waterside Marsh and burrow names. 25
FIGURE 2.3 - Photos and x-ray images of salt-marsh sediments. 27
FIGURE 2.4 - Photos of modern and recent tidal-creek deposits. 31
FIGURE 2.5 - Photos and sketches of modern and recent point-bar deposits. 35
FIGURE 2.6 - Schematic profiles of salt marsh and tidal-creek facies associations. 37

FIGURE 3.1 - Sketch of *Talorchestia longicornis*. 51
FIGURE 3.2 - Location of Waterside Beach, New Brunswick. 53
FIGURE 3.3 - Shore-normal schematic profile of the backshore and upper foreshore of Waterside Beach. 54
FIGURE 3.4 - Photos of burrows constructed in the backshore by amphipods. 58

FIGURE 4.1 - Location of Waterside Beach, New Brunswick. 71
FIGURE 4.2 - Sediment distribution map of the intertidal and sub-tidal components of Waterside Beach. 74
FIGURE 4.3 - X-ray images of box cores taken from the beach. 81
FIGURE 4.4 - Photos depicting the association of gravel bar, muddy gravel, and mud deposits. 84
FIGURE 4.5 - X-ray images of laminated mud beds. 86
FIGURE 4.6 - Theoretical strip logs constructed for transgressive gravel, mixed sand and gravel, and muddy gravel beaches. 90

FIGURE 5.1 - Location of Waterside Beach, New Brunswick. 109
FIGURE 5.2 - Maps of seismic surveys acquired in 2003 and 2004. 112
FIGURE 5.3 - Shore-normal seismic line and its line-drawing interpretation. 116
FIGURE 5.4 - Shore-normal seismic line and its line-drawing interpretation. 117
FIGURE 5.5 - Shore-parallel seismic line and its line-drawing interpretation. 119

List of Figures (cont.)

FIGURE 5.6 - Distribution of seismically and sedimentologically defined units. 120
FIGURE 5.7 - Three dimensional map generated from closely spaced seismic lines of the glacio-marine sediments that underlie Waterside Beach. 121
FIGURE 5.8 - X-ray images of drop cores taken from the laminated silty sand unit. ...123
FIGURE 5.9 - Photos of the *Glossifungites* surface developed in salt-marsh sediments exposed intertidally. 128
FIGURE 5.10 - Schematic, paleoenvironmental block diagrams of Waterside Beach from 12,000 years ago to present. 130

FIGURE 6.1 - Location map and air photos of Waterside Beach, Alma delta, and the Big Salmon River delta. 143
FIGURE 6.2 - Plot of average grain size versus sorting (standard deviation) for all three systems. 147
FIGURE 6.3 - Salinities of the Big Salmon River, Upper Salmon River (Alma), Long Marsh Creek (Waterside), and the Bay of Fundy. 149
FIGURE 6.4 - Sediment distribution maps. 153
FIGURE 6.5 - Gravel-bar locations and mud zones. 154
FIGURE 6.6 - Wave heights at Waterside. 155
FIGURE 6.7 - Shore-normal seismic line of the Alma delta. 156
FIGURE 6.8 - Air photos or maps of the Alma delta from 1953 to 2003. 157
FIGURE 6.9 - Shore-normal seismic line of Waterside Beach. 158
FIGURE 6.10 - Plot of average grain size versus areal extent of the intertidal zone for the three systems. 161
FIGURE 6.11 - Classification of Waterside Beach, Alma delta, and BSR delta based on hydraulic process (river, wave, tide). 166

CHAPTER 1: INTRODUCTION

Facies models developed from modern, marginal-marine depositional environments are used as analogues for sedimentary successions preserved in the rock record. Existing models tend to focus on the sedimentology and stratigraphy of clastic (mainly sandy) systems, and have only recently incorporated ichnology. Relative to sandy systems, gravel-dominated (conglomeratic) coasts have received little attention, of which, most studies have reported on the sedimentology of the deposits. The ichnology of conglomeratic coasts is virtually unknown. Stratigraphic models are constructed from rock-record examples due to a paucity of readily available three-dimensional data in the modern.

This thesis attempts to further understanding of the sedimentology, ichnology, and stratigraphy of conglomerates by conducting research on modern, gravel-dominated coasts in the Bay of Fundy, Canada (Fig. 1.1). Three systems on the New Brunswick coastline of the upper Bay of Fundy – Big Salmon River (BSR) delta (Fig. 1.2), Alma delta (Fig. 1.3), and Waterside Beach (Fig. 1.4) – are selected for analysis. Based on the results, this thesis: (1) improves understanding of the stratigraphy and sedimentology of conglomeratic systems, particularly within transgressive settings; (2) assesses the relationship between depositional environments (salt marsh and beach) within the same coastal zone; (3) where possible, semi-quantifies bioturbation rates and sedimentological relationships; and, (4) endeavours to determine hydraulic influences (especially tidal) on the geomorphology of gravel-dominated systems.

Gravel-Dominated Coasts

Gravel deposits are classified in terms of the relative energy contribution from rivers, waves, and tides. River-dominated systems include gravel deltas that exhibit distinct morphologies depending on their location relative to the shoreline, water depth

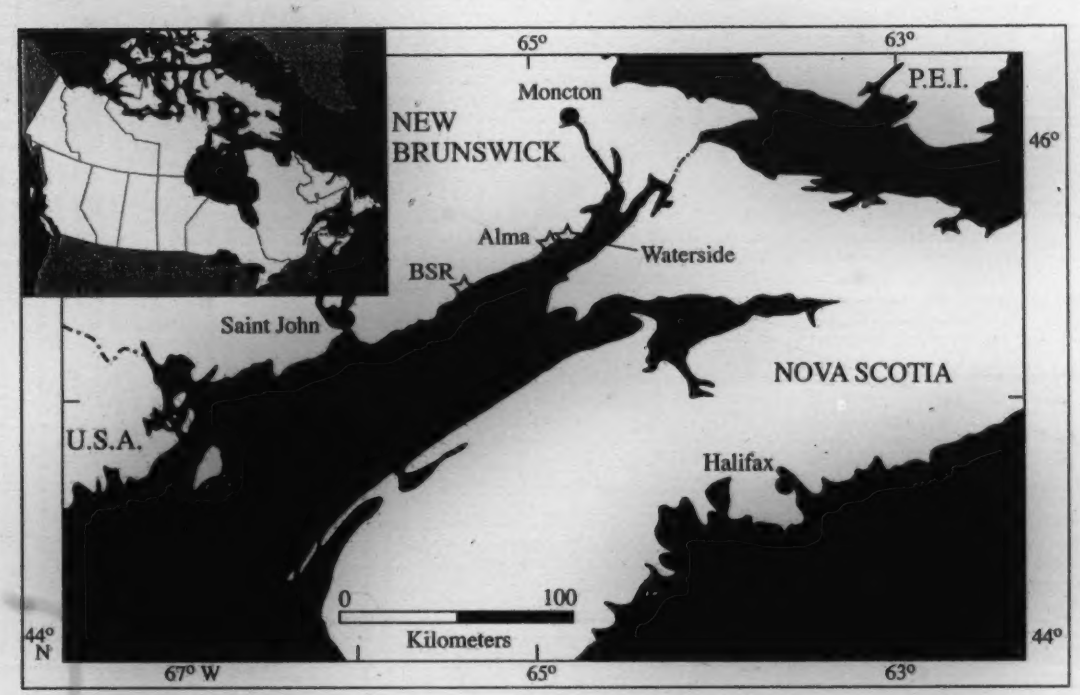

FIGURE 1.1 —Location of the Bay of Fundy within Canada and the three study areas within the bay.

of the receiving basin, and average grain size (Orton and Reading 1993; Postma 1990; Reading and Collinson 1996; Wescott and Ethridge 1980; Wescott and Ethridge 1982). Gravel deltas, commonly referred to as fan or Gilbert-type deltas, are small (compared to sand and mud-dominated ones), have steeply dipping (up to 15°) delta fronts (Colella 1988; Marzo and Anadón 1988; Postma 1990; Postma and Roep 1985; Reading and Collinson 1996; Wescott and Ethridge 1980), and decrease in size with increasing average grain size.

Wave-dominated gravel coasts encompass beaches and shorefaces. The first model of a gravel beach (Bluck 1967) depicted a narrow beach with shore-normal clast partitioning based on clast shape and size. This deposit type is recognized around the world and is considered typical for gravel beaches with limited fluvial input or sediment supply (Bartholomä et al. 1998; Bluck 1999; Carr 1969; Carr et al. 1970; Hart and Plint 1989; Maejima 1982; Postma and Nemec 1990). Bluck's (1967) model, however, does

FIGURE 1.2 —Airphoto of the Big Salmon River delta taken at low tide in 1993.

not encompass the full range of beaches that may develop and does not account for tidal influences on beach morphology.

Tide-dominated gravel systems are not defined because tidal influence decreases as grain size increases (Orton and Reading 1993; Reading and Collinson 1996). Tidally modified beaches though, are common and can be classified by the relationship between wave height and tidal range (Masselink 1993; Masselink and Short 1993; Short 1991; Wright and Short 1984). In macrotidal and megatidal (> 8 m tidal range) settings, sandy and mixed sand and gravel tidal beaches comprise a moderately dipping beachface (2-5°) passing rapidly offshore into a shallowly dipping (< 1°), concave-up sandy terrace (Anthony and Orford 2002; Masselink and Short 1993).

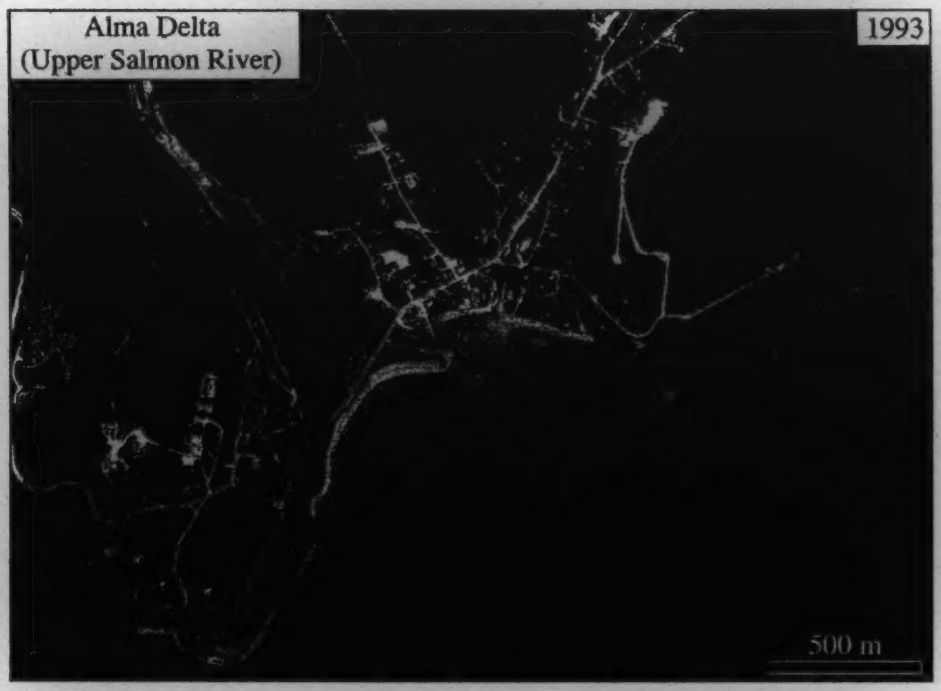

FIGURE 1.3 — Airphoto of the Alma delta taken in 1993 at low tide.

Bioturbation in gravels and conglomerates is limited due to the added and significant grain-size stress on infauna. Within the intertidal zone, burrowing organisms must contend with desiccation, salinity and temperature fluctuations, rapidly shifting substrates, energetic wave conditions, and predation when both subaerially and subaqueously exposed (Bromley 1990; Gingras et al. 2006; Pemberton et al. 1992; Pemberton et al. 2001). Of these, desiccation (subaerial exposure) is one of the main influences on sediment colonization by marine organisms. Subaerial exposure is greatest at the top of the foreshore and decreases in the basinward direction. Exposure time is also linked to grain size. In gravel systems the large pore spaces and permeable nature of the sediment results in rapid dewatering, which limits the ability of infauna to maintain ambient conditions (salinity, temperature, humidity, and water circulation) within their dwelling (MacEachern and Hobbs 2004). In addition, gravel-sized clasts are too large to

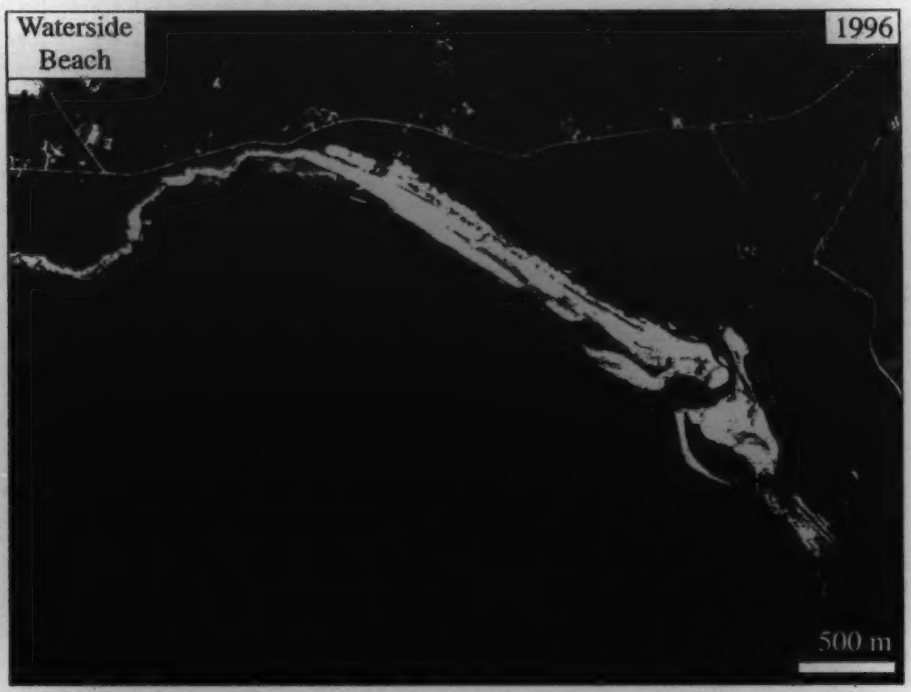

FIGURE 1.4 —Air photo of Waterside Beach taken between high and low tide in 1996.

be moved by most intertidal burrowers. This restricts the activity of motile organisms that tunnel though the sediment.

Bioturbation in conglomerates generally exhibits a similar distribution to sandy systems, where the degree of burrowing and colonization increases in an oceanward direction (MacEachern and Hobbs 2004). It differs, however, in that the overall intensity of burrowing is lower, and the structures tend to be thick-walled (Bann et al. 2006) and constructed mainly by sessile organisms. Neoichnological studies in gravel are not available.

Stratigraphic evolution of conglomerates is well established from rock-record examples (Clifton 1981; Marzo and Anadón 1988; Massari 1984; Plint et al. 1988; Walker 1983a; Walker 1983b; Zonneveld and Moslow 2004) and from the study of recent (Holocene) deposits (Browne and Naish 2003; Engels and Roberts 2005; Forbes and Taylor 1987; Forbes et al. 1991; Orford and Carter 1982; Orford et al. 1991; Shulmeister

and Kirk 1993; Wescott and Ethridge 1980). Conglomerates within these studies are classified as either regressive (progradational) or transgressive (Bourgeois and Leithold 1984; Postma and Nemec 1990; Wescott and Ethridge 1982). Gilbert-type and fan deltas occur in regressive, fluvial-dominated settings (Colella 1988; Ethridge and Wescott 1984; Marzo and Anadón 1988; Massari 1984; Nemec 1990; Postma 1984; Postma 1990; Postma and Roep 1985; Wescott and Ethridge 1980; Wescott and Ethridge 1982; Wescott and Ethridge 1983). During transgression, the deltas are flooded and either evolve into estuaries (Dalrymple et al. 1992) or wave-dominated fan-deltas (Marzo and Anadón 1988; Reading and Collinson 1996). Regressive gravel beaches tend to be characterized by repeating sequences of coarsening-upward conglomerates with internal erosional surfaces (Bourgeois and Leithold 1984), and by the preservation of foreshore sediments (Clifton 1981; Massari and Parea 1988). Beach transgression results in wave erosion of backshore and foreshore deposits such that the beach is sometimes manifest as a thin gravel lag (Bourgeois and Leithold 1984; Clifton 1981) overlain by middle and lower shoreface sediments or offshore marine shales.

Associated Depositional Environments

The coastal zone is commonly a composite of linked depositional environments. Within the Bay of Fundy, salt marshes develop in the coastal zone, including landward of gravel-dominated coasts. Understanding the relation between the salt marsh and the gravel beach or delta is therefore necessary for determining the morphology of the coastal zone and in predicting the response of the system to changes in relative sea level (RSL) and tidal regime. This in turn, requires an understanding of salt-marsh dynamics, sedimentology, and stratigraphic evolution.

Salt marshes develop within the coastal zone as a result of periodic flooding by marine waters. They can be divided into two main components: a vegetated platform that is periodically submerged by the tide, and a network of tidal channels that branch

and taper landward (Allen 1997; Allen 2000; Pethnick 1992). The tidal channels can be further subdivided into deep and wide main channels, and small creeks that dissect the marsh surface. During RSL fall and lowstand, the marsh surface is rarely flooded resulting in cessation of vertical aggradation and evolution into a freshwater swamp. During the swamp stage, tidal creeks tend to be poorly developed or absent (Allen 1990; Allen 1997; Allen 2000; Redfield 1972). Relative sea level rise results in regular flooding of the marsh at high tide and aggradation at a rate proportional to the rise (Allen 1997; Allen 2000). Early RSL rise is marked by an expansion (in cross-sectional area) of tidal creeks and an increase in the areal density of smaller creeks that dissect the marsh surface (French 1993; Pye and French 1993). With continued RSL rise, small tidal creeks silt in, whereas the main tidal channels expand in width and depth (Allen 1997).

Thesis Organization

This thesis is divided into seven chapters (including the introduction and conclusion) that assess the sedimentology, ichnology and / or stratigraphy of modern, conglomeratic depositional environments in the Bay of Fundy, Canada. Chapters 2 through 5 focus on subenvironments or components of the Waterside Beach coastal zone. Chapter 6 deals with all three systems – Waterside Beach, Alma delta, and the Big Salmon River (BSR) delta.

Chapter 2 focuses on Waterside Marsh (a component of the Waterside Beach coastal zone). Salt marshes are important marginal-marine depositional environments and have received a lot of attention in terms of their sedimentological character, capacity as a sediment sink and source, and as recorders of relative sea level change (Allen 1990; Allen 1997; Allen 1999; Allen 2000; Bayliss-Smith et al. 1979; French and Stoddart 1992; Gordon et al. 1985; Letzsch 1983; Letzsch and Frey 1980; Letzsch and Frey 1981). At Waterside Beach, recently deposited salt-marsh sediments exposed in the intertidal zone present an opportunity to define sedimentologically and ichnologically

distinct facies, establish marsh stratigraphy, and discuss the preservation potential of marsh facies. Special attention is given to the neoichnology (tracks, trails, and burrows made by modern organisms) of the salt marsh, and the relation between bioturbation and environmental conditions (subaerial exposure, substrate type, hydraulic energy). A discussion is also presented on marsh-beach dynamics and the impact of the beach on the marsh.

Chapter 3 is an attempt to semi-quantify bioturbation indices (ie. burrowing intensity) by quantifying the distribution of Talitrid amphipods and their burrows and comparing these values to burrowing rates in field aquaria (control sites). Talitrids burrow in washover-fan deposits of the marsh-beach transition and in aeolian sands deposited at the top of the beach. The burrows are easily identified, measured, and counted. The purpose of this chapter is to establish the minimum amount of time needed to surpass biortubation-index (BI) thresholds (the minimum percentage of a BI range). These ranges may then be used to assess depositional chronology in ancient deposits where similar structures are observed. Talitrid burrows as paleo-environmental markers and a recorder of tidal limit are also discussed.

Chapter 4 describes the sedimentology of intertidal and sub-tidal sediments of Waterside Beach. From these data: theoretical facies models are constructed for transgressive gravel beaches; tidal influences on beach morphology are discussed, and, mechanisms are presented for mud deposition in gravel systems and the development of muddy gravel. Facies models already exist for progradational gravel beaches (Clifton 1981; Massari and Parea 1988), but have yet to be defined for transgressive ones. In general, it is considered that transgressive gravel beaches are manifest as a gravel lag overlain by marine muds (Bourgeois and Leithold 1984; Clifton 1981; Massari and Parea 1988). Yet depending on the rate of transgression, sedimentation, and tidal regime these sequences may be much thicker and sedimentologically complex. Tidal influence on beach morphology is addressed in terms of beach and salt-marsh morphology, and

size of the tidal channels. Finally, a discussion is presented on the deposition of mud in gravel systems and the development of muddy conglomerates. Muddy conglomerates are common in the Western Canadian Sedimentary Basin; however, the formation of these deposits has not been reported from modern environments.

Chapter 5 focuses on the post-glacial evolution of Waterside Beach and its implications for high-resolution sequence-stratigraphic analysis. The Bay of Fundy, and in particular Chignecto Bay, have experienced relative sea level rise and fall of 55 m in the past 13,000 years (Amos et al. 1991; Grant 1970; Shaw et al. 2002). Sea level change has had a significant impact on the morphology of Chignecto Bay, tidal regime in the Bay of Fundy, and on the depositional style of Waterside Beach. Through seismic and sedimentologic mapping, deposits corresponding to different stages of sea level fall, lowstand and rise are identified. Paleoenvironmental block diagrams are used to illustrate the change in depositional character at the shoreline and the possible pitfalls these changes may present to high-resolution, sequence-stratigraphic analyses.

Chapter 6 describes the sedimentological character of Waterside Beach, Alma delta, and Big Salmon River delta and attempts to semi-quantify the relationship between hydraulic process (river, wave, tide) and coastal geomorphology. The relationship between average grain size of a gravel deposit and areal extent of the coastal zone is confirmed (Orton and Reading 1993; Reading and Collinson 1996). The presence of swash bars (King 1972; King and Williams 1949; McCave and Geiser 1978; Wright 1977) and surf-zone bars (Anthony et al. 2004; Kroon and Masselink 2002; Sunamura and Takeda 1984) as a function of fluvial discharge and wave conditions is presented. The three systems are then classified based on the relative contributions of river-, wave-, and tidal-energy.

As a whole, this thesis attempts to further understanding of conglomeratic, marginal-marine environments by assessing and comparing the sedimentology, ichnology, and stratigraphy of modern, gravel deposits in the Bay of Fundy, Canada. Relationships

are defined between linked depositional environments, and facies models constructed for salt marshes and transgressive gravel beaches. Where possible, ichnological and sedimentological characteristics of deposits or between deposits are semi-quantified. The effects of changes in relative sea level on the morphology of an embayed coastline are reported. Finally, hydraulic controls (particularly tidal) on the coastal geomorphology of gravel systems are determined.

REFERENCES

Allen, J.R.L., 1990, Salt-marsh growth and stratification: A numerical model with special reference to the Severn Estuary, southwest Britain: Marine Geology, v. 95, p. 77-96.

Allen, J.R.L., 1997, Simulation models of salt-marsh morphodynamics: some implications for high-intertidal sediment couplets related to sea level change: Sedimentary Geology, v. 113, p. 211-223.

Allen, J.R.L., 1999, Geological impacts on coastal wetland landscapes: Some general effects of sediment autocompaction in the Holocene of Northwest Europe: The Holocene, v. 9, p. 1-12.

Allen, J.R.L., 2000, Morphodynamics of Holocene salt marshes: a review sketch from the Atlantic and Southern North Sea coasts of Europe: Quaternary Science Reviews, v. 19, p. 1155-1231.

Amos, C.L., Tee, K.T., and Zaitlin, B.A., 1991, The post-glacial evolution of Chignecto Bay, Bay of Fundy, and its modern environment of deposition, *in* Smith, D.G., Reinson, G.E., Zaitlin, B.A., and Rahmani, R.A., eds., Clastic Tidal Sedimentology: Calgary, AB, Canada, Canadian Society of Petroleum Geologists, p. 59-89.

Anthony, E.J., Levoy, F., and Monfort, O., 2004, Morphodynamics of intertidal bars on a megatidal beach, Merlimont, Northern France: Marine Geology, v. 208, p. 73-100.

Anthony, E.J., and Orford, J.D., 2002, Between wave- and tide-dominated coasts: the middle ground revisited: Journal of Coastal Research Special Issue 36, p. 8-15.

Bann, K.L., MacEachern, J.A., Gingras, M.K., Dashtgard, S.E., and Saunders, T.D.A., 2006, Abundant and diverse *Rosselia*: An indicator of shallow marine high-latitude deposition: AAPG Annual Meeting.

Bartholomä, A., Ibbeken, H., and Schleyer, R., 1998, Modification of gravel during longshore transport (Bianco Beach, Calabria, southern Italy): Journal of Sedimentary Research, v. 68, p. 138-147.

Bayliss-Smith, T.P., Healey, R., Lailey, R., Spencer, T., and Stoddart, D.R., 1979, Tidal flow in salt marsh creeks: Estuarine, Coastal and Marine Science, v. 9, p. 235-255.

Bluck, B.J., 1967, Sedimentation of beach gravels: Examples from south Wales: Journal of Sedimentary Petrology, v. 37, p. 128-156.

Bluck, B.J., 1999, Clast assembling, bed-forms, and structure in gravel beaches: Transactions of the Royal Society of Edinburgh, Earth Sciences, v. 89, p. 291-323.

Bourgeois, J., and Leithold, E.L., 1984, Wave-worked conglomerates - depositional processes and criteria for recognition, *in* Koster, E.H., and Steel, R.J., eds., Sedimentology of Gravels and Conglomerates: Calgary, AB, Canada, Canadian Society of Petroleum Geologists, p. 331-343.

Bromley, R.G., 1990, Trace Fossils; Biology and Taphonomy: London, Unwin Hyman, 280 p.

Browne, G.H., and Naish, T.R., 2003, Facies development and sequence architecutre of a late Quaternary fluvial-marine transition, Canterbury Plains and shelf, New Zealand: implications for forced regressive deposits: Sedimentary Geology, v. 158, p. 57-86.

Carr, A.P., 1969, Size grading along a pebble beach: Chesil Beach, England: Journal of Sedimentary Petrology, v. 39, p. 297-311.

Carr, A.P., Gleason, R., and King, A., 1970, Significance of pebble size and shape in sorting by waves: Sedimentary Geology, v. 4, p. 89-101.

Clifton, H.E., 1981, Progradational sequences in Miocene shoreline deposits, southeastern Caliente range, California: Journal of Sedimentary Petrology, v. 51, p. 165-184.

Colella, A., 1988, Pliocene-Holocene fan deltas and braid deltas in the Crati Basin, southern Italy: a consequence of varying tectonic conditions, *in* Nemec, W., and Steel, R.J., eds., Fan Deltas: Sedimentology and Tectonic Settings: London, UK, Blackie, p. 50-74.

Dalrymple, R.W., Zaitlin, B.A., and Boyd, R., 1992, Estuarine facies models: conceptual basis and stratigraphic implications: Journal of Sedimentary Petrology, v. 62, p. 1130-1146.

Engels, S., and Roberts, M.C., 2005, The architecture of prograding sandy-gravel beach ridges formed during the last Holocene highstand: Southwestern British Columbia, Canada: Journal of Sedimentary Research, v. 75, p. 1052-1064.

Ethridge, F.G., and Wescott, W.A., 1984, Tectonic setting, recognition and hydrocarbon reservoir potential of fan-delta deposits, *in* Koster, E.H., and Steel, R.J., eds., Sedimentology of Gravels and Conglomerates: Calgary, Canadian Society of Petroleum Geologists, p. 217-235.

Forbes, D.L., and Taylor, R.B., 1987, Coarse-grained beach sedimentation under paraglacial conditions, Canadian Atlantic Coast, *in* FitzGerald, D.M., and Rosen, P.S., eds., Glaciated Coasts: San Diego, U.S.A., Academic Press, p. 51-86.

Forbes, D.L., Taylor, R.B., Orford, J.D., Carter, R.W.G., and J., S., 1991, Gravel-barrier migration and overstepping: Marine Geology, v. 97, p. 305-313.

French, J.R., 1993, Numerical simulation of vertical marsh growth and adjustment to accelerated sea-level rise, north Norfolk, U.K.: Earth Surface Processes and Landforms, v. 18, p. 63-81.

French, J.R., and Stoddart, D.R., 1992, Hydrodynamics of salt marsh creek systems: implications for marsh morphological development and material exchange: Earth Surface Processes and Landforms, v. 17, p. 235-252.

Gingras, M.K., Dashtgard, S.E., and Pemberton, S.G., 2006, Latitudinal (climatic) controls on neoichnological assemblages of modern, marginal-marine depositional environments: AAPG Annual Meeting.

Gordon, D.C.J., Cranford, P.J., and Desplanque, C., 1985, Observations on the ecological importance of salt marshes in the Cumberland Basin, a macrotidal estuary in the Bay of Fundy: Estuarine, Coastal and Shelf Science, v. 20, p. 205-227.

Grant, D.R., 1970, Recent coastal submergence of the Maritime Provinces, Canada: Canadian Journal of Earth Sciences, v. 7, p. 676-689.

Hart, B.S., and Plint, A.G., 1989, Gravelly shoreface deposits: a comparison of modern and ancient facies sequences: Sedimentology, v. 36, p. 551-557.

King, C.A.M., 1972, Beaches and Coasts: London, UK, Edward Arnold, 570 p.

King, C.A.M., and Williams, W.W., 1949, The formation and movement of sand bars by wave action: Geographical Journal, v. 113, p. 70-85.

Kirk, R.M., 1980, Mixed sand and gravel beaches: morphology, processes and sediments: Progress in Physical Geography, v. 4, p. 189-210.

Kroon, A., and Masselink, G., 2002, Morphodynamics of intertidal bar morphology on a macrotidal beach under low-energy wave conditions, North Lincolnshire, England: Marine Geology, v. 190, p. 591-608.

Letzsch, W.S., 1983, Seven year's measurement of deposition and erosion, Holocene salt marsh, Sapelo Island, Georgia: Senckenbergiana Maritima, v. 15, p. 157-165.

Letzsch, W.S., and Frey, R.W., 1980, Erosion of salt marsh tidal creek banks, Sapelo Island, Georgia: Senckenbergiana Maritima, v. 12, p. 201-212.

Letzsch, W.S., and Frey, R.W., 1981, Organic carbon in a Holocene salt marsh, Sapelo Island, Georgia: Georgia Journal of Science, v. 39, p. 15-23.

MacEachern, J.A., and Hobbs, T.W., 2004, The ichnological expression of marine and marginal marine conglomerates and conglomeratic intervals, Cretaceous Western Interior Seaway, Alberta and northeastern British Columbia: Bulletin of Canadian Petroleum Geology, v. 52, p. 77-104.

Maejima, W., 1982, Texture and stratification of gravelly beach sediments, Enju Beach, Kii Peninsula, Japan: Journal of Geosciences, Osaka City University, v. 25, p. 35-51.

Marzo, M., and Anadón, P., 1988, Anatomy of a conglomeratic fan-delta complex: the Eocene Montserrat Conglomerate, Ebro Basin, northeastern Spain, *in* Nemec, W., and Steel, R.J., eds., Fan Deltas: Sedimentology and Tectonic Settings: London, UK, Blackie, p. 318-340.

Massari, F., 1984, Resedimented conglomerates of a Miocene fan-delta complex, Southern Alps, Italy, *in* Koster, E.A., and Steel, R.J., eds., Sedimentology of Gravels and Conglomerates: Calgary, Canadian Society of Petroleum Geologists.

Massari, F., and Parea, G.C., 1988, Progradational gravel beach sequences in a moderate- to high-energy, microtidal marine environment: Sedimentology, v. 35, p. 881-913.

Masselink, G., 1993, Simulating the effects of tides on beach morphodynamics: Journal of Coastal Research Special Issue, v. 15, p. 180-197.

Masselink, G., and Short, A.D., 1993, The effect of tidal range on beach morphodynamics and morphology: a conceptual beach model: Journal of Coastal Research, v. 9, p. 785-800.

McCave, I.N., and Geiser, A.C., 1978, Megaripples, ridges and runnels on intertidal flats of the Wash, England: Sedimentology, v. 26, p. 353-369.

McLean, R.F., 1970, Variations in grain-size ans sorting on two Kaikoura beaches: New Zealand Journal of Marine and Freshwater Resources, v. 4, p. 141-164.

McLean, R.F., and Kirk, R.M., 1969, Relationships between grain size, size-sorting, and foreshore slope on mixed sand-shingle beaches: New Zealand Journal of Geology and Geophysics, v. 12, p. 138-155.

Nemec, W., 1990, Aspects of sediment movement on steep delta slopes: Special Publications of the International Association of Sedimentologists, v. 10, p. 29-73.

Orford, J.D., and Carter, R.W.G., 1982, Crestal overtop and washover sedimentation on a fringing sandy gravel barrier coast, Carnsore Point, southeast Ireland: Journal of Sedimentary Petrology, v. 52, p. 265-278.

Orford, J.D., Carter, R.W.G., and Forbes, D.L., 1991, Gravel barrier migration and sea level rise: some observations from Story Head, Nova Scotia, Canada: Journal of Coastal Research, v. 7, p. 477-488.

Orton, G.J., and Reading, H.G., 1993, Variability in deltaic processes in terms of sediment supply, with particular emphasis on grain size: Sedimentology, v. 40, p. 475-512.

Pemberton, S.G., MacEachern, J.A., and Frey, R.W., 1992, Trace Fossil Facies Models: Environmental and Allostratigraphic Significance, *in* Walker, R.G., and James, N.P., eds., Facies Models: Response to Sea Level Change: St. John's, Newfoundland, Geological Association of Canada, p. 47-72.

Pemberton, S.G., Spila, M., Pulham, A.J., Saunders, T., MacEachern, J.A., Robbins, D., and Sinclair, I.K., 2001, Ichnology and Sedimentology of Shallow to Marginal Marine Systems: Ben Nevis and Avalon Reservoirs, Jeanne d'Arc Basin: Geological Association of Canada Short Course, v. 15: St. John's, Geological Association of Canada, 343 p.

Pethnick, J.S., 1992, Saltmarsh geomorphology, *in* Allen, J.R.L., and Pye, K., eds., Saltmarshes: Morphodynamics, Conservation and Engineering Significance: Cambridge, U.K., Cambridge University Press, p. 41-62.

Plint, A.G., Walker, R.G., and Duke, W.L., 1988, An outcrop to subsurface correlation of the Cardium Formation in Alberta, *in* James, D.P., and Leckie, D.A., eds., Sequences, Stratigraphy, Sedimentology: Surface and Subsurface: Memoir: Calgary, p. 167-184.

Postma, G., 1984, Slumps and their deposits in fan delta front and slope: Geology, v. 12, p. 27-30.

Postma, G., 1990, Depositional architecture and facies of river and fan deltas: a synthesis, *in* Coella, A., and Prior, D.B., eds., Coarse-Grained Deltas, International Association of Sedimentologists, p. 13-27.

Postma, G., and Nemec, W., 1990, Regressive and transgressive sequences in a raised Holocene gravelly beach, southwestern Crete: Sedimentology, v. 37, p. 907-920.

Postma, G., and Roep, T.B., 1985, Resedimented conglomerates in the bottomsets of Gilbert-type gravel deltas: Journal of Sedimentary Petrology, v. 55, p. 874-885.

Pye, K., and French, P.W., 1993, Erosion and acretion processes on British Salt Marshes, Vol. 1, Introduction: Saltmarsh Processes and Morphology: Cambridge, U.K., Cambridge Environmental Research Consultants.

Reading, H.G., and Collinson, J.D., 1996, Clastic Coasts, *in* Reading, H.G., ed., Sedimentary Environments; Processes, Facies and Stratigraphy: Oxford, U.K., Blackwell Science, p. 154-231.

Redfield, A.C., 1972, Development of a New England Salt Marsh: Ecological Monographs, v. 42, p. 201-237.

Shaw, J., Gareau, P., and Courtney, R.C., 2002, Palaeogeography of Atlantic Canada 13-0 kyr: Quaternary Science Reviews, v. 21, p. 1861-1878.

Short, A.D., 1991, Macro-meso tidal beach morphodynamics: Journal of Coastal Research, v. 7, p. 417-436.

Shulmeister, J., and Kirk, R.M., 1993, Evolution of a mixed sand and gravel barrier system in North Canterbury, New Zealand, during Holocene sea-level rise and still-stand: Sedimentary Geology, v. 87, p. 215-235.

Sunamura, T., and Takeda, I., 1984, Landward migration of inner bars: Marine Geology, v. 60, p. 63-78.

Walker, R.G., 1983a, Cardium Formation 2. Sand-body geometry and stratigraphy in the Garrington-Caroline-Ricinus area, Alberta - the "ragged blanket" model: Bulletin of Canadian Petroleum Geology, v. 31, p. 14-26.

Walker, R.G., 1983b, Cardium Formation 3. Sedimentology and stratigraphy in the Garrington-Caroline area, Alberta: Bulletin of Canadian Petroleum Geology, v. 31, p. 213-230.

Wescott, W.A., and Ethridge, F.G., 1980, Fan-Delta sedimentology and tectonic setting - Yallahs Fan Delta, southeast Jamaica: American Assoication of Petroleum Geologists Bulletin, v. 64, p. 374-399.

Wescott, W.A., and Ethridge, F.G., 1982, Bathymetry and sediment dispersal dynamics along the Yallahs fan delta front, Jamaica: Marine Geology, v. 46, p. 245-260.

Wescott, W.A., and Ethridge, F.G., 1983, Eocene fan delta-submarine fan deposition in the Wagwater Trough, east-central Jamaica: Sedimentology, v. 30, p. 235-247.

Wright, L.D., 1977, Sediment transport and deposition at river mouths: A synthesis: Bulletin of the American Association of Petroleum Geologists, v. 88, p. 857-868.

Wright, L.D., and Short, A.D., 1984, Morphodynamic variability of surf zones and beaches: A synthesis: Marine Geology, v. 56, p. 93-118.

Zonneveld, J.-P., and Moslow, T.F., 2004, Exploration potential of the Falher G shoreface conglomerate trend: evidence from outcrop: Bulletin of Canadian Petroleum Geology, v. 52, p. 23-38.

CHAPTER 2: FACIES ARCHITECTURE AND ICHNOLOGY OF RECENT SALT-MARSH DEPOSITS: WATERSIDE MARSH, NEW BRUNSWICK, CANADA[1]

INTRODUCTION

Salt marshes represent areally significant components of both modern and ancient marginal-marine depositional environments. Occurring behind barrier islands, beaches, in estuaries and lagoons, salt marshes develop in response to tidal inundation of backshore environments, and thus are excellent indicators of marginal-marine conditions. It is the purpose of this paper to define facies and facies associations from salt-marsh sediments observed outcropping along tidal creeks at Waterside Beach, New Brunswick, Canada. These exposures correlate to deposits presently forming in the adjacent Waterside Marsh.

The two main components of salt marshes are a vegetated platform that is periodically submerged by the tide, and a network of tidal channels that branch and taper landward (Allen 1997, 2000; Pethnick 1992). Salt marshes are classified as mineralogenic – dominated by tidally derived inorganic sediment with less than 10% organic material – or organogenic – sedimentation dominated by organic sediment with only minor amounts of tidally derived inorganic sediment (Allen 2000). Sedimentation rates and tidal-creek patterns in salt marshes are complex and change with relative sea level (RSL), sediment composition, and tidal character (Allen 2000; French 1993; Pye and French 1993). During periods of stillstand or RSL fall, tidal waters rarely flood the marsh surface; thus, they tend to be organogenic. In these marshes, tidal channels are poorly developed or absent and the stratigraphy is dominated by extensive peat horizons (Allen 1990, 1997, 2000; Anderson and Race 1980; Redfield 1972). During RSL rise, organogenic marshes evolve into mineralogenic marshes and aggrade vertically at a rate proportional

[1]A version of this chapter has been published in the JOURNAL OF SEDIMENTARY RESEARCH, 2005, v. 75, p. 596-607 as "Facies architecture and ichnology of recent salt-marsh deposits: Waterside Marsh, New Brunswick, Canada", by: Shahin E. Dashtgard and Murray K. Gingras

to RSL rise. With prolonged RSL rise, the high-order tidal creeks expand and increase in frequency, the marsh matures, and the low-order tidal creeks that dissect the salt-marsh surface silt in (Allen 1997).

Detailed descriptions of modern salt marshes focus either on the regional stratigraphy of a deposit or on the sedimentary and biogenic structures present. Van Straaten, for example, described salt-marsh bedding (Van Straaten 1954), tidal-creek migration (Van Straaten 1961), and the depositional processes responsible for sedimentation in European salt-marshes. Similarly, Evans (1965) provided comprehensive descriptions of sedimentary structures observed in salt-marsh deposits at The Wash, England. Weimer et al. (1982) and, more recently, Allen (2000) summarized much of the work on the sedimentology and morphology of modern tidal flats and salt marshes. In North America, identification of sub-environments within salt marshes was undertaken at Sapelo Island, Georgia, U.S.A. (Basan and Frey 1977; Edwards and Frey 1977) and in New England, U.S.A. (Anderson and Race 1980; Redfield 1972). Edwards and Frey (1977), and Basan and Frey (1977) defined creek-bank, low-marsh, transitional, and high-marsh environments. Similarly, Redfield (1972) differentiated peat, intertidal-marsh, and high-marsh environments based on vegetation cover. These zonation schemes are botanically based, which may be difficult to apply to the rock record. In fact, Basan and Frey (1977) acknowledge that diagnostic sedimentological and ichnological criteria for identifying high-marsh deposits are few and that the presence or absence of characteristic plants is used to define the zonation. Easily recognized, sedimentologically and ichnologically centered facies have not been presented in the literature,

The probability of salt-marsh deposits passing into the rock record (preservation potential) is partly dependent upon changes in RSL. In the Bay of Fundy the preservation of coastal sediments has been strongly influenced by transgression resulting from rapid sea-level rise over the past 6000 years (Amos et al. 1991; Shaw and Courtney 2002). Transgression, especially on wave-dominated coasts, tends to result in headland erosion

(Reading and Collinson 1996; Roy et al. 1994), thus the upper foreshore and backshore deposits of many Bay of Fundy coastal systems will either be partially preserved or removed. At Waterside Beach, wave-induced coastal erosion and high tidal energy has resulted in the exposure of recently deposited sediments (the last ~ 200 y). Although these salt-marsh sediments exposed in the foreshore of Waterside Beach have a low preservation potential, they provide an opportunity to compare the architecture and structures of re-exhumed salt-marsh deposits to active depositional environments in the adjacent marsh. Through this comparison it is possible to establish sedimentologically and ichnologically distinct facies and facies associations that are characteristic of salt-marsh deposits. The proposed facies associations are intended to improve the framework for identifying salt-marsh facies in the rock record.

Study Area

On the north shore of the Bay of Fundy (Fig. 2.1) Waterside Marsh is situated landward of the northwest-southeast oriented Waterside Beach (Fig. 2.1C). The marsh exhibits an open-coast to open-embayment morphology (Allen 2000; Pye and French 1993) and is a mature (high) marsh. The beach-marsh system suffers a 12 m spring-tidal range that results in subaerial exposure of up to 1100 m of intertidal-zone sediments during spring low tides. Overmarsh flooding (Bayliss-Smith et al. 1979) occurs for only a few days during the high tide of spring-tidal cycles. Decapitated salt-marsh deposits sporadically crop out throughout the upper and middle intertidal zones at Waterside Beach. Where Newfoundland Creek debouches onto the beach from the marsh, downcutting by the tidal creek exposes vertical successions of older marsh deposits (Fig. 2.1C). Weathering of the sediment has enhanced the sedimentological and ichnological structures present in the deposits.

Anthropogenic modification of Waterside Marsh has been significant. In the 17th and 18th centuries farmers excavated many of the low-order tidal creeks that dissect

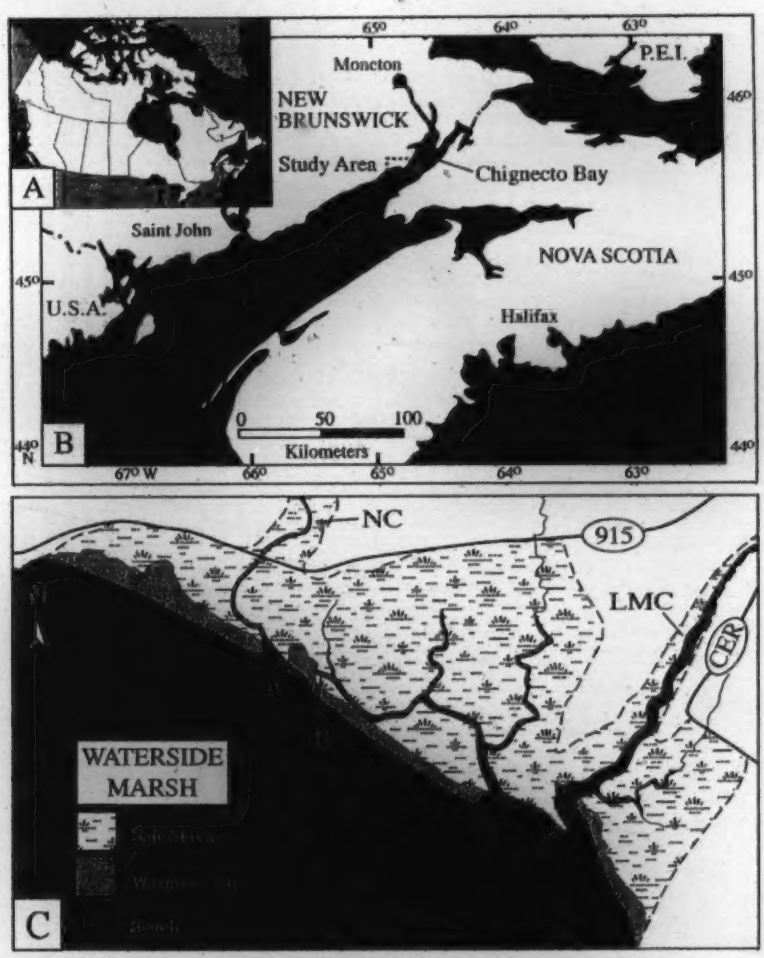

FIGURE 2.1 –Location map of Waterside Beach and Marsh. A) Map of Canada with Bay of Fundy identified by the dashed box. B) Schematic diagram of the study area in the Bay of Fundy. C) Schematic diagram of Waterside Beach and Marsh in 2001. Area A indicates the approximate location of salt-marsh outcrops. Area B is referred to in the text. (NC = Newfoundland Creek, LMC = Long Marsh Creek, CER = Cape Enrage Road)

the marsh surface. Similarly, salt-marsh erosion was hampered by the construction of a backshore dike system in the 1650s. Abandonment of the dike in the 1940s because of changes in demographics and regulations has resulted in rapid erosion via natural processes over the past 60 years. Of particular significance is the large washover deposit located directly north of the mouth of Newfoundland Creek (Fig. 2.1C). This resulted

from a 1997 storm that altered hydraulic flow and thereby the depositional and erosional patterns in the marsh.

Methods

Outcrops of palimpsest salt marsh located at the mouth of Newfoundland Creek were studied in detail in July 2003 (Fig. 2.1). Ichnological and sedimentological characteristics of the sedimentary facies were recorded, as was their spatial distribution and lateral variability. From these data, facies associations are inferred. Facies identified in historical deposits were compared to modern (active) marsh deposits. This comparison aided in the interpretation of sedimentological and ichnological structures observed in outcrop, and in drawing inferences pertaining to the preservation potential of the observed facies. In 2004 *in situ* sediment samples were collected from Waterside Marsh and Beach and imaged using x-ray radiography. Samples were collected with a 22.5 cm by 15 cm by 7.5 cm stainless steel box core as described in Bouma (1969). A slab, 22.5 cm by 14 cm by 2 cm thick, was then extracted using a plastic tray. This slab was x-rayed to assess sedimentary and biosedimentary structures.

Samples collected from salt-marsh outcrops were analyzed for grain size and organic carbon content. Pretreatment of samples involved an initial drying period of 24 hours at 105° C to remove interstitial water (McKeague 1978) followed by disaggregation with mortar and pestle. Total-organic-carbon content was measured through loss-on-ignition (LOI) analysis as outlined in Heiri et al. (2001). Disaggregated samples were dried for an additional 18 hours at 105° C and then heated to 550° C for 4 hours. Weight loss due to combustion of organic matter during LOI was determined with an electronic scale accurate to 0.001 g. X-ray absorption analysis with a Micromeritics Sedigraph 5100 was used to assess grain size. Samples were analyzed before and after the removal of organic carbon; however, the values reported herein for sand, silt, and clay are those for samples pretreated to remove organic carbon. Prior to x-ray analysis, samples were

sieved to remove grains larger than 250 μm (medium-grained sand). This coarse fraction was weighed and factored into the grain-size distribution of each sample. To prevent the flocculation of fines, 3 to 4 g of disaggregated sample was mixed with 30 to 40 mL of 0.05% sodium metaphosphate ($(NaPO_3)_x \cdot Na_2O$) . Each solution was thoroughly mixed with a magnetic mixer for 5 minutes and a sonic mixer for 1 minute before analysis. Data were plotted in continuous grain-size curves from 250 to 0.49 μm (ϕ 2 to 11) ± 2%. Grain-size nomenclature is assigned on the basis of Shepard's (1954) classification scheme with sand (S), silt (Z), and clay (C) fractions reported.

Airphotos of Waterside Marsh taken approximately every ten years from 1945 to 2001 and historical maps from 1789 and 1899 aided in assessing the extent and evolution of the salt marsh and in determining the possible depositional environments of facies observed in outcrop. We recognize that the term facies is normally reserved for descriptions of sedimentary rocks with a specific set of lithologic, structural, and organic characteristics. However, the terms facies and facies associations in this study are used to describe sediment, and genetically related sedimentary packages that otherwise meet the requirements of facies and facies associations. This is done in order to facilitate anticipated application and comparison to the rock record.

Herein, the degree of bioturbation is referred to as rare, low, moderate, high, or intense. These terms represent a range of burrowing intensities (Table 2.1) and are thus semiquantitative. The degree of bioturbation is partly dependent on the size of the organism. For example, the amphipod *Corophium volutator* rarely exceeds 1 cm long, 0.3 cm wide, and 0.15 cm thick. Within the Bay, burrow densities of *C. volutator* range up to 63,000 individuals/m^2 (Thurston 1990). Individual U-shaped burrows do not occupy a significant area, and intense burrowing is not apparent until there are at least 20,000 individuals/m^2. Conversely, shells of the bivalve *Mya arenaria* are measured up to 8 cm long, 5 cm wide, and 3.5 cm thick, requiring only 250 individuals/m^2 to intensely bioturbate a substrate. *Nereis* populations were difficult to assess because of the

	Rare	Low	Moderate	High	Intense
Mya arenaria	< 50	50 - 150	100 - 150	150 - 250	> 250
Macoma balthica	< 100	100 - 200	200 - 400	400 - 600	> 600
Corophium volutator	< 1,000	1,000 - 5,000	5,000 - 10,000	10,000 - 20,000	> 20,000
Nereis sp.	*Difficult to assess. Complex burrow networks				
Talitrid amphipods	< 50	50 - 100	100 - 300	300 - 600	> 600

TABLE 2.1 – Relative bioturbation levels for infauna observed in Waterside Marsh. Values are reported in burrows/m^2.

multiple burrow openings and complex burrow networks constructed by this polychete. The degree of bioturbation is proportional to the number of burrow openings, although counting openings cannot assess the population density of *Nereis*. In any case, *Nereis* is a minor bioturbator in the salt marsh and their burrow densities are generally low in both the palimpsest and modern substrates. Illustrations of the main bioturbating infauna observed in Waterside Marsh are provided in Figure 2.2. Figure 2.2 also schematically depicts the resultant biogenic sedimentary structures produced by each organism.

FACIES ASSOCIATIONS: DESCRIPTIONS AND INTERPRETATION

In the study area, salt-marsh deposits are divided into three facies associations: (FA1) salt-marsh deposits, (FA2) tidal-creek deposits, and (FA3) beach-related deposits. The three facies associations are further subdivided into nine sedimentary facies. All facies associations and facies are characterized by a distinctive suite of sedimentological and ichnological characteristics, which are summarized in Table 2.2.

Facies Association 1: Salt-Marsh Deposits

Facies Association 1 (FA1) facies are genetically related deposits that accumulate on the salt-marsh surface. FA1 comprises Facies 1, the main facies in the marsh, Facies 2, the sediments that accumulate in shallow salt-marsh pools or pannes, and Facies 3, a *Glossifungites*-demarcated surface (Bromley 1990; Gingras et al. 2001; Pemberton et al.

2001) formed via exhumation of F1 sediment at the base of the tidal creeks (Table 2.2). This is the most extensive and easily recognized facies association in the salt marsh. The three facies share similar sedimentological characteristics, but vary in both color and ichnological signature.

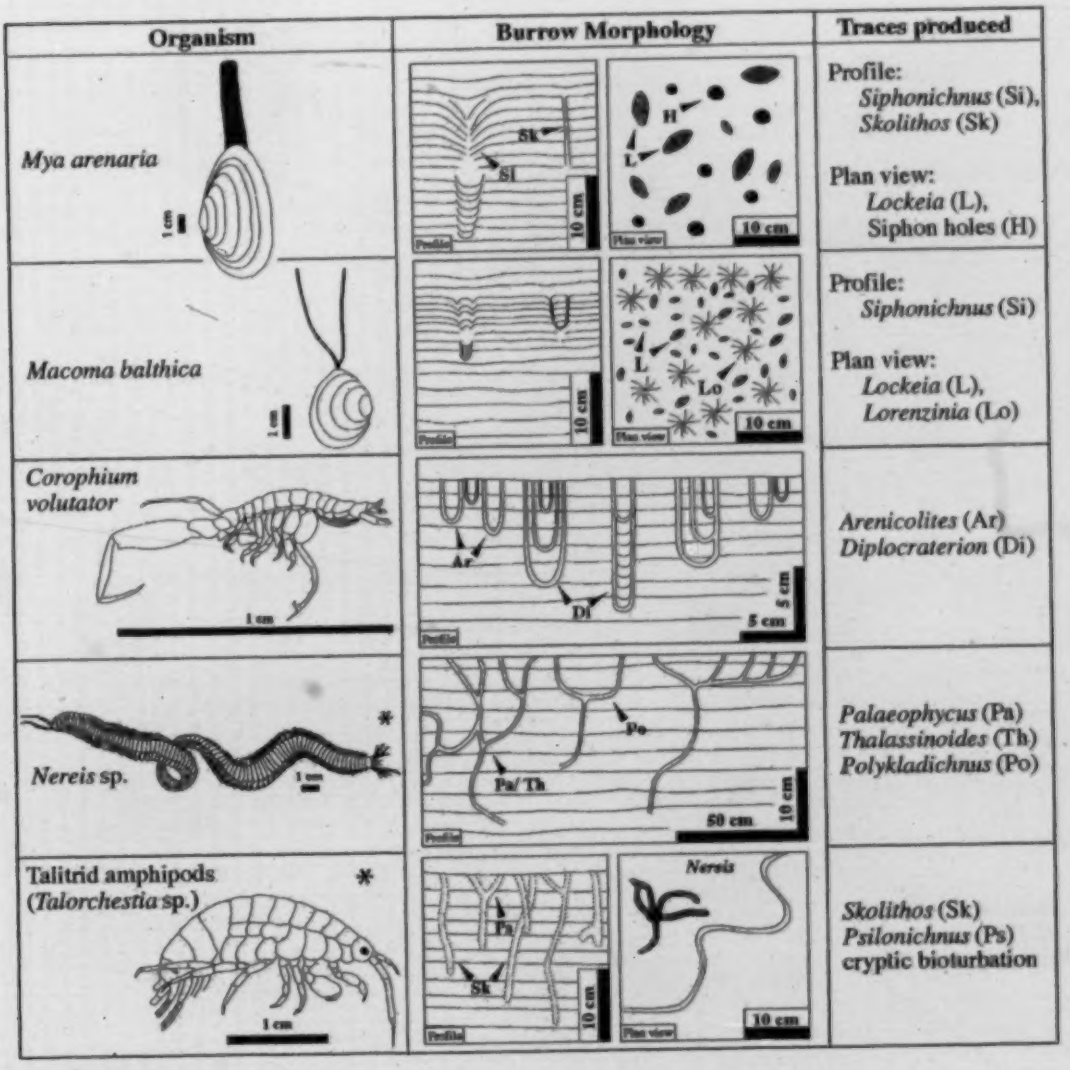

FIGURE 2.2 – Illustration of the major bioturbators observed in Waterside Marsh. Sketches of organisms, the traces they produce, and the incipient trace names are provided. (* = images modified from Gosner 1978).

Facies Association	Facies	Composition	Sedimentary Structures	Infauna / Vegetation	Incipient Bioturbation	Bioturbation Intensity	Depositional Environment / Comments	Distribution	Preservation Potential
FA1: salt-marsh deposits	F1	Silt (greenish-gray)	**Rhythmic laminae** Horizontal to subhistory laminations Scattered pebbles & cobbles	**Rooting**	**Root casts**	**Intense**	Sediment deposited on the salt-marsh surface Main salt-marsh facies	Very extensive, exposed throughout intertidal zone on beach	High
	F2	Clayey silt (gray)	**Very weakly laminated** Organic rich (> 10%)	Bird tracks	Not preserved	---	Peats deposits (shallow pools that form on the salt-marsh surface)	Extensive, occurs interbedded with F1 Likely more common lower in succession	High
	F3	Silt (reddish-brown to greenish-gray)	**Rhythmic laminae** Horizontal to subhistory laminations Scattered pebbles & cobbles	***M. arenaria*** ***C. volutator*** Rooting	**Sl, Sk, L** **Ar, Di** Root casts	**Local intense** **Mod** Mod to high	F1 deposits exhumed & colonized at the base of tidal creeks Upper contact is a *Glossifungites* surface	Occurs only at the base of tidal-creek successions	High
FA2: tidal-creek deposits	F4	**Clayey silt (brown) & silty gravel**	**Interbedded** Low-angle (axially oriented) bed dip Continuous matted-organic laminae	***M. arenaria*** ***M. balthica*** ***C. volutator*** *Nereis* sp.	**Sl, Sk, L** **Sl, L, Lo** **Ar, Di** **Pa, Th, Po**	**Local high** Low to high V. rare to high Low to mod	Tidal-creek deposits Accumulate via vertical aggradation at base of tidal creek	Confined to tidal-creek environments	High
	F5	Clayey silt (brown)	**Massive to chaotic bedding** **Slump blocks of F1** Parallel, low- to high-angle dipping laminae Rare gravel clasts	***M. balthica*** ***C. volutator***	**Sl, L, Lo** **Ar, Di**	Mod to high Mod to high (decreases to 0 at center of unit)	Channel-abandonment fill	Rare, confined to abandoned tidal-creek fairways	Mod to high
	F6	Silt (light reddish-brown)	**Medium angle (7-9°) lam.** **Rhythmic matted-organic laminae** Gravel lenses	***M. arenaria*** ***M. balthica*** ***C. volutator*** *Nereis* sp.	**Sl, Sk, L** **Sl, L, Lo** **Ar, Di** **Pa, Th, Po**	**Low to mod** **High to intense** **High to intense** Rare to low	Tidal-creek point-bar deposits	Confined to tidal-creek environments	High
	F7	Clayey silt (reddish-brown to dark gray)	**Pebble and shell lags** **Matted-organic laminae** Low angle (axially oriented) laminae	***M. arenaria*** ***C. volutator***	**Sl, Sk, L** **Ar, Di**	Intense Intense	Deposited in low-order tidal creeks that dissect F1 **Gradational upper contact with F1 or F2**	Abundant, but narrow and shallow Abundance increases lower in the succession	High
FA3: beach-related deposits	F8	**Sand & gravel**	**Steeply dipping (9-20°) beds**	---	---	---	Beach-derived sediment deposited in the tidal creeks	Rare, occurs only in tidal creeks within ~ 100 m of the seaward edge of the marsh	Mod
	F9	**Sand & gravel**	**Horizontal, to very low-angle (<4°) bedding** Some trough cross-bedding	**Talitrid amphipods** Rooting	**Sk, Ps** **Root casts**	**V. rare to rare** **Rare to mod**	Washover-fan deposits	Extensive on the marsh surface within ~ 100 m of the beach	Very Low

TABLE 2.2 – Summary table of facies and facies associations described in the text. See Figure 2.2 for definitions of incipient bioturbation and Table 2.1 for bioturbation intensities. Sedimentological and ichnological structures diagnostic of specific facies are highlighted in bold print.

Facies 1 (F1)

Facies 1 comprises greenish-gray, rooted, horizontal to undulatory, rhythmically laminated silt (Fig. 2.3A, B). The average grain size is 15.5 μm (S 2%, Z 90%, C 8%) with 6.9% organic carbon. Laminae sets are rhythmic (Fig. 2.3B, C) and continuous for at least tens of meters. Pebbles and cobbles are uncommon (Fig. 2.3A), and gravel occurrence decreases landwards from the seaward terminus of the salt marsh. Bioturbation is minimal, whereas rooting is common to abundant (Fig. 2.3B, C).

The rhythmic laminae sets of F1 are considered winter-summer couplets deposited on the salt-marsh surface during spring-tidal flooding. Depositional processes in this environment include sediment baffling by salt-marsh plants (Allen 2000; Nyman et al. 1993; Redfield 1972) and flocculation of fines (Christiansen et al. 2000). Laminae

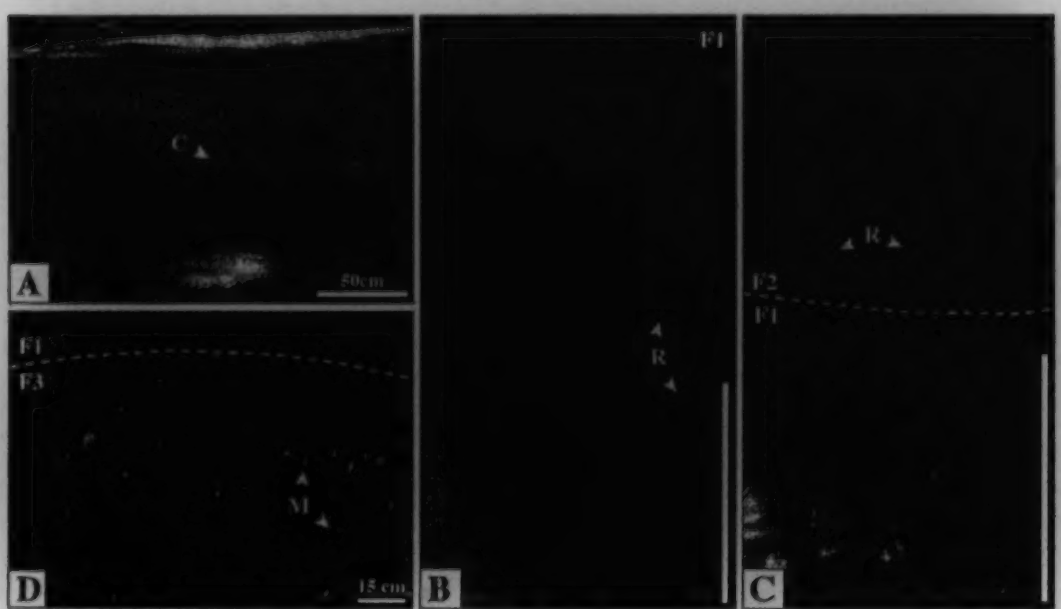

FIGURE 2.3 – Photos of FA1: salt-marsh deposits. A) Horizontally laminated, heavily rooted, greenish-gray clayey silt of F1. Note the large cobble (C) protruding from the sediment. B) An x-ray radiograph of laminated, heavily rooted (R) F1 sediment exposed by erosion on Waterside Beach. Light bands indicate silt laminae and dark, clayey silt laminae. C) X-ray radiograph profile of laminated, heavily rooted silt deposits of F1 overlain by organic-rich, clayey silt F2 sediments. Note the preservation of old Halophytic plant roots (R) near the base of F2, but no rooting near the top. Gradational contact between F1 and F2 is highlighted by the dashed line. D) Bedding-plane view of erosionally enhanced scours of *Mya arenaria* (M) burrows in exposed F3 deposits. Gradational contact between F1 and F3 is highlighted by the dashed line.

thickness decreases with distance from the immediate sediment source – either the seaward edge of the marsh or the tidal channels (Allen 2000; Davidson-Arnott et al. 2002). This process of sediment accumulation is not damped or interrupted by ponded water on the salt-marsh surface, because the laminae continue across vegetated zones and small ponds (Edwards and Frey 1977). The heavily vegetated, undulatory surface of the salt marsh represents the upper surface of F1 and is the primary depositional surface of this facies. Individual pebbles and cobbles (Fig. 2.3A) and thin, discontinuous gravel lenses, randomly distributed throughout F1, F2, and F3 are deposited by ice. Spring-tide flooding during the winter transports blocks of sediment-laden drift ice from the beach onto the marsh. Subsequent melting of the ice results in random deposition of coarse clastic material on the salt-marsh surface.

Facies 2 (F2)

Gray, very weakly laminated clayey silt (Fig. 2.3C) defines Facies 2. The average grain size is 4.3 μm (S 0%, Z 66%, C 34%) with 11.8% organic carbon. This facies was not observed in the outcrops, but it is defined from sediments presently accumulating at the base of pannes commonly encountered on the salt-marsh surface. Laminae and laminae sets are continuous for tens of meters but are composed of organic-rich soupy mud (Fig. 2.3C). Living plants are not apparent; however, the roots of old halophytic vegetation are commonly observed (Fig. 2.3C). Vegetation is restricted to algal growth at the base of the pool and in the water column. Large bird tracks, 20 cm long by 13 cm wide, are abundant and form depressions within the sediment. Shallow pannes dry out between overmarsh flooding events, resulting in desiccation and cracking of the exposed algal-matted surface.

Facies 2 sediments are deposited by the same processes as F1 with the addition of a longer-term low-energy depositional phase. Consequently, F2 deposits have considerably more clay than F1. The pannes in which F2 sediments are deposited tend

to be anoxic. A limited influx of oxygenated water and the significant accumulation of decaying organic matter severely limits the long-term oxygen supply, resulting in a predominantly anoxic environment that is inhospitable for infauna. Vegetation in pannes is restricted (Fig. 2.3C) because of the propensity of halophytes to avoid drowned environments (Allen 2000; Davidson-Arnott et al. 2002; Redfield 1972). Desiccation cracks develop between overmarsh flooding events when shallow pannes dry out.

Facies 3 (F3)

Facies 3 comprises light reddish-brown and greenish-gray, burrowed, rooted horizontal to undulatory, rhythmically laminated silt. Sedimentologically F3 is similar to F1, yet exhibits markedly different biogenic structures. Facies 3 suffers moderate to high degrees of rooting, moderate colonization by *Corophium volutator*, and locally intense bioturbation by the bivalve *Mya arenaria* (Fig. 2.3D).

Exhumation of Facies 1 sediment via tidal-creek migration and erosion results in the secondary alteration of F1 sediment to F3. Exposure to nutrient- and oxygen-rich water results in: (1) oxidation of the sediment; (2) decomposition of organic matter; and (3) colonization by *Mya arenaria* and *Corophium volutator*. Given the compacted nature of F3 and the postdepositional colonization of the exhumed sediment, the upper contact of this facies represents a *Glossifungites* ichnofacies (Fig. 2.3D). The light reddish-brown coloration of Facies 3 with no discernable change in grain-size composition relative to F1 is the result of oxidation of the reduced, greenish-gray F1 sediment. The low frequency of rooting in F3 occurs because of aerobic decomposition of roots in the oxygenated water of the tidal channels. Finally, the locally intense bioturbation by *M. arenaria* and moderate bioturbation by *C. volutator* is the result of exposure to nutrient- and oxygen-rich, mesohaline water in a sheltered environment (relative to the beach).

Facies Association 2: Tidal-Creek Deposits

Facies Association 2 (FA2) encompasses all sediment deposited in the naturally formed tidal creeks of Waterside Marsh. Areally, the tidal creeks are a minor component of the overall salt-marsh environment, yet are loci of rapid erosion and deposition. Deposition occurs when high-tide waters do not flood the marsh surface and erosion when they do (French and Stoddart 1992). Tidal-creek deposits are divided into four main facies: Facies 4 accumulates via vertical aggradation within a slowly migrating tidal creek; Facies 5 is a tidal-creek abandonment deposit; Facies 6 represents point-bar deposition associated with channel migration; and Facies 7 encompasses sediment that accumulates in low-order tidal creeks (Table 2.2).

Facies 4 (F4)

Facies 4 consists of brown, low-angle, interbedded clayey silt and silty gravel. The average grain size, excluding the gravel component, is 10.6 μm (S 3%, Z 70%, C 27%) with 2.8% organic carbon. Beds are continuous for tens of meters and are axially oriented (Fig. 2.4A). Small discontinuous gravel lenses and larger continuous gravel beds are common in the unit. Small, concave-down structures filled with steeply inclined silty gravel beds that laterally translate into tangential toeset beds are sporadically distributed throughout the unit. Continuous, low-angle, matted-organic laminae are regularly observed. Bioturbation in F4 is produced by *Corophium volutator, Macoma balthica,* and *Mya arenaria*, with minor populations of *Nereis*. *M. arenaria* is the main bioturbator and occurs in localized high-density populations. The population density of *C. volutator* is substrate dependent and varies from low to high. *C. volutator* populations are very rare to low in gravel-rich deposits but increase to high to intense in silt-dominated substrates. Similarly, the distribution of *Macoma balthica* is closely related to energy level and substrate caliber. In low-energy zones dominated by silt deposition, *M. balthica* is encountered in high-population densities. Conversely, in moderate-energy environments,

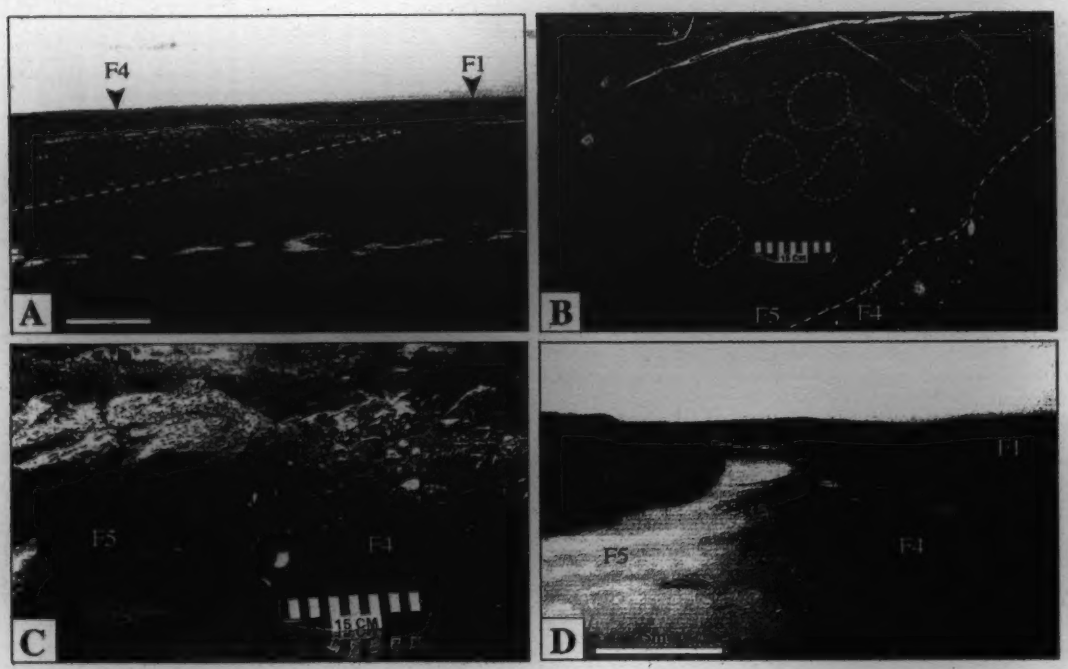

FIGURE 2.4 – Photos of FA2 – tidal-creek deposits. A) Contact between shallow-dipping, silty gravel beds of F4, and F1. B) Interpreted photo of non-oriented slump blocks in F5. C) Erosionally scoured contact between F4 and F5. D) Relationship of Facies 5 to F4 and F1 deposits in the active marsh.

low population densities are noted. *M. balthica* is not observed in substrates where the surface material is not mainly silt or clay. Burrowing by *Nereis* is low to moderate and generally increases as grain size decreases. Rooting is uncommon and discontinuous but increases towards the contact with Facies 5. Continuous laminae of matted-organic detritus (twigs, leaves, and grass material) accumulate parallel to the main bedding.

Interbedded silt and silty gravel beds in Facies 4 are deposited via vertical aggradation of sediment at the base of tidal creeks. Aggradation of sediment occurs either in response to RSL rise or from changing hydraulic conditions related to channel cutoff (Fig. 2.1C: Area B). Allen (2000) explained that channels expand in cross-sectional area with time, which is supported by historical data from Waterside Marsh. However, Facies 4 deposits accumulate as a result of base-level rise and aggradation of sediment at the bases of the channels and are not eroded by later channel expansion. During the

winter months, gravel is transported into the tidal creeks through both storm washover and slow, upstream transport and trapping of sediment by ice. The second process is postulated on the basis of data presented by Desplanque and Mossman (1998) regarding the accumulation and trapping of ice in tidal creeks. In the tidal creeks, there is a general landward decrease in the amount of gravel reflecting the landward dissipation of tidal (Weimer et al. 1982) and storm energy. Silt deposition is observed occurring over the summer in the active marsh. The bedding in F4 tends to follow the topography of the channel and dip toward the channel axis.

Bioturbation in F4 is mainly due to *Mya arenaria*. These bivalves easily tolerate extreme salinity fluctuations and salinities as low as 5 ppt (Gosner 1978) and are well adapted to colonize the brackish tidal creeks. Furthermore, *M. arenaria* larvae settle preferentially in sheltered sites (Snelgrove et al. 1999). The low-energy environment of the tidal creeks, as a result of upstream dissipation of tidal energy and no direct wave assault is thus favorable for *M. arenaria* colonization. The ichnological signature of this facies can vary depending on the salt-marsh architecture and local hydraulic conditions. Area B (Fig. 2.1C) is an example of a previously moderate-energy environment that now experiences low-energy conditions. This occurred when storm-driven infilling of the old channel fairway with beach-derived sand and gravel altered flow conditions in the marsh. Redirection of hydraulic energy away from Area B resulted in the establishment of an environment favorable for infaunal colonization by *Mya arenaria*, *Macoma balthica*, *Corophium volutator*, and *Nereis*.

Facies 5 (F5)

Facies 5 is brown, massive bedded to chaotically bedded clayey silt. The average grain size is 7.8 μm (S 5%, Z 74%, C 21%) with 2.9% organic carbon. Large blocks of F1 sediment with randomly oriented bedding are common in F5 (Fig. 2.4B). Parallel, low- to high-angle laminae are also common. Gravel clasts are rare (Fig. 2.4B, C).

Facies 5 is contained within a linear exposure oriented northwest-southeast that is 5 m wide and at least 100 m long. Large logs (greater than 1 m in length) are observed along and parallel to the central axis (Fig. 2.4B). Bioturbation is observed throughout F5. The highest burrow densities occur along the edges of the unit and abruptly diminish towards the center. *Corophium volutator* is the main bioturbator, varying from moderate to high burrow densities on the edges and decreasing to very rare in the middle. Burrowing by *Macoma balthica* is moderate to high on the edges as well, and displays a colonization pattern similar to that of *C. volutator.* Rooting reflects the primary bioturbation pattern with common to abundant rooting on the edges and decreasing rapidly towards the center of the unit. Macroscopic organic detritus (logs and branches) exhibits the reverse relationship to other detritus (i.e., grasses, leaves, and twigs) and is concentrated along the axis of the deposit and decreases rapidly towards the edge.

Facies 5 is deposited contemporaneously within and adjacent to the F4 sediment with the diverse trace assemblage described above. Upon establishment of a low-energy zone in the tidal channel (Fig. 2.1C: Area B), the channel begins to infill with clayey silt. The sharp contact between F4 and F5 is the result of this abrupt shift in facies (Fig. 2.4D). Interbedded silt and silty gravel beds of F4 are replaced by deposition of clayey silt (F5) in the old channel fairway. Slump blocks of F1 and large branches brought in on the flood tide are preserved in the mud. The distribution of bioturbation is strongly influenced by channel morphology. As seen in Figure 2.4D, the central channel axis maintains low-level flow at low tide as water seeps out of the surrounding salt marsh and channel sediment. Infauna preferentially colonize the water-saturated sediment that is emergent for part of the tidal cycle, and thus do not colonize the sediment along the central channel axis. This colonization pattern is reflected in the bioturbation pattern of exposed Facies 5 deposits where high to intense burrowing along the edges recedes rapidly to very rare along the central axis. Rooting patterns reflect the process of salt-marsh reestablishment over the abandoned channel. Vegetation colonizing the edges of the abandoned channel (Fig.

2.4D) increasingly encroaches upon the channel axis as it continues to fill with clayey silt. The central channel axis is therefore the last part of the abandoned channel to be colonized by vegetation. The resultant rooting pattern is manifested as high to intense rooting on the edges and receding rapidly towards the central axis.

Facies 6 (F6)

Facies 6 is light reddish-brown, low-angle, laminated silt (Fig. 2.5). The average grain size is 18.1 μm (S 8%, Z 80%, C 12%) with 2.5% organic carbon. Beds are continuous for more than 10 m and dip at medium dip angles (7-9°) in a landward direction (Fig. 2.5A, B). Silt beds are interrupted by regular laminae of matted organic material. The matted-organic laminae increase in number and frequency in the downdip direction and are typically discontinuous and distorted by postdepositional bioturbation (Fig. 2.5A, B). Silt beds and organic laminae form bedsets of relatively uniform thickness that repeat throughout the succession. Intermittent, discontinuous, bedding-parallel gravel lenses are uncommonly encountered. Generally, the number and thickness of gravel beds increases from rare to common in the updip or seaward direction. Gravel beds and matted-organic laminae share an inverse relationship with gravel content, increasing as organic laminae decrease. Shallow, U-shaped structures either lined or infilled with silty gravel are also encountered (Fig. 2.5A, B). In some occurrences, gravels in the U-structures dip steeply to tangentially towards the center. Otherwise, the shallow U-structures are infilled with either massive silt or downward-deflecting silt and organic laminae. Bioturbation is extensive in F6. High to intense bioturbation by *Corophium volutator* and *Macoma balthica* is encountered on bedding-plane surfaces in outcrop (Fig. 2.5C). Individual *C. volutator* burrows are difficult to discern in the vertical section because of their high density and partial destruction of burrows during compaction. Similarly, individual bivalve traces are poorly defined in the vertical sequence, although *Lockeia* are readily apparent on bedding planes. Low to moderate

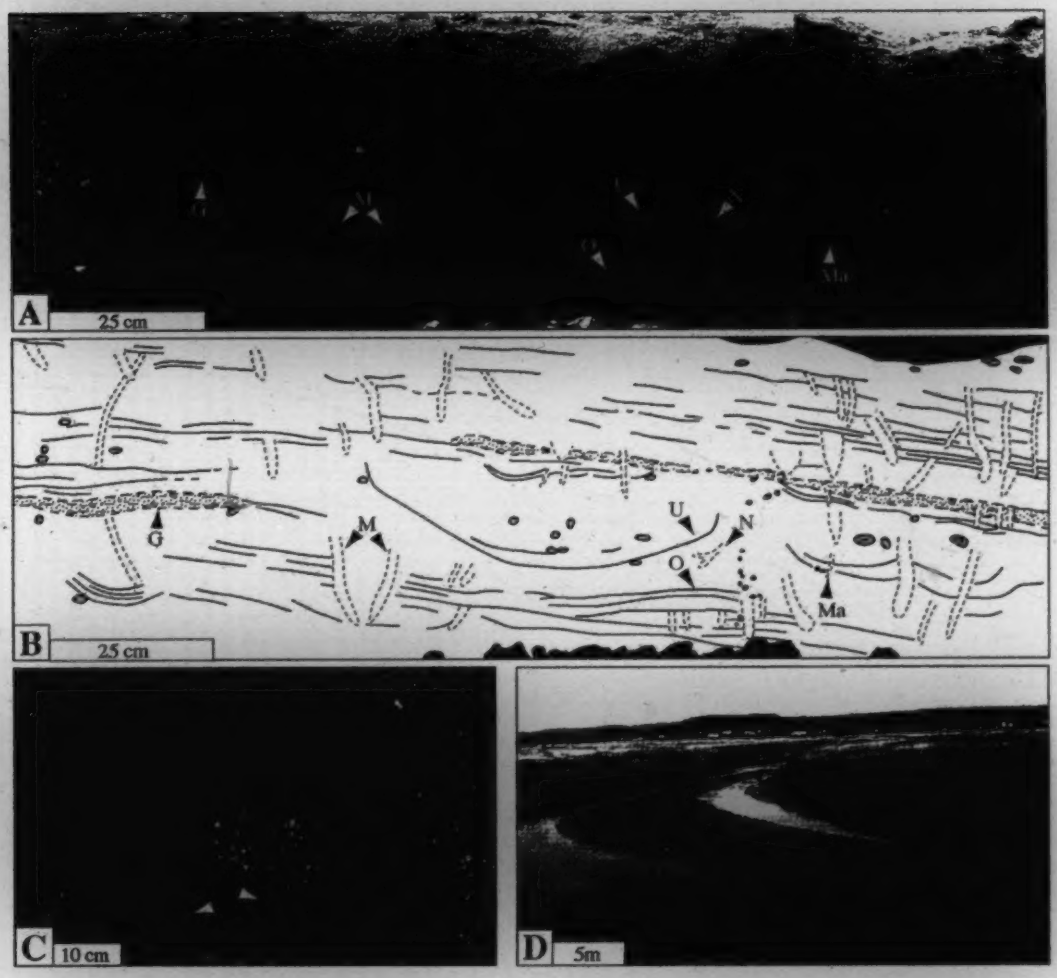

FIGURE 2.5 – Photos and schematics of F6, interpreted as point-bar deposits. A) Photo mosaic and B) interpreted schematic of light reddish-brown, low-angle, laminated silt and matted-organic laminae. Note: discontinuous gravel lenses (**G**), large burrows of *Mya arenaria* (**M**), matted-organic laminae (**O**), U-shaped structures (**U**), small *Nereis* (**N**) burrows, and *Macoma balthica* (**Ma**) burrows. C) Bedding-plane surface of F6. Arrows indicate examples of the high density of *Corophium volutator* burrows. D) Deposition of a point bar in the active salt marsh.

densities of vertical, unlined *Mya arenaria* burrows are observed originating at the tops of silt beds and penetrating down through both organic laminae and silt beds. These burrows are commonly greater than 1 cm wide and 10 cm long and sometimes are underlain by concave-down spreite. Low to rare *Nereis* burrows are observed. Rooting is essentially absent.

Facies 6 is interpreted to represent tidal-creek point-bar deposits (Fig. 2.5D). The lateral migration, or meander rate, of tidal channels in salt marshes is an order of magnitude slower than fluvial channels, as a consequence of the resistant nature of the heavily rooted salt-marsh sediment (Allen 2000; Letzsch 1983; Van Straaten 1961; Weimer et al. 1982). Sediment accumulation on point bars in tidal creeks is proportional to channel migration; thus, these deposits suffer repeated colonization and erosion. Repeated colonization obscures and distorts primary sedimentary structures. This is apparent at Waterside Marsh, where individual burrows and sedimentary structures are difficult to discern in the silt beds, and the matted-organic laminae are typically discontinuous and distorted by burrowing (Fig. 2.5A, B). The small, U-shaped structures commonly observed in Facies 6 represent small drainage channels that dissect the point-bar deposit. Similarly shaped structures were reported by van Straaten as channel-fill sediments at Veslen, The Netherlands (Weimer et al. 1982) and were considered common features of tidal-flat and tidal-channel sequences. Gravel layers encountered in F6 are deposited when storm-swash currents deposit coarse clastic material on the point bar. Rooting is not apparent, which is likely the result of the location of the facies at the base of the tidal creeks. Allen (2000) explains that halophytes are normally not encountered below the neap-tide high-water level. The point bars at Waterside Marsh are significantly below the neap high-water level, and thus are not likely to be colonized by halophytes (Figs. 2.5D, 2.6).

Facies 7 (F7)

Facies 7 comprises reddish-brown to dark-gray, bioturbated clayey silt. It is not observed in outcrop and is a minor depositional facies in Waterside Marsh. The average grain size is 6.0 μm (S 4%, Z 64%, C 32%) with 4.7% organic carbon. The grain size and sand content increases towards the main tidal channels and towards the seaward limit of the marsh. Pebble and shell lags and matted-organic laminae are commonly observed in

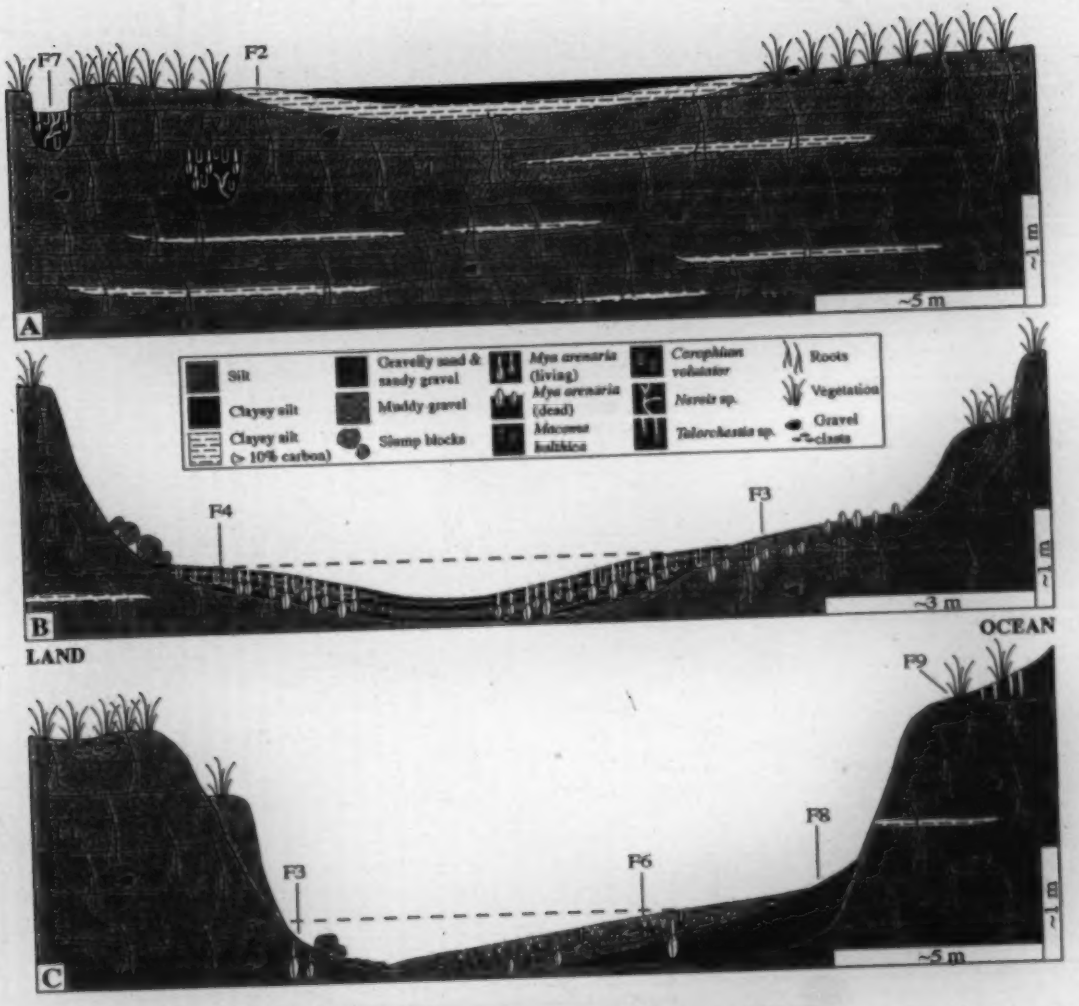

FIGURE 2.6 – Schematic diagrams depicting facies inter-relationships. A) Non-oriented profile through the salt marsh centering on a panne. B) Creek-normal section illustrating sediment deposition via channel aggradation. C) Shore-normal section through a tidal-creek point bar. Facies are indicated by (F#). The dashed line in B and C indicates the upper erosional boundary of sediments exposed in the foreshore of Waterside Beach.

this facies. Surface mud is soupy, but cohesiveness increases with depth. Rooting is not apparent. Bioturbation is common, with intense numbers of *Mya arenaria* and *Corophium volutator* burrows and low numbers of *Nereis* burrows.

Facies 7 represents sediments deposited in naturally formed, low-order tidal channels that dissect the marsh surface. The low-order creeks are a minor component of

the marsh and are inundated during every high tide. The incoming tide is relatively low-energy, resulting in the deposition and accumulation of microscopic organic material, fine silt, and clay. Consequently, these channels are ideal locations for colonization by sedentary organisms such as *M. arenaria* and motile but small organisms like *C. volutator*. Matted-organic beds form via trapping of organic detritus in pools at the bases of the creeks. Shell lags are deposited in a similar manner, whereas pebble lags are likely sourced from the melting of trapped ice blocks.

Facies Association 3: Beach-Related Deposits

Facies Association 3 (FA3) encompasses most beach-derived sediment. Coarse-grained material is deposited in the salt marsh as washover fans, storm-driven tidal-creek fill, and landward-migrating gravel bars. Identification of FA3 deposits is important in paleo-environmental reconstruction, especially as a beach proximity indicator. Waves and wave-generated currents rarely transport coarse clastic material more than 100 to 150 m inland; therefore, the presence of coarse clastic material in a salt-marsh succession is a good indicator of the adjacent beach. FA3 is composed of two recognized facies. Facies 8 represents sand and gravel beds deposited in the tidal channels and Facies 9 embodies sand and gravel deposited on the salt-marsh surface (Table 2.2).

Facies 8 (F8)

Facies 8 is defined by steeply dipping sand and gravel beds. These beds observed in outcrop typically dip landward at angles between 9° and 13° and a maximum angle of 20°. The predominant grain sizes are coarse-grained sand to small pebbles reflecting the palimpsest beach sediment. Grain-size composition changes rapidly in the landward direction from dominantly sand and gravel, to sandy, silty gravel, and finally gravelly, sandy silt. Facies 8 is devoid of bioturbation and rooting.

The steeply dipping sand and gravel beds of F8 are attributed mainly to storm-driven sedimentation in the tidal creeks (Fig. 2.6). During storms, large waves occasionally breach the narrow backshore dune complex and transport suspended sediment and traction-load coarse-grained sediment into the salt marsh. Where the sediment-laden swash encounters a tidal creek, rapid deposition forms steeply landward-dipping sand and gravel beds.

Facies 9 (F9)

Facies 9 is defined by nearly horizontal, parallel-laminated sand and gravel. These deposits occur on the present-day marsh surface, and as interbeds in vertical successions within Waterside Marsh. Facies 9 is subdivided into two related but sedimentologically distinct subfacies: 9A and 9B. Facies 9A is dominated by medium- and coarse-grained sand with minor gravel. It is deposited as relatively flat, lobate prisms of sediment on top of the salt marsh. Directly behind the narrow dune complex the sediment prism may exceed 2 m in thickness, but it pinches out within 50 to 70 m in the landward direction. A typical measurement of F9A indicates that the prism extends 63 m into the salt marsh with a depositional slope that decreases in the landward direction from 14.8° in the first 3.4 m to a relatively flat 0.71° over the main part of the lobe. Facies 9B is composed of very coarse sand to small pebbles (4-8 mm) deposited as a flat (less than 0.30°), sheet-like unit that extends between 80 and 100 m into the salt marsh. Facies 9B is usually deposited where the backshore dune is washed out or where the dune crest is significantly below the average dune-crest height. Bioturbation is rare in F9A and very rare in F9B. Where vegetation is low to moderate, rare burrowing by talitrid amphipods (Figs. 2.2, 2.6) is observed in F9A. In the sand-dominated fringe of F9B, very rare burrowing by talitrids is observed. Rooting is low to moderate over much of F9A and low to rare in F9B.

Facies 9A and 9B represent washover-fan deposits. These sediments are deposited on the salt-marsh surface when storm-driven sediment-laden swash breaches the backshore dune complex. In the transgressive Waterside Beach-Marsh system, storm processes have resulted in the coalescence of washover fans into a washover terrace that extends the full length of the beach (Fig. 2.1C).

DISCUSSION

Stratigraphy of Waterside Marsh

The facies identified at Waterside Marsh are representative of mineralogenic salt-marsh sediments deposited in a mature marsh during a stage of relative sea level rise. The facies associations identified correspond to three distinct sedimentary environments. Facies Association 1 encompasses sediment that accumulates or accumulated on the primary depositional surface of the marsh. FA2 includes deposits that form within the tidal creeks, and FA3 describes sediment that is sourced from the adjacent, coarse-grained beach. The interaction of processes and sediments from these three environments controls the facies architecture and stratigraphy of Waterside Marsh deposits.

Figure 2.6 schematically illustrates the horizontal and vertical relationship of the depositional environments and their associated facies. Scales are provided as approximations because the dimensions of the depositional environments vary with distance away from the seaward edge of the marsh and with time. In Figure 2.6A, the relationship of Facies 1, 2, and 7 are depicted. Both F1 and F2 are deposited on the salt-marsh surface. The interaction of these facies is laterally and vertically complex and changes as the salt marsh matures. Redfield (1972) delineates five stages in the evolution of a sand flat to a fully mature marsh. In particular, the marsh passes through a stage dominated by pannes (F2), which decrease in abundance during maturation (Redfield 1972). It is suggested that the frequency and thickness of Facies 2 deposits increases with depth, reflecting the earlier stages of marsh development. A shallow channel cutting

across the marsh surface and an infilled channel preserved in the vertical sequence represent Facies 7 (Fig. 2.6A). Studies concentrating on the stratigraphy of marshes in Europe indicate that during the early stages of sea-level rise and establishment of a mineralogenic marsh, low-order creeks are abundant and increase in density and depth with marsh accretion (French 1993; Pye and French 1993). As the marsh matures, the low-order creeks infill with silt (Allen 1997) and tidal energy is increasingly concentrated in the main tidal creeks. At Waterside Marsh, the early stages of marsh development were not evident in the exposed deposits; however, because this is a mature marsh in a transgressive system, it is assumed that low-order tidal channels (F7) are more abundant in the historical record than at present.

Tidal-creek facies relationships are illustrated in Figures 2.6B and 2.6C. In Figure 2.6B, the accumulation of sediment at the base of the tidal creek occurs in response to increased sedimentation rates and potentially RSL rise (i.e., base-level rise). Base-level rise results in the deposition and aggradation of sediments at the bases of the tidal creeks (F4). With time, the creeks expand and Facies 1 and 2 deposits are exposed along the channel walls and base. Those deposits exposed at the bases of the creeks are then colonized by *M. arenaria* and *C. volutator* (F3), thereby generating a *Glossifungites* ichnofacies (Bromley 1990; Gingras et al. 2001; Pemberton et al. 2001). It is important to note that this ichnofacies develops in response to autocyclic processes and is not regionally mappable.

Figure 2.6C illustrates the facies relationships in a tidal-creek point bar near the seaward edge of the marsh. In the salt marsh, point bars migrate very slowly because cutbanks erode into cohesive sediment stabilized by vegetation. Normally, this erosion is contemporaneous with establishment of low-marsh deposits on the inner edge of the point bar (Fig. 2.5D); however, Figure 2.6C depicts a point bar in the zone of storm-wave

swash that is sporadically inundated with beach-derived sediment (F8). This inhibits revegetation of the inner point bar. Facies 9, the washover fan, accumulates on the salt-marsh surface seaward of channel-bound F8 deposits.

Application to the Rock Record

Facies and facies associations defined from the Waterside Beach outcrops and from Waterside Marsh are applicable to mineralogenic salt-marsh deposits preserved in the rock record. The application of these results is dependent upon the preservation potential of the facies, which varies as a function of elevation in the vertical marsh succession, distance from the seaward edge of the marsh, RSL rise, and headland erosion rate. Salt-marsh deposits exposed in the foreshore of Waterside Beach are not likely to pass into the rock record. The upper 4 or 5 m of presently accreting marsh deposits located in close proximity to the beach will be eroded as transgression results in the landward shifting of facies and the erosion of the backshore (Reading and Collinson 1996; Roy et al. 1994). Conversely, sediments below 5 m depth in a salt-marsh sequence will be armored by sediment aggradation in the offshore (Reading and Collinson 1996; Roy et al. 1994), and therefore have a greater probability of preservation. In the landward direction, the preservation potential of recently deposited sediment increases because of accretion on the marsh surface and thickening of the vertical sequence. Consequently, the facies with the highest preservation potential, and thus the most applicable to the rock record, are those deposited either in topographic lows or well landward of the seaward edge of the marsh. On this basis, the facies can be ranked in terms of preservability as follows: F1, F2, F7, F3, F4, F6, F5, F8, and F9 (Table 2.2). Facies 1 and 2 are the most widely occurring deposits and have the greatest preservation potential. Facies 7 deposits extend deep into the marsh and also have a good chance of preservation. Tidal-creek facies – 3, 4, and 6 – are likely to be preserved because of their location at the bases of the channels. Facies 8 and 5 are considered to be anomalous and will not occur in most

marsh sequences. Facies 9 is deposited on the marsh surface in close proximity to the seaward edge and will generally be removed by subsequent transgression.

Application of these facies and facies associations to the rock record requires recognition of the sedimentological and ichnological characteristics and architecture (Fig. 2.6) of the overall deposit. In general, rooted, unbioturbated, rhythmically laminated silt observed in the rock record is akin to Facies 1 of this study and probably accumulated on the salt-marsh surface. Unbioturbated, very weakly laminated, organic-rich clayey silts (Fig. 2.3C) interbedded with F1 sediments represent the pannes (F2) that occur intermittently on the marsh surface. If rooted, rhythmic, horizontally laminated silt exhibits bioturbation – particularly with *Skolithos*, *Siphonichnus, Arenicolites*, and / or *Diplocraterion* – then the surface from which these traces originate was an erosionally exhumed *Glossifungites* surface (F3, Fig. 2.3D). If the surface is overlain by shallowly dipping, interbedded clayey silt and muddy gravel (F4, Fig. 2.4A) or by shallowly dipping interbedded silt and matted-organic laminae (F6, Fig. 2.6A), then it likely developed in response to autocyclic, tidal-creek processes. Rock-record examples of Facies 4 and 6 can be identified by their sedimentary structures, such as rhythmic bedding, and by their ichnological character. *Skolithos*, *Siphonichnus*, and *Arenicolites* may be observed between gravel clasts and in interbedded mud beds of vertical F4 successions. Rhythmic, dipping beds of silt and matted-organic laminae sets, and high degrees of bioturbation with *Arenicolites* (Fig. 2.5C), *Diplocraterion*, *Siphonichnus*, and *Skolithos* are diagnostic of Facies 6 (Table 2.2). Intensely bioturbated, laminated clayey silts that exhibit a gradational upper contact with either F1 or F3 is possibly similar to Facies 7 deposits of this study. Continuous beds of sand and gravel in a salt-marsh succession may be similar to Facies 8 or 9 and do not necessarily indicate a major change in depositional environment. These deposits, however, are proximity indicators of coarse-grained beach deposits.

The stratigraphic character of salt-marsh deposits varies as a function of climate, hydraulic conditions, and the morphology of the coastal system. Climate exerts a large influence on salt-marsh stratigraphy; thus, observations of temperate marshes cannot be directly applied to salt-marsh deposits globally. In Georgia, U.S.A., marshes, for example, decapods burrowing in tidal-creek banks is cited as a major form of bank erosion (Letzsch and Frey 1980). Conversely, randomly scattered ice-derived gravel clasts are not likely to be observed. Hydraulic conditions (influenced by tidal range and proximity to shore) also strongly influence sedimentation patterns (Allen 2000; Bayliss-Smith et al. 1979; Davidson-Arnott et al. 2002) and contribute to tidal-creek expansion (Pestrong 1965). Hydraulic processes are partly controlled by the morphology of the deposit (Pye and French 1993), which in turn determines whether a marsh is expanding, such as the Barnstable Marsh in Massachusetts, U.S.A. (Redfield 1972) or eroding, as in the case of Waterside Marsh. The location of a salt marsh relative to other marginal-marine environments not only influences the morphology of the deposit (Pye and French 1993) but also controls the extent and grain size of beach-derived sediment deposited in the salt marsh. Salt marshes landward of mud flats do not develop muddy-gravel deposits at the bases of their tidal creeks. Similarly, salt marshes landward of sand beaches likely exhibit an increased sand content in all salt-marsh facies, particularly in the creek facies.

Salt-marsh successions in the rock record are not present prior to the evolution of grasses. Although the first pollen grains of grasses are reported from the Maastrichtian, these plants were not dominant until the Paleocene (Kellogg 2000). Consequently, the earliest salt marshes probably date back to the early Cenozoic and not before.

CONCLUSIONS

The sedimentological and ichnological characteristics of salt-marsh facies vary with changes in RSL, climate, hydraulic conditions, and associated marginal-marine environments. However, the general facies relationships and architecture do not vary

significantly between marshes. Modern and exposed historical deposits at Waterside Beach and in Waterside Marsh provide an opportunity to describe and define salt-marsh facies and facies associations in a temperate, mineralogenic salt marsh.

Three facies associations are identified: (1) salt-marsh deposits, (2) tidal-creek deposits, and (3) beach-related deposits. These represent the three main components of the Waterside Marsh depositional system. The facies associations are subdivided into nine facies, of which six (Facies 1, 2, 3, 4, 6, and 7) have a high preservation potential and are applicable to rock-record successions. In general, sediments that accumulate far landward of the seaward edge of the marsh or at the bases of the tidal creeks have a high probability of being preserved.

In a vertical salt-marsh succession preserved in the rock record, the six facies likely to be encountered can be identified by their sedimentological and ichnological character and by their relationship to other facies. Facies 1 and 2 occur together in the marsh and are interbedded. Low-order tidal creeks that dissect the marsh surface are manifested in preserved sediment as thin and narrow Facies 7 deposits and can be identified by an upper gradational contact with either F1 or F2 sediments. Facies 3, 4, and 6 represent deposition in the main tidal creek. Facies 3 commonly defines the basal contact of the tidal creeks and is overlain by either F4 or F6 deposits. The beach-derived deposits of FA3 are not likely to be preserved in a transgressive system because of their proximity to the beach and their location near the top of the salt-marsh surface. If either Facies 8 or 9 is observed, then it is an excellent indicator of an adjacent beach environment.

REFERENCES

Allen, J.R.L., 1990, Salt-marsh growth and stratification: A numerical model with special reference to the Severn Estuary, southwest Britain: Marine Geology, v. 95, p. 77-96.

Allen, J.R.L., 1997, Simulation models of salt-marsh morphodynamics: some implications for high-intertidal sediment couplets related to sea level change: Sedimentary Geology, v. 113, p. 211-223.

Allen, J.R.L., 2000, Morphodynamics of Holocene salt marshes: a review sketch from the Atlantic and Southern North Sea coasts of Europe: Quaternary Science Reviews, v. 19, p. 1155-1231.

Amos, C.L., Tee, K.T., and Zaitlin, B.A., 1991, The post-glacial evolution of Chignecto Bay, Bay of Fundy, and its modern environment of deposition, *in* Smith, D.G., Reinson, G.E., Zaitlin, B.A., and Rahmani, R.A., eds., Clastic Tidal Sedimentology: Calgary, AB, Canada, Canadian Society of Petroleum Geologists, p. 59-89.

Anderson, R.S., and Race, C.D., 1980, Investigation of salt marsh stratigraphy as an indicator of sea level rise in coastal Maine: Maine Geological Survey, Open File 80-1, 11 p.

Basan, P.B., and Frey, R.W., 1977, Actual-palaeontology and neoichnology of salt marshes near Sapelo Island, Georgia, *in* Crimes, T.P., and Harper, J.C., eds., Trace Fossils 2: Geological Journal Special Issue No. 9, p. 41-70.

Bayliss-Smith, T.P., Healey, R., Lailey, R., Spencer, T., and Stoddart, D.R., 1979, Tidal flow in salt marsh creeks: Estuarine, Coastal and Marine Science, v. 9, p. 235-255.

Bouma, A.H., 1969, Methods for the Study of Sedimentary Structures: New York, John Wiley & Sons, 458 p.

Bromley, R.G., 1990, Trace Fossils; Biology and Taphonomy: London, Unwin Hyman, 280 p.

Christiansen, T., Wiberg, P.L., and Milligan, T.G., 2000, Flow and sediment transport on a tidal marsh surface: Estuarine, Coastal and Shelf Science, v. 50, p. 315-331.

Davidson-Arnott, R.G.D., Van Proosdij, D., Ollerhead, J., and Schostak, L., 2002, Hydrodynamics and sedimentation in salt marshes: examples from a macrotidal marsh, Bay of Fundy: Geomorphology, v. 48, p. 209-231.

Desplanque, C., and Mossman, D.J., 1998, A review of ice and tide observations in the Bay of Fundy: Atlantic Geology, v. 34, p. 195-209.

Edwards, J.M., and Frey, R.W., 1977, Substrate characteristics within a Holocene salt marsh, Sapelo Island, Georgia: Senckenbergiana Maritima, v. 9, p. 215-259.

Evans, G., 1965, Intertidal flat sediments and their environments of deposition in the Wash: Geological Society of London Quarterly Journal, v. 121, p. 209-241.

French, J.R., 1993, Numerical simulation of vertical marsh growth and adjustment to accelerated sea-level rise, north Norfolk, U.K.: Earth Surface Processes and Landforms, v. 18, p. 63-81.

French, J.R., and Stoddart, D.R., 1992, Hydrodynamics of salt marsh creek systems: implications for marsh morphological development and material exchange: Earth Surface Processes and Landforms, v. 17, p. 235-252.

Gingras, M.K., Pemberton, S.G., and Saunders, T., 2001, Bathymetry, sediment texture, and substrate cohesiveness; their impact on modern *Glossifungites* trace assemblages at Willapa Bay, Washington: Palaeogeography, Palaeoclimatology, Palaeoecology, v. 169, p. 1-21.

Gosner, K.L., 1978, Atlantic Seashore: A Field Guide to Sponges, Jellyfish, Sea urchins, and More: Peterson Field Guides: New York, Houghton Mifflin Company, 329 p.

Heiri, O., Lotter, A.F., and Lemcke, G., 2001, Loss on ignition as a method for estimating organic and carbonate content in sediments: reproducibility and comparability of results: Journal of Paleolimnology, v. 25, p. 101-110.

Kellogg, E.A., 2000, The grasses: A case study in macroevolution: Annual Review of Ecology and Systematics, v. 31, p. 217-238.

Letzsch, W.S., 1983, Seven year's measurement of deposition and erosion, Holocene salt marsh, Sapelo Island, Georgia: Senckenbergiana Maritima, v. 15, p. 157-165.

Letzsch, W.S., and Frey, R.W., 1980, Erosion of salt marsh tidal creek banks, Sapelo Island, Georgia: Senckenbergiana Maritima, v. 12, p. 201-212.

Mckeague, J.A., 1978, Manual on Soil Sampling and Methods of Analysis, Canadian Society of Soil Science, 212 p.

Nyman, J.A., Delaune, R.D., Roberts, H.H., and Patrick, W.H.J., 1993, Relationship between vegetation and soil formation in a rapidly submerging coastal salt marsh: Marine Ecology Progress Series, v. 96, p. 269-279.

Pemberton, S.G., Spila, M., Pulham, A.J., Saunders, T., Maceachern, J.A., Robbins, D., and Sinclair, I.K., 2001, Ichnology and Sedimentology of Shallow to Marginal Marine Systems: Ben Nevis and Avalon Reservoirs, Jeanne d'Arc Basin: Geological Association of Canada Short Course, v. 15: St. John's, Geological Association of Canada, 343 p.

Pestrong, R., 1965, The development of drainage patterns in tidal marshes: Stanford University Publications in Earth Science, v. 10, p. 1-87.

Pethnick, J.S., 1992, Saltmarsh geomorphology, *in* Allen, J.R.L., and Pye, K., eds., Saltmarshes: Morphodynamics, Conservation and Engineering Significance: Cambridge, U.K., Cambridge University Press, p. 41-62.

Pye, K., and French, P.W., 1993, Erosion and acretion processes on British Salt Marshes, Vol. 1, Introduction: Saltmarsh Processes and Morphology: Cambridge, U.K., Cambridge Environmental Research Consultants.

Reading, H.G., and Collinson, J.D., 1996, Clastic Coasts, *in* Reading, H.G., ed., Sedimentary Environments; Processes, Facies and Stratigraphy: Oxford, U.K., Blackwell Science, p. 154-231.

Redfield, A.C., 1972, Development of a New England Salt Marsh: Ecological Monographs, v. 42, p. 201-237.

Roy, P.S., Cowell, P.J., Ferland, M.A., and Thom, B.G., 1994, Wave-dominated coasts, *in* Carter, R.W.G., and Woodroffe, C.D., eds., Coastal Evolution: Late Quaternary Shoreline Morphodynamics: Cambridge, U.K., Cambridge University Press, p. 121-186.

Shaw, J., and Courtney, R.C., 2002, Postglacial coastlines of Atlantic Canada: digital images: Geological Survey of Canada Open File #4302.

Shepard, F.P., 1954, Nomenclature based on sand-silt-clay ratios: Journal of Sedimentary Petrology, v. 24, p. 151-158.

Snelgrove, P.V.R., Grant, J., and Pilditch, C.A., 1999, Habitat selection and adult-larvae interactions in settling larvae of soft-shell clam *Mya arenaria*: Marine Ecology Progress Series, v. 182, p. 149-159.

Thurston, H., 1990, Tidal Life; A Natural History of the Bay of Fundy: Halifax, Nimbus Publishing, 167 p.

Van Straaten, L.M.J.U., 1954, Composition and structure of recent marine sediments in the Netherlands: Leidse Geologische Mededelingen, v. 19, p. 1-110.

Van Straaten, L.M.J.U., 1961, Sedimentation in tidal flat areas: Journal of the Alberta Society of Petroleum Geologists, v. 9, p. 203-213, 216-226.

Weimer, R.J., Howard, J.D., and Lindsay, D.R., 1982, Tidal flats and associated tidal channels, *in* Scholle, P.A., and Spearing, D., eds., Sandstone Depositional Environments: Tulsa, U.S.A., American Association of Petroleum Geologists, p. 191-245.

CHAPTER 3: THE TEMPORAL SIGNIFICANCE OF BIOTURBATION IN BACKSHORE DEPOSITS: WATERSIDE BEACH, NEW BRUNSWICK, CANADA[2]

INTRODUCTION

This paper provides an estimate of the temporal significance and environmental implications of bioturbation in modern upper foreshore and backshore deposits resulting from the burrowing activity of Talitrid amphipods. Short-term preservation potential is assessed by comparing shore-normal variations in burrow morphologies and densities to grain-size distribution, hydraulic, and eolian processes. Application of results to ancient upper foreshore and backshore deposits is discussed in terms of: (1) paleoenvironmental implication; and, (2) the temporal nature of bioturbation indices in these environments.

Degree of Bioturbation

The degree of bioturbation provides a means to compare ichnofabrics between facies (Bottjer and Droser 1991; Droser and Bottjer 1993) and is considered an important tool in facies analysis. A semi-quantitative assessment of bioturbation intensity was first proposed by Reineck (1963) to describe the destruction of primary bedding by burrowing (Reineck and Singh 1980). Utilizing Reineck's classification scheme, Taylor and Goldring (1993) proposed a non-linear bioturbation index (BI), in which they defined: BI 1 (1-5%) as sparse bioturbation with a few discrete traces, BI 2 (6-30%) by distinct bedding and low trace diversity, BI 3 (31-60%) as sharp bedding boundaries and distinct traces, and BI 4 (61-90%) by indistinct bedding boundaries and high trace diversity with common overlap. These categories are defined from ancient sedimentary deposits and have not been quantified temporally from modern settings. By quantifying the degree of

[2]A version of this paper is published in PALAIOS, 2005, v. 20, p. 589-595 as "The temporal significance of bioturbation in backshore deposits: Waterside Beach, New Brunswick, Canada" by Shahin E. Dashtgard and Murray K. Gingras

bioturbation, bioturbation indices could feasibly be used to estimate depositional rates and processes, and thus aid in paleoenvironmental reconstructions.

Talitrid Distribution

Talitrid amphipods, commonly known as sand hoppers, inhabit the backshore of sandy beaches (Fig. 3.1). During the day, they sleep under seaweed or in shallow (up to 25 cm deep) burrows excavated in sand above the high-tide line. At night, during the low tide, they exit their burrows to forage on algae, seaweed, and diatoms washed up by the surf (Fallaci et al. 1999; Pank 2003). With the coming dawn, sand hoppers either re-occupy an existing burrow (often deepening it) or excavate a new one.

Burrowing by Talitrid amphipods is common in the backshore of modern beaches (Basan and Frey 1977; Colombini et al. 2002; Fallaci et al. 1999; Frey et al. 1989; Howard and Frey 1975; Vader 1970; Weslawski et al. 2000) and has also been described from the rock record (Clifton 1981). Howard and Frey (1975) and Basan and Frey (1977) report Talitrid amphipod burrowing in backshore environments of Georgia, U.S.A. estuaries and beaches. Similarly, the uneven distribution of Talitrid amphipods on beaches in Europe and northern Africa is well documented (Colombini et al. 2002; Fallaci et al.

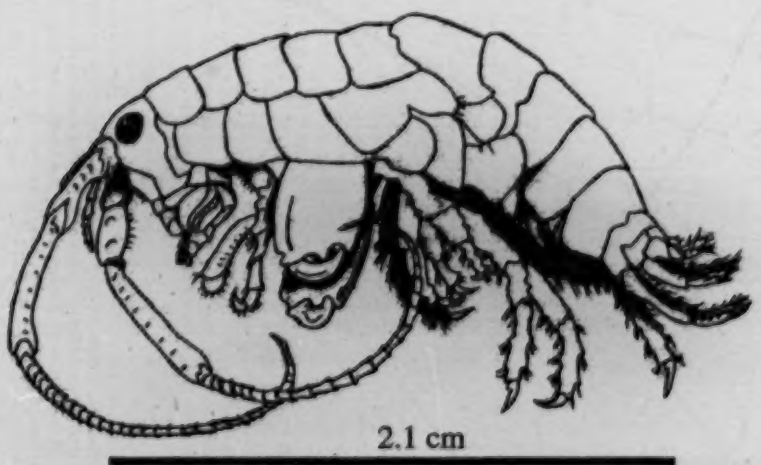

FIGURE 3.1 – Sketch of *Talorchestia longicornis* (by T. Hauck).

1999; Weslawski et al. 2000). Ancient examples of these burrows is limited; although, Clifton (1981) observed them in upper foreshore and backshore units of progradational Miocene shoreline deposits in California, U.S.A.

Talorchestia longicornis is the dominant amphipod in the upper foreshore and backshore of Waterside Beach. Moreover, the distribution of adult *T. longicornis* there is qualitatively similar to Talitrid populations on beaches in Europe, northwest Africa, and the southeast U.S.A. (Basan and Frey 1977; Colombini et al. 2002; Fallaci et al. 1999; Howard and Frey 1975; Vader 1970; Weslawski et al. 2000).

Study Area

Waterside Beach is situated on the north shore of the Bay of Fundy, near Fundy National Park (Fig. 3.2). Oriented northwest-southeast, the beach is approximately 4 km long and has a mean tidal range of 9 m. Tide heights range from 6 m during neap tides to 12 m during spring tides. At spring high tide, the high-water level extends to the base of the backshore dune. During neap tides, the high-water level is 40 m seaward of spring high water; thus, a 40 m-wide zone is present that is alternately dominated by upper foreshore (wave) and backshore (eolian) processes.

Waterside Beach is a wave-dominated beach in the macrotidal Bay of Fundy. It is a mixed sand and gravel system with beach-normal and beach-parallel heterogeneous grain-size partitioning. In general, the northwest half of the beach is sandy while the southeast end is gravel-rich. This study was conducted in the sandy northwest end of the beach (Fig. 3.2).

Methods

Three beach-normal transects, spaced 250 m apart, document the beach slope and distribution of sediment grain size, structure, and bioturbation. Transects, averaging 42 m in length, began at the top of the vegetated dune and extended slightly past the high-water

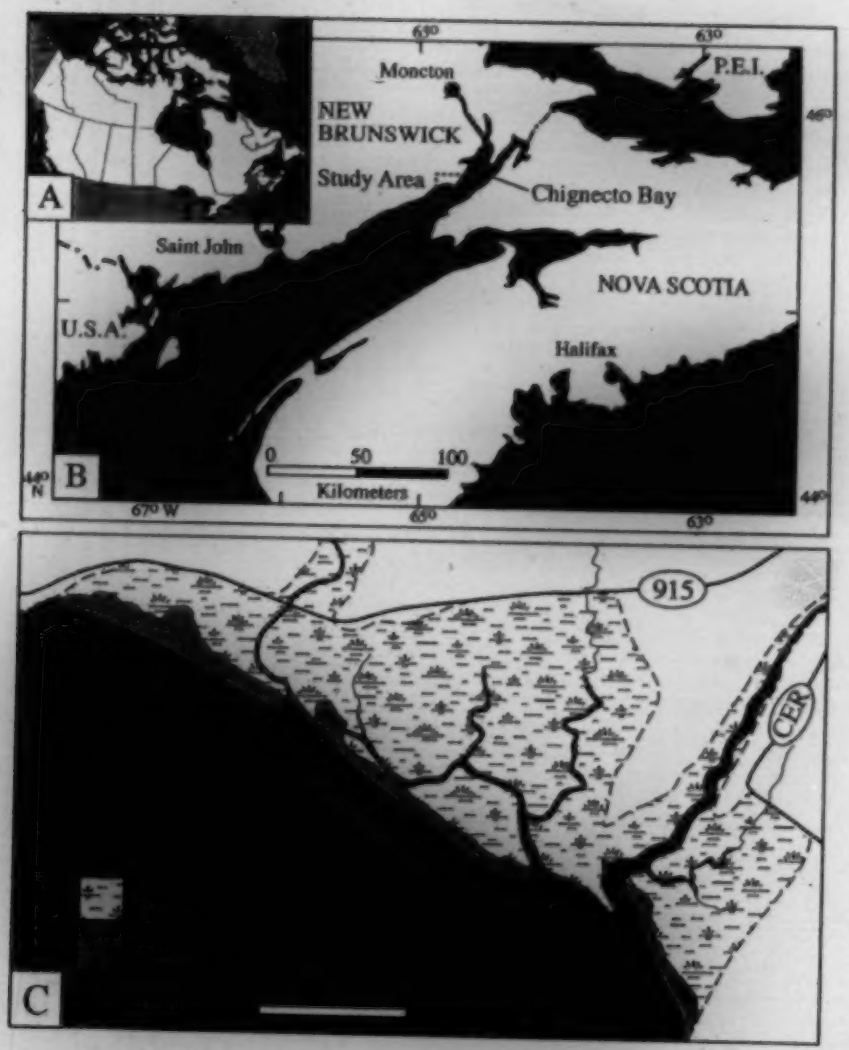

FIGURE 3.2 – Map of the study area. (A) Location of the Bay of Fundy in Canada. (B) Position of study area in the Bay of Fundy. (C) Close-up of Waterside Beach. Positions of transects indicated (1, 2, and 3). (CER = Cape Enrage Road)

mark (Fig. 3.3). Transects were subdivided into zones based on the approximation of spring, average, and neap high-tide levels (Fig. 3.3). Zone 1 extends from the dune top to the spring tide high-water level (SHWL) locally demarcated by the most landward band of seaweed and stranded disc-shaped clasts. Zone 2 extends from the SHWL to the mean high-water level (MHWL), and zone 3 from the MHWL to the neap tide high-water level

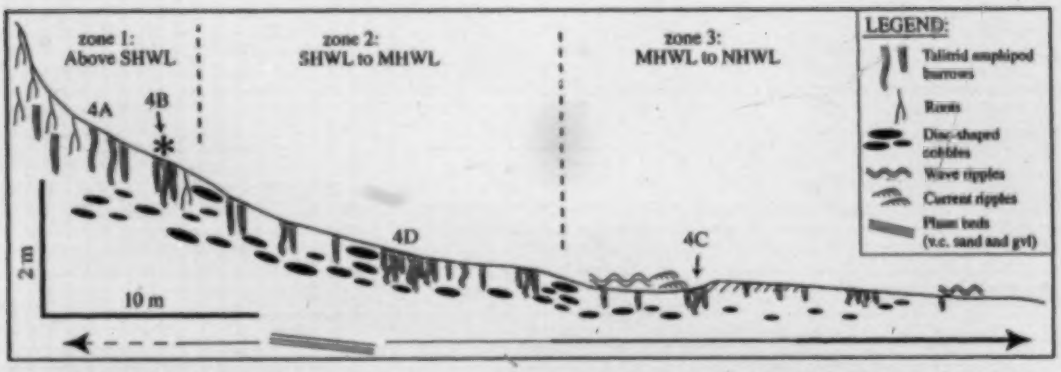

FIGURE 3.3 – Schematic summary of the zonation along a beach-normal profile. Locations 4A-D indicate location of photos in Figure 3.4. (* refers to the beach-normal location of aquaria). SHWL = spring-tide high-water level; MHWL = mean high-water level; and, NHWL = neap-tide high-water level.

(NHWL). Burrow-density counts were conducted by zone to evaluate the shore-normal distribution of burrows (Table 3.1).

Burrow densities were determined at 24 stations along the three transects. Burrow-depth measurements were taken from trenches excavated at seven stations, of which, four stations were chosen for burrow-aperture measurements. Six population counts of amphipods greater than 3 mm in length were conducted (two per zone). Burrows with aperture diameters below 2 mm and juvenile amphipods (< 3 mm long) were not included in counts as they were both related to biogenic structures with negligible preservation potential. At eleven stations, the sediment was sieved and amphipods collected for species identification. Over 200 specimens were collected and identified by comparing to descriptions and sketches of Gammaridean amphipods in Bousfield (1973).

Zone	Avg. burrow density (burrows/m^2)	Max. burrow density (burrows/m^2)	Avg. burrow height (cm)	Avg. burrow apeture diameter (cm)	Biogenic-reworking rate %/day	Days required to exceed BI thresholds			
						BI 1 (1%) (days)	BI 2 (6%) (days)	BI 3 (31%) (days)	BI 4 (61%) (days)
1	142.1	241	17.7	0.59	0.038	26	157	811	1595
2	285.8	1183	11.4	0.56	0.126	8	48	248	488
3	312	1100	~3	0.47	0.54	2	11	58	113

TABLE 3.1 – Distribution and dimensions of Talitrid burrows and days needed to exceed bioturbation index thresholds.

Zone	granule %	v.c. sand %	c. sand %	m. sand %	f. sand %
1	0	1	25	71	3
2	9	4	7	74	6
3	15	7	22	54	2

TABLE 3.2 – Grain-size distribution (1 phi-size increments).

In the backshore of transect one, five aquaria were buried (Fig. 3.3). Aquaria were 25 cm long, 0.9 cm wide, and 25 cm deep, and filled with either granules, very coarse-, coarse-, medium-, or fine-grained sand. These grain sizes reflect the most common grain sizes found in the upper 25 cm of upper foreshore and backshore deposits (Table 3.2). In order to reconstruct natural conditions and eliminate burrowing bias based on aquaria exposure, all five aquaria were covered by 2 to 3 cm of the surrounding dry sand.

Burrowing rates measured in the medium-sand aquarium were used to estimate burrow-deepening rates. The average initial burrow depth (after 1 day) was ~5 cm versus 13.3 cm after 7 days. Therefore, the average burrow was deepened at (13.3 – 5)/(7-1) = 1.38 cm/day. This value was then used to calculate the number of days (X) needed to excavate an average burrow in each shore-normal zone:

$$X = \left[\frac{(h-5)}{1.38}\right] + 1$$

Where *h* is the average burrow height (Table 3.1). Assuming cylindrical burrow morphology, burrow volume and X are used to calculate biogenic-reworking rates (BRR):

$$BRR = \frac{\pi \cdot r^2 \cdot B_D}{100 \cdot X}$$

Where B_D is the average burrow density and r is one half the average burrow-aperture diameter (Table 3.1). Biogenic-reworking rates are expressed as a percentage (of total sediment volume) per day. Finally, it is possible to calculate the number of days (Y) required for cumulative bioturbation to exceed bioturbation-index thresholds (BI_T) using the BRR:

$$Y = \frac{BI_T}{BRR}$$

Bioturbation-index thresholds are the minimum percentages of bioturbation indices – i.e., BI 1 (1%), BI 2 (6%), BI 3 (31%), BI 4 (61%).

Calculating the biogenic-reworking rate and Y require making three assumptions. These are:

(1) The study area is a closed system, where the Talitrid population neither increases nor decreases significantly over the course of the study.

(2) Shore-parallel migration of the Talitrid population was negligible during the study.

(3) The burrow deepening rates measured in the medium-sand aquarium are representative of the Talitrid population.

The first assumption is reasonable as the upper foreshore and backshore zones at the northwest end of Waterside Beach are isolated by cliffs to the northwest and a wide tidal creek to the southeast (Fig. 3.2). Similarly, migration between the small, sporadically distributed communities of the washover fan and the beach community is unlikely to significantly increase or decrease the beach population. The second assumption at first glance appears to introduce significant error as Talitrid populations have been shown to migrate in both a beach-parallel and beach-normal direction between seasons (Colombini et al. 2002; Weslawski et al. 2000) and over the course of a tidal cycle (Fallaci et al. 1999). In this study, the three transects were spaced across the center of the 1100 m long beach and are considered representative of at least the central 750 m (Fig. 3.2). Any shore-parallel migration would likely be accounted for by averaging measurements from the three transects. Moreover, the measurements for this study were taken over a nine-day period during a neap- to mean-tide cycle. As a result the Talitrid population was distributed across the upper foreshore and backshore. This suggests

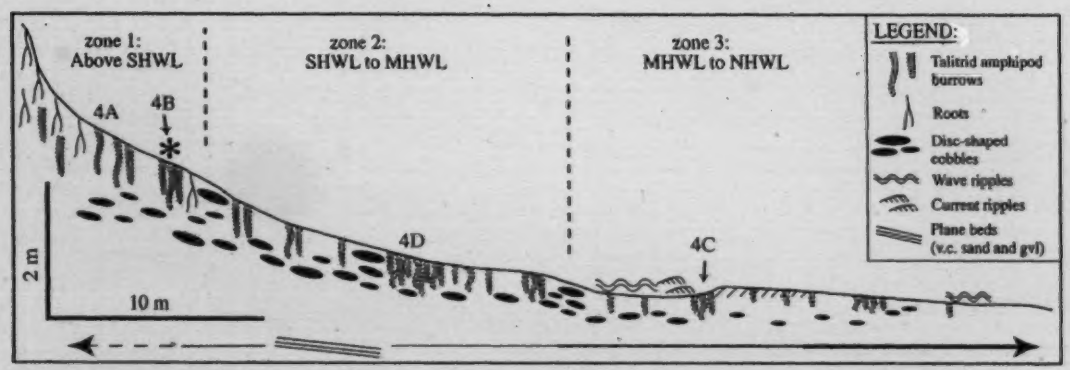

FIGURE 3.3 – Schematic summary of the zonation along a beach-normal profile. Locations 4A-D indicate location of photos in Figure 3.4. (* refers to the beach-normal location of aquaria). SHWL = spring-tide high-water level; MHWL = mean high-water level; and, NHWL = neap-tide high-water level.

(NHWL). Burrow-density counts were conducted by zone to evaluate the shore-normal distribution of burrows (Table 3.1).

Burrow densities were determined at 24 stations along the three transects. Burrow-depth measurements were taken from trenches excavated at seven stations, of which, four stations were chosen for burrow-aperture measurements. Six population counts of amphipods greater than 3 mm in length were conducted (two per zone). Burrows with aperture diameters below 2 mm and juvenile amphipods (< 3 mm long) were not included in counts as they were both related to biogenic structures with negligible preservation potential. At eleven stations, the sediment was sieved and amphipods collected for species identification. Over 200 specimens were collected and identified by comparing to descriptions and sketches of Gammaridean amphipods in Bousfield (1973).

Zone	Avg. burrow density (burrows/m^2)	Max. burrow density (burrows/m^2)	Avg. burrow height (cm)	Avg. burrow apeture diameter (cm)	Biogenic-reworking rate %/day	Days required to exceed BI thresholds			
						BI 1 (1%) (days)	BI 2 (6%) (days)	BI 3 (31%) (days)	BI 4 (61%) (days)
1	142.1	241	17.7	0.59	0.038	26	157	811	1595
2	285.8	1183	11.4	0.56	0.126	8	48	248	488
3	312	1100	~3	0.47	0.54	2	11	58	113

TABLE 3.1 – Distribution and dimensions of Talitrid burrows and days needed to exceed bioturbation index thresholds.

dipping sand plane beds are common on the surface, whereas, very coarse-grained sand and gravel plane beds dominate the vertical stratigraphy. Landward-migrating dunes of steeply dipping sand and gravel beds are also common. Landward of these dunes, temporary, shore-parallel troughs are dominated by wave- and current-rippled sand with abundant disc-shaped cobbles (Fig. 3.3).

Overall, sediment coarsens from the backshore into the upper foreshore (Table 3.2). This trend corresponds to an increasing dominance of very coarse-grained sand- and gravel- plane beds (Fig. 3.3). Plane beds are the dominant sedimentary structure; however, in zones 2 and 3, landward-migrating dunes and troughs are common. Disc-shaped cobbles are prevalent in the upper foreshore and are uncommon in the backshore. Conversely, rooting is restricted to the backshore.

FIGURE 3.4 – Photos of Talitrid amphipod burrows at Waterside Beach. (A) Cross-section of burrows in zone 1. (B) Burrows preserved in the medium-sand aquarium after seven days. (C) High density burrowing in zone 3. (D) Intense burrowing adjacent to a laterally extensive band of seaweed in zone 2.

Bioturbation

Talitrid amphipods at Waterside Beach excavate vertical to slightly inclined, unlined burrows in moist, medium- and coarse-grained sand (Fig. 3.4). Burrows are unlined, but are relatively competent due to the presence of moist sand. Burrows depths average 17.7 cm in the backshore (zone 1) and decrease to about 3 cm near the high-tide mark (zone 3) of the neap tide (Table 3.1). Burrow morphology ranges from simple, vertical to slightly inclined forms to branching and merging forms (Fig. 3.4B). Burrow apertures are asymmetric, although they are treated as symmetric in this study (see methods). Aperture diameters decrease slightly from an average 5.9 mm in the backshore, to 4.7 mm at the neap high-tide level. Consequently, burrow aperture to depth ratios decrease from 30:1 in the backshore to 6:1 at the NHWL. Burrow densities are lowest in zone 1 and increase towards zone 3 (Fig. 3.3). Burrowing was not observed below the NHWL.

The average measured burrow density for zone 1 is 142 burrows/m^2 with an average burrow depth of 17.7 cm (Table 3.1). Population counts indicate there are approximately 300 amphipods/m^2 (~20% small adults) during a normal period of the tidal cycle. Burrowing in zone 1 is highest adjacent to the SHWL and decreases in the landward direction. Using the aquaria-based results for burrow deepening presented above, it requires an average of 10.2 days to excavate a 17.7 cm burrow. Therefore, the biogenic-reworking rate by volume in the upper 17.7 cm is 0.038%/day. Consequently, a minimum 157 days are required to develop a BI 2 or 811 days for a BI 3 (Table 3.1).

Zone 2 has moderate burrow densities of 286 burrows/m^2 with an average burrow depth of 11.4 cm (Table 3.1). Population counts indicate there are approximately 410 amphipods/m^2 (~90% small adults) during a normal period of the tidal cycle. During the neap phase of the tidal cycle, average burrow densities vary from moderate (100 to 300 burrows/m^2) to intense (greater than 600 burrows/m^2). During the spring tide, this zone is submerged at high tide and experiences no burrowing. The BRR in the upper 11.4 cm of

zone 2 is 0.126%/day. Therefore, a minimum 48 days are required to develop a BI 2 and 248 for a BI 3 (Table 3.1).

Burrowing densities are highest in zone 3 averaging 312 burrows/m^2 (Table 3.1) with an approximate burrow depth of 3 cm. Population counts at the landward end of the zone indicate there are approximately 92 amphipods/m^2 (~75% small adults) during a normal period of the tidal cycle. Burrowing occurs during the neap tide. During mean and spring tides no burrowing is observed in this zone. Burrows in zone 3 are shallow and are likely excavated daily. The BRR for the upper 3 cm of zone 3 is 0.54%/day. This suggests only 11 days are needed to develop a BI 2 and 58 days for a BI 3 (Table 3.1).

DISCUSSION

The degree of bioturbation generated in each zone is directly related to the degree of wave reworking and grain size. Wave swash-backwash reworks surface sediment, resulting in the deposition of very coarse-sand and gravel plane beds (Clifton 1981; Clifton et al. 1971; Ethridge and Wescott 1984; Massari and Parea 1988) and destruction of palimpsest biogenic and sedimentary structures occurring at shallow depths. Consequently, decreased exposure to wave action equates to increased short-term preservation potential of burrows. Grain size controls the depth and location of burrowing. Talitrid amphipods preferentially burrow in medium- to coarse-grained sand and avoid burrowing in very coarse-sand and gravel. Therefore, burrow penetration is greater in thick-sand beds uninterrupted by very coarse-sand and gravel plane beds.

Wave reworking increases proportionally to a decrease in eolian depositional processes from zone 1 to 3 (Fig. 3.3). Eolian processes are responsible for the deposition of well-sorted medium-grained sand in the surface sediment of zone 1, whereas, swash-backwash results in deposition of very coarse-grained sand and gravel plane beds and an overall shift towards coarser sediment in zones 2 and 3 (Table 3.2, Fig. 3.3). The increased frequency of gravel plane beds from zone 1 to 3 hinders Talitrid amphipod

burrowing resulting in a significant decrease in burrow depths in the seaward direction (Table 3.1).

Zone 1 deposits are subjected to little or no wave reworking during the summer and are dominated by thick beds of medium-grained sand (Table 3.2). Therefore, burrows penetrate deepest in this zone and have the highest preservation potential of the upper foreshore and proximal backshore. Over the course of a summer season (May to September) it is feasible that 5.8% of the upper 17.7 cm of sediment is reworked generating a BI that straddles the one/two boundary. Higher bioturbation indices would require multiple years of colonization to develop.

Burrow preservation potential decreases rapidly from zone 1 to 2, as do burrow depths (Table 3.1). In a single summer, 19% of the upper 11.4 cm of sediment in zone 2 will be reworked. However, cyclical submergence of the upper foreshore during spring high tides and exposure to wave swash-backwash effectively obliterates the resultant ichnofabric. A BI greater than one would not be expected in zone 2. Similarly, preservation of the ichnofabric generated by Talitrid amphipods in zone 3 is very low. Burrows excavated during neap tides in zone 3 tend to be very shallow (Table 3.1) and are destroyed by wave reworking at high tide over most of the tidal cycle. The expected preserved bioturbation index of this zone is zero.

Taken as a whole, the preserved ichnofacies consists of unlined *Skolithos*. Additionally, partially collapsed burrows may resemble the ichnogenus *Monocraterion*. Locally, y-shaped burrows resembling small *Psilonichnus* or *Polykladichnus* may be preserved, but these should represent only a small fraction of the represented traces. Because the burrows can completely collapse, not all burrows will be discernible.

Application to the rock record

The data and conclusions presented refer to autocyclic, short-term processes and preservation potential. In the rock record, however, preservation potential of burrows

is dependent on preservation of upper foreshore and backshore deposits, which in turn is dependent on longer-term allocyclic processes. On transgressive coastlines, such as Waterside Beach, preservation of upper foreshore and backshore sediments is not likely (Bourgeois and Leithold 1984; Reading and Collinson 1996); thus, long-term burrow preservation potential is zero. On progradational coastlines preservation of upper foreshore and backshore sediments increases significantly (Bourgeois and Leithold 1984; Clifton 1981; Massari and Parea 1988). Therefore, these results are more appropriately applied to progradational sequences in the rock record.

The distribution of burrows, biogenic-reworking rates, and temporal constraints on bioturbation indices presented herein provide a means for assessing short-term, autocyclic processes in progradational successions preserved in the rock record. Primarily, the initial occurrence of burrowing in a vertical sequence of upper foreshore and backshore deposits (preserved in the rock record) is an excellent indicator of the transition from the foreshore to the backshore. Secondly, the degree of bioturbation may be used to predict the length of time backshore sediments were subjected to Talitrid colonization. This in turn, provides a means to estimate depositional rates and processes responsible for sedimentation in the backshore. Based on the Waterside Beach example, bioturbation indices of two or less indicate a single season of colonization, whereas, BI's of two (upper end of range) and higher would require multiple seasons of colonization. A high BI may indicate that the backshore environment was protected from wave reworking or erosion (particularly during storms) and/or was subjected to low eolian sedimentation rates.

Burrowing in backshore deposits may either be obscured by post-depositional diagenesis or partly responsible for the destruction of bedding. For example, the progradational Miocene shoreline successions reported by Clifton (1981) exhibit small, vertical burrows described as amphipod burrows near the foreshore/backshore facies contact. Overlying this contact, backshore deposits are massive appearing. Clifton (1981)

attributed the lack of bedding in the upper beach or backshore to soil development and plant growth. However, multiple years of burrowing by amphipods or similar organisms may, in part, contribute to bedding destruction and should be considered as a possible mechanism for sediment homogenization.

Burrowing by amphipods in the backshore is a geologically recent occurrence. Suborder Gammaridea, to which Talitrid amphipods belong, is first documented from the late Eocene (~35 M.a.) (Bousfield 1973; Bousfield and Shih 1994; Hessler 1982). Suborder Gammaridea belongs to Superorder Peracarida, which extends back to the early Carboniferous (~350 M.a.). This suggests that the burrowing described herein will occur in sediments deposited after the Eocene. It is also possible that organisms of Superorder Peracarida may have exploited the same niche and employed a similar burrowing strategy as Talitrids as far back as the early Carboniferous.

CONCLUSIONS

The development of an ichnofabric – in this case within the *Psilonichnus* Ichnofacies (Frey and Pemberton 1987; Pemberton et al. 2001) – in the upper foreshore and proximal backshore of high-energy, conglomeratic beaches is most probable in the backshore environment. Although bioturbation occurs in the upper foreshore, wave reworking continually obliterates the resultant ichnofabric. In the backshore limited wave-reworking and the dominance of eolian-deposited medium-grained sand produces an environment favorable for colonization, and thus, the development of an ichnofabric.

Bioturbation in progradational foreshore and backshore successions provides a means for predicting short-term, autocyclic processes in the rock record. Firstly, the initial occurrence of burrowing marks the transition from the foreshore to the backshore. Secondly, the degree of bioturbation may be used to estimate the length of time backshore sediments were subjected to Talitrid colonization. This in turn, provides a means to estimate depositional rates and processes responsible for sedimentation in

the backshore. Based on the Waterside Beach example, bioturbation indices of two or less indicate a single season of colonization, whereas, BI's of two (upper end of range) and higher would require multiple seasons of colonization. A high BI may indicate that the backshore environment was protected from wave reworking or erosion (particularly during storms) and/or was subjected to minor eolian sedimentation.

Application of these results is dependent upon long-term allocyclic processes. In general, upper foreshore and backshore deposits have low preservation potential in transgressive systems and moderate preservation potential in progradational systems (Bourgeois and Leithold 1984). Consequently, these results are of limited use in transgressive deposits and may be more applicable to progradational sequences in the rock record.

REFERENCES

Basan, P.B., and Frey, R.W., 1977, Actual-palaeontology and neoichnology of salt marshes near Sapelo Island, Georgia, *in* Crimes, T.P., and Harper, J.C., eds., Trace Fossils 2: Geological Journal Special Issue No. 9, p. 41-70.

Bottjer, D.J., and Droser, M.L., 1991, Ichnofabric and basin analysis: Palaios, v. 6, p. 199-205.

Bourgeois, J., and Leithold, E.L., 1984, Wave-worked conglomerates - depositional processes and criteria for recognition, *in* Koster, E.H., and Steel, R.J., eds., Sedimentology of Gravels and Conglomerates: Calgary, AB, Canada, Canadian Society of Petroleum Geologists, p. 331-343.

Bousfield, E.L., 1973, Shallow-water Gammaridean Amphipoda of New England: London, Cornell University Press, 312 p.

Bousfield, E.L., and Shih, C.-T., 1994, The phyletic classification of amphipod crustaceans: problems in resolution: Amphipacifica, v. 1, p. 76-134.

Clifton, H.E., 1981, Progradational sequences in Miocene shoreline deposits, southeastern Caliente range, California: Journal of Sedimentary Petrology, v. 51, p. 165-184.

Clifton, H.E., Hunter, R.E., and Phillips, R.L., 1971, Depositional structures and processes in the non-barred high-energy nearshore: Journal of Sedimentary Petrology, v. 41, p. 651-670.

Colombini, I., Aloia, A., Bouslama, M.F., Elgtari, M., Fallaci, M., Ronconi, L., Scapini, F., and Chelazzi, L., 2002, Small-scale spatial and seasonal differences in the distribution of beach arthropods on the northwestern Tunisian coast. Are species evenly distributed along the shore?: Marine Biology, v. 140, p. 1001-1012.

Droser, M.L., and Bottjer, D.J., 1993, Trends and patterns of Phanerozoic ichnofabrics: Annual Review of Earth and Planetary Sciences, v. 21, p. 205-225.

Ethridge, F.G., and Wescott, W.A., 1984, Tectonic setting, recognition and hydrocarbon reservoir potential of fan-delta deposits, *in* Koster, E.H., and Steel, R.J., eds., Sedimentology of Gravels and Conglomerates: Calgary, Canadian Society of Petroleum Geologists, p. 217-235.

Fallaci, M., Aloia, A., Audoglio, M., Colombini, I., Scapini, F., and Chelazzi, L., 1999, Differences in behavioural strategies between two sympatric talitrids (Amphipoda) inhabiting an exposed sandy beach of the French Atlantic coast: Estuarine, Coastal and Shelf Science, v. 48, p. 469-482.

Frey, R.W., Howard, J.D., and Dorjes, J., 1989, Coastal sediments and patterns of bioturbation, eastern Buzzards Bay, Massachusetts: Journal of Sedimentary Petrology, v. 59, p. 1022-1035.

Frey, R.W., and Pemberton, S.G., 1987, The *Psilonichnus* ichnocoenose and its relationship to adjacent marine and nonmarine ichnocoenoses along the Georgia coast: Bulletin of Canadian Petroleum Geology, v. 35, p. 333-357.

Hessler, R.R., 1982, Evolution within Crustacea, Part 1: General: Remipedia, Branchiopoda and Malacostraca, *in* Abele, L.G., ed., The Biology of Crustacea - Systematics, the Fossil Record and Biogeography: New York, Academic Press, p. 150-185.

Howard, J.D., and Frey, R.W., 1975, Regional animal-sediment characteristics of Georgia estuaries: Senckenbergiana Maritima, v. 7, p. 33-107.

Massari, F., and Parea, G.C., 1988, Progradational gravel beach sequences in a moderate- to high-energy, microtidal marine environment: Sedimentology, v. 35, p. 881-913.

Pank, B., 2003, Beach hoppers, the sandy shore custodians, http://www.museums.org.za/bio/articles/pank/beach_hoppers.htm: Cape Town, South Africa, Iziko Museums.

Pemberton, S.G., Spila, M., Pulham, A.J., Saunders, T., Maceachern, J.A., Robbins, D., and Sinclair, I.K., 2001, Ichnology and Sedimentology of Shallow to Marginal Marine Systems: Ben Nevis and Avalon Reservoirs, Jeanne d'Arc Basin: Geological Association of Canada Short Course, v. 15: St. John's, Geological Association of Canada, 343 p.

Reading, H.G., and Collinson, J.D., 1996, Clastic Coasts, *in* Reading, H.G., ed., Sedimentary Environments; Processes, Facies and Stratigraphy: Oxford, U.K., Blackwell Science, p. 154-231.

Reineck, H.-E., 1963, Sedimentgefüge im Bereich der südlichen Nordsee, v. 505: Stuttgart, Abhandlungen der Senckenbergischen Naturforschenden Gesellschaft, 138 p.

Reineck, H.-E., and Singh, I.B., 1980, Depositional Sedimentary Environments, 2nd Ed.: Berlin, Springer-Verlag, 551 p.

Taylor, A.M., and Goldring, R., 1993, Descriptions and analysis of bioturbation and ichnofabric: Journal of the Geological Society (London), v. 150, p. 141-148.

Vader, W., 1970, *Talorchestia brito* Stebbing (Amphipoda, Talitridae): Notes on distribution, taxonomy, and biology: Sarsia, v. 42, p. 83-96.

Weslawski, J.M., Kupidura, T., and Zabicki, M., 2000, Sandhoppers, *Talitrus saltator* (Montagu, 1808) (Amphipoda, Gammaridea), at the Polish Baltic coast: Seasonal and spatial distribution patterns: Crustaceana, v. 73, p. 961-969.

CHAPTER 4: SEDIMENTOLOGY AND STRATIGRAPHY OF A TRANSGRESSIVE, MUDDY GRAVEL BEACH: WATERSIDE BEACH, BAY OF FUNDY, CANADA[3]

INTRODUCTION

Studies of modern, transgressive gravel beaches provide important information regarding facies relationships and organization of ancient conglomerates. In particular, determining sedimentological and stratigraphic relationships on modern beaches aids in predicting the extent, thickness, and morphology of conglomerates in the subsurface. Waterside Beach is a transgressive, muddy gravel beach in the megatidal Bay of Fundy. Due to the area's extreme tidal range (up to 12 m), foreshore (and shoreface equivalent) sediments are exceptionally well exposed at spring low tide. This provides an opportunity to assess the sedimentological characteristics of conglomerates deposited at water depths equivalent to the upper and lower shoreface (i.e. deposited due to shoaling, breaker, surf, and swash processes). In this paper: (1) sedimentologically distinct deposits are reported; (2) mechanisms for depositing mud beds and muddy conglomerates on gravel beaches are described; and, (3) inferred stratigraphic successions of transgressive gravel beaches are proposed.

Sedimentological descriptions of modern, wave-dominated gravel foreshores and backshores are common in geological literature. The original model presented by Bluck (1967) recognized distinct, shore-parallel zones based on clast-shape selection. This shore-normal zonation is observed from gravel beaches around the world (Bartholomä et al. 1998; Bluck 1999; Carr 1969; Carr et al. 1970; Hart and Plint 1989; Maejima 1982; Postma and Nemec 1990) and may be considered typical of high-energy, wave-dominated shorelines with a limited fluvial- or marine- sediment supply. The above model, however,

[3]A version of this chapter has been published in SEDIMENTOLOGY, 2006, v. 53, p. 279-296 as "Sedimentology and stratigraphy of a transgressive, muddy gravel beach: Waterside Beach, Bay of Fundy, Canada" by Shahin E. Dashtgard, Murray K. Gingras, and Karl E. Butler

is limited to a narrow (average 100–200 m wide) beach-normal zone that includes the steeply dipping beachface (foreshore), berm, and backshore (Bluck 1967; Carr et al. 1970; Kirk 1980; Maejima 1982; Postma and Nemec 1990). Modern nearshore (shoreface) and more basinal conglomerate facies have been described (Hart and Plint 1989), but are generally poorly understood. Shoreface conglomerate models are therefore, mainly derived from outcrop and core (Caddell and Moslow 2004; Clifton 1981, 1988; Hart and Plint 1989, 2003; Massari and Parea 1988; Zonneveld and Moslow 2004). As a result, most modern depositional models for conglomerates are a composite of modern foreshore deposits, and ancient shoreface and more basinal deposits (Bourgeois and Leithold 1984).

Shoreface conglomerates are broadly subdivided as transgressive and regressive (Bourgeois and Leithold 1984; Postma and Nemec 1990; Wescott and Ethridge 1982). Transgressive conglomerate successions encountered in the rock record tend to lack backshore and foreshore deposits as a result of erosion during transgression (Bourgeois and Leithold 1984). Regressive (progradational) gravel beaches tend to be characterized by repeating sequences of coarsening-upward conglomerates with internal erosional surfaces (Bourgeois and Leithold 1984), and by the preservation of foreshore sediments (Clifton 1981; Massari and Parea 1988).

Waterside Beach, New Brunswick, Canada is a transgressive, muddy gravel beach in the megatidal Bay of Fundy. It is considered that the structures and morphology of the intertidal deposits partly result from depositional processes (shoaling, breaker, surf, and swash zone processes) and water depths equivalent to the upper and lower shoreface. Examination of these modern deposits, therefore, provides insights into the facies and facies relationships of hydraulically reworked shoreface conglomerates.

Study Area

Waterside Beach is located on the New Brunswick coastline of Chignecto Bay (Fig. 4.1). Oriented northwest-southeast the beach is perpendicular to the dominant southwest winds (Amos and Asprey 1979). During winter cyclones (mainly November through January) it experiences peak significant wave heights of 3 m and wave periods of 10 seconds (Amos et al. 1991). Overall, most significant waves heights (79%) are below 1.25 m with periods of 7 seconds or less (Amos et al. 1991). Waterside Beach experiences a mean tidal range of 9 m. Vertical tidal range varies from 6 m during neap tides to 12 m during spring tides resulting in exposure of up to 1200 m of intertidal zone at low tide. Additionally, up to 650 m of beach/shoreface sediments occur subtidally (Fig. 4.2). The toe of the beach is demarcated by a step that is locally steep (1°), but generally weakly defined. On the landward edge, backshore and beachface deposits abut either salt marsh or bedrock cliffs (Fig. 4.1C).

At the northwest end of the beach, sand with minor gravel is the dominant sediment; whereas, gravel is present near the mouth of Long Marsh Creek (Figs. 4.1B and 4.2). A maintained dike backs the beach in the southeast (Fig. 4.1B, C). The dike has significantly hindered transgression, yet does not appear to interrupt beach sedimentation patterns in the intertidal and subtidal zones (Fig. 4.2).

Methods

Fieldwork on Waterside Beach was undertaken in 2003 and 2004. Beach-normal and beach-parallel transects were conducted to establish beach zonation and morphology. Line-and-level measurements were used to document changes in slope and to establish major changes in morphology. In total, 5.6 km of line-and-level measurements were taken in the shore-normal direction and 1.1 km in the alongshore direction. Stations were then erected at intervals in both directions. In areas where sediment distribution was heterogeneous, additional stations were established to characterize the sedimentological

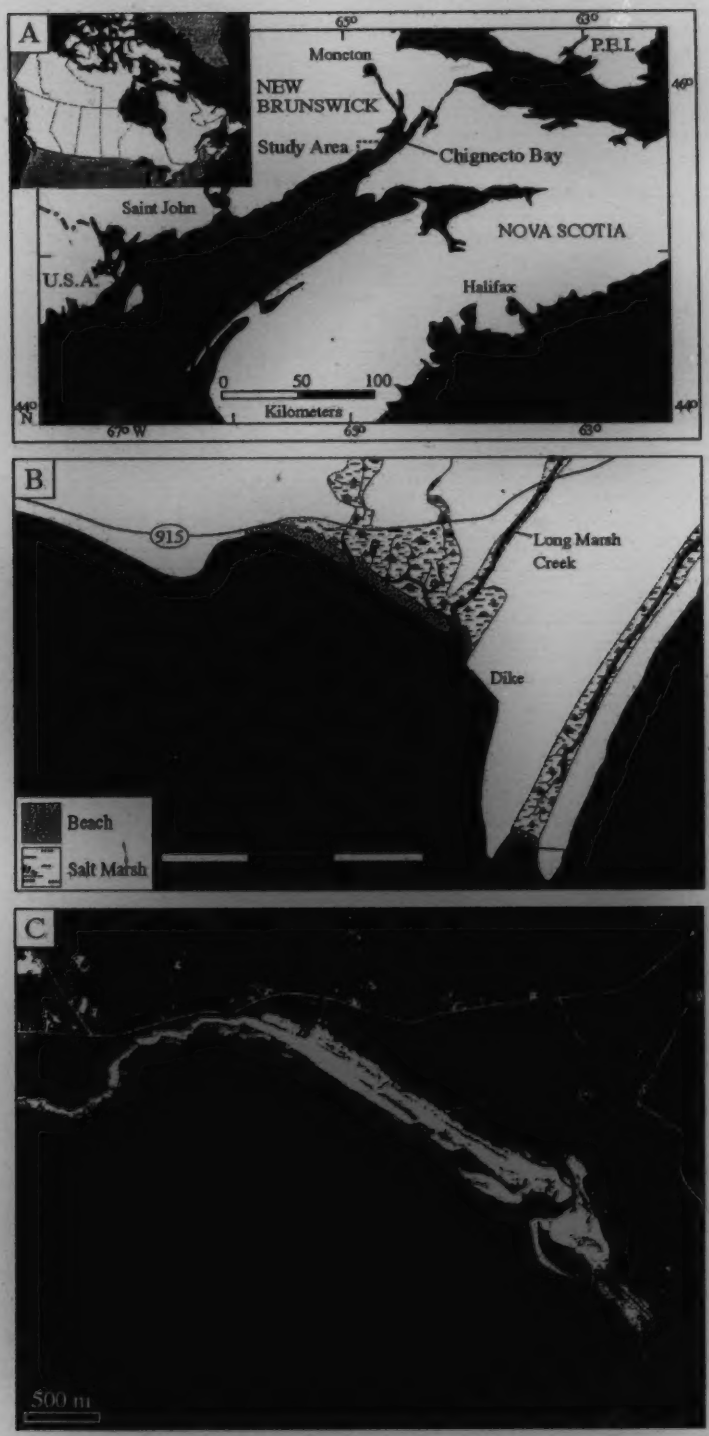

FIGURE 4.1 – Location map of the study area. (A) Location of the Bay of Fundy in Canada, and Waterside Beach in the Bay of Fundy. (B) Diagram of Waterside Beach. (C) Airphoto of Waterside Beach in 1996.

characteristics of each zone. At each station, sedimentary structures were recorded from the surface and from trenches dug mainly perpendicular to depositional strike. Box cores were collected at most stations for x-ray imaging.

High-resolution, single-channel seismic profiles were acquired in 2003 and 2004. These surveys were used to map out the toe of the beach (Fig. 4.2), but otherwise are not presented in this paper. In 2005, a grab-sampling program was undertaken to sample subtidal beach and offshore sediments. Samples collected during this program are incorporated into the grain-size data and are used to map out the horizontal distribution of sediments in the subtidal zone (Fig. 4.2).

Grain-size distribution on Waterside Beach was determined using one of three techniques: (1) grid sampling, (2) bulk-sample dry sieving, and (3) x-ray absorption. (1) Grid sampling (Hoey 2004; Rice and Church 1996; Wolman 1954) was employed for deposits with significant quantities of cobble- and boulder-sized clasts. This method involved establishing a 5 m x 5 m or 10 m x 10 m grid in an area considered representative of a deposit, and measuring the b-axis of clasts (> 4 mm) encountered every 0.5 m or 1 m across the grid (Church et al. 1987; Wolman 1954). A matrix sample of sediment < 4 mm was then collected from each grid and sieved to accurately determine the grain-size distribution of the matrix. (2) Three hundred and fifteen kilograms of sediment (60 samples) was collected for dry sieving. In the field, samples were dried, sieved, and weighed and the coarse fraction (particle diameter > 1 ϕ) discarded. Representative sub-samples were extracted from the remaining sample and dry sieved in the laboratory in one phi-size increments to the sand-silt break (4 ϕ). Grain-size statistics included in this paper are reported for all grab samples, and for intertidal samples where the total sample mass is equal too or greater than 100 times the mass of the largest clast observed. This is smaller than sample sizes suggested by Church et al. (1987) and Hoey (2004); but still provides reasonable grain-size information for comparison between

FIGURE 4.2 – Sediment distribution maps from 2003 and 2004 and profiles of Waterside Beach. Note the significant differences in the size of the mud zone (D11), bar locations (D8), and tidal-creek braid plain (D6) from 2003 to 2004. All lithologies on the 2003 map correspond to deposits described in Tables 4.1 and 4.2 except for the cross-hatch pattern, which demarcates a rock platform of Paleozoic bedrock exposed in the intertidal zone. P1 and P2 indicate the locations of profiles 1 and 2. Points 1 and 2 are referred to **(cont.)** in the text. The thick, dashed line on the 2004 map indicates the approximate edge of salt-marsh sediments exposed or buried shallowly on Waterside Beach. Between the two lines the beach is deeply incised into the salt marsh.

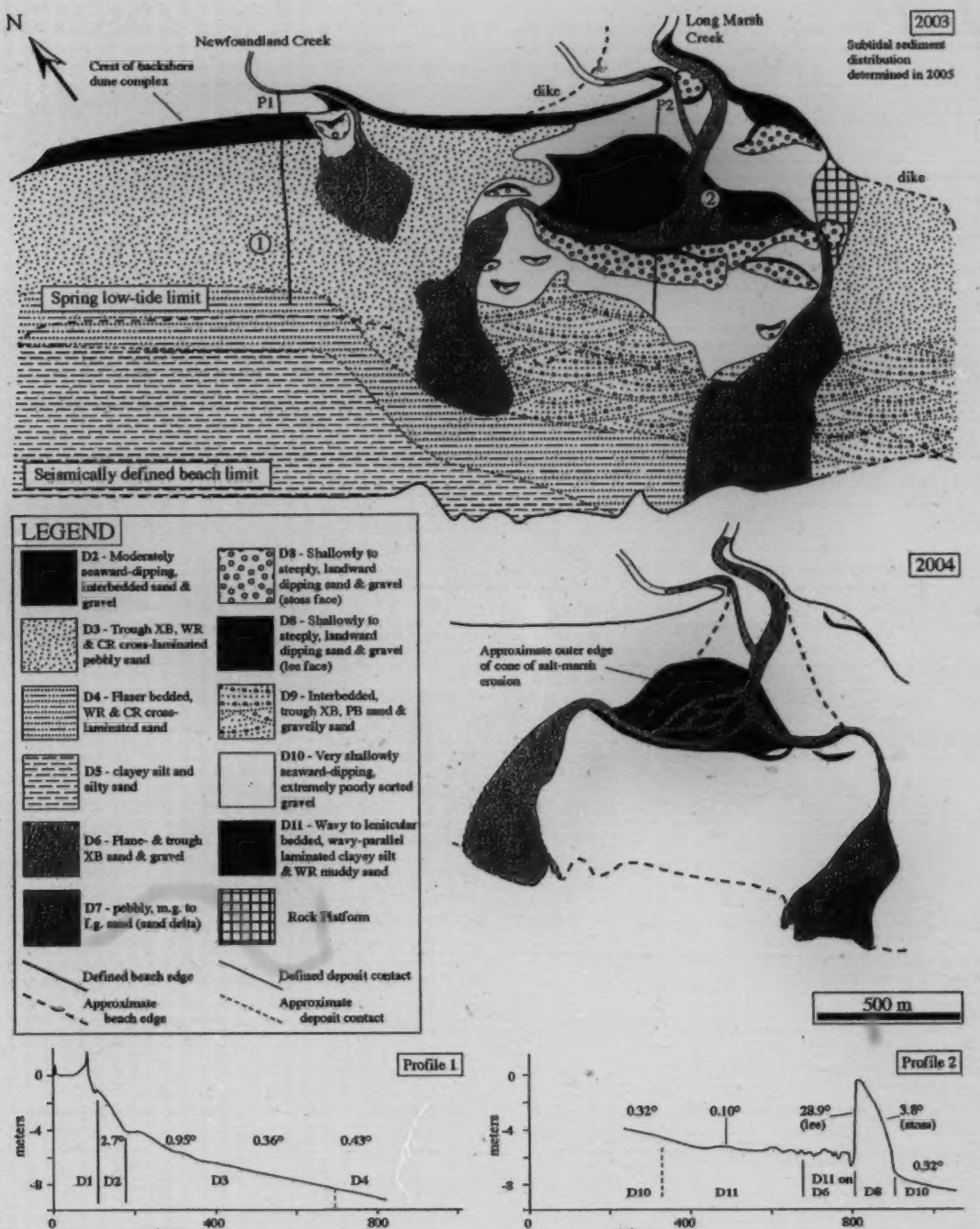
N
Newfoundland Creek
Crest of backshore dune complex
P1
P2
dike
Long Marsh Creek
2003
Subtidal sediment distribution determined in 2005
dike
2
1
Spring low-tide limit
Seismically defined beach limit
LEGEND
D2 - Moderately seaward-dipping, interbedded sand & gravel
D3 - Trough XB, WR & CR cross-laminated pebbly sand
D4 - Flaser bedded, WR & CR cross-laminated sand
D5 - clayey silt and silty sand
D6 - Plane- & trough XB sand & gravel
D7 - pebbly, m.g. to f.g. sand (sand delta)
D8 - Shallowly to steeply, landward dipping sand & gravel (stoss face)
D8 - Shallowly to steeply, landward dipping sand & gravel (lee face)
D9 - Interbedded, trough XB, PB sand & gravelly sand
D10 - Very shallowly seaward-dipping, extremely poorly sorted gravel
D11 - Wavy to lenticular bedded, wavy-parallel laminated clayey silt & WR muddy sand
Rock Platform
Defined beach edge
Approximate beach edge
Defined deposit contact
Approximate deposit contact
2004
Approximate outer edge of cone of salt-marsh erosion
500 m
Profile 1
meters
0
-4
-8
2.7°
0.95°
0.36°
0.43°
D1
D2
D3
D4
0
400
800
meters
Profile 2
meters
0
-4
-8
0.32°
0.10°
28.9° (lee)
3.8° (stoss)
0.32°
D10
D11
D11 on D6
D8
D10
0
400
800
meters

deposits (Hoey 2004). (3) Silt and clay fractions of samples with a significant fine-grained component (> 2% silt and clay) were determined by x-ray absorption.

Mean grain size (ϕ), sorting (σ), and skewness (Sk) were calculated by graphical analysis (Folk and Ward 1957) and the method of moments (Boggs 1995; Krumbein and Pettijohn 1938). Reported mean grain-size values are arithmetic means derived by the method of moments using millimeter values. For ease of comparison these values are converted to the phi scale. Sorting and skewness values are derived from graphical analysis of phi-scale, cumulative grain-size curves allowing for easy comparison of the Waterside Beach sediments to standard sorting and skewness scales (Boggs 1995; Folk and Ward 1957; Hoey 2004). Reported values are an average of all samples in each deposit (D1 to D11; Tables 4.1 and 4.2), but do not encompass the full range of mean grain sizes, sorting, and skewness measurements. These values offer a means for easy comparison of sediment properties between deposits.

In situ sediment samples were collected and imaged using x-ray radiography. Samples were collected with a 22.5 cm x 15 cm x 7.5 cm stainless-steel box core as described in Bouma (1969). From this, a 22.5 cm x 14 cm x 2 cm thick slab was extracted and x-rayed to assess sedimentary and biogenic sedimentary structures. By combining grain-size data, x-ray images, photos, field descriptions, and GPS measurements, sediment distribution maps were generated for the backshore, intertidal, and subtidal zones of Waterside Beach (Fig. 4.2).

RESULTS

Sediment Source

Sediment deposited on Waterside Beach is derived from three main sources. Mud is sourced from the bay; sand from the outcrops surrounding Waterside Beach; and, gravel and sand from reworking of glacial deposits exposed subtidally. Sediment sourced from the Bay of Fundy is primarily fine-grained, comprising silt and clay derived

from erosion of the seafloor and Paleozoic cliffs surrounding Chignecto Bay (Amos 1987; Amos and Asprey 1979; Amos et al. 1991). In particular, Amos (1987) reports that suspended particulate matter in upper Chignecto Bay comprises 70–90% silt with approximately 10–20% clay and minor sand. This grain-size distribution is similar (but slightly more silt-rich) to those of mud deposits (D5 and D11) on Waterside Beach, which yield an average grain-size distribution (and range) of 4% (1–7%) sand, 58% (50–66%) silt, and 38% (28–48%) clay.

Erosion of Paleozoic and Triassic outcrops fringing Waterside Beach and Long Marsh Creek present a second major source of sediment. These outcrops predominantly comprise siltstone and sandstone with recessive shale beds (Amos 1987; Amos and Asprey 1979; McLeod and Johnson 1999; Plint 1986; St. Peter 1996). Blocks eroded from the cliffs are friable and disaggregate into component grains and clasts. This is manifested as a decrease in outcrop-derived gravel aggregates away from the cliffs and abrasion platforms fringing the beach. It is considered that the outcrops provide a significant volume of sand to the beach, but are only a minor contributor of gravel. A second major source of sand and the main source of gravel are glacial deposits exposed subtidally. These sediments are considered to be glacial based on their sedimentological character, mineralogy, and from reconstructed glacial flow maps presented by Rampton et al. (1984). The distribution of the deposits is seismically mapped and the composition determined by grab sampling. They are exposed immediately seaward of the beach in the southeast, but are covered by beach sediments in the northwest.

Beach Sedimentology

Beach and shoreface sediments are subdivided into eleven zones (D1 to D11), which represent sedimentologically distinct deposits observed in the subtidal, intertidal, and supratidal zones of Waterside Beach. Sediment textures and structures observed in each deposit are summarized in Tables 4.1 and 4.2 and Figures 4.3, 4.4 and 4.5. The

deposits are broadly divided into three categories: (1) sandy foreshore and shoreface (D1 to D5); (2) tidal-creek braid-plain and delta (D6 and D7); and, (3) wave-formed gravel and sand bars, and associated deposits (D8 to D11). The relationship between these deposits is complex and their boundaries are commonly gradational. Nevertheless, the deposit interrelationships are tractable, thereby permitting the development of a characteristic facies model.

Deposits 1 through 5

Deposits 1 to 5 encompass sandy foreshore and shoreface sediments (Table 4.1; Figs. 4.2 and 4.3). They form a shore-normal continuum of sediments deposited from the backshore (D1) to the subtidal zone (D5). Below the moderately dipping beachface (D2), deposits 3 to 5 occur as a laterally extensive, shallowly seaward-dipping terrace (Fig. 4.2). The intertidal component of the terrace is referred to as a low-tide terrace (Masselink and Short 1993) and is the equivalent of the foreshore and upper shoreface. The subtidal component represents the lower shoreface. Terrace sediments exposed at low tide are submerged up to 12 m during high tide. Consequently, sedimentation and sediment transport on the terrace (D3 to D5) is almost completely dominated by shoaling waves. Swash-backwash and surf-zone processes dominate deposition on the beachface (D2).

Deposit 1 is well-sorted, medium-grained aeolian sand (Table 4.1) situated in the backshore (Profile 1, Fig. 4.2). The basal contact of D1 (underlain by D2) is gradational and marked by layers of disc-shaped cobbles. Deposit 2 tends to be very poorly sorted with interbedded, moderately well-sorted sands. All beds dip 3 to 5° seawards. Deposit 2 is analogous to narrow beachface–foreshore deposits reported from gravel, and mixed sand and gravel beaches (Bourgeois and Leithold 1984; Clifton 1981; Forbes and Taylor 1987; Kirk 1980; Massari and Parea 1988; McLean and Kirk 1969). Deposit 2 differs from those narrower, more gravel-rich beaches in that it lacks an imbricate disc zone or

	Deposit description	Sediment Texture	Sedimentary Structures: Major	Sedimentary Structures: Minor	Depositional environment & Contacts
D1	Weakly bedded, rooted well-sorted sand	Well sorted, coarse skewed m.g. sand (1.21 ϕ; 0.49 σ; -0.17 Sk (10))	Weakly defined bedding, Common disc-shaped cobbles near contact with D2		Backshore dune complex and washover fan Gradational contact with D2
D2	Moderately seaward-dipping, interbedded pebbly sand & gravel	Moderately well sorted, very coarse skewed c.g. sand (0.58 ϕ; 0.80 σ; -0.38 Sk (4)) Very-poorly sorted gravel (-2.81 ϕ; 2.16 σ; -0.02 Sk (1))	Moderately seaward dipping (3 - 5°), planar-parallel beds of pebbly sand & gravel	Trough XB (landward dip) & common disc-shaped cbls near contact with D1	Beachface / foreshore Gradational contact with D1; sharp with D3, 6
D3	Trough cross-bedded, WR & CR cross-laminated pebbly sand	Moderately well sorted, m.g. sand (1.22 ϕ; 0.62 σ; -0.09 Sk (14))	Beach cusps, Trough XB (landward & seaward dip), WR to CR (landward & seaward dip) cross-laminated, PB, Gravel lenses, Scattered pebbles, Bubble sand	Interbedded WR muddy sand	LTT / upper to middle shoreface equivalent Sharp contact with D2, 6, 8; gradational with D4, 7, 9; Interbedded with D11
D4	Flaser bedded, WR & CR cross-laminated sand	Moderately well sorted f.g. sand (2.41 ϕ; 0.60 σ; 0.1 Sk (4))	Current-modified WR, Discontinuous, lunate mud lenses (up to 2 cm thick),	PB, Discontinuous gravel lenses, Scattered pebbles	LTT/ middle to lower shoreface equivalent Transitional between D3 & D5 Gradational contact with D3, 5, 7, 9
D5	Clayey silt and silty sand	Clayey silt (6.01 ϕ, 2.3% sand, 52.2% silt, 45.5% clay (2)) Very poorly sorted, silty v.f.g. sand (3.28 ϕ; 2.23 σ; 0.06 Sk (2))	Scattered pebbles, sand lenses		ST/ lower shoreface equivalent Gradational contact with D4, 7, 9

TABLE 4.1 – Summary table of sedimentary deposits 1 to 5 at Waterside Beach. The values in brackets after skewness values indicate the number of samples included in the reported values and a star next to the number indicates grid-by-number sampling. Abbreviations are used in this table for wave ripples (WR), current ripples (CR), plane beds (PB), cross-bedding (XB), and for grain size: fine- (f.g.), medium- (m.g.), coarse- (c.g.), and very coarse- (v.c.g.) grained sand. Under depositional environments, LTT represents low-tide terrace and ST for subtidal terrace.

Deposit description		Sediment Texture	Sedimentary Structures		Depositional environment & Contacts
			Major	Minor	
D6	Plane- & trough cross-bedded sand & gravel	Heterogeneous grain-size distribution (-3.65 to 0.97 ϕ (generally decreases offshore); 0.69 to 2.22 σ; -0.15 to 0.42 Sk (3))	PB, Trough XB (landward dip), CR & WR sand	Trough XB (seaward dip), Mud layers in WR troughs, Gravel WR	LTT/ tidal-creek braid plain Sharp contact with D2, 3; gradational with D4, 7, 9, 10 Interbedded with D8, 10, 11
D7	Offshore fining, sandy gravel to f.g. sand	Heterogenous grain-size distribution (-1.14 ϕ; 1.40 σ; 0.42 Sk grades offshore to 2.15 ϕ; 0.60 σ; 0.09 Sk (4))	Unknown	Unknown	ST/ tidal-creek sand 'delta' Sharp contact with D8, 10; gradational with D3, 4, 5, 9 Interbedded with D6, 8, 10, 11
D8	Shallowly to steeply, landward-dipping sand & gravel beds	Very-pooly sorted gravel (-3.26 ϕ; 2.05 σ; 0.04 Sk (4))	Steeply (up to 29°) to shallowly, landward-dipping interbeds of gravel & pebbly sand, Trough XB (landward dip)	Interbedded shallow, seaward-dipping gravel & pebbly sand	LTT & ST / wave-generated gravel bars Sharp contact with D3, 4, 5, 6, 7, 9, 11; gradational with D10 Interbedded with D5, 6, 7, 9, 10, 11
D9	Interbedded, trough cross-bedded PB sand & gravelly sand	Poorly sorted, very coarse skewed v.c.g. sand (-0.48 ϕ; 1.24 σ; -0.32 Sk (4))	Trough XB (dom. landward dip) gravelly sand, PB sand, WR, CR	Thin, discontinuous mud laminae	LTT & ST / wave-generated sand bars Sharp contact with D6, 8, 10; gradational with D3, 4, 5, 7 Interbedded with D5, 6, 8, 10
D10	Very shallowly seaward dipping, extremely poorly sorted gravel	Very-poorly sorted, very fine skewed gravel (-5.93 ϕ; 2.47 σ; 0.48 Sk (2°))	Shallowly (< 1°) seaward -dipping gravel, PB sand between clasts	WR & CR sand & mud	LTT & ST / gravel lag (deflation of D8) Sharp contact with D5, 6, 7, 8, 9, 11; Interbedded with D5, 6, 7, 8, 9, 11
D11	Wavy to lenticular bedded, wavy-parallel laminated clayey silt & WR muddy sand	Clayey silt (5.60 ϕ, 4.7% sand, 39.5% silt, 35.7% clay (6)) Poorly sorted sand (1.29 ϕ; 1.57 σ; 0.08 Sk, 7.4% mud (2))	Wavy-parallel laminated mud, Interbedded WR & PB sand & pebbly sand, Scattered pebbles and gravel leases	Mud cracks, Flame structures, Runzelmarkken	LTT / mud Sharp contact with D6, 7, 8, 10; gradational with D8 Interbedded with D3, 8, 9, 10

TABLE 4.2 – Summary table of sedimentary deposits 6 to 11. Abbreviations are the same as in Table 4.1.

well-defined clast segregation. The toesets of D2 are marked by rounded cobbles and pebbles that accumulate at the base of the foreshore during storms (Bluck 1967, 1999). These sediments overlie a wave-scoured surface cut into salt-marsh deposits that is excavated during transgression (Dashtgard and Gingras 2005). Deposit 3 sands onlap the cobble toesets of D2 and are derived from onshore-directed currents developed under fair-weather conditions (Table 4.1; Roy et al., 1994; Reading and Collinson, 1996). Along depositional strike at the top of D3, sand is distributed into low-amplitude bars spaced equidistantly (~ 100–200 m). Grain size and sorting of bar sediments is ideal for trapping air; hence, these zones tend to be dominated by bubble sand (i.e. air trapped in sand; Fig. 4.3A) in the upper 0.1 to 0.15 m. Runoff zones dominated by silty sand and silt deposition occur between the bars. Mud deposited in these zones may be up to 5 cm thick, but is typically eroded when the bars shift position. High-energy wave conditions are manifested as onshore-directed trough cross-beds in D3 (Fig. 4.3A), gravel layers at the base of scours (Fig. 4.3B), and by gravel-dune foresets.

Deposit 4 encompasses sediment deposited below the mean-tide low-water level and is a transitional zone between D3 and D5 (i.e. equivalent to the middle shoreface). This zone is dominated by wave-ripples with silt infilling ripple troughs. The silt deposits are generally thin, lunate, and discontinuous, but may exceed 6 cm in thickness. Throughout D3 and D4, wave- and current-ripple laminae are developed under fair-weather conditions (Fig. 4.3A, B). When initially exposed by the falling tide, the terrace is covered by wave-ripples, probably resulting from shoaling-waves (Masselink 1993; Masselink and Short 1993; Wright et al. 1982). With continued exposure, sheet-like surface drainage reworks many of the wave ripples into offshore-directed current ripples resulting in preservation of ebb-current modified wave-ripples (Fig. 4.3B).

Deposit 5 is the lowest most unit of the terrace and only occurs subtidally. It is considered the equivalent of the lower shoreface (Fig. 4.2). This zone is dominated by clayey silt and silty very-fine grained sand deposition (Table 4.1) with interbedded thin

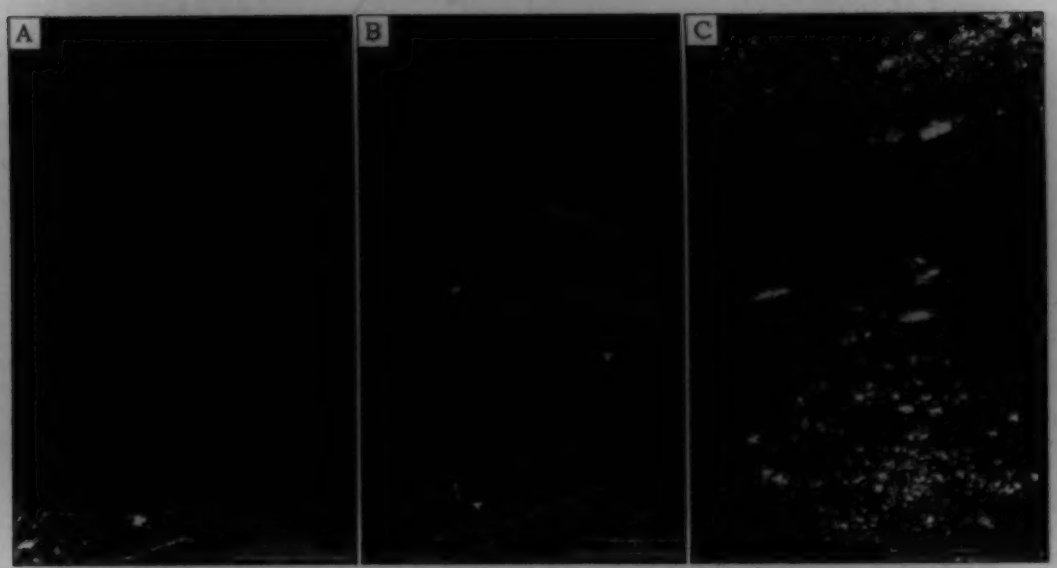

FIGURE 4.3 – X-ray images of D3, D4, and D6. All images are taken from box cores oriented beach-normal (seaward direction to the right). (A) Example of landward-dipping trough cross-beds overlain by seaward-dipping current-ripple laminae in D3. Trough cross-bedding is enhanced by air bubbles (dark holes) developed along bedding planes. (B) Deposit 4 dominated by wave- and current-ripple laminae, and plane-bedded sand. Dark laminae indicate more mud –rich sediments and light laminae more sand-rich. Note the gravel-lined scour near the base of the image (black arrow) and pervasive bioturbation (white arrows). (C) Plane-bedded sandy gravel of D6. The lighter beds are gravel-rich versus the gray, sandier beds. Black spots are pores spaces.

pebbly sand lenses. The offshore pinchout of D5 corresponds to the toe of the shoreface, and is demarcated by a weakly defined step and a decrease in the slope of the seafloor.

Deposits 6 and 7

Deposits 6 and 7 comprise plane and trough cross-bedded sand and gravel deposited as a result of tidal-creek processes active on the low-tide terrace at low tide. Water transported up the creeks at high tide (particularly spring high tide) flood the salt marsh and drain into two tidal lakes, 2 and 10 kilometers landward of the beach. During the falling tide, bay waters drain off the marsh and out of the lakes at a relatively constant rate – maintaining a relatively steady flow rate within the creeks throughout falling- and low-tide. Tidal-creek waters winnow fine gravel and sand from upper terrace

deposits and transports it to the lower intertidal and subtidal zones. As a result, upper and middle terrace sediments exhibit improved sorting and a general shift towards coarsely skewed sediment. The tidal creeks also redistribute low-tide terrace sediments into creek-parallel sand and gravel beds. These deposits form a braided outwash plain with a very heterogeneous distribution of grain size, sorting, and skewness (D6, Table 4.2). The hydraulic energy of a braid channel determines whether gravel, sand or mud is actively deposited and the thickness of that deposit. Moreover, sedimentary structures observed in a particular area of the braid plain are related to sediment grain size and hydraulic energy. High-energy streams (active channels) are erosive and remove up to pebble-sized clasts from the underlying deposit. In moderate-energy channels, sand and gravel is deposited as plane beds (Fig. 4.3C) with intermittent steeply dipping foresets of stream-parallel and stream-normal channel bars. Grain-size distribution is heterogeneous; however, there is an overall decrease in grain size offshore (Table 4.2). At the seaward end of D6, sand and fine gravel winnowed out of upper and middle terrace deposits is deposited as a sand 'delta' (D7). The delta extends from the lower intertidal seaward to the toe of the shoreface (Fig. 4.2) where it develops a pronounced (1°) step. This sediment is likely the source for the landward-migrating sand dunes and bars of deposit 9.

Deposits 8 through 11

Deposits 8 to 11 are reworked by high-energy waves. Deposit 8 encompasses sediment laid down as large (up to 800 m long), landward-migrating gravel bars (Figs. 4.2 and 4.4A). In Figure 4.4A, the gravel bar on the right of the photo comprises a 5.5 m high lee face and 6.7 m high stoss face (Profile 2, Fig. 4.2). Overall, the bars are composed of steeply landward-dipping foresets of very-poorly sorted gravel and sand (Table 4.2) Sediment migrates up the stoss face of the large bars and avalanches down

the lee slope forming foresets that dip up to 29° (Figs. 4.2, 4.4C, E and 4.6). Interbedded with these sediments are better sorted, coarsely skewed gravels representing hydraulically winnowed surface sediment.

The Waterside gravel bars develop in the shallow subtidal zone (lower shoreface) and increase in volume as they migrate onshore. Measurements of bar migration indicates that annual landward migration along the bar front is variable, ranging from 0 to over 50 m year^{-1} (Maps 2003 and 2004, Fig. 4.2). At the landward limit of the beach the bars either accrete to the beachface (D2) or infill the tidal creeks (Strip logs 2A, 2B, and 2C, Fig. 4.6). Small bars (< 2 m high) tend to be washed out by storm waves in the intertidal zone whereas large bars are more resilient and migrate landward during storms. Under fair-weather conditions, migration of the large bars is minimal and is restricted to small, low-amplitude, mixed sand and gravel dunes that migrate up and over the stoss face of the bar.

In sandy systems, bar-forms similar to, but smaller than, the Waterside bars are common and have been the subject of numerous studies (Anthony et al. 2004; Greenwood and Davidson-Arnott 1979; King and Williams 1949; Kroon and Masselink 2002; McCave and Geiser 1978; Yang et al. 2005). Initially, these intertidal bars were considered to form as a result of swash processes and destroyed by surf processes (King 1972; King and Williams 1949). However, recent work by Kroon and Masselink (2002) shows that onshore bar-migration results mainly from surf-zone processes and that swash processes play a secondary role. The Waterside bars may then be considered intertidal bars that are akin to subtidal, inner surf-zone bars (Kroon and Masselink 2002; Sunamura and Takeda 1984).

Deposit 9 refers to sediment deposited from sandy, low amplitude (< 1 m) bars with gently dipping lee and stoss slopes. D9 bars are composed of poorly sorted sand and gravel, but tend to be predominantly gravelly sand (Table 4.2; Fig. 4.6). The increased sand content is partly the result of wave reworking of D7 sand-delta sediments in the

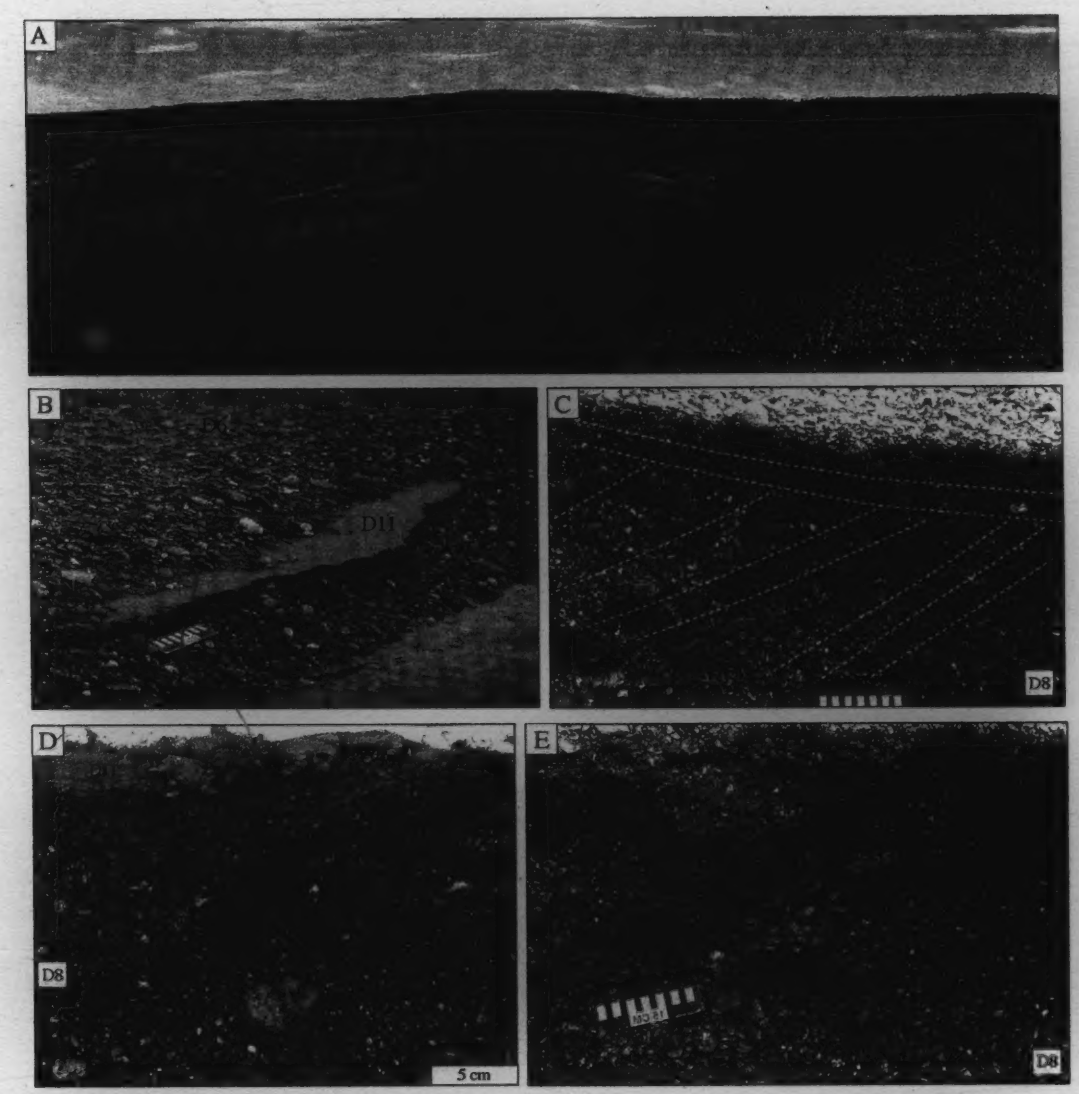

FIGURE 4.4 – Photos of D6 to D11. (A) Panoramic view of the relationship between the 5.5 m high gravel bar (D8), braided channel of Long Marsh Creek (D6), and zone of mud deposition (D11). Panoramic taken from the top of the gravel bar looking east, the bay is to the right of the photo and land to the left. (B) Example of interbedded D6 and D11. The mud layer is 0.04 m thick and the scale is 0.15 m long. (C) Trench excavated normal to the beach on the backside of the gravel bar in photo A (D8). The dashed white lines highlight steeply landward-dipping gravel beds overlain by shallowly seaward-dipping gravel. Scale is 0.15 m long. (D) Photo of a trench excavated normal to the beach in the zone of mud deposition (D11) on photo A. Note the mud-coated gravel within the upper 0.15 m of sediment and steeply landward-dipping sand and gravel beds (D8) preserved below mud beds (D11). (E) Image of a beach-normal trench excavated approximately 1 m above the base of the gravel bar in photo A on its stoss face. All gravel clasts 0.10 m below the bar surface are coated in mud. Scale is 0.15 m long.

lower intertidal and subtidal zones (Fig. 4.2). Sedimentary structures are dominated by trough cross-bedding (dipping in all directions) and plane beds that form as a result of water flowing over and off the bar forms. These bars are highly unstable and are akin to the Type 2 bars reported by Greenwood and Davidson-Arnott (1979). They are also considered to result from similar processes (Anthony et al. 2004; Kroon and Masselink 2002) as the larger gravel bars (D8) and may be considered analogous to subtidal, inner surf-zone bars as well.

Deposit 10 is a wave-winnowed pebble and cobble lag (Fig. 4.2) deposited to seaward of the landward-migrating gravel bars (D8). The upper layer of D10 is wave-reworked into weakly defined horizontal to gently seaward-dipping beds (Fig. 4.6). Hydraulic winnowing of the primary deposit (D8) removes most fines and concentrates large pebbles and cobbles on the beach surface. Secondary infilling of interstitial pores with sand (D9) and mud (D5 and D11) results in an increased proportion of fines, hence the fine skew and very-poor sorting (Table 4.2). Deposit 10 may occur from the top of the low-tide terrace (foreshore) to the base of the shoreface (Fig. 4.2).

The development of large gravel bars (D8) is both an important mechanism for gravel transport and deposition, and is necessary for the occurrence of extensive mud deposition landward of the bars (Fig. 4.2). The gravel bars dissipate and reflect wave-energy resulting in the development of quiescent zones dominated by clayey silt deposition (Figs. 4.2, 4.4A and 4.5). Below a threshold bar-height (~ 1.5 m) mud deposition is negligible. With increased height the mud zone extends landward (Fig. 4.2). This mud is deposited on top of the existing sediment (Figs. 4.2 and 4.4A, B) and pinches or swells in response to the antecedent topography (Fig. 4.6). In abandoned channel lows (D6) or depressions in the underlying surface, mud deposits (D11) are commonly 0.15 to 0.2 m thick. Mud up to 0.4 m thick has been observed. On topographic highs, mud

thickness rarely exceeds 0.07 m. The clayey silt is wavy parallel laminated (Fig. 4.5A) to wave-ripple laminated (Fig. 4.5B) and is commonly interbedded with sand and sandy gravel beds deposited during storms or by ice (Fig. 4.5B).

DISCUSSION

Muddy Conglomerates and Mud Beds in Conglomerates

Understanding the relationship between the mud deposits (D11), channel deposits (D6), gravel bars (D8), and lag deposits (D10) on Waterside Beach provides a mechanism for mud deposition in conglomeratic systems and for the formation of muddy conglomerates. Landward of the gravel bars, mud is deposited as thin layers on top of braided-channel bars and in abandoned channels of D6 (Figs. 4.4A, B and 4.5). Initially, the mud is soupy and easily resuspended by low-energy hydraulic currents. Subsequent desiccation, dewatering, and / or bacterial (or algal) binding renders it firm – forming resistant mud beds. An example of this is shown in Figure 4.4B where a 0.04 m thick mud bed is interbedded with braided-channel gravel-bar deposits of D6. Muddy clast- and matrix-supported conglomerates develop in front of the landward-migrating gravel bars (D8). Gravel transported up the seaward (stoss) side of the bar avalanches down the landward (lee) face and either accumulates on the face or in the mud at the base of the bar. The area directly in front of the bar is not affected by wave- or tidal-energy; hence,

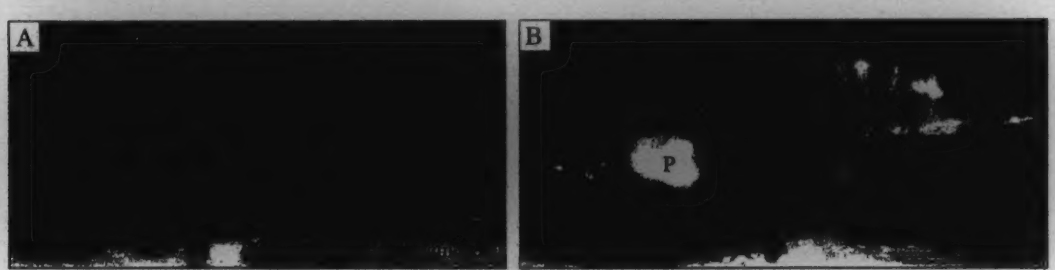

FIGURE 4.5 - (A) X-ray image of the wavy-parallel laminated clayey silt (dark layers) and silty sand (light layers) of D9, overlying gravelly sand. U-shaped *Corophium volutator* burrows (Co) are prevalent throughout the mud. (B) X-ray image of D9 showing the variability in the lithology of the deposit. Dark layers are clayey silt, dark grey areas sandy mud, and light layers are gravelly sand. Note the large pebble (P), *Corophium volutator* burrows (Co) and wave ripples (WR).

the mud is not eroded during bar migration. Gravel avalanching down the lee face either rests on top of the mud or sinks into it resulting in mud infilling the spaces between gravel clasts. This relationship is represented on Strip log 2A (Fig. 4.6) by muddy gravel in the basal portion of each D8 deposit.

Muddy conglomerates also develop when mud-rich seawater seeps through the beach sediments (Fig. 4.4D, E). Figure 4.4D is an example of muddy gravel that occurs below the zone of mud deposition. Mud-laden seawater percolating down through the gravel rapidly loses velocity below the surface resulting in mud deposition in the near-surface beach sediment. The mud tends to coat grains instead of infilling the pore spaces. Figure 4.4E depicts muddy gravels encountered in a trench approximately 1 m above the low-tide terrace on the stoss side of a gravel bar (D8). In this case, mud-laden seawater passing through the gravel bar coats sand and gravel clasts with mud. In both cases muddy gravels are developed, although the depth (relative to the beach surface) at which they occur differs. Below the zone of mud deposition (D11, Fig. 4.2) muddy gravels occur in the near-surface sediment (upper 0.15 m) and overly mud-free sand and gravel. Within the gravel bars, muddy gravels occur below the upper 0.1 to 0.15 m resulting from wave winnowing of the near-surface sediment.

The two mechanisms presented for the development of muddy, matrix- and clast-supported conglomerates and for the deposition of mud beds in conglomerates provide a means to assess environmental conditions of the paleo-depositional environment that otherwise may not be discernable. The latter mechanism (requiring gravel deposits and mud-laden seawater) suggests that the occurrence of muddy conglomerate is a good indicator that seawater at the time of conglomerate deposition was muddy. The first mechanism necessitates bar formation and migration, which is dependent on the location of the bars relative to the beach and on the local tidal range. Intertidal bars exhibit characteristics that are distinct to an intertidal environment and thus, may be distinguished from their subtidal equivalents. Primarily, the height of intertidal bars is

restricted by tidal range where bar height cannot exceed the maximum tide height. This in turn, controls the occurrence of mud deposits on the landward side of the gravel bars. Short (< 1.5 m high) bars tend not to permit the development of mud beds. Subtidal gravel bars are not restricted by tidal range and may occur in microtidal to megatidal settings.

Intertidal bars are subaerially exposed twice a day, resulting in dewatering, desiccation, and algal binding of the mud beds that develop landward of the bars. In a subtidal environment dewatering and possibly algal binding may also render mud beds firm, but is less likely too occur. Moreover, bar migration rates are likely to be higher in a subtidal setting as a result of prolonged exposure to surf-zone processes. Consequently, the occurrence of mud beds in a conglomeratic succession may indicate an intertidal environment and upper mesotidal to megatidal conditions. The occurrence of muddy conglomerates however, is less restrictive and may either indicate subtidally formed gravel bars, intertidal bars or mud-laden seawater. If bedding is apparent in a muddy conglomerate it most likely developed from mud-laden seawater seeping through the gravel; whereas, a lack of bedding may be more indicative of bar migration over soupy mud deposits in either a subtidal or intertidal setting.

Transgressive, Muddy Gravel Beach Sequences

Waterside Beach occurs in a megatidal setting where the dominance of wave-processes will result in a facies architecture that corresponds to that of a transgressive gravel beach. Figure 4.6 illustrates six idealized successions that can be predicted if continued transgression resulted in burial and preservation of Waterside Beach in the rock record. Strip logs 1A, 1B, and 1C (Fig. 4.6) relate to point 1, and strip logs 2A, 2B, and 2C relate to point 2 on Map 2003, Figure 4.2. The stratigraphic successions presented for points 1 and 2 represent end members of the possible stratigraphic relationships that exist on Waterside Beach. Strip logs 1A and 2A are complete transgressive sequences that may

FIGURE 4.6 – Idealized sections that may be expected if Waterside Beach is preserved in the rock record. Strip logs 1A, 1B, and1C refer to sections for point 1, and strip logs 2A, 2B, and 2C for point 2 (2003 map, Fig. 4.2). The logs are discussed extensively in the text. Lithology is not indicated on the strip log unless it differs from the indicated lithology type (i.e. gravel beds in a sand unit). The vertical bars and D#'s on the right side of each log refer to the vertical distribution of each deposit type in the section. Scale is in meters.

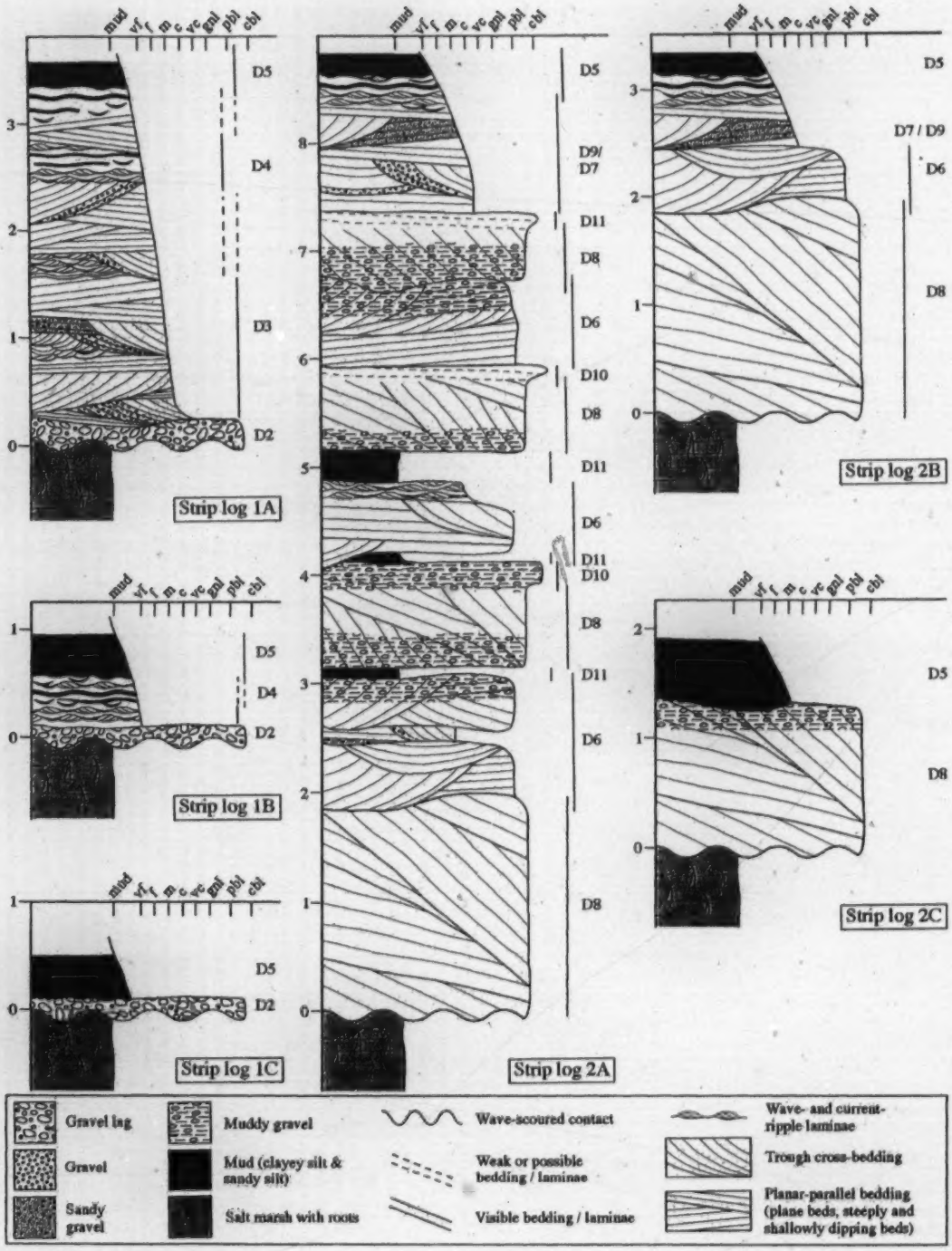
mud vf f m c vc gnl pbl cbl
Strip log 1A
Strip log 1B
Strip log 1C
Strip log 2A
Strip log 2B
Strip log 2C
D2
D3
D4
D5
D6
D7 / D9
D8
D9/ D7
D10
D11
Gravel lag
Gravel
Sandy gravel
Muddy gravel
Mud (clayey silt & sandy silt)
Salt marsh with roots
Wave-scoured contact
Weak or possible bedding / laminae
Visible bedding / laminae
Wave- and current-ripple laminae
Trough cross-bedding
Planar-parallel bedding (plane beds, steeply and shallowly dipping beds)

either be encountered in systems with high sedimentation rates or that may develop at or near the maximum transgressive shoreline. Strip logs 1B and 2B present the expected preserved succession that may be encountered in areas with moderate sedimentation, or at the early or late stages of transgression. Strip logs 1C and 2C show sedimentary successions that will develop in rapidly transgressing systems. Continued transgression of present day Waterside Beach should result in preservation of a succession that resembles either strip logs 1B and 2B or 1C and 2C.

The (extreme) difference in thickness between sequences constructed for points 1 and 2 is due to erosion of the salt marsh at the mouth of Long Marsh Creek (LMC; Fig. 4.2). This in turn, is controlled by tidal range, where the cross-sectional area of a tidal-inlet throat (i.e. where LMC debouches onto the beach) is related to the tidal prism (Allen 1997, 2000; French 1993; Pye and French 1993). On the megatidal Waterside Beach the tidal prism is large; hence the cross-sectional area of LMC is also large (8.2 m deep, 54 m wide; Dashtgard and Gingras, 2005). Depth measurements taken from the beach and within marsh indicate that at the landward end of the beach (seaward limit of the marsh), LMC is filled with 4.5 m of gravel and sand derived from the beach, and is presently filling in a landward direction. Seaward of LMC, the erosional profile of underlying salt-marsh sediments flares laterally and vertically (as a cone opening seawards) from the mouth of the creek to beyond the outer edges of the gravel bars (Map 2004, Fig. 4.2). Within this cone the beach and shoreface deposit is much thicker; thus, the successions presented in strip logs 2A, 2B, and 2C (i.e. near tidal-channel complex) are nearly three times thicker than those in strip logs 1A, 1B, and 1C, respectively (i.e. ambient beach; Fig. 4.6).

Strip logs 1A, 1B, and 1C

Assuming Waterside Beach is preserved in the rock record, strip logs 1A, 1B, and 1C (Fig. 4.6) are idealized sections of the sedimentary succession that may be expected at point 1 (Map 2003, Fig. 4.2). The three sections are presented to illustrate variations in the preserved succession that can occur under varying rates of transgression and / or sedimentation. In general, a complete sedimentological record will be relatively thin and dominated by middle to lower terrace deposits representing mainly shoaling-wave (shoreface) processes. In transgressive systems, backshore and beachface deposits are normally eroded (Bourgeois and Leithold 1984; Nemec and Steel 1984); whereas, shoreface and offshore facies tend to be preserved (Reading and Collinson 1996; Roy et al. 1994). This is likely to be the case for Waterside Beach with the vertically significant, but laterally restricted D1 and D2 deposits (Profile 1, Fig. 4.2) having a limited to nil chance of preservation. The rest of the succession consists of a deepening-upward trend.

Strip logs 1A, 1B, and 1C depict the facies evolution on top of a wave-scoured contact (wave-ravinement surface) cut into underlying salt-marsh deposits that develops during transgression (Fig. 4.6). This contact is in turn overlain by a thin transgressive lag that is sedimentologically similar to the transgressive lag described by Massari and Parea (1988) and Clifton (1981). The lag comprises toeset sediments of D2 that are partly wave-reworked resulting in destruction of bedding (Fig. 4.6). Above the lag, the rates of transgression and sedimentation controls the thickness of the preserved succession and the deposit relationships observed.

Three scenarios are presented for the expected preserved succession at point 1 (Map 2003, Fig. 4.2). In strip log 1A, the lag (D2) is sharply overlain by D3, then D4, and finally D5 sediments that form a continuum of decreasing grain size upward in the succession. This trend is accompanied by an increase in mud deposition and ripple cross-lamination, and a decrease in trough cross-bedding and gravel content. Strip log 1B illustrates the case of moderate sedimentation rates relative to transgression resulting in

increased erosion of the low-tide terrace deposits (foreshore and upper shoreface) and deposition of middle and lower shoreface sediments (D4 and D5) sediments on top of the gravel lag. Finally, strip log 1C presents a succession that is likely to develop in a rapidly transgressive setting with low sedimentation. In this scenario, the entire foreshore and upper shoreface sequence is removed (D2 to D4), with lower shoreface sediments (D5) overlying the gravel lag. Because the beach has an abundant source of sand and gravel (i.e. glacial deposits exposed subtidally) and experiences relatively rapid transgression, it is considered that either strip log 1B or 1C (Fig. 4.6) represents the most likely succession that will be preserved if Waterside Beach passes into the rock record.

Strip logs 2A, 2B, and 2C

Strip logs 2A, 2B, and 2C (Fig. 4.6) depict a much thicker beach and shoreface sequence that may be expected at point 2 (Map 2003, Fig. 4.2). As discussed above, erosion of the salt marsh is much more pronounced near the mouth of Long Marsh Creek and extends seaward as a cone of relatively deeply incised beach sediment (Map 2004, Fig. 4.2). The complete sequences are a vertical representation of the complex stratigraphic relationships between deposits 6 to 11 observed on the beach surface (Fig. 4.2). The depositional conditions – rates of transgression and sedimentation – for strip logs 2A, 2B, and 2C are the same as those for strip logs 1A, 1B, and 1C, respectively.

The base of the successions is demarcated by a tidally scoured contact cut into salt-marsh deposits (Strip logs 2A, 2B, and 2C, Fig. 4.6). In strip log 2A, this surface is directly overlain by a 3 m thick unit of gravel bar (D8) then channel (D6) deposits representing the initial filling episode of LMC by gravel-bar sediments. The upper part of the bar sediments are hydraulically reworked by tidal-creek waters to form D6. From 3 m to nearly 5 m is a typical sedimentary package for this succession. Mud deposition (D11) occurs on top of the channel sediments (D6) as a result of gravel-bar formation. Downward percolating seawater coats sand and gravel clasts in the sediment immediately

below the mud beds resulting in the development of muddy gravel. Subsequent landward migration of the bar, deposits a thick bedset of steeply dipping sand and gravel (D8) on top of the mud. The basal third of the bar deposit is dominated by muddy gravel as a result of mud being forced into the pore spaces between gravel clasts. The surface sediments of the bar-deposited bedset (D8) are hydraulically winnowed and reworked by waves into weakly developed seaward-dipping plane beds (D10). Once the bar reaches the beachface or is washed out by waves, braided drainage channels of LMC are re-established on the low-tide terrace forming channel-bar deposits (D6). This sedimentation cycle is repeated vertically. After the last bar, channel, and mud unit (at approximately 7.5 m), the D10 beds are sharply overlain by either low-relief sand-bar (D9) or sand-delta (D7) sediments representing the lowermost intertidal and subtidal zones (Strip log 2A, Fig. 4.6).

Strip logs 2B and 2C (Fig. 4.6) depict the same sequence as in 2A, but under varying rates of transgression and / or sedimentation. Similar to strip log 1A, strip log 2A should be preserved in a setting with high sedimentation rates and slow transgression, such as at or near the maximum transgressive shoreline. Strip log 2B will be preserved where sedimentation rates are high enough to result in some aggradation during transgression. This results in erosion of the foreshore by transgressive wave ravinement, and partial preservation of middle and lower shoreface sediments (D4 and D5; Strip log 2B, Fig. 4.6). Strip log 2C illustrates a sequence that will be preserved when sedimentation rates are much lower than transgression rates. Transgressive wave ravinement removes most of the intertidal (foreshore and upper shoreface) and subtidal (middle and upper lower shoreface) deposits. Lower shoreface muds then accumulate on top of the wave-scoured sediments. The resultant package therefore, consists of foreshore and upper shoreface sediments that infilled the tidal creeks, decapitated by wave ravinement, and capped by lower shoreface muds (Strip log 2C, Fig. 4.6).

Application to the Rock Record

The sedimentological relationships and theoretical stratigraphy of Waterside Beach provides important information for facies and facies relationships of transgressive gravel-, muddy gravel-, and mixed sand and gravel-beaches preserved in the rock record. Firstly, it is observed that architecture, thickness, and extent of transgressive gravel-beach deposits are significantly influenced by the occurrence and size of associated tidal creeks. The size of these creeks is a function of the tidal prism (Allen 1997, 2000; French 1993; Pye and French 1993). The successions in strip logs 2A, 2B, and 2C are very thick reflecting the megatidal nature of Waterside Beach. The thickness of these units will decrease with a reduction in tidal range; hence, the thick deposits observed in these strip logs are applicable to upper mesotidal to megatidal settings. Strip logs 1A, 1B, and 1C depict much thinner sedimentary successions typical of beach and shoreface sediments deposited outside the zone of tidal-creek influence (Fig. 4.2). The thickness of these deposits is controlled by the rate of sedimentation, transgression, and by wave action, and is independent of tidal range. Strip logs 1A, 1B, and 1C are therefore, applicable to transgressive gravel, muddy gravel, and mixed sand and gravel successions in any tidal setting.

Secondly, sedimentation rate versus trangression rate controls the thickness and architecture of the preserved succession. In rapidly transgressing systems and / or those with limited sediment supply, the preserved succession tends to be thin, either manifested as a gravel lag (Strip log 1C, Fig. 4.6) or as a thin (< 2 m thick) shore-normal gravel deposit where tidal creeks debouch onto the beach (Strip log 2C, Fig. 4.6). In both cases the successions are capped by lower shoreface silty sand and clayey silt deposits. This depositional setting is similar to described transgressive beach successions and the transgressive components of progradational deposits, which tend to be thin (commonly manifested as a wave-winnowed, gravel lag) and grade quickly upward into offshore, muddy marine facies (Bourgeois and Leithold 1984; Clifton 1981;

Massari and Parea 1988). A beach and shoreface succession that results from a rapidly transgressing shoreline with a limited sediment supply represents one end member of possible successions that may occur. The other end member is illustrated in strip logs 1A and 2A, which are the expected successions when the sedimentation rate is high relative to the transgression rate. These deposits tend to be much thicker and occur at or near the maximum transgressive shoreline.

The stratigraphic successions depicted in strip logs 2A, 2B, and 2C (Fig. 4.6) develop over an erosional surface into salt-marsh deposits scoured by Long Marsh Creek and enhanced by wave action on the beach (Map 2004, Fig. 4.2). Consequently, the zone of thick beach deposits develops perpendicular to the strike of the beach and may be mistaken for fluvial or estuarine deposits. This is a significant problem in rapidly transgressing systems where the beach tends to be manifested as a thin gravel lag and the tidal-creek influenced deposit as a shore-normal gravel unit up to 2 m thick (Strip logs 1C and 2C, Fig. 4.6). The original depositional environment may be ascertained if sedimentary structures, such as steeply landward-dipping gravel beds (D8), horizontal mud beds (D11), and muddy conglomerates (D8) are observed.

CONCLUSIONS

Waterside Beach deposit can be subdivided into eleven sedimentologically distinct deposits that represent three main depositional environments: (1) sandy foreshore and shoreface; (2) tidal-creek braid-plain and delta; and, (3) wave-deposited gravel and sand bars, and associated deposits. Sandy foreshore and shoreface deposits encompass aeolian-deposited sand of the backshore (D1), moderately seaward-dipping (3–5°) mixed sand and gravel of the beachface (D2), and a shallowly seaward-dipping terrace comprising intertidal sand (D3) and silty sand (D4), and subtidal silty sand and clayey silt deposits (D5). Deposit 6 includes terrace sediments reworked or deposited by tidal creeks. Sand and fine gravel removed from the upper and middle intertidal is deposited

in the lower intertidal and subtidal components of the terrace forming a sand 'delta' (D7). This sediment is then transported onshore by waves as unstable, low-amplitude sandy bars of D9. Deposits 8 and 10 represent gravel deposited by large, landward-migrating gravel bars (up to 5.5 m high, 800 m long). These bars form and migrate in response to surf-zone processes (Kroon and Masselink 2002) and are considered subtidal (shoreface) features exposed as a result of the extreme tidal range. D11 represents the zones of mud deposition developed on the landward side of large gravel bars.

The occurrence of mud beds in a conglomeratic succession is most indicative of upper mesotidal to megatidal conditions at the time of deposition, and may indicate subaerial exposure of mud beds resulting in dewatering, desiccation, and algal binding of the mud. Muddy, clast- and matrix-supported conglomerates may develop from subtidally formed gravel bars, intertidal bars or mud-laden seawater. If bedding is apparent in a muddy conglomerate it more likely develops from mud-laden seawater seeping through the gravel. A lack of bedding may be more indicative of bar migration over soupy mud deposits in either a subtidal or intertidal setting.

The thickness and preservation of transgressive gravel beaches is dependent on tidal regime, sedimentation rate, and transgression rate. In areas where tidal creeks do not influence sedimentation on the beach, a preserved sequence will be thin, consisting of an upward-deepening (fining) profile (Strip logs 1A, 1B, and 1C, Fig. 4.6). Conversely, where tidal creeks do occur landward of the beach, the beach sequence tends to be much thicker (Strip log 2A, 2B, and 2C, Fig. 4.6). The thickness of the succession is largely controlled by the occurrence and size of tidal creeks, which is proportional to the tidal prism. At Waterside Beach, the tidal prism is large, thus the preserved succession is thick. The thickness of the preserved succession is also strongly influenced by the rates of sedimentation and transgression. Where sedimentation is low and transgression rapid, the preserved deposits are thin – comprising either a thin conglomerate lag (Strip log 1C, Fig. 4.6) or a thin (< 2 m thick) gravel unit oriented shore-normally (Strip log 2C, Fig.

4.6). These successions would typically be capped by lower shoreface mud. At or near the maximum transgressive shoreline or in transgressive settings with high sedimentation rates the preserved gravel deposits are predicted to be much thicker (Strip logs 1A and 2A, Fig. 4.6).

REFERENCES

Allen, J.R.L., 1997, Simulation models of salt-marsh morphodynamics: some implications for high-intertidal sediment couplets related to sea level change: Sedimentary Geology, v. 113, p. 211-223.

Allen, J.R.L., 2000, Morphodynamics of Holocene salt marshes: a review sketch from the Atlantic and Southern North Sea coasts of Europe: Quaternary Science Reviews, v. 19, p. 1155-1231.

Amos, C.L., 1987, Fine-grained sediment transport in Chignecto Bay, Bay of Fundy, Canada: Continental Shelf Research, v. 7, p. 1295-1300.

Amos, C.L., and Asprey, K.W., 1979, Geophysical and sedimentary studies in the Chignecto Bay system, Bay of Fundy - a progress report, Geological Survey of Canada, p. 245-252.

Amos, C.L., Tee, K.T., and Zaitlin, B.A., 1991, The post-glacial evolution of Chignecto Bay, Bay of Fundy, and its modern environment of deposition, *in* Smith, D.G., Reinson, G.E., Zaitlin, B.A., and Rahmani, R.A., eds., Clastic Tidal Sedimentology: Calgary, AB, Canada, Canadian Society of Petroleum Geologists, p. 59-89.

Anthony, E.J., Levoy, F., and Monfort, O., 2004, Morphodynamics of intertidal bars on a megatidal beach, Merlimont, Northern France: Marine Geology, v. 208, p. 73-100.

Bartholomä, A., Ibbeken, H., and Schleyer, R., 1998, Modification of gravel during longshore transport (Bianco Beach, Calabria, southern Italy): Journal of Sedimentary Research, v. 68, p. 138-147.

Bluck, B.J., 1967, Sedimentation of beach gravels: Examples from south Wales: Journal of Sedimentary Petrology, v. 37, p. 128-156.

Bluck, B.J., 1999, Clast assembling, bed-forms, and structure in gravel beaches: Transactions of the Royal Society of Edinburgh, Earth Sciences, v. 89, p. 291-323.

Boggs, S., Jr., 1995, Principles of Sedimentology and Stratigraphy, 2nd edition: New Jersey, Prentice-Hall, 774 p.

Bouma, A.H., 1969, Methods for the Study of Sedimentary Structures: New York, John Wiley & Sons, 458 p.

Bourgeois, J., and Leithold, E.L., 1984, Wave-worked conglomerates - depositional processes and criteria for recognition, *in* Koster, E.H., and Steel, R.J., eds., Sedimentology of Gravels and Conglomerates: Calgary, AB, Canada, Canadian Society of Petroleum Geologists, p. 331-343.

Caddell, E.M., and Moslow, T.F., 2004, Outcrop sedimentology and stratal architecture of the Lower Albian Falher C sub-Member, Spirit River Formation, Bullmoose Mountain, northeastern British Columbia: Bulletin of Canadian Petroleum Geology, v. 52, p. 4-22.

Carr, A.P., 1969, Size grading along a pebble beach: Chesil Beach, England: Journal of Sedimentary Petrology, v. 39, p. 297-311.

Carr, A.P., Gleason, R., and King, A., 1970, Significance of pebble size and shape in sorting by waves: Sedimentary Geology, v. 4, p. 89-101.

Church, M.A., Mclean, D.G., and Wolcott, J.F., 1987, River bed gravels: Sampling and analysis, *in* Thorne, C.R., Bathurst, J.C., and Hey, R.D., eds., Sediment Transport in Gravel-Bed Rivers: Chichester, U.K., John Wiley & Sons, p. 43-79.

Clifton, H.E., 1981, Progradational sequences in Miocene shoreline deposits, southeastern Caliente range, California: Journal of Sedimentary Petrology, v. 51, p. 165-184.

Clifton, H.E., 1988, Sedimentologic approaches to paleobathymetry, with applications to the Merced Formation of central California: Palaios, v. 3, p. 507-522.

Dashtgard, S.E., and Gingras, M.K., 2005, Facies architecture and ichnology of recent salt-marsh deposits: Waterside Marsh, New Brunswick, Canada: Journal of Sedimentary Research, v. 75, p. 596-607.

Folk, R.L., and Ward, W.C., 1957, Brazos River bar: A study in the significance of grain size parameters: Journal of Sedimentary Petrology, v. 27, p. 3-26.

Forbes, D.L., and Taylor, R.B., 1987, Coarse-grained beach sedimentation under paraglacial conditions, Canadian Atlantic Coast, *in* FitzGerald, D.M., and Rosen, P.S., eds., Glaciated Coasts: San Diego, U.S.A., Academic Press, p. 51-86.

French, J.R., 1993, Numerical simulation of vertical marsh growth and adjustment to accelerated sea-level rise, north Norfolk, U.K.: Earth Surface Processes and Landforms, v. 18, p. 63-81.

Greenwood, B., and Davidson-Arnott, R.G.D., 1979, Sedimentation and equilibrium in wave-formed bars: a review and case study: Canadian Journal of Earth Sciences, v. 16, p. 312-332.

Hart, B.S., and Plint, A.G., 1989, Gravelly shoreface deposits: a comparison of modern and ancient facies sequences: Sedimentology, v. 36, p. 551-557.

Hart, B.S., and Plint, A.G., 2003, Stratigraphy and sedimentology of shoreface and fluvial conglomerates: insights from the Cardium Formation in NW Alberta and adjacent British Columbia: Bulletin of Canadian Petroleum Geology, v. 51, p. 437-464.

Hoey, T.B., 2004, The size of sedimentary particles, *in* Evans, D.J.A., and Benn, D.I., eds., A Practical Guide to the Study of Glacial Sediments: London, U.K., Arnold Publishers, p. 52-77.

King, C.A.M., 1972, Beaches and Coasts: London, UK, Edward Arnold, 570 p.

King, C.A.M., and Williams, W.W., 1949, The formation and movement of sand bars by wave action: Geographical Journal, v. 113, p. 70-85.

Kirk, R.M., 1980, Mixed sand and gravel beaches: morphology, processes and sediments: Progress in Physical Geography, v. 4, p. 189-210.

Kroon, A., and Masselink, G., 2002, Morphodynamics of intertidal bar morphology on a macrotidal beach under low-energy wave conditions, North Lincolnshire, England: Marine Geology, v. 190, p. 591-608.

Krumbein, W.C., and Pettijohn, F.J., 1938, Manual of Sedimentary Petrology: New York, Appleton-Century Crofts, 549 p.

Maejima, W., 1982, Texture and stratification of gravelly beach sediments, Enju Beach, Kii Peninsula, Japan: Journal of Geosciences, Osaka City University, v. 25, p. 35-51.

Massari, F., and Parea, G.C., 1988, Progradational gravel beach sequences in a moderate- to high-energy, microtidal marine environment: Sedimentology, v. 35, p. 881-913.

Masselink, G., 1993, Simulating the effects of tides on beach morphodynamics: Journal of Coastal Research Special Issue, v. 15, p. 180-197.

Masselink, G., and Short, A.D., 1993, The effect of tidal range on beach morphodynamics and morphology: a conceptual beach model: Journal of Coastal Research, v. 9, p. 785-800.

Mccave, I.N., and Geiser, A.C., 1978, Megaripples, ridges and runnels on intertidal flats of the Wash, England: Sedimentology, v. 26, p. 353-369.

Mclean, R.F., and Kirk, R.M., 1969, Relationships between grain size, size-sorting, and foreshore slope on mixed sand-shingle beaches: New Zealand Journal of Geology and Geophysics, v. 12, p. 138-155.

Mcleod, M.J., and Johnson, S.C., 1999, Bedrock geological compilation of the Alma map area (NTS 21 H/14), Albert County, New Brunswick: New Brunswick Department of Natural Resources and Energy, Minerals and Energy Division.

Nemec, W., and Steel, R.J., 1984, Alluvial and coastal conglomerates: their significant features and some comments on gravelly mass-flow deposits, *in* Koster, E.H., and Steel, R.J., eds., Sedimentology of Gravels and Conglomerates: Calgary, AB, Canada, Canadian Society of Petroleum Geologists, p. 1-31.

Plint, A.G., 1986, Slump blocks, intraformational conglomerates and associated erosional structures in Pennsylvanian fluvial strata of eastern Canada: Sedimentology, v. 33, p. 387-399.

Postma, G., and Nemec, W., 1990, Regressive and transgressive sequences in a raised Holocene gravelly beach, southwestern Crete: Sedimentology, v. 37, p. 907-920.

Pye, K., and French, P.W., 1993, Erosion and acretion processes on British Salt Marshes, Vol. 1, Introduction: Saltmarsh Processes and Morphology: Cambridge, U.K., Cambridge Environmental Research Consultants.

Rampton, V.N., Gauthier, R.C., Thibault, J., and Seaman, A.A., 1984, Quaternary Geology of New Brunswick, v. Memoir 416: Ottawa, Geological Survey of Canada.

Reading, H.G., and Collinson, J.D., 1996, Clastic Coasts, *in* Reading, H.G., ed., Sedimentary Environments; Processes, Facies and Stratigraphy: Oxford, U.K., Blackwell Science, p. 154-231.

Rice, S., and Church, M.A., 1996, Sampling surficial fluvial gravels: The precision of size distribution percentile estimates: Journal of Sedimentary Research, v. 66, p. 654-665.

Roy, P.S., Cowell, P.J., Ferland, M.A., and Thom, B.G., 1994, Wave-dominated coasts, *in* Carter, R.W.G., and Woodroffe, C.D., eds., Coastal Evolution: Late Quaternary Shoreline Morphodynamics: Cambridge, U.K., Cambridge University Press, p. 121-186.

St. Peter, C., 1996, Carboniferous geology of the Waterside-Midway area (NTS 21 H/ 10f), Albert County, New Brunswick: New Brunswick Department of Natural Resources and Energy, Minerals and Energy Division.

Sunamura, T., and Takeda, I., 1984, Landward migration of inner bars: Marine Geology, v. 60, p. 63-78.

Wescott, W.A., and Ethridge, F.G., 1982, Bathymetry and sediment dispersal dynamics along the Yallahs fan delta front, Jamaica: Marine Geology, v. 46, p. 245-260.

Wolman, M.G., 1954, A method for sampling coarse river-bed material: Transactions, American Geophysical Union, v. 35, p. 951-956.

Wright, L.D., Nielsen, P., Short, A.D., and Green, M.O., 1982, Morphodynamics of a macrotidal beach: Marine Geology, v. 50, p. 97-128.

Yang, B.C., Dalrymple, R.W., and Chun, S.S., 2005, Sedimentation on a wave-dominated, open-coast tidal flat, south-western Korea: a summer tidal flat - winter shoreface: Sedimentology, v. 52, p. 235-252.

Zonneveld, J.-P., and Moslow, T.F., 2004, Exploration potential of the Falher G shoreface conglomerate trend: evidence from outcrop: Bulletin of Canadian Petroleum Geology, v. 52, p. 23-38.

CHAPTER 5: EFFECTS OF RELATIVE SEA LEVEL CHANGE ON THE DEPOSITIONAL ARCHITECTURE OF AN EMBAYED BEACH, BAY OF FUNDY, CANADA[4]

INTRODUCTION

High-resolution sequence stratigraphy is an important tool in determining the distribution of sediments in the rock record and for predicting basin evolution. In modern settings high-resolution sequence stratigraphic studies are uncommon due to the relatively short time scale represented by modern deposits, the lack of accessibility of historical sediment-stacking patterns and a paucity of geophysical data. At Waterside Beach, New Brunswick, Canada joint geologic and geophysical investigations of shallow-marine sediments provide an opportunity to examine the evolution of an embayed gravel-dominated coastal setting (in this case within Chignecto Bay) as a function of relative sea level change. The resulting model is used to refine existing paleoenvironmental reconstructions (Amos et al. 1991; Amos and Zaitlin 1985) of the bay over the past 13 000 years. Understanding the near-shore response of dynamic sedimentary patterns has important implications for high-resolution sequence stratigraphic analyses. This is because the evolution of a beach is controlled not only by local hydraulic conditions, but reflects changes in basin configuration and is a tangible product of the evolution of the entire embayment. The embayment is, in turn, greatly influenced by changes in relative sea level.

Sequence stratigraphy provides a mechanism to predict the extent and evolution of sedimentary systems as a function of change in relative sea level (RSL) or base level (Catuneanu 2002, 2006; Embry 1993; Hunt and Tucker 1992; Posamentier and Allen 1999; Van Wagoner et al. 1990). In open-marine systems, RSL changes result

[4]A version of this chapter is being reviewed for publication in MARINE GEOLOGY as "Effects of relative sea level change on the depositional architecture of an embayed beach, Bay of Fundy, Canada" by Shahin E. Dashtgard, Richardo O. White , Karl E. Butler, and Murray K. Gingras

in predictable changes in the depositional style at and near the coastline (Catuneanu 2002; Dalrymple et al. 1992; Reading and Collinson 1996; Roy et al. 1994). However, within bays and other semi-enclosed seaways, similar changes can significantly alter the depositional style throughout the sedimentary basin. In Chignecto Bay, RSL fall and rise over the past 13 000 years has considerably influenced local hydraulic conditions – particularly tides (Amos et al. 1991; Shaw et al. 2002). These changes in tidal regime have altered the depositional style and architecture of both the embayment (Amos et al. 1991; Amos and Zaitlin 1985) and the coastal zone, including salt marshes (Allen 2000; Dashtgard and Gingras 2005; Pye and French 1993; Redfield 1972) and beaches (Dashtgard et al. 2006; Masselink 1993; Masselink and Short 1993; Short 1991).

Salt marshes mainly comprise a vegetated platform and a network of tidal channels (Allen 1997, 2000). The tidal channels may be subdivided into two groups: deep and wide main channels, and small creeks that dissect the marsh surface. During RSL fall and lowstand, vertical aggradation of the salt-marsh is minimal as it is rarely flooded and tidal creeks tend to be poorly developed or absent (Allen 1990, 1997, 2000; Redfield 1972). During RSL rise, the marsh is regularly flooded at high tide and aggrades at a rate proportional to the rise (Allen 1997, 2000). Early RSL rise is marked by an expansion (in cross-sectional area) of tidal creeks and an increase in the areal density of smaller creeks that dissect the marsh surface (French 1993; Pye and French 1993). With continued RSL rise, small tidal creeks tend to silt in, whereas the main tidal channels expand in width and depth (Allen 1997). The salt marsh plays a pivotal role in beach morphodynamics partly because of its resistance to erosion, and partly in its capacity as a major sediment sink and productive zone for organic material (Allen 2000; Davidson-Arnott et al. 2002; Gordon et al. 1985; Gordon and Desplanque 1983). The tidal creeks are even more important in megatidal settings as they regulate the distribution, extent and thickness of sediment deposited on the beach.

Evolution of beach and shoreface systems in response to sea-level change is well documented (Catuneanu 2002; Roy et al. 1994; Walker and Plint 1992). During regression beaches tend to prograde with an accumulation of sediment in the foreshore and upper shoreface: this is accompanied by erosion in the lower shoreface (Reading and Collinson 1996; Roy et al. 1994). These deposits tend to be thick and preferentially preserve upper shoreface and foreshore sediments (Bourgeois and Leithold 1984; Clifton 1981; Engels and Roberts 2005; Massari and Parea 1988; Walker and Plint 1992). Conversely, during transgression, beaches display erosion in the foreshore and upper shoreface and deposition in the lower shoreface and offshore (Reading and Collinson 1996; Roy et al. 1994). Transgressive beach (shoreface) deposits tend to be thin with a basinward shift in facies vertically up through the succession (Bourgeois and Leithold 1984; Dashtgard et al. 2006).

Waterside Beach is a trangressive beach backed by a salt marsh along much of its length. The relationship between salt marsh and beach is dynamic and the presence of each influences the depositional style of the other (Dashtgard and Gingras 2005; Dashtgard et al. 2006). Consequently, these two systems must be considered together when considering their sedimentary response to changes in sea level and tidal regime.

Tides and Relative Sea Level in the Bay of Fundy

The Bay of Fundy is famous for having the highest tides in the world – amplified from a mean tidal range of 5 m at the bay mouth to over 12 m at the head of the Minas Basin (Fig. 5.1; Desplanque and Mossman, 2001). Tidal amplification is a relatively recent phenomenon; however, having occurred only in the past 7 000 to 6 000 years (Grant 1970; Scott and Greenberg 1983; Shaw et al. 2002). In consequence, strongly macrotidal (i.e. megatidal) conditions are limited to the past 4 000 years (Scott and Greenberg 1983). This change in tidal conditions resulted from forebulge migration and post-glacial uplift of Georges Banks restricting water flow in and out of the Bay of Fundy

/ Gulf of Maine system (Fig. 5.1) and is considered to be independent of relative sea-level changes in the Bay of Fundy (Grant 1970, 1980; Quinlan and Beaumont 1981; Scott and Greenberg 1983; Shaw and Courtney 2002).

Post-glacial changes in sea level are more complex than changes in tidal range. Approximately 13 000 years ago (13 ka), the upper Bay of Fundy was submerged 30 m below present-day sea level (Amos et al. 1991; Grant 1970; Shaw and Courtney 2002). From 13 to 6.5 ka isostatic rebound resulted in emergence of the bay reaching a maximum lowstand 25 to 30 m below present sea level (Amos et al. 1991; Amos and Zaitlin 1985; Grant 1980; Scott and Greenberg 1983; Shaw et al. 2002). This drop in RSL was significant as Chignecto Bay evolved into a wave-dominated estuary separated from the rest of the Bay of Fundy by a gravel spit across its mouth – 15 km southwest of Waterside Beach (Fig. 5.1B; Amos et al., 1991). The past 6 500 years is marked by transgression, partly resulting from RSL rise and partly from tidal amplification up the bay (Amos et al. 1991; Grant 1970; Scott and Greenberg 1983). These different periods of sea-level rise and fall are recorded in the preserved sedimentary sequence at the base of the bay and are described in detail by Amos and Zaitlin (1985) and Amos et al. (1991).

The post-glacial record of Waterside Beach reflects the changes in RSL and tidal amplitude of the Bay of Fundy. This paper attempts to examine the Quaternary succession at Waterside Beach through seismic interpretation and sedimentological characteristics, and thereby, establish sedimentary units representing the different stages of RSL rise and fall. The relationship between the different units is described and the evolution of the beach discussed. Finally, a discussion is presented on the implications of this study to high-resolution sequence stratigraphic analyses conducted within embayed settings.

Study Area

Waterside Beach, New Brunswick, Canada occurs on the north shore of Chignecto Bay (Fig. 5.1). It experiences megatidal (> 6 m spring-tide range) conditions and is oriented perpendicular to the dominant wind direction (Amos and Asprey 1979; Amos et al. 1991). The spring-tide range exceeds 11.5 m, whereas the neap-tide range is 6 m. The beach is oriented northwest-southeast and is perpendicular to the full fetch of the Bay of Fundy (Fig. 5.1). Under fair-weather conditions significant wave heights (H_s) rarely exceed 0.75 m with periods (T) of 6 s or less (Amos et al., 1991). During storms, H_s may exceed 3.0 m (T > 10 s; Amos et al., 1991). Waterside is a transgressive beach that comprises a narrow backshore; moderately dipping (2–5°) beachface; and a 1.5 to 2 km wide, low angle (generally < 0.5°) intertidal and subtidal terrace composed of sand and/or gravel (Dashtgard et al. 2006). Within the intertidal zone, from the mouth of Newfoundland Creek southeast to the mouth of Long Marsh Creek, salt-marsh deposits are sporadically exposed (Fig. 5.1C). These deposits form the base upon which the beach resides.

Methods

Seismic Acquisition and Processing

This study incorporates two sets of shallow-marine seismic profiles collected over the intertidal and subtidal zones of Waterside Beach (Fig. 5.2) during a reconnaissance survey in 2003 and a detailed follow-up survey in 2004 (White et al. 2006). The data were acquired using the high-resolution IKB Seistec™ profiler, which is equipped with a broadband electrodynamic boomer source (~ 1 to 10 kHz bandwidth) and a special vertical line-in-cone receiver. Both the boomer and receiver are mounted on a floating catamaran frame (Simpkin and Davis 1993). The fixed geometry and short distance (70 cm) between the source and receiver make this system particularly well suited for

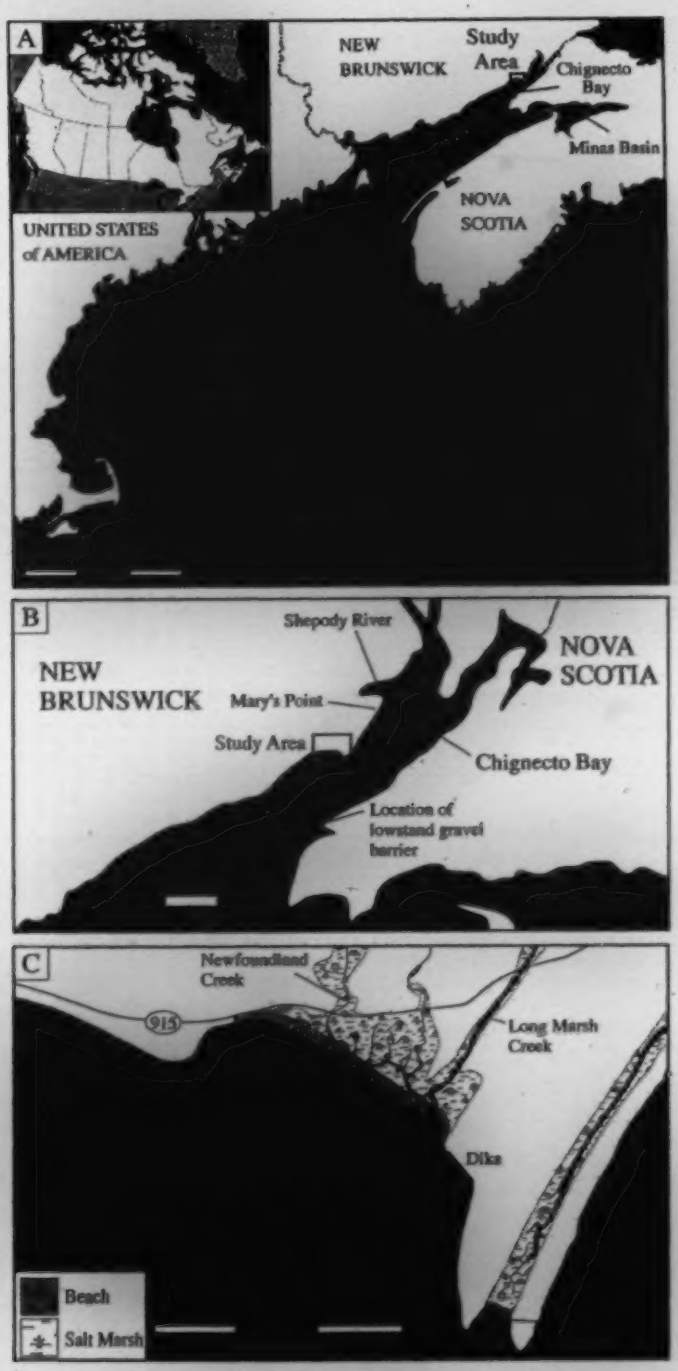

FIGURE 5.1 – Location map of the study area. (A) Map of the Gulf of Maine / Bay of Fundy system with the location of the study area indicated. (B) Close up map of Chignecto Bay. Mary's Point and Shepody River are areas of active mud deposition referred to in the text. The black line across the bay indicates the approximate location of the lowstand gravel barrier reported by Amos et al. (1991) that is referred to in the text. (C) Close up of Waterside Beach.

operations in very shallow water. Sub-bottom reflections exhibit a dominant frequency of approximately 4.5 kHz and provide a vertical resolution on the order of 20 cm in unconsolidated sediments.

The boomer source was fired at intervals ranging from 0.25 to 0.5 s, thereby providing trace spacing of 0.5 to 1 m at an average boat speed of 2 m/s (4 knots). In 2003, positions were recorded using a sub-meter precision DGPS while in 2004 positions were recorded using a dual frequency differential global positioning system (DGPS with a local base station providing centimeter precision. Approximately 19 km of data were collected during the 2003 survey. In 2004, we used an experimental dual profiler approach (see White et al., 2006) to acquire 50 km of seismic. The centerlines of the dual profilers were approximately 50 m apart, with two to three profiles collected per swath. The results presented here, however, are based on results from one profiler only. The 2003 seismic data was reduced to Canadian Hydrographic Service Chart Datum using predicted tidal values for the area. The 2004 data was reduced to a datum of 4 m above mean sea level (to avoid truncating shallow reflections in the intertidal zone) by using tides inferred from the measured DGPS heights. A uniform seismic velocity of 1500 m/s - the nominal speed of sound in water at the temperatures and salinities typical of those in the Bay of Fundy - was used for time-to-depth conversions. This provides minimum estimates of sub-bottom depths and sediment thicknesses given that acoustic velocities measured for sediments in shallow (~ 1 m deep) drop cores averaged approximately 1580 m/s.

Following data acquisition, the seismic data were debiased, band pass filtered and resampled from 10 to 20 microseconds. A spherical divergence correction and exponential gain function and were applied to boost the amplitudes of deeper reflections. Heave was removed from the data by applying a zero phase moving average filter to the

water bottom arrival times (White et al., 2006). This process of water bottom smoothing was effective, but, as a side effect it also smoothed any short wavelength bottom topography having a wavelength less than or comparable to the distance traveled by the profiler.

Sedimentological Methods

The sedimentological character of the beach was determined in the intertidal and backshore zones through surface sampling and GPS mapping in 2003 and 2004. Subtidal sediments were sampled in 2005 through a combination of drop coring and grab sampling. Six drop cores were collected from 32 attempts and were analyzed at the Bedford Institute of Oceanography (BIO) in Dartmouth, Nova Scotia, Canada. The orientation of the drop cores was initially assumed to be vertical; however, the steep dip of beds and laminae in the recovered mud suggests that most of the cores entered the sediment at an angle. More importantly, the bedding dips increase down through the core suggesting that the coring device continued to tip over after entering the sediment. This likely resulted from strong tidal currents (up to 1 m/s) and boat movement causing the coring device to deviate from a vertical orientation before and during penetration of the sea bottom. Cores were subjected to full-diameter and split-core analyses. Full-diameter tests included: (1) multi-sensor track analysis to establish density, horizontal acoustic velocity, and magnetic susceptibility; and, (2) x-ray imaging to determine the dominant dip direction. The core was then split along the dominant dip direction, logged, and photographed. Further split-core analysis included: spectral reflectance; shear strength from plugs (every 10 cm); assessment of water content to estimate porosity (by comparing to density measurements); and, vertical and horizontal acoustic velocity measurements (taken every 10 cm). Finally, 1 cm thick slabs were extracted from the face of the split core and x-rayed to observe sedimentological and ichnological characteristics of the sediment.

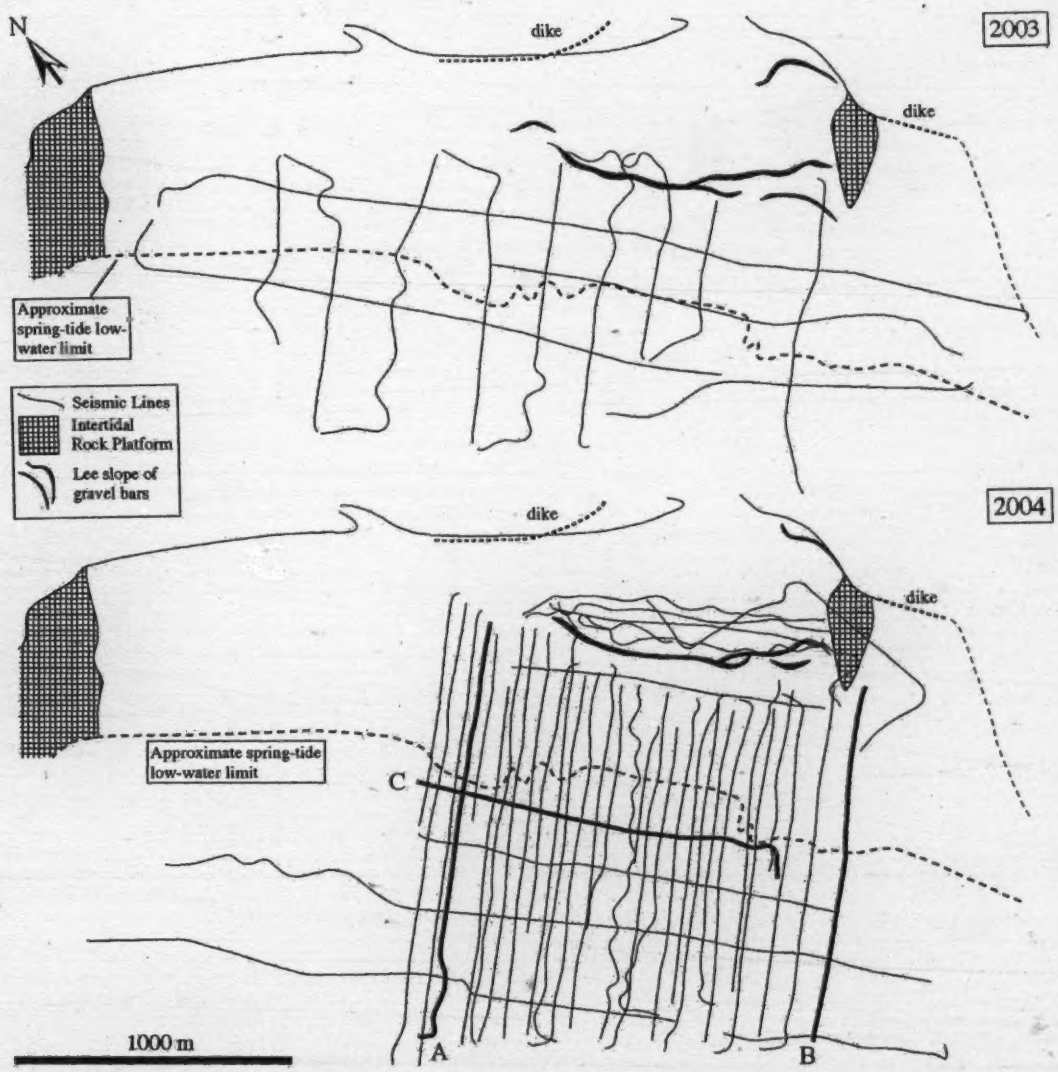

FIGURE 5.2 – Maps of Waterside Beach indicating the location of seismic surveys collected in 2003 and 2004. The heavy lines labeled A, B, and C on the 2004 survey map indicate lines presented in Figures 5.3, 5.4, and 5.5, respectively.

Thirty grab samples were attempted resulting in the acquisition of 27 samples. Grab samples were dried at 105° C for 24 hours and then disaggregated using a mortar and pestle. The disaggregated samples were then dry sieved at one phi-size intervals to the fine-grained / very-fine grained sand break (3 ϕ). A representative sub-sample was then extracted from the remaining sediment and analyzed on a Micrometrics Sedigraph

5100. Grain-size data are arithmetic means determined using the method of moments converted to the phi scale. Average sand, silt, and clay contents are also reported.

RESULTS AND DISCUSSION

Interpretation of seismic surveys in conjunction with the data provided from surface mapping, grab sampling, and drop coring resulted in the identification of bedrock, a glacio-marine unit, and three post-glacially deposited units to a depth of 20 m (depth of seismic penetration) below Waterside Beach (Figs. 5.3, 5.4, and 5.5). Line A in Figure 5.3 is a shore-normal profile that delineates the four glacial and post-glacial units. The glacio-marine deposit is identified by the occurrence of moderately dipping reflectors (2-4°) within the deposit. Basinward of this is the laminated silty sand unit (LSSU) characterized by shallow seaward-dipping reflectors. Overlying the glacial sediments and landward of the LSSU are salt-marsh sediments, and capping the whole sequence are mixed sand and gravel beach sediments. The bedrock surface (Carboniferous and Triassic rock), underlying the sediments can be seen dipping seaward at an apparent angle of 1.7° at the landward end of Line B (Fig. 5.4). Figure 5.6 is a plan-view map of Waterside Beach revealing where the various seismic units outcrop on the seafloor. In the case of the salt-marsh unit, it does not outcrop, but subcrops below the beach sediments (Fig. 5.6).

Steeply Dipping Reflector Unit (SDRU)

The deepest unit discernable on the seismic profiles is characterized by reflectors that exhibit an apparent dip of up to 4° towards the southwest on the shore-normal profiles (Figs. 5.3 and 5.4) and 3° to the southeast on the alongshore profiles (Fig. 5.5). The seismic character of this deposit varies along strike of the beach (Fig. 5.5). Towards the southeast, the apparent dip of the reflectors shallows to nearly horizontal. The basal contact is not discernable because of the limited depth of penetration of the seismic. The SDRU underlies all other deposits and hence, shares a contact with the laminated

silty sand unit, salt-marsh deposits, and beach sediments depending on the location of observation. This unit is exposed on the seafloor seaward of the beach in the southeast, where it forms a topographically positive feature 11.5 m below present-day mean sea level (Figs. 5.3, 5.6 and 5.7). Seismic mapping of the ridge depicts a linear feature that parallels the present-day shoreline (Fig. 5.7; White et al., 2006).

Grab samples of this unit recovered little to no sediment. Where sediment was recovered, it consisted of metamorphic and igneous cobbles and pebbles covered in barnacles and coated with mud. Recovered mud is soupy to semi-soupy and comprises clayey silt (8.3% sand, 59.9% silt, 31.8% clay) with a mean grain size of 5.5 ϕ. This composition and grain size is similar to those reported in Dashtgard et al. (2006) for modern mud deposits of the lower shoreface. Consequently, the interstitial mud accumulations retrieved during the grab sampling are considered to be post-depositional.

The SDRU is interpreted to be a glacio-marine unit equivalent to either the G4 (15 to 13.3 ka) or G3 (13 to 9 ka) deposits of Amos et al. (1991). The base of this deposit was not discernable on the seismic and therefore, its relationship to the underlying bedrock is unknown. If equivalent to G4, then the unit was deposited while glaciers of the Chignecto phase were retreating from the area and the SDRU comprises glacial-outwash material laid down in a marine setting. However, if equivalent to G3, the unit either comprises reworked till or gravel deposited at the paleo-shoreline between 13 and 9 ka. The above two scenarios are consistent with the internal architecture of the deposit and it's presence at depths 20 m below present sea level.

In the first scenario, this unit is considered to be glacial outwash comprising poorly sorted sand and gravel deposited as the glaciers of the Chignecto phase retreated approximately 13.5 ka (Rampton et al. 1984; Shaw et al. 2002; Stea 2005). Late Wisconsin glaciation of the Bay of Fundy area is complex, comprising 6 phases (Rampton et al. 1984). The oldest of these phases, from 18 to 13.5 ka, is referred to as the Chignecto phase, where ice flowed from the Escuminac Ice Center in the Gulf of

St. Lawrence, towards the southwest. The direction of ice flow was parallel to the main outcrop ridges in the area suggesting a major influence on the geography of Waterside Beach. The presence of internal reflectors with consistent dips suggests that this deposit is not a moraine or composed of poorly sorted till. Therefore, if the retreating glaciers deposited this unit, it is a glacial-outwash deposited in a marine setting. This hypothesis is supported by the composition and texture of pebbles and cobbles recovered while grab sampling (rounded to sub-rounded, metamorphic and igneous clasts), which do not reflect the composition of the local bedrock cliffs, but of rocks exposed 50 km to the northeast and 5 km NW of the beach. Moreover, the sediment would have been laid down in a marine environment as late Wisconsin glacial retreat was tracked by simultaneous marine advance over the isostatically depressed continent and continental shelf (Shaw et al. 2002).

The second scenario suggests that the SDRU is a paleo-beach that developed at the same time that G3 gravels were being deposited across Chignecto Bay between 13 and 9 ka (Amos et al. 1991). Initially, the G3 gravel was attributed to macrotidal conditions in the bay from 13.3 to 10 ka resulting in deflation of the sea bottom and development of a gravel pavement (Amos et al. 1991). However, macrotidal conditions at the time were not likely as tide heights in the bay are dependent on water exchange with the open ocean at Georges Bank (Fig. 5.1A). Recent modeling has shown that this exchange was restricted until ~ 8 ka; thus, the tidal range would likely have been microtidal (Scott and Greenberg 1983; Shaw and Courtney 2002; Shaw et al. 2002). It is possible that the SDRU developed as a beach during the Younger Dryas (~ 10.8 ka) glacial period (Stea 2005). Stea (2005) suggests that glaciation during the Younger Dryas was widespread across Nova Scotia and persisted for 800 years. This presents the possibility that ice rafting and deposition from the base of icebergs may be responsible for the widespread distribution of gravel at that time. Additionally, rapid melting of the Younger Dryas ice sheet and warming of the area could have resulted in increased

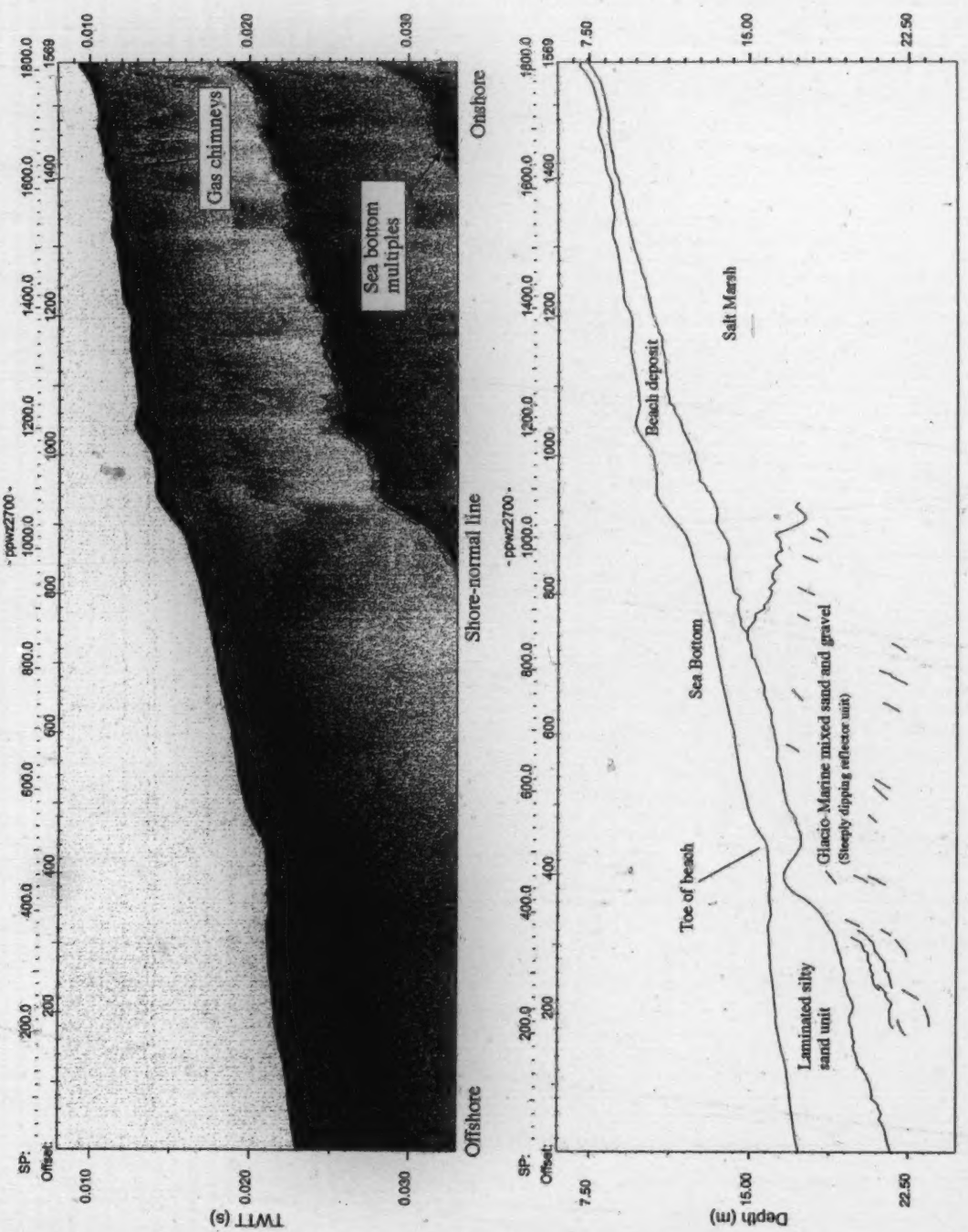

FIGURE 5.3 – Shore-normal Seistec profile A acquired near the central part of Waterside Beach (as shown in Fig. 5.2) and its line drawing interpretation. The 1500 m long profile is plotted with a vertical exaggeration of 30 times. Depths are expressed in meters below mean sea level.

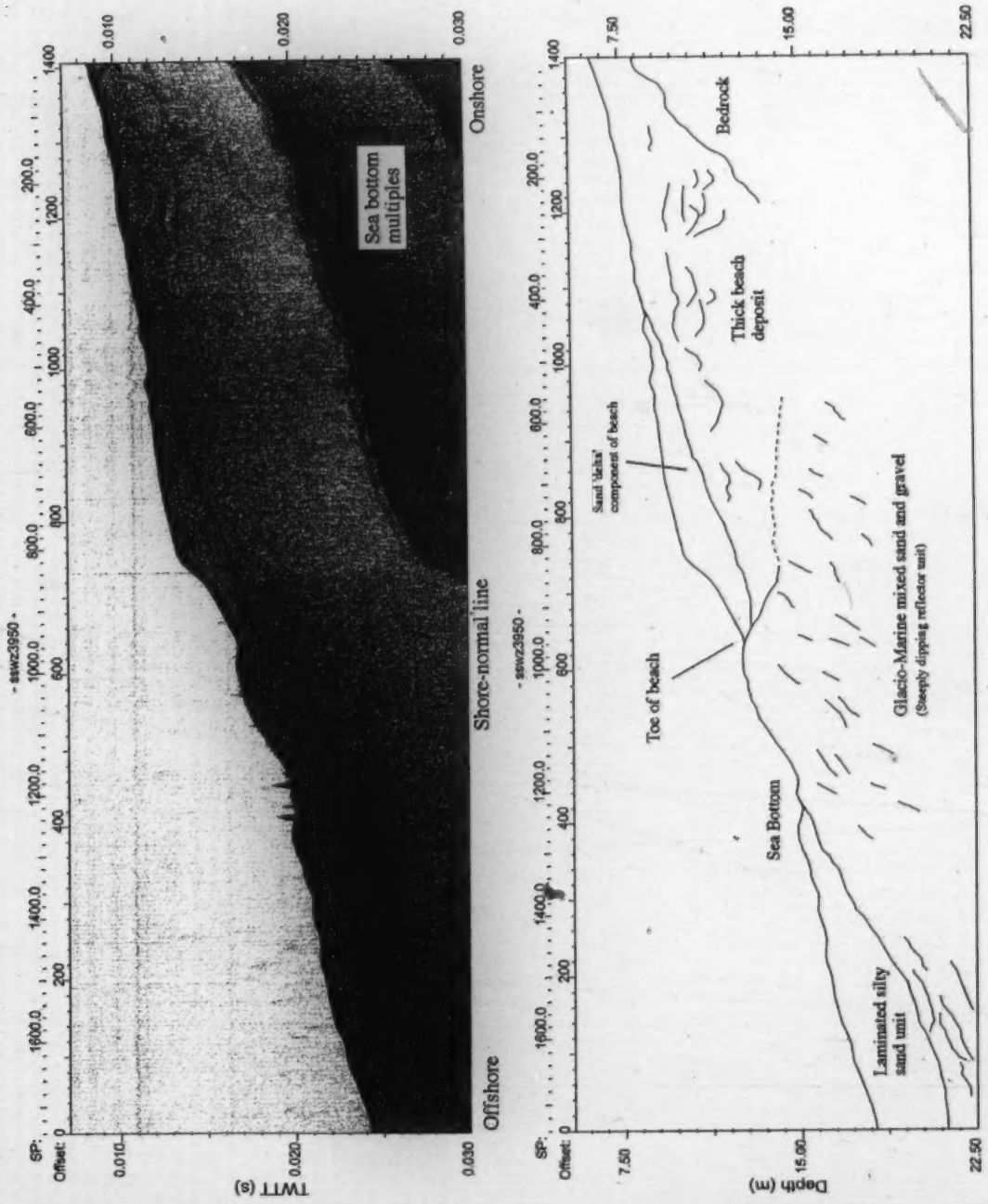

FIGURE 5.4 - Shore-normal Seistec profile B acquired near the southeastern end of Waterside Beach (as shown in Fig. 5.2) and its line drawing interpretation. The 1400 m long profile is plotted with a vertical exaggeration of 30 times. The sea-bottom parallel events that seem to cut through the bedrock reflector at the landward end of this line are though to be reverberations within the seismic profiler that were excited by the very strong sea-bottom reflection.

FIGURE 5.5 - Shore-parallel Seistec profile C located near the limit of the intertidal zone at Waterside Beach (as shown in Fig. 5.2) and its line drawing interpretation. The 1440 m long profile is plotted with a vertical exaggeration of 29 times. The contact between the salt marsh and underlying glacio-marine, steeply dipping reflector unit is clearly visible in the central to northwestern part of the profile.

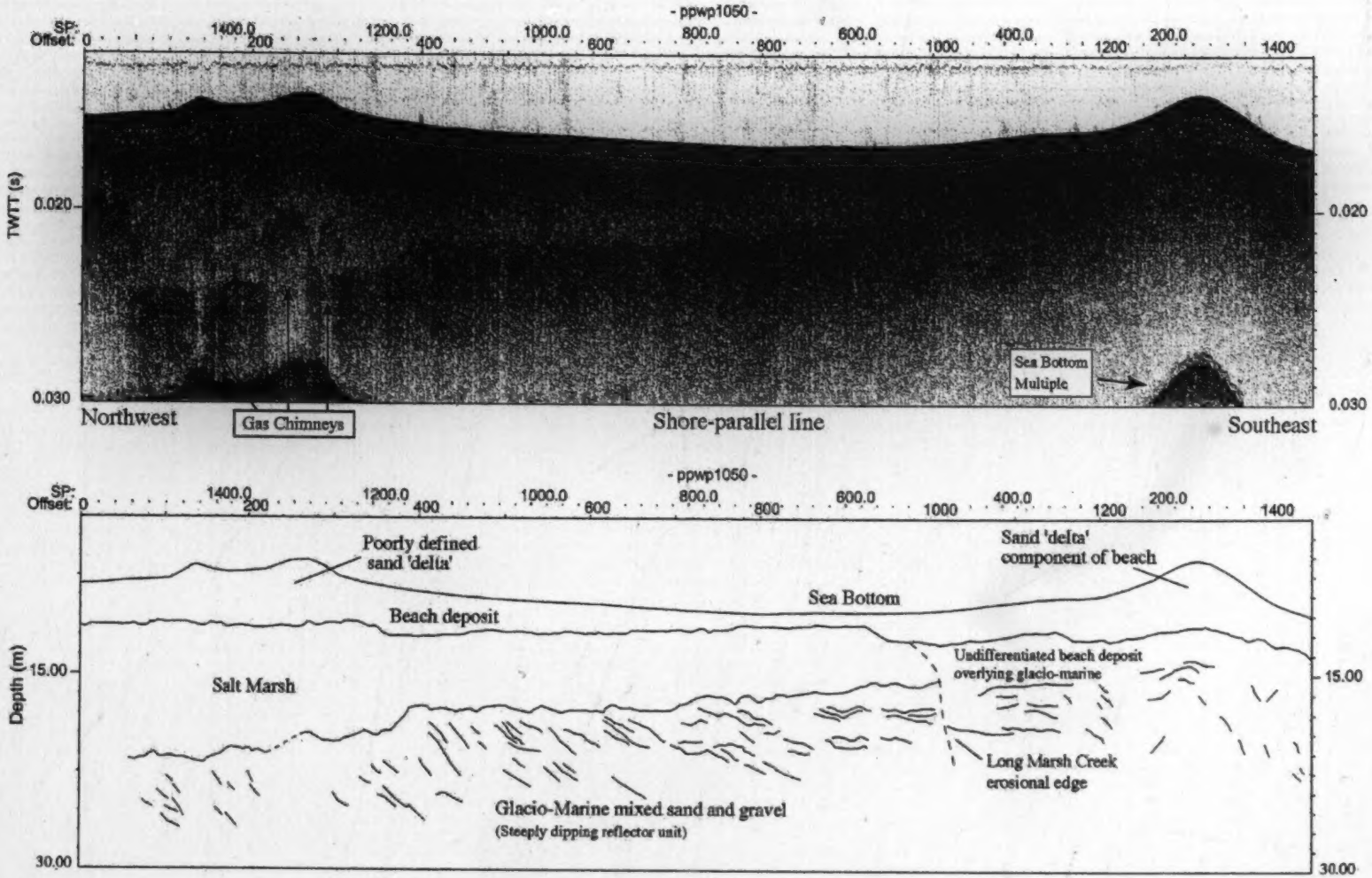
- ppwp1050 -
SP:
Offset:
TWTT (s)
0.020
0.030
Sea Bottom
Multiple
Northwest
Gas Chimneys
Shore-parallel line
Southeast
- ppwp1050 -
Depth (m)
15.00
30.00
Poorly defined
sand 'delta'
Sand 'delta'
component of beach
Sea Bottom
Beach deposit
Undifferentiated beach deposit
overlying glacio-marine
Salt Marsh
Long Marsh Creek
erosional edge
Glacio-Marine mixed sand and gravel
(Steeply dipping reflector unit)

headland erosion (of till deposited during the Chignecto phase) and deposition at the paleo-shoreline. The SDRU would then equate to a paleo-shoreline deposit that accumulated during a period of base-level fall and would be progradational. This hypothesis is supported by the orientation of the unit parallel to the modern shoreline, the dip of the beds (2-4°) – closely mirroring the dips of the present day beachface – and by the apparent shallowing of reflectors in a basinward direction (Figs. 5.3, 5.4, and 5.5).

Both hypotheses have merit for the formation of the SDRU. It is likely that the unit is a glacial-outwash deposit that developed in shallow-marine setting as the Chignecto phase glaciers retreated from the area. It is also likely that the unit was modified by waves during RSL fall and rise into a linear ridge that parallels the present-day shoreline and is perpendicular to the main fetch of the Bay of Fundy / Gulf of Maine system (Fig. 5.1). As a result of the uncertainty surrounding the genesis of this unit, it is referred to as a glacio-marine deposit.

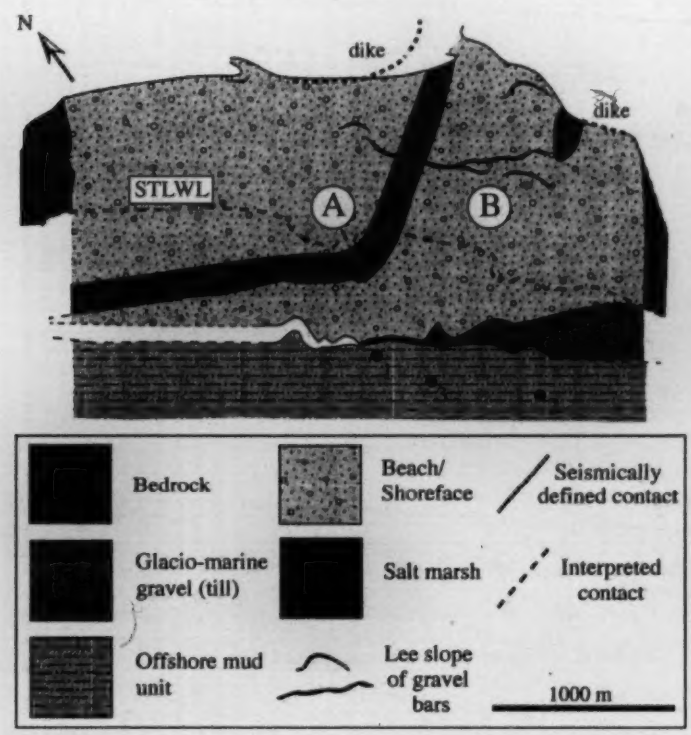

FIGURE 5.6 – Surface expressions of the units identified in this study. Note that the salt-marsh deposits subcrop below the beach sediments and do not outcrop on the sea bottom. The basinward depositional edge of the offshore mud unit was not encountered in this study. "A" refers to the area of the beach underlain by thick salt-marsh sediments. "B" indicates the region where the salt-marsh deposits are scoured into by the tidal creek resulting in deposition of a thick beach deposit. STLWL is the spring-tide low-water level. Points 1, 2, and 3 are the location of drop cores 1, 2, and 3 in Fig. 5.8, respectively.

Laminated Silty Sand Unit (LSSU)

Basinward of and overlying the SDRU is a unit comprising shallowly seaward dipping to horizontal reflectors. This unit only occurs basinward of the SDRU and is detached from the overlying beach deposits and laterally adjacent salt-marsh sediments (Figs. 5.3, 5.4, and 5.6). The sediments comprise semi-firm, silty sand with minor gravel (4.2% gravel, 45.7% sand, 33.4% silt, 16.8% clay). The mean grain size is 1.8 ϕ, but ranges from –1.9 to 3.3 ϕ. X-ray images of the upper 1.2 m of the unit (maximum drop-core penetration depth) indicate that sedimentary structures comprise horizontal to steeply dipping, interlaminated silty sand and sandy silt (Fig. 5.8). The laminae are wavy-parallel with interspersed thin sandy gravel lenses and organic detritus. Laminae are a few mm to cm thick and increase in dip from 8-10° near the surface (upper 20 cm) to over 25°, 60 cm below the sea bottom (Fig. 5.8). The dip of the laminae increases with depth as a result of the coring device entering the sediment at an angle and continuing to tip over

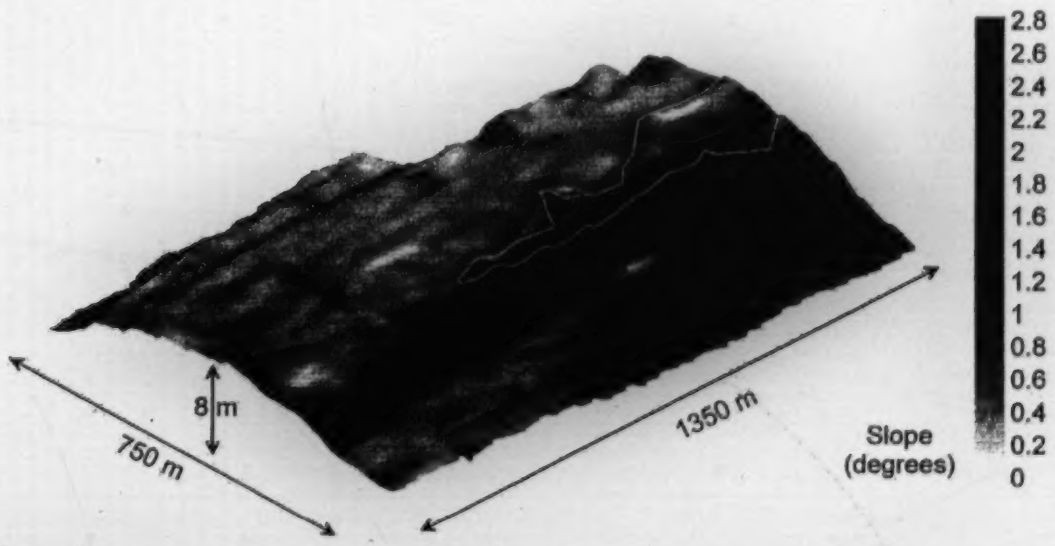

FIGURE 5.7 – Three-dimensional view, looking east, of the top of the glacio-marine steeply dipping reflector unit (SDRU) as mapped from sub-bottom profiles acquired in 2004 over the area shown in Fig. 5.2. The slope of the surface is superimposed as a grayscale map. A narrow zone outlined in white indicates where the glacio-marine unit is exposed on the seafloor offshore at the southeast end of Waterside Beach. The linear troughs and ridges oriented perpendicular to the shoreline are artifacts (line effects) related to slight inconsistencies in the way that the reflector was picked on adjacent lines.

after initial penetration. It is therefore likely that the bedding dips observed in the core are apparent and reflect core disturbance and not the true bed dips. Seismically, the LSSU is represented by discontinuous, sub-horizontal, sub-parallel reflectors (Figs. 5.3, 5.4; White et al., 2006. Throughout all cores, burrowing is uncommon, and includes *Planolites*; *Skolithos*; and, round, large-diameter, sand- or mud-filled *Thalassinoides* and *Teichichnus* (Fig. 5.8). Feeding structures or *Piscichnus*, are also common, and predominantly result from the feeding activity of Atlantic Sturgeon (Pearson et al. in press).

The laminated silty sand unit, as sampled with grabs and shallow drop cores, is compositionally similar to G1 (6 to 3 ka) deposits of Amos et al. (1991) and Amos and Zaitlin (1985). G2 (9 to 6 ka) deposits, comprising mud with minor sand, were presumably not encountered in the core. Amos et al. (1991) proposed that similar sediments (G1) located near the head of Chignecto Bay (northeast of the beach) were deposited via lateral accretion on tidal-creek point bars in an intertidal and shallow subtidal setting. A similar depositional setting is proposed for the LSSU; although, the seismic character suggests sheet-like deposition (tidal flat) and the ichnological character of the upper meter of the unit suggests it is comprised nearly entirely of subtidal deposits.

The subtidal character of the deposits is ichnologically evidenced in two ways. First, present-day mud flats and tidal point bar deposits in the bay comprise seasonal bedsets of laminated (winter) and bioturbated (summer) mud (Pearson and Gingras in press). The LSSU deposits do not exhibit this cyclicity. Second, the bioturbated component of modern intertidal flats (Mary's Point; Fig. 5.1B) and tidal point bars (Shepody River; Fig. 5.1B) in Chignecto Bay are nearly completely dominated by incipient *Planolites* and *Palaeophycus*, and by *Arenicolites* and *Diplocraterion* – constructed by *Nereis* sp. (polychaete) and *Corophium volutator* (amphipod), respectively (Pearson and Gingras in press). *C. volutator* is nearly exclusively confined to the intertidal zone; hence, the lack of structures produced by this amphipod in the LSSU suggests that an intertidal setting is not likely.

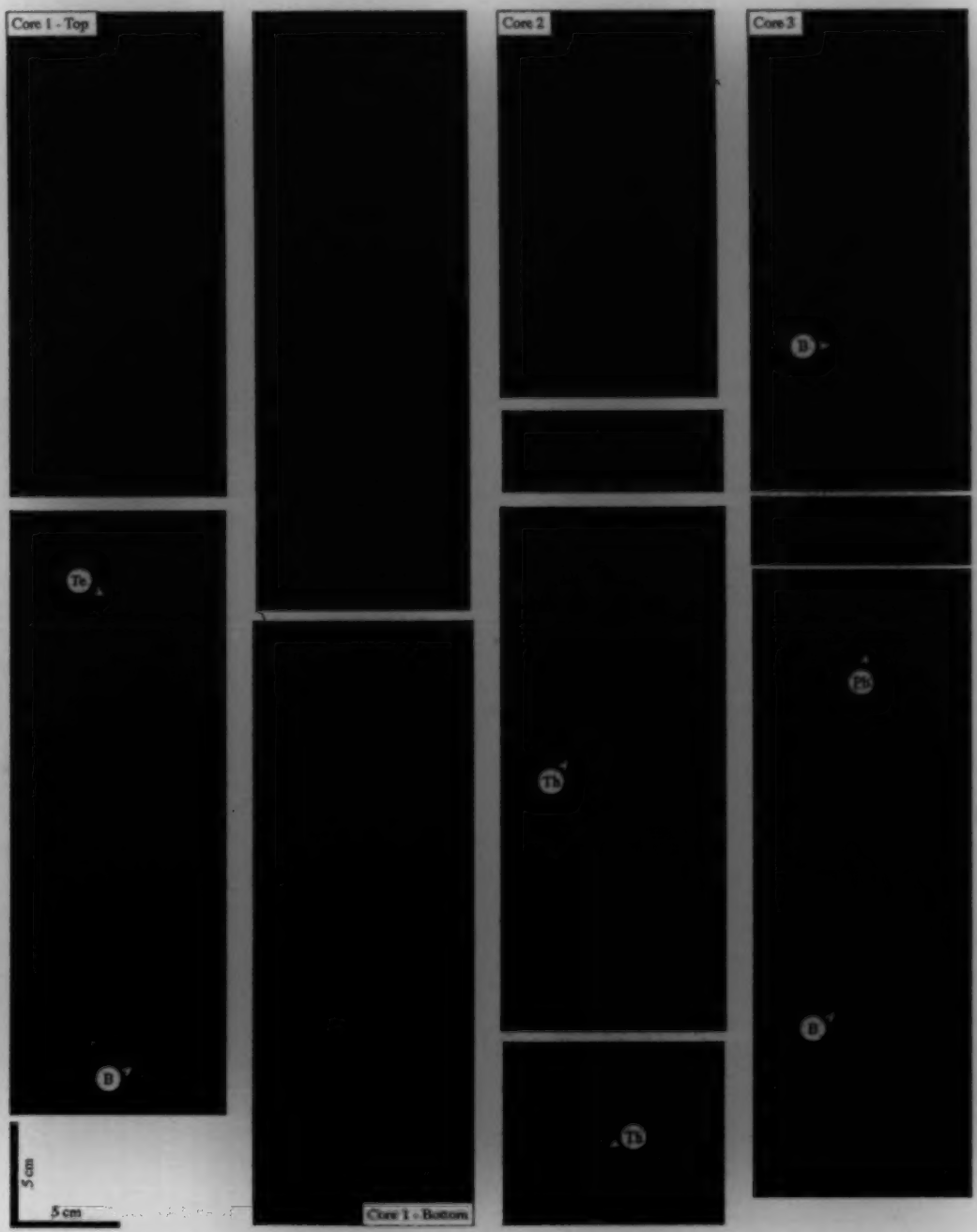

FIGURE 5.8 – X-ray radiographs of drop cores collected from the laminated silty sand unit (LSSU) in 2005. Cores were split along the maximum-dip direction, although the direction of dip of the laminae is unknown. Laminae dips observed in the core are not true dips and increase with depth as a result of the coring device entering the sediment at an angle and continuing to tip over during the collection process. The top, bottom and edges of each core were disturbed during the coring process. Darker colours indicate more mud-rich sediment and light, more sand-rich. Large-diameter *Thalassinoides* (Th), *Teichichnus* (Te), undefined burrowing (B), and pebble layers (Pb) are indicated in the cores.

The ichnological character of the laminated silty sand unit; mainly the presence of large-diameter, oval to round *Thalassinoides* and *Teichichnus*; supports the hypothesis that hydraulic conditions and overall depositional setting at Waterside Beach have undergone significant change between 6.5 ka and present (Amos et al. 1991). *Thalassinoides* and *Teichichnus* of the size and shape observed in the core (Fig. 5.8) are usually constructed by deep-burrowing crabs, particularly in estuarine environments (Gingras et al. 1999). However, in the present Bay of Fundy, there are no deep-burrowing crabs reported from the intertidal or subtidal zones. The presence of these structures thus supports the interpretation that Chignecto Bay was an estuary during deposition of the LSSU. With RSL rise and tidal amplification, and overstepping of the gravel spit across the mouth of the bay, the protected central estuarine setting at Waterside Beach evolved to the present conditions with tidal currents in excess of 1 m/s and storm waves exceeding 3 m (Amos et al. 1991). This in turn, would influence the fauna colonizing the mud, such that burrowing crabs were replaced by polychaetes resulting in a change in the trace assemblage from large-diameter *Thalassinoides* and *Teichichnus* to smaller structures such as *Palaeophycus*, *Skolithos*, and *Planolites*.

Based on sedimentological, ichnological, and seismic character of the laminated silty sand unit, the subtidal component of a moderate- to low-energy estuarine setting is considered the most likely depositional environment for this unit. Moreover, deposits of the LSSU are considered to have accumulated via aggradation of subtidal mud flats in a central estuary subjected to macro- to lower megatidal conditions. The LSSU may therefore be considered a subtidal mud-flat that aggraded with base-level rise between 6 and 3 ka.

Salt-Marsh Deposits

Directly overlying the SDRU and laterally adjacent to (on the landward side) the laminated silty sand unit are salt-marsh sediments. These deposits are characterized

seismically by scattered occurrences of 'gas chimneys' (seen most clearly in Figs. 5.3 and 5.5), which are zones of limited seismic penetration beneath pockets of shallow gas, sometimes capped by strong reflections of negative polarity. Moreover, limited impedance between salt-marsh beds results in the unit exhibiting a relatively uniform (low reflectivity) appearance. The lower contact of the salt-marsh sediments is likely conformable with underlying strata due to a brief period of salt-marsh development during base-level fall. Continued fall, however, would result in the evolution of the marsh into a freshwater marsh (Fig. 5.10) dominated by peat deposition (Allen 1990, 1997, 2000; Anderson and Race 1980; Redfield 1972). The SDRU forms a natural barrier to salt marsh progradation where, as noted in Figures 5.3 and 5.5, the marsh pinches out against it. The upper marsh contact is a ravinement surface eroded by wave action within the upper shoreface. This contact between beach and salt-marsh deposits is well defined on the seismic data at the northwest end of the beach (Figs. 5.3 and 5.5), but becomes hard to follow towards the southeast (Figs. 5.4 and 5.5). The strong reflector at the base of the salt marsh also disappears towards the southeast. We infer that the salt-marsh deposits in the southeast were removed by down cutting of Long Marsh Creek (Fig. 5.1C) and widening of the tidal-creek incision by wave-action within the foreshore and upper shoreface upon transgression (Fig. 5.6). Consequently it is considered that salt-marsh deposits are either not preserved in the southeast or are thin and seismically masked by thick overlying beach deposits.

A description of the salt-marsh sediments is presented in Dashtgard and Gingras (2005) and is not re-iterated here. However, the presence of the marsh and the timing of its aggradation can be related to the architecture of post-glacial deposits at Waterside Beach. Firstly, aside from the marsh deposits that accumulated during base-level fall and peat deposits during lowstand, Waterside Marsh aggraded strongly during base-level rise (Fig. 5.10). Accompanying aggradation, during the early stages of tidal amplification, would be a component of progradation as was reported from the Barnstable Marsh,

Massachusetts, USA (Redfield 1972). It is also possible that with continued aggradation and progradation of the salt marsh between 6 and 3 ka, and with aggradation of the LSSU due to accretion that these two deposits are partly contemporaneous.

Somewhere between 6 ka to 3 ka, RSL rise coupled with tidal amplification up the bay resulted in a switch from aggradation and progradation of the marsh, to aggradation and transgression. It is likely that this transition occurred around 4 to 3 ka, when tides in the bay were considered to have reached 75% of their present amplitude (Desplanque and Mossman 2001; Scott and Greenberg 1983). Breaching of the Chignecto estuary-mouth probably exposed the area to substantially increased wave energy. From 3 ka to present the salt marsh has been in a state of erosion. Where exposed in the intertidal zone (upper shoreface), the surface is burrowed, forming a *Glossifungites* surface (Gingras et al. 2000, 2001; Pemberton and Frey 1985; Pemberton et al. 2001). This surface is colonized by *Mya arenaria* (Fig. 5.9C), *Corophium volutator* (Fig. 5.9A, B), and *Nereis* sp. (polychaete), which develop the incipient traces: *Siphonichnus* (Fig. 5.9C), *Skolithos*, *Lockeia*, *Arenicolites* (Fig. 5.9B), *Diplocraterion* (Fig. 5.9A), *Palaeophycus*, *Thalassinoides*, and *Polykladichnus* (Bromley 1990; Dashtgard and Gingras 2005; Gingras et al. 1999).

Beach Deposits

The youngest unit preserved at Waterside Beach is the modern beach. The sedimentological character and distribution of the beach deposits is described extensively in Dashtgard et al. (2006). In general, the beach can be subdivided into two main zones: (1) a thin beach deposit in the northwest; and, (2) a thick beach deposit basinward of the mouth of Long Marsh Creek (Fig. 5.1C). The thin beach sequence is characterized by an offshore fining in grain size from mixed course-grained sand and fine gravel to interbedded silty sand and sandy silt. This trend is manifested geomorphologically by an offshore decrease in beach slope from 3° to 0.3°. It rests on a wave-ravinement

The ichnological character of the laminated silty sand unit; mainly the presence of large-diameter, oval to round *Thalassinoides* and *Teichichnus*; supports the hypothesis that hydraulic conditions and overall depositional setting at Waterside Beach have undergone significant change between 6.5 ka and present (Amos et al. 1991). *Thalassinoides* and *Teichichnus* of the size and shape observed in the core (Fig. 5.8) are usually constructed by deep-burrowing crabs, particularly in estuarine environments (Gingras et al. 1999). However, in the present Bay of Fundy, there are no deep-burrowing crabs reported from the intertidal or subtidal zones. The presence of these structures thus supports the interpretation that Chignecto Bay was an estuary during deposition of the LSSU. With RSL rise and tidal amplification, and overstepping of the gravel spit across the mouth of the bay, the protected central estuarine setting at Waterside Beach evolved to the present conditions with tidal currents in excess of 1 m/s and storm waves exceeding 3 m (Amos et al. 1991). This in turn, would influence the fauna colonizing the mud, such that burrowing crabs were replaced by polychaetes resulting in a change in the trace assemblage from large-diameter *Thalassinoides* and *Teichichnus* to smaller structures such as *Palaeophycus*, *Skolithos*, and *Planolites*.

Based on sedimentological, ichnological, and seismic character of the laminated silty sand unit, the subtidal component of a moderate- to low-energy estuarine setting is considered the most likely depositional environment for this unit. Moreover, deposits of the LSSU are considered to have accumulated via aggradation of subtidal mud flats in a central estuary subjected to macro- to lower megatidal conditions. The LSSU may therefore be considered a subtidal mud-flat that aggraded with base-level rise between 6 and 3 ka.

Salt-Marsh Deposits

Directly overlying the SDRU and laterally adjacent to (on the landward side) the laminated silty sand unit are salt-marsh sediments. These deposits are characterized

FIGURE 5.9 – Images of burrows and organisms colonizing the *Glossifungites* surface developed between the salt marsh and beach sediments. (A) Sand-filled *Diplocraterion* constructed by *Corophium volutator* into salt-marsh exposed in the upper intertidal. (B) Intensely colonized salt marsh. Burrowing dominated by *Arenicolites*, which is also constructed by *C. volutator*. Note the thin sediment-starved wave ripples developed on top. (C) Close up of a *Mya arenaria* burrow into salt marsh. Note the sand lining around the siphon hole.

a considerable influence on what will ultimately be preserved of the beach succession, including the thickness, orientation, and sedimentological character of the preserved deposit.

Implications for High-Resolution Sequence Stratigraphy

Waterside Beach presents an interesting case of the variability in depositional architecture that may occur at a coastline as a function of base-level change. Sequence stratigraphic analysis is based on changes in the position of the shoreline (Catuneanu 2002, 2006). However, changes in base level may result in profound changes in depositional environments, basin configuration, and hydraulic conditions – particularly in embayments. This is the case of Waterside Beach, Chignecto Bay, Bay of Fundy. The Bay of Fundy has experienced significant changes in relative sea level and tidal range over the past 15 ka (Amos et al. 1991; Grant 1970, 1980; Scott and Greenberg 1983; Shaw et al. 2002). Following an immediate post-glacial submergence of the coastline, 55 m below present-day sea level, isostatic rebound resulted in a drop in RSL to 25 m below present level by 6.5 ka (Fig. 5.10; Amos et al. 1991). Coupled with these significant changes in RSL are equally large changes in tidal range – where the bay likely experienced

micro- to mesotidal conditions until 8 ka (Grant 1970; Scott and Greenberg 1983). More importantly for Waterside Beach, a significant change in the morphology of Chignecto Bay occured with the development of a gravel barrier across the mouth of the bay, 15 km to the southwest (Amos et al. 1991). Developed at or near the maximum regressive shoreline, this barrier would have baffled incoming waves resulting in quiescent depositional conditions to the northeast.

The present depositional setting for Waterside Beach is a relatively recent occurrence resulting from changes in the basin architecture of Chignecto Bay. Reconstruction of the paleo-shoreline over the past 13 ka, suggests that Waterside Beach was dominated by mud deposition until ~ 3 ka (Fig. 5.10). This is partly the result of larger scale changes in the configuration of the bay, which controlled the intensity of wave activity at the shoreline. Variation in tidal conditions and the availability of coarse-grained sediment also contributed greatly to the changing depositional styles. Consequently, high-resolution sequence stratigraphic analysis of Waterside Beach requires inferring the paleo-shoreline and understanding changes in depositional environments with changes in RSL and hydraulic (energy) conditions. This in turn is not possible without detailed knowledge and modeling of the entire system as changes at the shoreline are influenced by changes to the entire bay. Sequence stratigraphic analysis of the beach is therefore difficult, as shifts in the position of the shoreline cannot easily be determined.

A second component controlling the morphology of Waterside Beach is the availability of coarse and fine sediment. In this sense, the glacial history of the beach plays a significant role in its evolution. The presence of the ridge of glacio-marine deposits (SDRU) acted to baffle waves and effectively compartmentalize the shoreline during RSL fall and early rise (13 to 4 ka). From 3 ka to present, wave-reworking of the SDRU upon transgression has sourced most of the gravel that comprises the beach. It is likely that without this unit, Waterside Beach would be sandy and narrow (in a

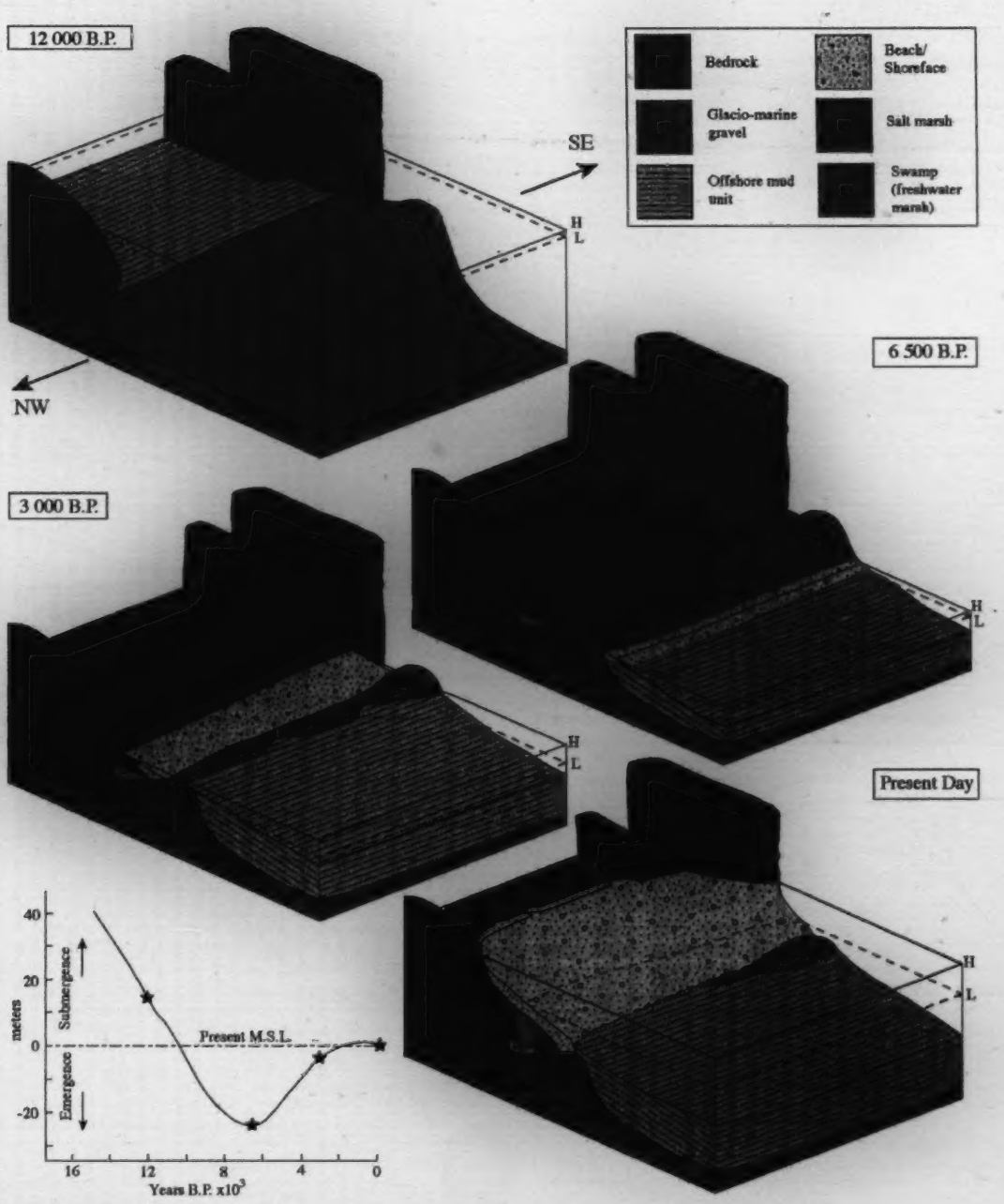

FIGURE 5.10 – Schematic, paleo-environmental block diagrams recording shoreline shifts and evolution of the coastal architecture at Waterside Beach. The diagrams relate to various stages of post-glacial RSL fall and rise and were chosen to illustrate environmental conditions at the time of deposition of the four units identified in this study. The relative sea level curve is modified after Amos et al. (1991) and printed with permission from the Canadian Society of Petroleum Geologists.

shore-normal direction). This again has sedimentological and sequence-stratigraphic implications in that the changes in the morphology and depositional character of the bay and in the local hydraulic conditions continue to influence sedimentation in an area for a long time after sediment is deposited. More importantly, the source of sand and gravel is not immediately evident at the beach, yet that does not necessitate sediment be derived from either a landward direction or from longshore transport.

CONCLUSIONS

Geological interpretation of shallow-seismic profiles collected at Waterside Beach, Chignecto Bay, Canada reveals a varied post-glacial depositional history for the shore and nearshore system. During glacial retreat, a glacio-marine unit was developed comprising glacial outwash. Immediately following deglaciation, the land surface was depressed and submerged below 55 m of ocean. From 13.5 to 6.5 ka, isostatic rebound resulted in RSL fall (Amos et al. 1991; Grant 1970; Scott and Greenberg 1983; Shaw et al. 2002) and a shift of the shoreline basinward. During the same period, the coastal sequence landward of the glacio-marine unit evolved from an area of mud deposition to salt marsh as the coastline regressed. The initial salt marsh evolved into a freshwater marsh as falling RSL limited salt-water incursion into the emergent coastal area. Falling sea level resulted in wave-modification of the glacio-marine unit into a gravel barrier (SDRU), and in the development of mixed mud and sand, subtidal mud flats basinward of the barrier. Between ~8 and 4 ka (end of RSL fall, maximum lowstand, and start of RSL rise), wave and tide influence on the beach was minimal because of the presence of a gravel spit across the mouth of Chignecto Bay, 15 km southwest (Amos et al. 1991). This resulted in aggradation and progradation of the mud flat. RSL rise beginning at 6.5 ka to present was accompanied by an increase in tide heights from mesotidal to megatidal (Scott and Greenberg 1983). At Waterside Beach, rising sea-level and tidal amplification led to flooding of the freshwater marsh and wave-reworking of the glacio-marine deposit.

In consequence, the marsh evolved into the present-day aggrading salt marsh, and landward transport of sand and gravel from the glacio-marine deposit supplied the newly formed, transgressive, mixed sand and gravel, Waterside Beach.

The post-glacial evolution of Waterside Beach presents some interesting implications for high-resolution sequence stratigraphic studies within embayments. Mainly, the hydraulic conditions, configuration of the basin, and availability of sediment that control the depositional character of the coastline are all extremely sensitive to changes in RSL. The present gravel beach is a relatively recent phenomenon (past 3 ka); whereas, for the majority of post-glacial time Waterside has been a mud flat or dominated by mud deposition. Mapping out the position of the shoreline, is therefore difficult, as the beach did not shift position. Instead it underwent drastic changes in depositional character as hydraulic conditions and the availability of sediment changed as sea level fell and rose.

REFERENCES

Allen, J.R.L., 1990, Salt-marsh growth and stratification: A numerical model with special reference to the Severn Estuary, southwest Britain: Marine Geology, v. 95, p. 77-96.

Allen, J.R.L., 1997, Simulation models of salt-marsh morphodynamics: some implications for high-intertidal sediment couplets related to sea level change: Sedimentary Geology, v. 113, p. 211-223.

Allen, J.R.L., 2000, Morphodynamics of Holocene salt marshes: a review sketch from the Atlantic and Southern North Sea coasts of Europe: Quaternary Science Reviews, v. 19, p. 1155-1231.

Amos, C.L., and Asprey, K.W., 1979, Geophysical and sedimentary studies in the Chignecto Bay system, Bay of Fundy - a progress report, Geological Survey of Canada, p. 245-252.

Amos, C.L., Tee, K.T., and Zaitlin, B.A., 1991, The post-glacial evolution of Chignecto Bay, Bay of Fundy, and its modern environment of deposition, *in* Smith, D.G., Reinson, G.E., Zaitlin, B.A., and Rahmani, R.A., eds., Clastic Tidal Sedimentology: Calgary, AB, Canada, Canadian Society of Petroleum Geologists, p. 59-89.

Amos, C.L., and Zaitlin, B.A., 1985, The effect of changes in tidal range on a sublittoral macrotidal sequence, Bay of Fundy, Canada: Geo-Marine Letters, v. 4, p. 161-169.

Anderson, R.S., and Race, C.D., 1980, Investigation of salt marsh stratigraphy as an indicator of sea level rise in coastal Maine: Maine Geological Survey, Open File 80-1, 11 p.

Bourgeois, J., and Leithold, E.L., 1984, Wave-worked conglomerates - depositional processes and criteria for recognition, *in* Koster, E.H., and Steel, R.J., eds., Sedimentology of Gravels and Conglomerates: Calgary, AB, Canada, Canadian Society of Petroleum Geologists, p. 331-343.

Bromley, R.G., 1990, Trace Fossils; Biology and Taphonomy: London, Unwin Hyman, 280 p.

Catuneanu, O., 2002, Sequence stratigraphy of clastic systems: concepts, merits, and pitfalls: Journal of African Earth Sciences, v. 35, p. 1-43.

Catuneanu, O., 2006, Principles of Sequence Stratigraphy: Amsterdam, Elsevier, 336 p.

Clifton, H.E., 1981, Progradational sequences in Miocene shoreline deposits, southeastern Caliente range, California: Journal of Sedimentary Petrology, v. 51, p. 165-184.

Dalrymple, R.W., Zaitlin, B.A., and Boyd, R., 1992, Estuarine facies models: conceptual basis and stratigraphic implications: Journal of Sedimentary Petrology, v. 62, p. 1130-1146.

Dashtgard, S.E., and Gingras, M.K., 2005, Facies architecture and ichnology of recent salt-marsh deposits: Waterside Marsh, New Brunswick, Canada: Journal of Sedimentary Research, v. 75, p. 596-607.

Dashtgard, S.E., Gingras, M.K., and Butler, K.E., 2006, Sedimentology and stratigraphy of a transgressive, muddy gravel beach: Waterside Beach, Bay of Fundy, Canada: Sedimentology, v. 53, p. 279-296.

Davidson-Arnott, R.G.D., Van Proosdij, D., Ollerhead, J., and Schostak, L., 2002, Hydrodynamics and sedimentation in salt marshes: examples from a macrotidal marsh, Bay of Fundy: Geomorphology, v. 48, p. 209-231.

Desplanque, C., and Mossman, D.J., 2001, Bay of Fundy tides: Geoscience Canada, v. 28, p. 1-11.

Embry, A.F., 1993, Transgressive-regressive (T-R) sequence analysis of the Jurassic succession of the Sverdrup Basin, Canadian Arctic Archipelago: Canadian Journal of Earth Sciences, v. 30, p. 301-320.

Engels, S., and Roberts, M.C., 2005, The architecture of prograding sandy-gravel beach ridges formed during the last Holocene highstand: Southwestern British Columbia, Canada: Journal of Sedimentary Research, v. 75, p. 1052-1064.

French, J.R., 1993, Numerical simulation of vertical marsh growth and adjustment to accelerated sea-level rise, north Norfolk, U.K.: Earth Surface Processes and Landforms, v. 18, p. 63-81.

Gingras, M.K., Pemberton, S.G., and Saunders, T., 2000, Firmness profiles associated with tidal-creek deposits: the temporal significance of *Glossifungites* assemblages: Journal of Sedimentary Research, v. 70, p. 1017-1025.

Gingras, M.K., Pemberton, S.G., and Saunders, T., 2001, Bathymetry, sediment texture, and substrate cohesiveness; their impact on modern *Glossifungites* trace assemblages at Willapa Bay, Washington: Palaeogeography, Palaeoclimatology, Palaeoecology, v. 169, p. 1-21.

Gingras, M.K., Pemberton, S.G., Saunders, T., and Clifton, H.E., 1999, The ichnology of modern and Pleistocene brackish-water deposits at Willapa Bay, Washington: variability in estuarine settings: Palaios, v. 14, p. 352-374.

Gordon, D.C.J., Cranford, P.J., and Desplanque, C., 1985, Observations on the ecological importance of salt marshes in the Cumberland Basin, a macrotidal estuary in the Bay of Fundy: Estuarine, Coastal and Shelf Science, v. 20, p. 205-227.

Gordon, D.C.J., and Desplanque, C., 1983, Dynamics and environmental effects of ice in the Cumberland Basin of the Bay of Fundy: Canadian Journal of Fisheries and Aquatic Sciences, v. 40, p. 1331-1342.

Grant, D.R., 1970, Recent coastal submergence of the Maritime Provinces, Canada: Canadian Journal of Earth Sciences, v. 7, p. 676-689.

Grant, D.R., 1980, Quaternary sea-level change in Atlantic Canada as an indication of crustal delevelling, *in* Mörner, N.-A., ed., Earth Rheology, Istostasy and Eustasy: London, John Wiley and Sons, p. 201-214.

Hunt, D., and Tucker, M.E., 1992, Stranded parasequences and the forced regressive wedge systems tract: deposition during base-level fall: Sedimentary Geology, v. 81, p. 1-9.

Massari, F., and Parea, G.C., 1988, Progradational gravel beach sequences in a moderate- to high-energy, microtidal marine environment: Sedimentology, v. 35, p. 881-913.

Masselink, G., 1993, Simulating the effects of tides on beach morphodynamics: Journal of Coastal Research Special Issue, v. 15, p. 180-197.

Masselink, G., and Short, A.D., 1993, The effect of tidal range on beach morphodynamics and morphology: a conceptual beach model: Journal of Coastal Research, v. 9, p. 785-800.

Pearson, N.J., and Gingras, M.K., in press, An ichnological and sedimentological facies model for muddy point-bar deposits: Journal of Sedimentary Research.

Pearson, N.J., Gingras, M.K., Armitage, I.A., and Pemberton, S.G., in press, The significance of Atlantic Sturgeon feeding excavations, Mary's Point, Bay of Fundy, New Brunswick, Canada: Palaios.

Pemberton, S.G., and Frey, R.W., 1985, The *Glossifungites* ichnofacies: modern examples from the Georgia Coast, U.S.A., *in* Curran, H.A., ed., Biogenic Structures: Their use in Interpreting Depositional Environments: Tulsa, Oklahoma, SEPM, p. 237-259.

Pemberton, S.G., Spila, M., Pulham, A.J., Saunders, T., Maceachern, J.A., Robbins, D., and Sinclair, I.K., 2001, Ichnology and Sedimentology of Shallow to Marginal Marine Systems: Ben Nevis and Avalon Reservoirs, Jeanne d'Arc Basin: Geological Association of Canada Short Course, v. 15: St. John's, Geological Association of Canada, 343 p.

Posamentier, H.W., and Allen, G.P., 1999, Siliciclastic Sequence Stratigraphy - Concepts and Applications: SEPM Concepts in Sedimentology and Paleontology 7: Tulsa, SEPM (society for Sedimentary Geology), 210 p.

Pye, K., and French, P.W., 1993, Erosion and acretion processes on British Salt Marshes, Vol. 1, Introduction: Saltmarsh Processes and Morphology: Cambridge, U.K., Cambridge Environmental Research Consultants.

Quinlan, G., and Beaumont, C., 1981, A comparison of observed and theoretical postglacial relative sea level in Atlantic Canada: Canadian Journal of Earth Sciences, v. 18, p. 1146-1163.

Rampton, V.N., Gauthier, R.C., Thibault, J., and Seaman, A.A., 1984, Quaternary Geology of New Brunswick, v. Memoir 416: Ottawa, Geological Survey of Canada.

Reading, H.G., and Collinson, J.D., 1996, Clastic Coasts, *in* Reading, H.G., ed., Sedimentary Environments; Processes, Facies and Stratigraphy: Oxford, U.K., Blackwell Science, p. 154-231.

Redfield, A.C., 1972, Development of a New England Salt Marsh: Ecological Monographs, v. 42, p. 201-237.

Roy, P.S., Cowell, P.J., Ferland, M.A., and Thom, B.G., 1994, Wave-dominated coasts, *in* Carter, R.W.G., and Woodroffe, C.D., eds., Coastal Evolution: Late Quaternary Shoreline Morphodynamics: Cambridge, U.K., Cambridge University Press, p. 121-186.

Scott, D.B., and Greenberg, D.A., 1983, Relative sea-level rise and tidal development in the Fundy tidal system: Canadian Journal of Earth Sciences, v. 20, p. 1554-1564.

Shaw, J., and Courtney, R.C., 2002, Postglacial coastlines of Atlantic Canada: digital images: Geological Survey of Canada Open File #4302.

Shaw, J., Gareau, P., and Courtney, R.C., 2002, Palaeogeography of Atlantic Canada 13-0 kyr: Quaternary Science Reviews, v. 21, p. 1861-1878.

Short, A.D., 1991, Macro-meso tidal beach morphodynamics: Journal of Coastal Research, v. 7, p. 417-436.

Simpkin, P.G., and Davis, A., 1993, For seismic profiling in very shallow water, a novel receiver: Sea Technology, v. 34, p. 21-28.

Stea, R.R., 2005, Virtual field trip website, http://www.gov.ns.ca/NATR/MEB/field/glacier.htm#chignecto, Mineral Resources Branch, Department of Natural Resources, Nova Scotia.

Van Wagoner, J.C., Mitchum Jr., R.M., Campion, K.M., and Rahmanian, V.D., 1990, Siliciclastic sequence stratigraphy in well logs, core, and outcrops: concepts for high-resolution correlation of time and facies: American Association of Petroleum Geologists Methods in Exploration Series 7: Tulsa, AAPG, 55 p.

Walker, R.G., and Plint, A.G., 1992, Wave- and storm-dominated shallow marine systems, *in* Walker, R.G., and James, N.P., eds., Facies Models, Response to Sea Level Change: St. John's, NF, Canada, Geological Association of Canada, p. 219-238.

White, R.O., Butler, K.E., Simpkin, P.G., and Dashtgard, S.E., 2006, Pseudo-3D sub-bottom imaging of a dynamic beach environment in the Bay of Fundy, New Brunswick, Canada: 19th Symposuim on the Application of Geophysics to Engineering and Environmental Problems.

CHAPTER 6: GRAVEL DELTAS TO SHOREFACES – LINKING HYDRAULIC PROCESS TO COASTAL GEOMORPHOLOGY AND SEDIMENTOLOGY IN THE BAY OF FUNDY, CANADA[5]

INTRODUCTION

Sedimentological research conducted in modern coastal settings has focused on the continuum that exists between wave- and tide-dominated depositional environments (Anthony and Orford 2002; Dalrymple et al. 1992; Engels and Roberts 2005; Masselink 1993; Masselink and Short 1993; Short 1984; Yang et al. 2005). A similar continuum occurs between fluvial- to wave-dominated settings, yet this has received little attention. On the New Brunswick coastline of the megatidal (> 8 m tidal range; Levoy et al. 2000) Bay of Fundy, three coarse-grained systems exhibit distinct morphologies reflecting relative differences in fluvial-, wave-, and tidal-energy input. Consequently, these systems present an opportunity to compare sedimentological and morphological characteristics of gravel-dominated deposits through a range of hydraulic process. In this paper: (1) the relationship between grain size and areal extent of the coastal zone is examined; (2) a discussion of the occurrence of swash- and surf-zone bars, particularly as an indirect function of fluvial discharge is presented; and, (3) three bay-margin deposits are compared to assess the influence of hydraulic process on the morphology and sedimentology of gravel-dominated systems.

Marginal-marine depositional environments are commonly grouped into river-, wave-, and tide-dominated categories depending on the morphology and sedimentology of the coastal zone (Boggs 1995; Dalrymple et al. 1992; Galloway 1975; Reading and Collinson 1996). This tripartite division is applicable to gravel-dominated coasts as

[5] A version of this chapter is being reviewed for publication in the JOURNAL OF SEDIMENTARY RESEARCH as "Gravel deltas to shorefaces — Linking hydraulic process to coastal geomorphology and sedimentology in the Bay of Fundy, Canada" by Shahin E. Dashtgard and Murray K. Gingras

long as the grain-size distribution is considered. River-dominated coarse-grained coastal systems are represented by gravel deltas, which tend to be small (relative to sand- and mud-dominated ones) and are commonly referred to as either fan or, in special cases, Gilbert-type deltas (Colella 1988; Marzo and Anadón 1988; Postma 1990; Postma and Roep 1985; Reading and Collinson 1996; Wescott and Ethridge 1980). The morphology, size, and sedimentological character of these deltas is dependent on the location relative to the shoreline, gradient of the backshore, water depth of the receiving basin, average grain-size (Orton and Reading 1993; Postma 1990; Reading and Collinson 1996; Wescott and Ethridge 1980, 1982) and the nature and provenance of the fluvial system (Allen 1997b; Schumm 1977).

Wave-dominated gravel systems encompass beaches and shorefaces that commonly exhibit a shore-normal partitioning based on clast shape and size (Bluck 1967, 1999; Hart and Plint 1989, 2003; Massari and Parea 1988). These systems demonstrate a degree of tidal influence that can be defined by the relationship between wave energy and tide height (Davis and Hayes 1984; Masselink 1993; Masselink and Short 1993; Short 1991; Wright and Short 1984), which is manifested in the topography and morphology of the beach. Beaches in strongly macrotidal to megatidal environments comprise a moderately dipping (2-5°) beachface that grades rapidly seaward to a shallowly dipping (< 1°), concave-up sandy terrace (Forbes and Taylor 1987; Masselink and Short 1993; Wright and Short 1984). Within the shallow shoreface, tidal currents may result in the development of two-dimensional gravel waves or sand ridges (Anthony and Orford 2002; Dyer and Huntley 1999). Tidal beach and shoreface morphology is similar in both regressive (Anthony 2000; Anthony and Orford 2002) and transgressive settings (Dashtgard et al. 2006). However, tidal influences on morphology decrease with increasing grain size such that gravel systems are rarely, if ever, tide dominated (Orton and Reading 1993; Reading and Collinson 1996).

Tidal affects on the morphology of gravel systems can also be indirect, resulting from the impact of tides on the regional morphology of a basin margin, and on the distribution and relationships between depositional environments within the coastal zone (Amos et al. 1991; Amos and Zaitlin 1985). In the upper Bay of Fundy, coarse-grained beaches and deltas commonly develop on the seaward margin of salt marshes. These marshes are dissected by tidal channels whose cross-sectional area and frequency is a function of the tidal prism (Allen 1997a; Bayliss-Smith et al. 1979; Davidson-Arnott et al. 2002; Pestrong 1965; Pye and French 1993; Van Straaten 1961). In macrotidal and megatidal settings the tidal prism, and in turn, the cross-sectional area (width and depth) of tidal creeks is large. Where these creeks debouch onto a coarse-grained beach, they are infilled with beach sediments resulting in deposition of substantially thicker beach deposits than may be expected in micro- or mesotidal settings (Dashtgard et al. 2006; Dashtgard et al. in review).

Relative sea level (RSL) change is another factor that impacts the depositional style of gravel-dominated coasts. Gilbert-type and fan deltas occur in regressive (progradational) fluvial-dominated settings (Arnott 2004; Colella 1988; Ethridge and Wescott 1984; Marzo and Anadón 1988; Massari 1984; Nemec 1990; Postma 1984, 1990; Postma and Roep 1985; Wescott and Ethridge 1980, 1982, 1983). During transgression, these deposits are drowned and evolve into either estuaries (Dalrymple et al. 1992) or wave-dominated fan-deltas (Marzo and Anadón 1988; Reading and Collinson 1996). Gravel beaches can also be subdivided as regressive and transgressive systems. Regressive beaches are generally thick, and preserve upper shoreface and foreshore deposits (Anthony 2000; Bourgeois and Leithold 1984; Clifton 1981; Engels and Roberts 2005; Massari and Parea 1988). Transgressive gravel beaches are manifest as a thin gravel lag overlain by lower shoreface to offshore sand and muds (Clifton 1981; Dashtgard et al. 2006; Massari and Parea 1988).

Relative sea-level change can result in significant variation in tidal regime, particularly within embayments (Amos et al. 1991; Amos and Zaitlin 1985; Scott and Greenberg 1983). For example, in the Bay of Fundy, and particularly Chignecto Bay, RSL rise and fall has resulted in tides increasing from microtidal approximately 8000 years ago to megatidal today (Amos et al. 1991; Grant 1970; Scott and Greenberg 1983). This has had a considerable impact on the depositional style of Chignecto Bay (Amos et al. 1991; Amos and Zaitlin 1985) and especially on coastal zones within the bay that occur seaward of salt marshes or tidal creeks (Dashtgard et al. in review).

Study Area

The three study sites are situated along the New Brunswick coastline of the upper Bay of Fundy, Canada (Fig. 6.1). The Big Salmon River (BSR) delta is situated at the mouth of the Big Salmon River near the town of St. Martins. Fifty kilometers to the northeast is the Alma delta at the mouth of the Upper Salmon River (USR). Waterside Beach is a further 10 km up bay, near Cape Enrage, New Brunswick.

The Big Salmon River is entrenched within a canyon cut into igneous and metamorphic bedrock (Proterozoic) of the Caledonian Highlands. Within the lower 1 km stretch, the canyon opens up and the river enters a slightly wider (~ 150 m) valley. The seaward end of the valley is partly constricted by a large terrace of till, beyond which the delta occurs. The delta is backed by either bedrock or till cliffs with a small salt marsh developed within the valley (Fig. 6.1). Alma delta occurs at the mouth of the Upper Salmon River (USR), which drains a region of the Caledonian Highlands. In the lower 1.3 km the river exits the highlands and enters a valley that increases in width from 50 m to over 200 m at the coastline. The delta (developed at the coastline) is backed either by tall bedrock cliffs, till, salt marsh, or the village of Alma (Fig. 6.1). Waterside Beach, a mixed sand and gravel deposit, has no major fluvial point source, but is characterized

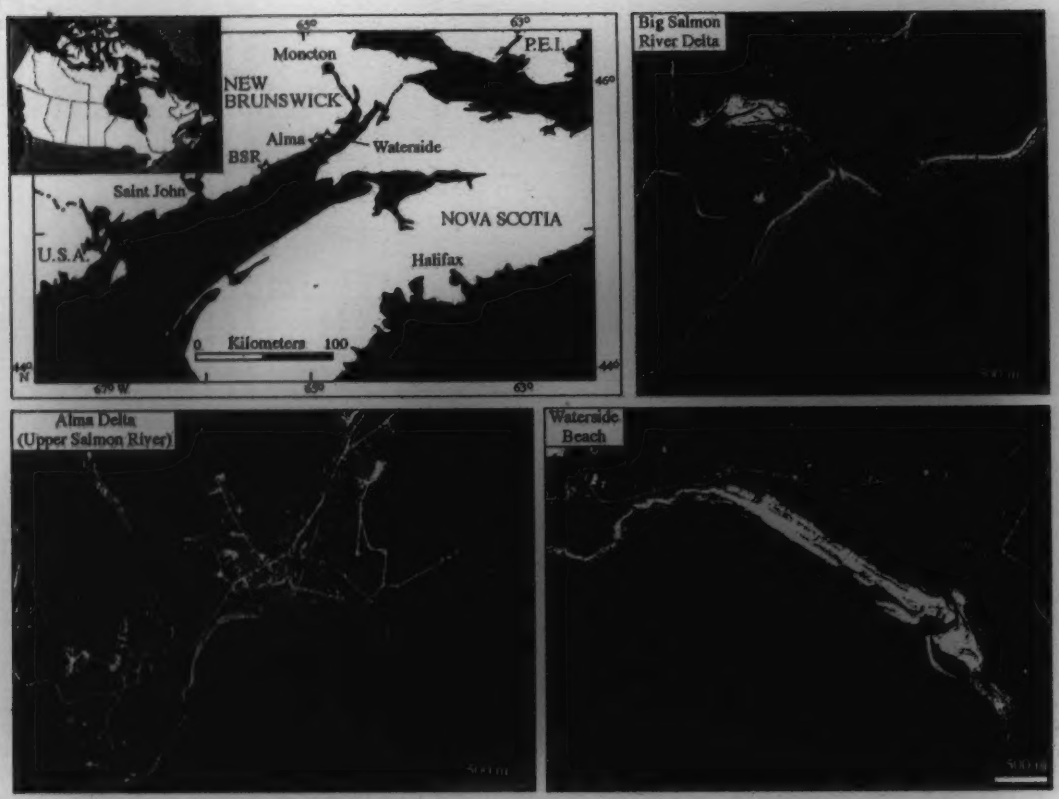

FIGURE 6.1 – Location map and air photos of the study areas. The location of the Big Salmon River (BSR) delta, Alma delta, and Waterside Beach are indicated on the Bay of Fundy map. North is to the top of the air photos.

by large tidal creeks. At the northwest end, the beach abuts low cliffs of Triassic bedrock (mainly sandstone and shale) and Carboniferous bedrock in the southeast. Between these cliffs the beach is backed by salt marsh.

Methods

Fieldwork was conducted in 2003, 2004, and 2005. The sedimentology of the intertidal zones of the three systems was determined with GPS mapping, sediment sampling, trenching, and x-ray imaging of sediment box cores. GPS mapping of Waterside Beach and Alma delta was conducted in 2003, and of the BSR delta in 2004. Follow-up surveys in 2004 and 2005 along the crests of landward-migrating gravel bars

recorded movements of the large bed-forms on each system. Sediment mapping of the intertidal zone was compared to high-resolution, single-channel seismic profiles acquired in 2003 and 2004 over Waterside and Alma. These surveys were used to map out the sub-tidal component of Waterside Beach and to establish the dip of the delta front of the Alma delta. The areal extents of the intertidal and sub-tidal zones were calculated from mapping and seismic. The areas were also determined by assuming a 10 m tidal range (the spring-tide range of the BSR delta) to enable comparisons of the BSR delta to Alma and Waterside. In 2005, a grab-sampling program was undertaken to sample sub-tidal beach and offshore sediments at Waterside and Alma. The grab samples are incorporated into the grain-size data and used, where possible, to map out the sub-tidal sediment distribution. Sampling was not uniform for the three sites (68 from Waterside, 27 from Alma, and 13 from BSR). Despite inequitable sampling, the overall sedimentological trends can be determined from the data and can be used for comparative purposes between the three systems.

Sediment grain size was determined for 108 stations using one of three techniques: (1) grid sampling, (2) bulk-sample dry sieving, and (3) x-ray absorption, depending on the maximum size (weight) of a clast population. Church et al. (1987) and Hoey (2004) suggest sample sizes of 100 times the size of the largest clast when the maximum clast size exceeds 32 mm. This standard was generally employed, however, as clast sizes surpassed 100 mm, the sample size required exceeded what was practical to obtain. Where cobbles and boulders were observed in a unit, grid sampling was employed. Grid sampling involves setting up a 5 m x 5 m or 10 m x 10 m grid and measuring the b-axis of the clast encountered every 0.5 m or 1 m across the grid (Rice and Church 1996; Wolman 1954). Where clasts < 4 mm were encountered, they were categorized as matrix, of which a representative sample was collected and dry sieved in the lab. For sampling sites where the sediment was dominated by clasts 32 mm and below, a sediment sample was collected for dry sieving. These samples were dried and

sieved in one phi-size increments to the coarse-grained sand break (1 ϕ). Each grain fraction was then weighed. A sub-sample was collected from the remaining sediment (< 1 ϕ) for mechanical sieving in the lab. Grain size of the finest fraction of sieved samples (< 4 ϕ) and those dominated by very fine-grained sand, silt, and clay was determined using x-ray absorption. These samples were dried for 24 hours at 105° C, crushed with mortar and pestle, and then processed on a Micrometrics Sedigraph 5100.

Mean grain size (ϕ) and sorting (σ) were calculated by graphical analysis (Folk and Ward 1957) and the method of moments (Krumbein and Pettijohn 1938). Reported mean grain-size values are arithmetic means derived by the method of moments using millimeter values. For ease of comparison these values are converted to the phi scale. Sorting values are derived from graphical analysis of phi-scale, cumulative grain-size curves allowing for easy comparison of the results to standard sorting scales (Boggs 1995; Folk and Ward 1957; Hoey 2004). Plots of mean grain size versus standard deviation are used to define the main sediment groupings mapped out on Waterside Beach, Alma delta and Big Salmon River delta. For Waterside Beach, the sediment distribution map is a simplified version of that published in Dashtgard et al. (2006).

Fluvial and tidal-creek discharge was determined using the velocity-area method as suggested by Wahl et al. (1995). Measurements were taken over three 24-hour periods in July 2005 with light precipitation at night and clear days during the spring stage of the tidal cycle. Salinity was measured using a salinity-calibrated Fisher© conductivity probe. The volume of freshwater was determined by comparing the salinity of the river and tidal-creek samples to that of the bay and determining what proportion of the discharge was freshwater. Discharge measurements neither reflect the full range of flow from the streams nor provide a means of determining flood discharge; however, they reflect the size of the drainage catchments and may be used to quickly assess the relative output of the fluvial systems. For quantitative analysis, drainage-catchment areas are

used. The three deposits experience similar climatic conditions including precipitation (Table 6.1; Weather Office 2005). The annual discharge of each river should therefore be proportional to the size of the catchment area.

RESULTS

Waterside Beach, Alma delta, and Big Salmon River delta were compared for grain size, hydraulic input and water chemistry, and deposit morphology. Figure 6.2 presents statistical grain-size data for the three deposits. These data are plotted together and then subdivided into generalized groupings that are used to map out sediment distribution on Figure 6.4. Table 6.1 details catchment-basin areas, average annual precipitation within the catchment, stream-flow data, tide ranges, and recorded salinities. Figure 6.3 graphically displays the salinity measurements. Figure 6.4 incorporates GPS and seismic mapping, and grain-size data from the three environments. Figure 6.5 is a simplified version of Figure 6.4, but focuses on movement of gravel bars from 2003 to 2005.

Grain Size

The combined grain-size distribution for Waterside Beach, Alma delta, and BSR delta spans 14 phi sizes that are grouped into four main categories: (1) silt and clay, and sandy silt; (2) silty sand and sand; (3) fine gravel, and mixed sand and gravel; and, (4) coarse gravel (All systems, Fig. 6.2). With the exception of the silt and clay group, sorting decreases as grain-size increases. The coarsest grain sizes (-6 ϕ and above) tend to be very poorly sorted. Comparison of the grain-size plots for each system suggests that grain size increases and sorting decreases (standard deviation increases) from Waterside to Alma to BSR (Fig. 6.2). At Waterside, samples exhibit a linear decrease in sorting from 2.5 to –6 ϕ, such that standard deviation increases by 0.3 σ for every 1 ϕ increase in grain size (i.e. 0 to –1 ϕ). Excluding mud samples, and eleven mainly sand samples collected

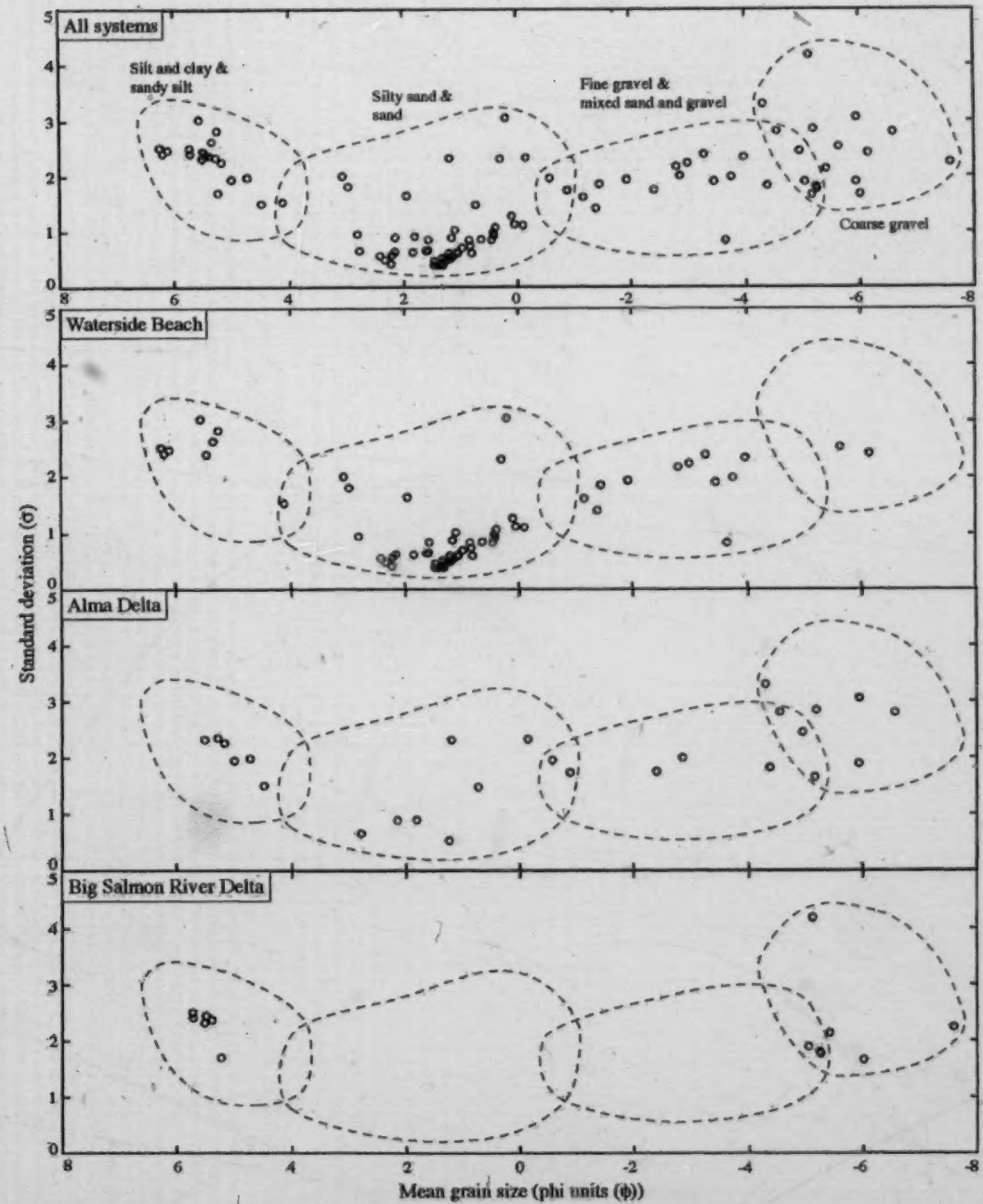

FIGURE 6.2 – Plots of average grain size versus standard deviation (sorting) for all three systems (108 samples), and by location – Waterside (68 samples), Alma (27), and BSR (13). Average grain sizes are arithmetic means determined by the method of moments using millimeter values converted to phi scale for comparison. Standard deviation is graphically determined. The four main grain-size categories are used to map out sediment distribution in Figure 6.4.

as part of a localized study, the average grain size for Waterside is –2.05 ϕ and sorting 1.24 σ. Alma also exhibits a decrease in sorting with increasing grain size, however, the degree of scatter in the sorting values is much higher than at Waterside and there is a shift towards coarser grain sizes. The Alma samples (excluding the silt and clay category) have an average grain size of –4.29 ϕ and sorting of 1.86 σ. Big Salmon River delta is the coarsest grained of the three deposits. The average grain size excluding mud is –5.99 ϕ and sorting of 2.23 σ. Coarse-gravel samples at BSR are generally better sorted than those of Alma and Waterside (Fig. 6.2).

The silt and clay, and sandy-silt category exhibits the least variability in average grain size and sorting of the four categories. Waterside Beach silt and clay samples tend to have high clay content and are very poorly sorted. Alma muds are coarser grained and better sorted than Waterside muds; whereas BSR mud samples are poorly sorted and slightly finer than the Alma samples. BSR muds exhibit very limited variation in grain size and sorting (Fig. 6.2).

Water Chemistry and Hydraulic-Energy Inputs

Table 6.1 presents the water chemistry, drainage-basin area, precipitation, and freshwater-discharge data for the main fluvial (or tidal) systems at each site. The Big Salmon River drains an area of 278 km^2, and the Upper Salmon River (Alma) 176 km^2. The other freshwater streams are small, with catchments of ~8 km^2 (Dickson Brook, Alma) and 15 km^2 (Cleavland Brook, Alma). The tidal creeks are dominated by marine water (Table 6.1, Fig. 6.3). However, all three creeks behind Waterside Beach drain tidal and/or freshwater lakes, have small catchment areas, and include a component of freshwater in their discharge. Precipitation was relatively consistent, suggesting that over the long-term the size of the catchment basin is proportional to the fluvial discharge. Freshwater salinity is 0 to 0.1 parts per thousand salt (ppt), whereas the upper Bay of Fundy is lower polyhaline with 31.4 ppt (i.e. nearly marine). For BSR and Alma, the

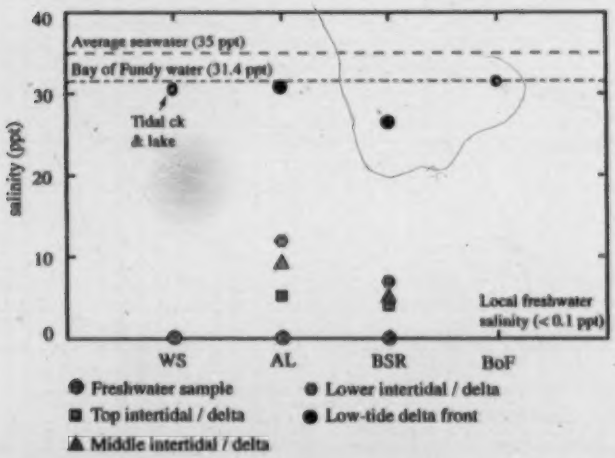

FIGURE 6.3 – Plot of salinity versus location. Samples were taken during the spring-tide phase of the tidal cycle and indicate that upper Bay of Fundy salinity is 31.4 ppt (11 samples) and that freshwater is 0.0 ppt (3 samples). Also note the increase in salinity of samples collected from the rivers, at Alma and BSR, from the top of the intertidal zone to the low-tide level. This suggests that a significant volume of salt-water seeps out of the sediment into the channel during the low-tide stage.

volume of freshwater is equal to the measured fluvial-discharge rate (Table 6.1; see Fig. 6.4 for location of rivers). Determining freshwater output at Waterside was only attempted for Long Marsh Creek 10 km landward of the beach. The site selected was just downstream (ebb) of a tidal lake (Lockhart Lake), which is considered the main freshwater catchment for the creek. Salinity taken at the stream-gauging site was 30.4 ppt (Fig. 6.3), which is slightly lower than bay water. Freshwater mixing produces this reduced salinity such that of the 4.16 m^3/s of discharge, only 0.15 m^3/s comprises freshwater.

The upper Bay of Fundy is megatidal with tides amplified up the bay. Tidal range increases from an approximate average spring range of 10 m at BSR delta to 11 m at Alma delta, and 11.5 m at Waterside Beach (Table 6.1; Canadian Hydrographic Service, 2005). Wave measurements in the upper Bay of Fundy indicate it is sheltered relative to the open ocean. A nine-month wave survey conducted in 1978 and 1979 near Waterside Beach (Fig. 6.6; Amos and Asprey, 1979; Amos et al., 1991; Ocean Sciences, 2005) provides the best predictions of the wave conditions at the three sites.

	Stream	Drainage Basin (km^2)	Avg. annual Precipitation (cm)	Measured dischagre (m^3/s)	Avg Salinity (ppt)	Freshwater discharge (m^3/s)	Spring-tide Range (m)	Neap-tide Range (m)
Waterside Beach	Total	16.3	153.1				11.5	6.5
	Long Marsh Ck	4.8		4.16	30.4	0.15		
	Horn Ck	1.6						
	Newfoundland Ck	3.6						
	Freshwater				0.1			
Alma Delta	Total	200	153.1				11.0	6.0
	Upper Salmon River	176.3		1.22	0.0	1.22		
	Cleavland Brook	15.3		0.053		0.053		
	Dickson Brook	8.4		0.023		0.023		
BSR Delta			139.0*				10.0	5.2
	Big Salmon River	278.2		6.57	0.0	6.57		
Bay of Fundy					31.4			

TABLE 6.1 — Summary table of hydraulic data from Waterside Beach, Alma delta, and the Big Salmon River delta. Under the stream heading, italicized names indicate tidal creeks and normal font fluvial ones. Catchment basin areas were determined from detailed land maps (1:25 000 scale). Precipitation data was obtained from the Weather Office (2005). Alma and Waterside are closely spaced and therefore are covered by the same weather station at Alma. The Big Salmon River is not near a station, so the value reported is for the nearest station at Saint John, New Brunswick (*), which is southwest of the delta. Freshwater discharge is the freshwater component of measured discharge based on stream salinities and measured flow rates. Tidal ranges are based on predicted values provided by the Canadian Hydrographic Service (2005).

This data indicates that Waterside Beach experiences relatively low wave energy under fair-weather conditions (< 0.75 m) and storm waves up to 3 m high (Fig. 6.6). The wave environment of the beach differs from that at BSR and Alma, as the latter two systems are exposed to waves generated from the southwest, southeast, and northeast. Waterside only experiences waves from the southwest (Fig. 6.1). In addition, Alma is partly protected by a headland to the southwest, which results in refraction of waves around the headland. Consequently, waves approach from both the southwest and south-southwest (see 1953 air photo, Fig. 6.8). Regardless of the differences in exposure to waves and wave approach, wave conditions are similar for all three systems as they all occur on the north shore of the upper Bay of Fundy and are susceptible to modification by the largest waves – those generated from the southwest (Fig. 6.1).

Geomorphology

Figure 6.4 presents maps of surface-sediment distribution for the three systems in the years indicated. In plan-view, the morphology of the deposits varies from deltaic (BSR and Alma) to beach (Waterside). The Big Salmon River delta occurs at the mouth of the Big Salmon River and comprises mainly coarse and fine gravel. The Alma delta occurs at the mouth of the Upper Salmon River, and comprises fine gravel with secondary sand and coarse gravel. Waterside Beach does not occur at the mouth of a fluvial system, but is associated with a salt marsh and tidal creeks, mainly Long Marsh Creek. Waterside is dominated by sand and fine gravel accumulations in the intertidal zone, and by sand and mud deposition in the sub-tidal zone (Figs. 6.2 and 6.4).

The coarsest-grained system is the Big Salmon River delta. At spring low tide (10 m tidal range), 1.0 km^2 of intertidal zone is exposed. It is nearly entirely composed of coarse gravel with secondary fine gravel (Fig. 6.4). The Big Salmon River cuts across the intertidal delta plain at low tide. During storms and floods, the channel shifts position across the plain through channel avulsion and lateral migration (compare river location in Fig. 6.1 to Fig. 6.5). Avulsion commonly results in the development of abandoned channel fairways, which become sites of active mud deposition. The delta occurs along a northeast-southwest trending shoreline. Consequently, waves generated along the full fetch of the bay (from the southwest) hit the delta obliquely. This is manifest on the delta plain by gravel bars migrating at an oblique angle to the shoreline (Fig. 6.5). Coarse-gravel deposits occur as flat to shallowly seaward-dipping beds. Fine-gravel deposits occur either as flat beds or more commonly as gravel bars (up to 2 m high) that migrate in a landward direction. Gravel bars are especially common near the mouth of the river, where they tend to have a short wavelength (100 to 200 m long) and low-amplitude (< 1 m). Landward of the bars and within the abandoned channels, mud deposition takes place. Areas of active mud deposition cover approximately 4.5% of the intertidal area of the delta. The mud is predominantly soupy.

FIGURE 6.4 – Sediment distribution maps of the Big Salmon River delta, Alma delta, and Waterside Beach. Main grain-size categories are defined in Figure 6.2. Intertidal mapping was conducted using GPS, sediment sampling, trenching, and x-ray imaging of sediment box cores. Sub-tidal sediment mapping (Waterisde only) is based on grab samples collected in 2005 and seismic mapping from surveys collected in 2004. The Waterside map is modified from Dashtgard et al. (2006). Areal extents of the intertidal and sub-tidal zones are given based on extrapolated spring-tide low-water levels (Table 6.1) and assuming a 10 m spring-tide range (10 m STR). Ten meters in the spring tide range of the Big Salmon River delta.

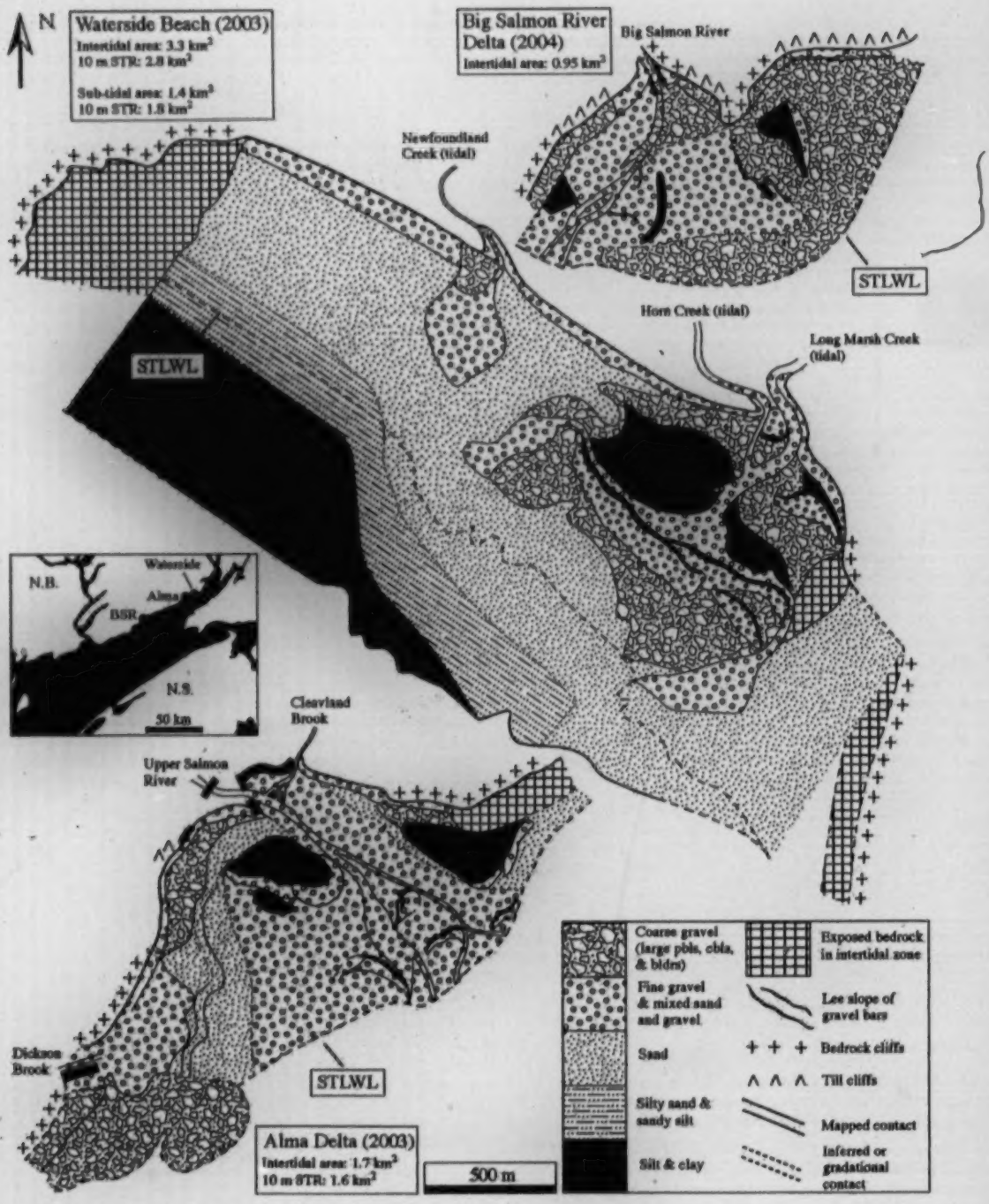
N
Waterside Beach (2003)
Intertidal area: 3.3 km²
10 m STR: 2.8 km²
Sub-tidal area: 1.4 km²
10 m STR: 1.8 km²
Big Salmon River Delta (2004)
Intertidal area: 0.95 km²
Big Salmon River
Newfoundland Creek (tidal)
STLWL
Horn Creek (tidal)
Long Marsh Creek (tidal)
STLWL
N.B.
Waterside
Alma
BSR
N.S.
50 km
Cleaviand Brook
Upper Salmon River
Dickson Brook
STLWL
Alma Delta (2003)
Intertidal area: 1.7 km²
10 m STR: 1.6 km²
500 m
Coarse gravel (large pbls, cbls, & bldrs)
Fine gravel & mixed sand and gravel
Sand
Silty sand & sandy silt
Silt & clay
Exposed bedrock in intertidal zone
Lee slope of gravel bars
Bedrock cliffs
Till cliffs
Mapped contact
Inferred or gradational contact

In terms of the areal extent of the coastal zone and grain size, Alma is intermediate between the BSR delta and Waterside Beach (Figs. 6.2 and 6.4). The intertidal zone covers approximately 1.7 km^2 at spring low tide (1.6 km^2 if the tidal range was 10 m) and is an amalgamation of deltas deposited at the mouths of the Upper Salmon River (USR) and Dickson Brook. The dip of the Alma delta front measured on shore-normal seismic lines varies between 1.6° and 2.3° (Fig. 6.7). Average grain size fines offshore with a seaward shift in the trend where the Upper Salmon River debouches into the bay at low tide. During storms or floods the USR migrates across the delta plain (Ali 1964). The frequency of these shifts is decadal (Fig. 6.8) versus the annual to semi-decadal shifts noted for the BSR. On the delta surface, both large and small, landward-

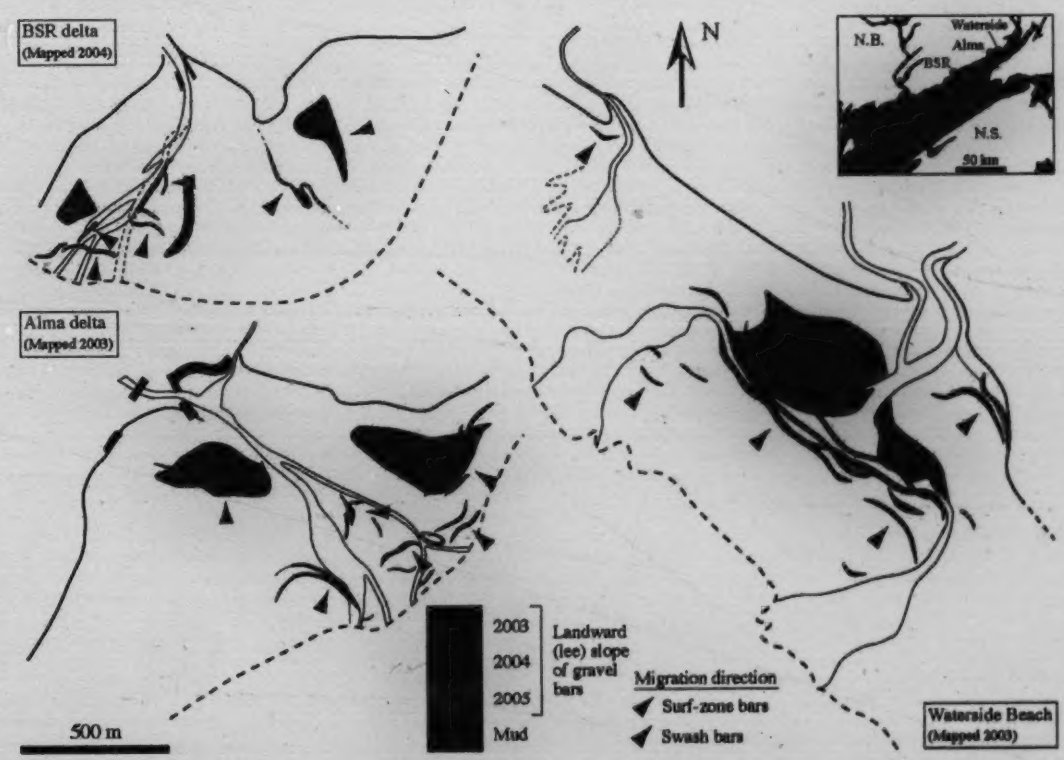

FIGURE 6.5 – Simplified sediment-distribution maps indicating shifts in the position of the gravel bars from 2003 to 2005. The thin coloured zones represent the steeply landward-dipping (lee) face of the bars. The position of mud deposits in the first year they were mapped (2003 for Alma and Waterside and 2004 for BSR) are indicated as a means to assess bar migration. Black arrows indicate the migration direction of surf-zone bars and grey arrows indicate the migration direction of swash bars.

migrating gravel bars (up to 2 m high and 500 m long) are present. Surface sediment of the Alma delta is dominated by fine gravel and mixed sand and gravel. This sediment tends to be deposited by either the river or the gravel bars and therefore accumulates in channel-shaped structures or as steeply landward-dipping plane beds. On the landward (lee) side of the bars mud deposition is commonly observed. The mud is predominantly sandy silt (Fig. 6.2) and drapes the underlying topography. In abandoned channel lows, interbedded mud and sand can be up to 20 cm thick. Mud beds are relatively resistant and palimpsest mud beds may be exposed on the delta plain after the gravel bars have migrated over the deposit (Fig. 6.4). Continuous mud beds cover approximately 6% of the intertidal delta plain. Sand and pebbly sand infill the paleo-channel fairway (channel location in 1962; Fig. 6.8). Course gravel dominates in the present-day river channel and along the margins of the delta (Fig. 6.4). Fine and coarse gravel deposits occur within the central part of the delta plain and are completely covered in small to medium-sized barnacles. Barnacle size (likely 2-3 years old; Schäfer 1972) suggests the gravels experience infrequent transport (stable substrate) and/or minor sedimentation after initial deposition.

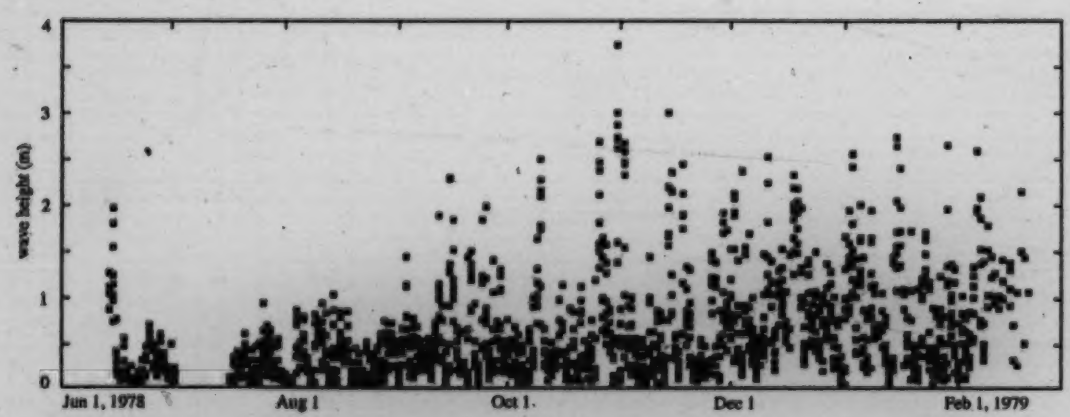

FIGURE 6.6 – Nine months of wave data collected offshore of Waterside Beach every three hours from June 1978 to February 1979. Storm-wave heights are measured up to 3 m, whereas fair-weather waves are generally below 0.75 m. This data is modified from Amos et al. (1991) and is available online at Ocean Sciences (2005).

Waterside Beach is the largest and most sand-rich of the three systems (Figs. 6.2 and 6.4). The intertidal zone covers 3.3 km² (at spring low tide) with an additional 1.4 km² occurring sub-tidally. However, if the spring tide range were 10 m, the intertidal area would be 2.8 km² and the subtidal zone 1.8 km². The beach is oriented perpendicular to the main fetch of the Bay of Fundy and experiences some of the highest-energy waves in the bay (Figs. 6.1 and 6.6). Cross-cutting the beach and associated salt marsh are tidal channels that significantly influence the sedimentological character of the beach (Fig. 6.4). These tidal channels are widest and deepest (LMC is 54 m wide and 8 m deep) where they debouch onto the beach and taper in a landward direction (Dashtgard and Gingras 2005).The banks of the tidal creeks are either eroded or are widened by wave-scour within the intertidal and sub-tidal zones (Dashtgard et al. 2006; Dashtgard et al. in review).

Waterside Beach can be subdivided into three main sedimentological zones: (1) a rocky intertidal platform; (2) a thin, mixed sand and gravel deposit that occurs outside the area of tidal-creek down cutting; and, (3) a thick beach deposit of interbedded sand,

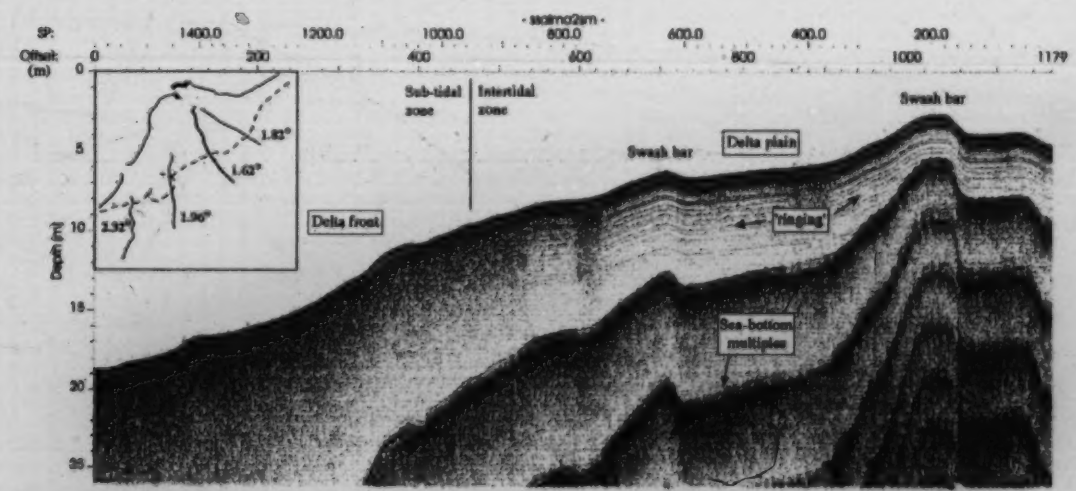

FIGURE 6.7 – Shore-normal seismic survey of Alma delta illustrating the shallow slope of the delta front. The "ringing" effect results from a lack of seismic penetration because of air trapped in the sediment. Sea-bottom multiples result from seismic reflections bouncing off the sea-bottom and water surface. The location of the line is indicated on the map and is highlighted in bold. Maximum dip angles of the delta front are indicated on the map.

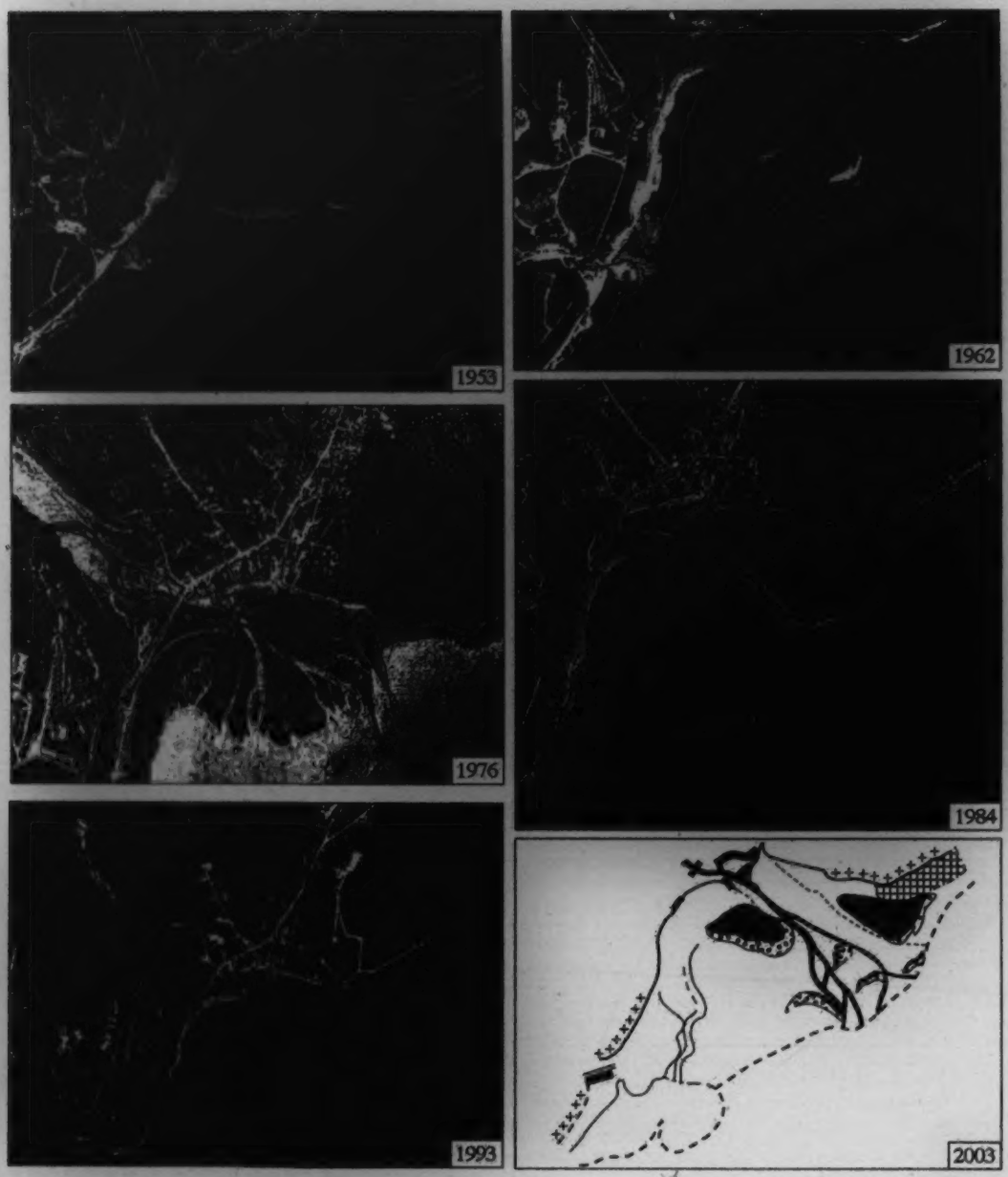

FIGURE 6.8 – Air photos and map of Alma delta from 1953 to present. Note the changes in the location of the bars on the delta plain and in the channel pathway. Also note the refraction of waves around the headland at the southwest end of the beach in the 1953 air photo. The channel has not significantly shifted position since at least 1976.

gravel, and mud situated where the tidal creeks debouch onto the beach (Fig. 6.9). The rocky platform is developed as a result of wave-erosion of cliffs at the northwest and southeast ends of the beach. The platform covers 0.3 km^2 of the intertidal zone and is either exposed on the beach surface or covered by a thin veneer of sediment (Fig. 6.4). The second zone is typical of mixed sand and gravel beaches developed in megatidal settings (Anthony and Orford 2002; Forbes and Taylor 1987; Masselink and Short 1993; Short 1991; Wright and Short 1984). The beach is generally less than 2 m thick with a concave-up morphology. Below a moderately steep, seaward-dipping beachface of mixed sand and gravel is a shallowly seaward-dipping terrace of coarse-grained sand fining offshore to silty sand and finally sandy silt at the toe of the beach (Fig. 6.4). The third

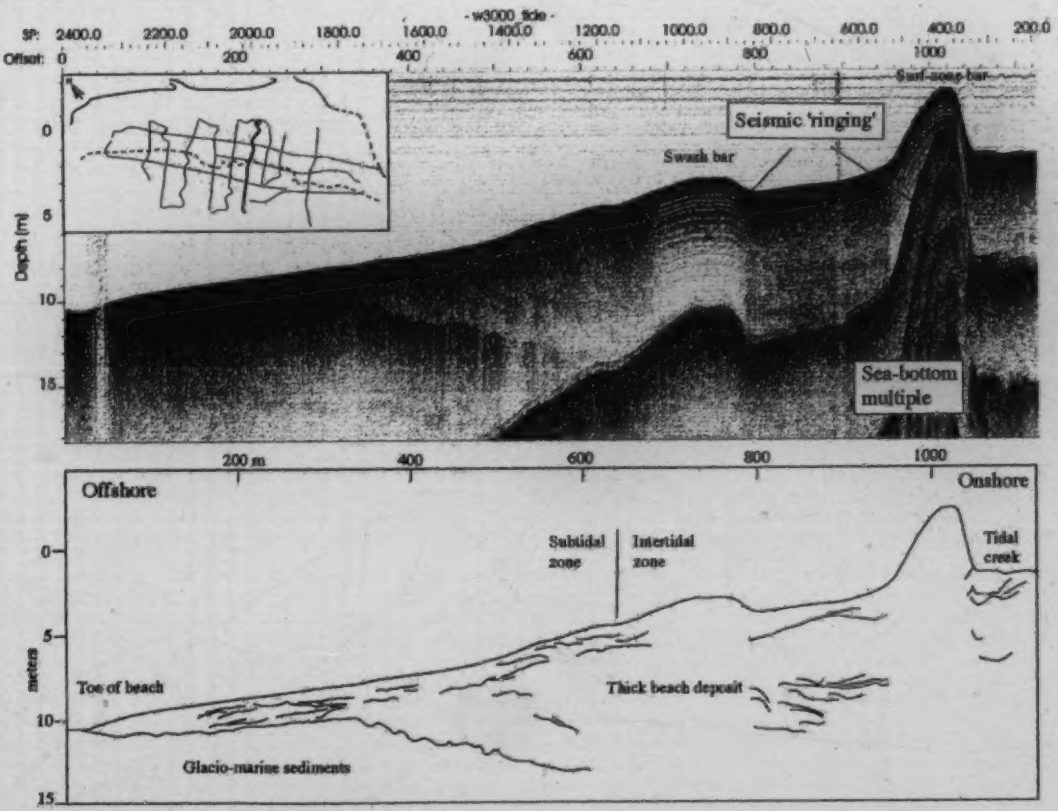

FIGURE 6.9 – Shore-normal seismic line of Waterside Beach. Imaged on the line are a large, landward-migrating surf-zone bar and a thick beach sequence deposited within the zone of tidal creek down cutting. For a detailed discussion of the seismic and post-glacial history of Waterside Beach see Dashtgard et al. (in review).

zone occurs where Long Marsh Creek debouches onto the beach at low tide. Here, the beach sequence is much thicker (Fig. 6.9) and comprises interbedded gravel, sand, and mud. Sedimentation results from tidal-creek processes (fine gravel and sand), landward-migrating gravel bars (coarse and fine gravel, and sand), or from suspension (mud) in quiescent zones developed landward of the gravel bars. In 2003, mud deposits covered approximately 7.3 % of the intertidal zone.

DISCUSSION

By comparing hydraulic process (river, wave, tidal) to the grain size and geomorphology of the Big Salmon River delta, Alma delta, and Waterside Beach it is possible to semi-quantify the relationship between hydraulic conditions, sedimentological characteristics, and morphology. Three relationships are derived from the results: (1) decreasing areal extent (size) of the coastal zone is proportional to increasing average grain size; (2) the occurrence of swash and surf-zone bars is a function of wave-energy and indirectly of fluvial input; and (3) the amount of bar-associated mud deposition in the coastal zone can be used to predict the development, type and frequency of gravel bars. Finally, hydraulic controls on classification of gravel-dominated systems are discussed.

Grain Size and Areal Extent of the Coastal Zone

The relationship between grain size and delta dimensions in plan view derived in this study supports the conclusion that deltas decrease in areal extent with increasing grain size (Orton and Reading 1993; Reading and Collinson 1996). The delta plain (approximately equivalent to the intertidal zone) of the coarse-gravel-dominated BSR delta is areally the smallest (1.0 km^2), whereas the finer-grained Alma delta is 1.6 times larger at 1.6 km^2 (assuming a 10 m spring-tide range, Fig. 6.4). Comparing these values to average grain size and sorting, the increase in delta area is accompanied by a decrease in average grain size from –5.99 to –4.29 ϕ (Fig. 6.2) and improved sorting from very

poorly (2.23 σ) sorted to poorly (1.86 σ) sorted. This relationship can be extended to non-deltaic, gravel-dominated coasts. Such is the case for Waterside Beach, where the intertidal zone (2.8 km^2) is 1.8 times larger than the Alma delta and 3.0 times larger than the BSR delta (Fig. 6.4). Comparing grain size and sorting of Waterside (-2.05 ϕ, 1.24 σ) to Alma and BSR, it is clear that Waterside is much finer grained and better sorted (Fig. 6.2). In fact, grain size (phi scale) and the area occupied by the intertidal zone (assuming a 10 m spring-tide range) exhibit a log-linear relationship (Fig. 6.10), where areal extent increases by 0.5 km^2 for every one-phi increase (i.e. –2 to –1 ϕ) in grain size.

It is also evident from Figure 6.10 that for hydraulically transported coastal deposits there is potentially a maximum average grain size for a deposit. This empirical value is semi-quantifiable and appears to occur in the coarse-cobble grain-size class (-7.75 ϕ or 215 mm). A theoretical maximum is predictable for hydraulically transported sediment based on the fluid dynamics of water. Lift and drag forces exerted on the bedload by a fluid act to move the sediment, while gravitational and frictional forces act against it (Allen 1997b; Middleton and Southard 1984). Grain size increases result in a greater gravitational force exerted on the clast, requiring higher drag and lift forces. Lift and drag forces are a function of fluid density, hydraulic radius (width and depth of the stream) and slope such that larger streams and higher slopes (faster flow rates) are required to transport larger clasts (Allen 1997b; Schumm 1977). The relationship between lift and drag (fluid) forces, gravitational forces, and grain size is best illustrated by the Shields diagram (Allen 1997b; Shields 1936). With increasing grain size there is a corresponding increase in the grain-Reynolds number and decrease in the ratio of fluid to gravitational forces. Consequently, the slope and size of the stream transporting the bed load must increase to transport large clasts (Miller et al. 1977). In natural systems, a maximum transportable clast size will be reached at a realistic maximum value for stream slope and wetted perimeter (width and depth).

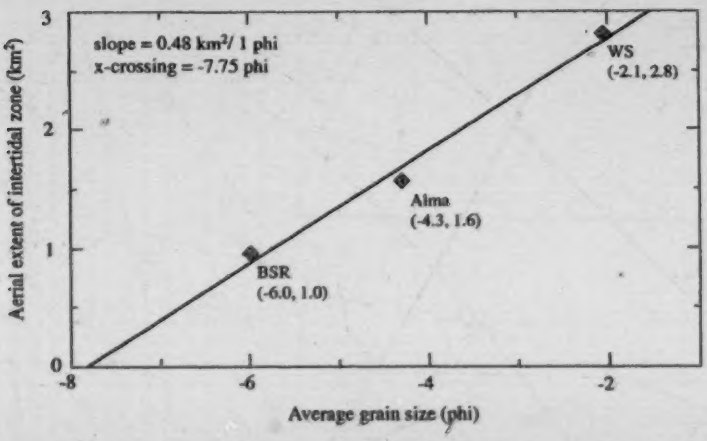

FIGURE 6.10 – Graph of the areal extent of the intertidal zone (assuming a 10 m spring tide range) versus average grain size (in phi scale) of the three systems. The three points describe a log-linear relationship where coastal zone area decreases with increasing grain size. The data also suggest there is a maximum average grain size for coastal deposits that are hydraulically transported. In this study that value is –7.75 ϕ or 215 mm.

Swash and Surf-Zone Bars

At Waterside, Alma, and Big Salmon River, both large and small, landward-migrating gravel bars were observed and mapped. Trenching and sampling of the bars indicates that all bars are composed of moderately to steeply, landward-dipping beds of fine gravel and mixed sand and gravel. The bars differ, however, in their size and frequency (Figs. 6.4 and 6.5). Nearly all the gravel bars on the BSR delta are relatively poorly developed, of low amplitude (< 1 m), and less than 200 m long (Fig. 6.5). Alma has small, low-amplitude bars developed at and near the mouth of the river and larger more permanent ones (up to 2 m high and 500 m long) developed away from the channel mouth. At Waterside, the gravel bars are generally quite large – up to 5.5 m high (Fig. 6.9) and 800 m long.

The small low-amplitude bars (grey arrows, Fig. 6.5) are considered swash bars (King 1972; King and Williams 1949) that develop as waves rework onshore, sediment deposited at or near the low-tide limit of the channels. These gravel bars are common around river mouths (Bluck 1999; Reading and Collinson 1996; Wright 1977)

and on tidal flats (McCave and Geiser 1978; Yang et al. 2005). The swash bars form near the low-tide level, migrate rapidly landward under fair-weather conditions, and are obliterated during storms. They are short lived and exhibit a significant degree of variation in orientation depending on the prevalent wave (wind) direction at the time of their formation. The larger, more permanent bars (black arrows, Fig. 6.5) are only partly developed as a result of swash processes and are considered akin to inner surf-zone bars (Anthony et al. 2004; Kroon and Masselink 2002; Sunamura and Takeda 1984). These structures mainly develop in the shallow sub-tidal zone and migrate onshore during storms (Dashtgard et al. 2006; Kroon and Masselink 2002; Sunamura and Takeda 1984). Migration rates along surf-zone bar crests were measured up to 50 m/year at Waterside and nearly 100 m/year at Alma. As these bars migrate onshore, they gain amplitude and size from the sub-tidal to lower intertidal zone. However, from the middle to upper intertidal, bar height is regulated by tidal range such that bars decrease in amplitude and length landward. At the landward terminus of the beach or delta they either accrete to the beachface or are washed out by storms.

The dominance of one bar type or the other can be related to channel stability, which is a function of the local fluvial discharge. Higher discharge tends to correlate to higher frequency of channel avulsion and migration across the coastal plain resulting in the dominance of swash bars over surf-zone bars. For the BSR delta, the river shifted position drastically between 1993 (Fig. 6.1) and 2004 (Fig. 6.4), and migrated 100 m (southward) between 2004 and 2005 (Fig. 6.5). The Upper Salmon River (Alma) drains a catchment area that is 0.7 times that of the BSR. The smaller catchment is reflected in the lower flow rates (Table 6.1), which in turn, results in greater stability of distributary channels on the Alma delta plain. Because the Upper Salmon River has not shifted position significantly since 1976 (Fig. 6.8), large surf-zone bars are developed on the delta plain and remain for years and possibly decades. Swash bars are also present on the Alma delta, but these are generally restricted to a localized region where the USR

drains into the bay at low tide. Waterside Beach is ornamented with both surf-zone and swash bars (Fig. 6.4) that mainly developed seaward of where Long Marsh Creek empties into the bay at low tide. Both bar types at Waterside exhibit the same orientation. This is partly because the beach is oriented perpendicular to the main fetch of the Bay of Fundy, but mostly because the beach is flanked by land on three sides and does not experience waves from any other direction. The flow in and out of LMC is nearly completely (96.4%) tidally driven. At low tide, it is confined to shallow channels that form a braided drainage network in which flow lacks sufficient energy to erode the large, surf-zone bars (Figs. 6.4 and 6.5). Consequently, these bars survive for longer periods of time and migrate slowly (0 to 50 m year^{-1}) onshore. Swash bars on Waterside Beach are relatively unstable, easily eroded, and are generally not mappable from year to year.

Mud deposition is often associated with the gravel bars (Fig. 6.5). The extent and amount of deposition is crudely linked to bar size such that mud deposition is common on the landward (lee) side of larger surf-zone bars and is uncommon behind bars less than 1.5 m high (i.e. swash bars; Dashtgard et al. 2006). The larger bars are relatively stable and baffle wave-energy resulting in the deposition of thick, continuous mud beds on the delta plain or beach. Mud deposition is generally not associated with swash bars however, because of their instability and low amplitude. Where deposition does occur the mud tends to be very soupy such that as the bars migrate, gravel avalanching down the lee face sinks into the mud and forms muddy gravels. Eventually the bar is destroyed by wave action resulting in the rapid erosion of related mud deposits.

As discussed, bar type is a function of fluvial discharge, and the degree of mud deposition a function of bar type. It follows then that the degree of mud deposition is indirectly related to fluvial discharge. For the three study areas, the BSR delta, with mainly swash bars and the highest discharge, has the least amount of mud deposition (4.5%). This value increases to 6% at Alma, and to 7.3% for Waterside. Waterside is

dominated by surf-zone bars, and has the lowest fluvial discharge (Fig. 6.5). The extent of mud deposition (associated with the gravel bars) in the intertidal zone may therefore be used as a tool for predicting bar type and coastal morphology in conglomeratic successions preserved in the rock record.

It is noted that the relationship between the amount of mud deposition and fluvial input just described differs from the traditional relationship. Typically, mud is sourced from rivers and upon mixing with marine water, flocculates and accumulates in the zone of turbidity maximum (Eisma 1986). In the Bay of Fundy, erosion of Holocene muds from the sea floor is the main source of suspended material (Amos 1987; Amos et al. 1991). In fact, this source contributes nearly all of the suspended material in the bay. Mud deposition on the coast is therefore, not directly proportional to fluvial input, but instead exhibits the indirect relationship described.

Hydraulic Controls on the Classification of Gravel-Dominated Coasts

Waterside Beach, Alma delta, and Big Salmon River delta exhibit sedimentological and/or morphological characteristics that can be attributed to fluvial, wave, and tidal processes. By establishing relative energy contributions from rivers, waves, and tides, it is thereby possible to classify these systems using the tripartite division of marginal-marine depositional environments. Tidal range is similar for the three systems (greater than 10 m spring range). Relative wave-energy input is less uniform, but for comparative purposes it is assumed that wave conditions (Fig. 6.6) are similar because of the close proximity of the three deposits (Fig. 6.1) and exposure to waves generated along the full fetch of the bay. With these assumptions in mind, variations in sedimentology and morphology can be attributed to fluvial-energy input (reported as drainage-catchment area) relative to uniform wave- and tidal-energy contributions.

The Big Salmon River delta is river-dominated with low to moderate wave influence (Fig. 6.11). River catchment area is 1.4 times higher than at Alma (USR) and over 17 times greater than the total drainage area of Waterside's tidal creeks (Table 6.1). The BSR delta is also the smallest and coarsest grained (Figs. 6.2 and 6.4), and is considered to occur near the river-dominated apex of the tripartite division of gravel-dominated depositional environments (Dalrymple et al. 1992; Galloway 1975; Hayes 1979; Orton and Reading 1993). Wave effects on the delta are manifest as small, short-lived, gravel swash bars and occasional surf-zone bars that develop on the delta plain (Fig. 6.5).

Waterside Beach is a mixed sand and gravel beach (wave dominated) whose morphology is directly and indirectly influenced by tides (see geomorphology section of results). The beach is the largest of the three sites (Fig. 6.4), the finest grained (Fig. 6.2), and is oriented perpendicular to the main fetch of the bay. In addition, landward-migrating, gravel surf-zone and swash bars are developed on the beach surface. Direct tidal influence is evidenced in that beach topography is similar to that of tidal beaches reported by Masselink and Short (1993), and Anthony et al. (2002). Indirect tidal influence is manifest through tidal controls on the width and depth of tidal creeks. In trangressive settings, this can result in deposition of thick beach sequences (Fig. 6.9; Dashtgard et al. 2006). Fluvial-energy input is insignificant relative to tidal contributions, and is mainly limited to freshwater mixing within the tidal creeks and lakes. For Long Marsh Creek, which has a flow rate (near the landward limit of the creek) that is 0.6 times that of BSR, only 3.2% of the flow is freshwater. Taken as a whole, the negligible fluvial input, presence of tidal channels, beach topography, and dominance of wave-formed structures and morphology suggests that Waterside is a highly tide-modified, wave-dominated beach (Fig. 6.11).

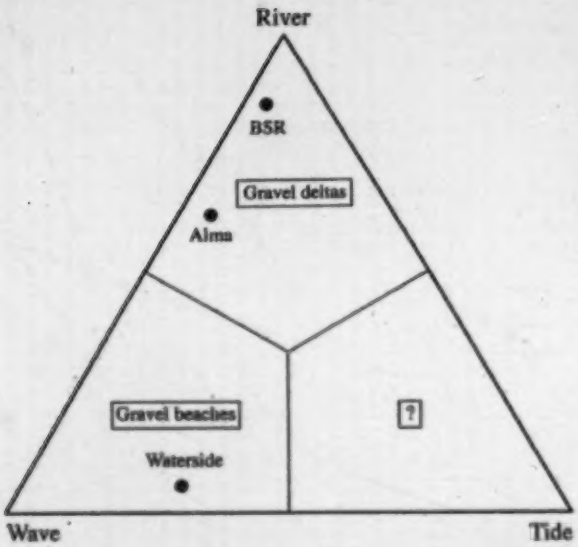

FIGURE 6.11 – Classification of the Big Salmon River delta, Alma delta, and Waterside Beach using a tripartite classification scheme based on hydraulic process. The BSR delta is river-dominated with low to moderate wave modification. Alma delta is also river-dominated with high wave-modification. Waterside is a highly tide-modified, wave-dominated beach.

Between these systems is the river-dominated, highly wave-modified, Alma delta (Fig. 6.11). The delta occurs at the mouths of the Upper Salmon River, Dickson Brook, and Cleavland Brook whose combined catchment area is 0.7 times that of the Big Salmon River (Table 6.1). Areally, the delta is smaller and coarser-grained than Waterside Beach, but bigger and finer grained than the BSR delta (Figs. 6.2 and 6.4). The USR migrates across the delta plain during floods, although the occurrence of this migration is much lower than for the BSR (Fig. 6.8). Limited channel avulsion and low discharge rates have resulted in wave-formed bed forms dominating the delta plain (Figs. 6.4 and 6.5). Wave-modification of the delta is further evidenced by the shallow dip of the delta front (< 2.5°; Fig. 6.7) compared to typical gravel-delta fronts (Colella 1988; Marzo and Anadón 1988; Massari 1984; Postma 1990; Reading and Collinson 1996; Wescott and Ethridge 1980, 1982, 1983). Consequently, the Alma delta is considered a highly wave-modified, river-dominated gravel delta that acts partly like a delta – in that the main sediment source is the river and it is a shoreline proturbance – and partly like a beach with wave processes dominating depositional architecture over much of the delta plain.

CONCLUSIONS

Comparison of the three gravel-dominated, marginal-marine environments in the megatidal Bay of Fundy provides insights into the relationships between hydraulic process (fluvial, wave, tidal), grain size, and geomorphology. Four main conclusions are drawn.

(1) For gravel-dominated coasts, the areal extent of the coastal zone increases inversely with average grain size (Figs. 6.2, 6.4, and 6.10). In this study, there is a 0.5 km^2 increase in size of the coastal zone for every one-phi increase (i.e. –2 to -1 phi) in grain size (Fig. 6.10). The smallest system, Big Salmon River delta (1.0 km^2 intertidal zone), also exhibits the coarsest grain size (avg –5.99 ϕ) and occurs at the mouth of the river with the largest drainage basin (278 km^2). Alternatively, the most areally extensive system, Waterside Beach (2.8 km^2 intertidal area assuming the same tidal range as BSR, Table 1), is also the finest grained (-2.05 ϕ). The tidal channels at Waterside define a small catchment basin (16 km^2 combined) that is masked by tidal flow within the creeks. Alma delta is between these two at 1.6 km^2 and an average grain size of –4.29 ϕ. The combined drainage area for Alma tributaries (Upper Salmon River, Dickson Brook, and Cleavland Brook) is 200 km^2.

(2) The occurrence of swash and surf-zone bars is a function of fluvial input and wave energy. Swash bars are small (< 1 m high, 100 to 200 m long, Fig. 6.5), develop as a result of swash processes, migrate rapidly onshore, and are washed out during storms or by river erosion. Surf-zone bars tend to be larger (up to 5.5 m high and 800 m long; Fig. 6.9) and more permanent than swash bars. Surf-zone bars migrate landward during storms and are not destroyed by tidal currents or lower-energy distributary channels. Swash bars are more common on the BSR delta, whereas surf-zone bars are more common at Waterside and Alma (Fig. 6.5).

It is hypothesized that rapid river migration (scale of years versus decades) on the BSR delta restricts the longevity of surf-zone bars, thus favoring short-lived swash bars.

(3) Landward of surf-zone bars and occasionally of swash bars, zones of mud deposition develop. Mud in these deposits is sourced from the Bay of Fundy and not from rivers. The degree of bar-associated mud deposition on the coastal plain is proportional to the type and number of gravel bars. Therefore, the amount of mud encountered in a coarse-grained deposit can be used to predict the morphology of the coastal zone.

(4) The classification of gravel-dominated coasts, based on coastal morphology and sedimentology, is dependent on relative energy contributions from river-, wave-, and tidal-processes. The BSR delta with the largest catchment area and coarsest grain size is a river-dominated gravel delta with low to moderate wave-modification. Alma delta is a highly wave-modified, river-dominated delta. It is deltaic in that it has a fluvial point source (Upper Salmon River) and protrudes from the shoreline. However, wave-processes dominate deposition over much of the delta plain, and have smoothed the delta front, such that it dips at a much shallower angle (< 2.5°) than typical gravel deltas. Waterside is a tide-modified, wave-dominated beach. Tides indirectly determine beach morphology by influencing the morphology of associated depositional environments. (1) For Waterside Beach, tides control the cross-sectional area of tidal creeks, which in turn locally determines beach thickness and sedimentological character.

Much of the work presented herein suggests some interesting trends between hydraulic process, and the sedimentology and geomorphology of gravel-dominated systems. This work is at a preliminary stage however, and requires additional data to confirm or refute the findings. In particular, the Big Salmon River delta, Alma

delta, and Waterside Beach occur within a megatidal embayment that is not typical of most coastlines. Incorporating these results into existing models for open coasts and examining these deposits as a function of quantified hydraulic processes may allow us to better compare this work to existing classifications of gravel-dominated systems. Moreover, further examination and quantification of gravel-dominated systems may render possible the development of a classification scheme for conglomerates that more accurately represents the depositional environments that may occur under varying relative contributions of river-, wave-, and tidal-energy.

REFERENCES

Ali, S.I., 1964, Study of recent sediments of the beach and delta at the mouth of the Alma River (Bay of Fundy) [unpublished Master's thesis]: University of New Brunswick, Fredericton, New Brunswick, 123 p.

Allen, J.R.L., 1997a, Simulation models of salt-marsh morphodynamics: some implications for high-intertidal sediment couplets related to sea level change: Sedimentary Geology, v. 113, p. 211-223.

Allen, P.A., 1997b, Earth Surface Processes: London, UK, Blackwell Science, 404 p.

Amos, C.L., 1987, Fine-grained sediment transport in Chignecto Bay, Bay of Fundy, Canada: Continental Shelf Research, v. 7, p. 1295-1300.

Amos, C.L., and Asprey, K.W., 1979, Geophysical and sedimentary studies in the Chignecto Bay system, Bay of Fundy - a progress report, Geological Survey of Canada, p. 245-252.

Amos, C.L., Tee, K.T., and Zaitlin, B.A., 1991, The post-glacial evolution of Chignecto Bay, Bay of Fundy, and its modern environment of deposition, *in* Smith, D.G., Reinson, G.E., Zaitlin, B.A., and Rahmani, R.A., eds., Clastic Tidal Sedimentology: Calgary, AB, Canada, Canadian Society of Petroleum Geologists, p. 59-89.

Amos, C.L., and Zaitlin, B.A., 1985, The effect of changes in tidal range on a sublittoral macrotidal sequence, Bay of Fundy, Canada: Geo-Marine Letters, v. 4, p. 161-169.

Anthony, E.J., 2000, Marine sand supply and Holocene coastal sedimentation in northern France between the Seine estuary and Belgium, *in* Pye, K., and Allen, J.R.L., eds., Coastal and Estuarine Environments - Sedimentology, Geomorphology and Geoarchaeology: London, UK, Special Publications of the Geological Society of London, p. 87-97.

Anthony, E.J., Levoy, F., and Monfort, O., 2004, Morphodynamics of intertidal bars on a megatidal beach, Merlimont, Northern France: Marine Geology, v. 208, p. 73-100.

Anthony, E.J., and Orford, J.D., 2002, Between wave- and tide-dominated coasts: the middle ground revisited: Journal of Coastal Research Special Issue 36, p. 8-15.

Arnott, R.W.C., 2004, The role of fluid- and sediment-gravity flow processes during deposition of deltaic conglomerates (Cardium Formation, Upper Cretaceous), west-central Alberta: Bulletin of Canadian Petroleum Geology, v. 51, p. 426-436.

Bayliss-Smith, T.P., Healey, R., Lailey, R., Spencer, T., and Stoddart, D.R., 1979, Tidal flow in salt marsh creeks: Estuarine, Coastal and Marine Science, v. 9, p. 235-255.

Bluck, B.J., 1967, Sedimentation of beach gravels: Examples from south Wales: Journal of Sedimentary Petrology, v. 37, p. 128-156.

Bluck, B.J., 1999, Clast assembling, bed-forms, and structure in gravel beaches: Transactions of the Royal Society of Edinburgh, Earth Sciences, v. 89, p. 291-323.

Boggs, S., Jr., 1995, Principles of Sedimentology and Stratigraphy, 2nd edition: New Jersey, Prentice-Hall, 774 p.

Bourgeois, J., and Leithold, E.L., 1984, Wave-worked conglomerates - depositional processes and criteria for recognition, *in* Koster, E.H., and Steel, R.J., eds., Sedimentology of Gravels and Conglomerates: Calgary, AB, Canada, Canadian Society of Petroleum Geologists, p. 331-343.

Canadian Hydrographic Service, 2005. Tides, Currents, and Water Levels. www.waterlevels.gc.ca. Department of Fisheries and Oceans Canada.

Church, M.A., Mclean, D.G., and Wolcott, J.F., 1987, River bed gravels: Sampling and analysis, *in* Thorne, C.R., Bathurst, J.C., and Hey, R.D., eds., Sediment Transport in Gravel-Bed Rivers: Chichester, U.K., John Wiley & Sons, p. 43-79.

Clifton, H.E., 1981, Progradational sequences in Miocene shoreline deposits, southeastern Caliente range, California: Journal of Sedimentary Petrology, v. 51, p. 165-184.

Colella, A., 1988, Pliocene-Holocene fan deltas and braid deltas in the Crati Basin, southern Italy: a consequence of varying tectonic conditions, *in* Nemec, W., and Steel, R.J., eds., Fan Deltas: Sedimentology and Tectonic Settings: London, UK, Blackie, p. 50-74.

Dalrymple, R.W., Zaitlin, B.A., and Boyd, R., 1992, Estuarine facies models: conceptual basis and stratigraphic implications: Journal of Sedimentary Petrology, v. 62, p. 1130-1146.

Dashtgard, S.E., and Gingras, M.K., 2005, Facies architecture and ichnology of recent salt-marsh deposits: Waterside Marsh, New Brunswick, Canada: Journal of Sedimentary Research, v. 75, p. 596-607.

Dashtgard, S.E., Gingras, M.K., and Butler, K.E., 2006, Sedimentology and stratigraphy of a transgressive, muddy gravel beach: Waterside Beach, Bay of Fundy, Canada: Sedimentology, v. 53, p. 279-296.

Dashtgard, S.E., White, R.O., Butler, K.E., and Gingras, M.K., in review, Effects of relative sea level change on the depositional architecture of an embayed beach, Waterside Beach, Bay of Fundy, Canada: Marine Geology.

Davidson-Arnott, R.G.D., Van Proosdij, D., Ollerhead, J., and Schostak, L., 2002, Hydrodynamics and sedimentation in salt marshes: examples from a macrotidal marsh, Bay of Fundy: Geomorphology, v. 48, p. 209-231.

Davis, R.A.J., and Hayes, M.O., 1984, What is a wave-dominated coast?: Marine Geology, v. 60, p. 313-329.

Dyer, K.R., and Huntley, D.A., 1999, The origin, classification and modelling of sand banks and ridges: Continental Shelf Research, v. 19, p. 1285-1330.

Eisma, D., 1986, Flocculation and de-flocculation of suspended matter in estuaries: Netherlands Journal of Sea Research, v. 20, p. 183-199.

Engels, S., and Roberts, M.C., 2005, The architecture of prograding sandy-gravel beach ridges formed during the last Holocene highstand: Southwestern British Columbia, Canada: Journal of Sedimentary Research, v. 75, p. 1052-1064.

Ethridge, F.G., and Wescott, W.A., 1984, Tectonic setting, recognition and hydrocarbon reservoir potential of fan-delta deposits, *in* Koster, E.H., and Steel, R.J., eds., Sedimentology of Gravels and Conglomerates: Calgary, Canadian Society of Petroleum Geologists, p. 217-235.

Folk, R.L., and Ward, W.C., 1957, Brazos River bar: A study in the significance of grain size parameters: Journal of Sedimentary Petrology, v. 27, p. 3-26.

Forbes, D.L., and Taylor, R.B., 1987, Coarse-grained beach sedimentation under paraglacial conditions, Canadian Atlantic Coast, *in* FitzGerald, D.M., and Rosen, P.S., eds., Glaciated Coasts: San Diego, U.S.A., Academic Press, p. 51-86.

Galloway, W.E., 1975, Process framework for describing the morphologic and stratigraphic evolution of deltaic depositional systems, *in* Broussard, M.L., ed., Deltas, Models for Exploration: Houston, Texas, Houston Geological Society, p. 87-98.

Grant, D.R., 1970, Recent coastal submergence of the Maritime Provinces, Canada: Canadian Journal of Earth Sciences, v. 7, p. 676-689.

Hart, B.S., and Plint, A.G., 1989, Gravelly shoreface deposits: a comparison of modern and ancient facies sequences: Sedimentology, v. 36, p. 551-557.

Hart, B.S., and Plint, A.G., 2003, Stratigraphy and sedimentology of shoreface and fluvial conglomerates: insights from the Cardium Formation in NW Alberta and adjacent British Columbia: Bulletin of Canadian Petroleum Geology, v. 51, p. 437-464.

Hayes, M.O., 1979, Barrier island morphology as a function of tidal and wave regime, *in* Leatherman, S.P., ed., Barrier Islands - from the Gulf of St. Lawrence to the Gulf of Mexico: New York, Academic Press, p. 1-27.

Hoey, T.B., 2004, The size of sedimentary particles, *in* Evans, D.J.A., and Benn, D.I., eds., A Practical Guide to the Study of Glacial Sediments: London, U.K., Arnold Publishers, p. 52-77.

King, C.A.M., 1972, Beaches and Coasts: London, UK, Edward Arnold, 570 p.

King, C.A.M., and Williams, W.W., 1949, The formation and movement of sand bars by wave action: Geographical Journal, v. 113, p. 70-85.

Kroon, A., and Masselink, G., 2002, Morphodynamics of intertidal bar morphology on a macrotidal beach under low-energy wave conditions, North Lincolnshire, England: Marine Geology, v. 190, p. 591-608.

Krumbein, W.C., and Pettijohn, F.J., 1938, Manual of Sedimentary Petrology: New York, Appleton-Century Crofts, 549 p.

Levoy, F., Anthony, E.J., Monfort, O., and Larsonneur, C., 2000, The morphodynamics of megatidal beaches in Normandy, France: Marine Geology, v. 171, p. 39-59.

Marzo, M., and Anadón, P., 1988, Anatomy of a conglomeratic fan-delta complex: the Eocene Montserrat Conglomerate, Ebro Basin, northeastern Spain, *in* Nemec, W., and Steel, R.J., eds., Fan Deltas: Sedimentology and Tectonic Settings: London, UK, Blackie, p. 318-340.

Massari, F., 1984, Resedimented conglomerates of a Miocene fan-delta complex, Southern Alps, Italy, *in* Koster, E.A., and Steel, R.J., eds., Sedimentology of Gravels and Conglomerates: Calgary, Canadian Society of Petroleum Geologists, p. 259-278.

Massari, F., and Parea, G.C., 1988, Progradational gravel beach sequences in a moderate- to high-energy, microtidal marine environment: Sedimentology, v. 35, p. 881-913.

Masselink, G., 1993, Simulating the effects of tides on beach morphodynamics: Journal of Coastal Research Special Issue, v. 15, p. 180-197.

Masselink, G., and Short, A.D., 1993, The effect of tidal range on beach morphodynamics and morphology: a conceptual beach model: Journal of Coastal Research, v. 9, p. 785-800.

Mccave, I.N., and Geiser, A.C., 1978, Megaripples, ridges and runnels on intertidal flats of the Wash, England: Sedimentology, v. 26, p. 353-369.

Middleton, G.V., and Southard, J.B., 1984, Mechanics of sediment movement, 2nd Edn, Short Course notes no. 3: Tulsa, USA, Society of Economic Paleontologists and Mineralogists, Eastern Section, p. 401.,

Miller, M.C., Mccave, I.N., and Komar, P.D., 1977, Threshold of sediment motion under unidirectional currents: Sedimentology, v. 24, p. 507-527.

Nemec, W., 1990, Aspects of sediment movement on steep delta slopes: Special Publications of the International Association of Sedimentologists, v. 10, p. 29-73.

Ocean Sciences, 2005. Ocean Data Inventory. www.mar.dfo-mpo.gc.ca/science/oceans/database. Department of Fisheries and Oceans Canada.

Orton, G.J., and Reading, H.G., 1993, Variability in deltaic processes in terms of sediment supply, with particular emphasis on grain size: Sedimentology, v. 40, p. 475-512.

Pestrong, R., 1965, The development of drainage patterns in tidal marshes: Stanford University Publications in Earth Science, v. 10, p. 1-87.

Postma, G., 1984, Slumps and their deposits in fan delta front and slope: Geology, v. 12, p. 27-30.

Postma, G., 1990, Depositional architecture and facies of river and fan deltas: a synthesis, *in* Coella, A., and Prior, D.B., eds., Coarse-Grained Deltas, International Association of Sedimentologists, p. 13-27.

Postma, G., and Roep, T.B., 1985, Resedimented conglomerates in the bottomsets of Gilbert-type gravel deltas: Journal of Sedimentary Petrology, v. 55, p. 874-885.

Pye, K., and French, P.W., 1993, Erosion and acretion processes on British Salt Marshes, Vol. 1, Introduction: Saltmarsh Processes and Morphology: Cambridge, U.K., Cambridge Environmental Research Consultants.

Reading, H.G., and Collinson, J.D., 1996, Clastic Coasts, *in* Reading, H.G., ed., Sedimentary Environments; Processes, Facies and Stratigraphy: Oxford, U.K., Blackwell Science, p. 154-231.

Rice, S., and Church, M.A., 1996, Sampling surficial fluvial gravels: The precision of size distribution percentile estimates: Journal of Sedimentary Research, v. 66, p. 654-665.

Schäfer, W., 1972, Ecology and Paleoecology of Marine Environments: Edinburgh, Oliver and Boyd, 568 p.

Schumm, S.A., 1977, The Fluvial System: Toronto, Canada, John Wiley and Sons, 338 p.

Scott, D.B., and Greenberg, D.A., 1983, Relative sea-level rise and tidal development in the Fundy tidal system: Canadian Journal of Earth Sciences, v. 20, p. 1554-1564.

Shields, A., 1936, Anwendung der Ähnlichkeitsmechanik der Turbulenzforschung auf die Geschiebebewegung: Mitteilungen der Preussichen Versuchsansalt für Wasserbau und Schiffbau, v. 26, p. 26.

Short, A.D., 1984, Beach and nearshore facies: southeast Australia: Marine Geology, v. 60, p. 261-282.

Short, A.D., 1991, Macro-meso tidal beach morphodynamics: Journal of Coastal Research, v. 7, p. 417-436.

Sunamura, T., and Takeda, I., 1984, Landward migration of inner bars: Marine Geology, v. 60, p. 63-78.

Van Straaten, L.M.J.U., 1961, Sedimentation in tidal flat areas: Journal of the Alberta Society of Petroleum Geologists, v. 9, p. 203-213, 216-226.

Wahl, K.L., Thomas, W.O.J., and Hirsch, R.M., 1995, The stream-gaging program of the U.S. Geological Survey, United States Geological Survey Circular Report C1123: Reston, VA, United States Geological Survey, p. 22.

Weather Office 2005. Canadian Climate Normals 1971-2000. www.climate.weatheroffice.ec.gc.ca/climate_normals. Environment Canada.

Wescott, W.A., and Ethridge, F.G., 1980, Fan-Delta sedimentology and tectonic setting - Yallahs Fan Delta, southeast Jamaica: American Assoication of Petroleum Geologists Bulletin, v. 64, p. 374-399.

Wescott, W.A., and Ethridge, F.G., 1982, Bathymetry and sediment dispersal dynamics along the Yallahs fan delta front, Jamaica: Marine Geology, v. 46, p. 245-260.

Wescott, W.A., and Ethridge, F.G., 1983, Eocene fan delta-submarine fan deposition in the Wagwater Trough, east-central Jamaica: Sedimentology, v. 30, p. 235-247.

Wolman, M.G., 1954, A method for sampling coarse river-bed material: Transactions, American Geophysical Union, v. 35, p. 951-956.

Wright, L.D., 1977, Sediment transport and deposition at river mouths: A synthesis: Bulletin of the American Association of Petroleum Geologists, v. 88, p. 857-868.

Wright, L.D., and Short, A.D., 1984, Morphodynamic variability of surf zones and beaches: A synthesis: Marine Geology, v. 56, p. 93-118.

Yang, B.C., Dalrymple, R.W., and Chun, S.S., 2005, Sedimentation on a wave-dominated, open-coast tidal flat, south-western Korea: a summer tidal flat - winter shoreface: Sedimentology, v. 52, p. 235-252.

CHAPTER 7: CONCLUSION

The study of modern gravel deltas and beaches in the Bay of Fundy, Canada provides insights into the sedimentology, ichnology, and stratigraphy of gravel-dominated coasts. Four main goals are achieved in this thesis. Firstly, the stratigraphy and sedimentology of conglomeratic systems, particularly within transgressive settings is described in chapters 4, 5, and 6. Secondly, the relation between the salt marsh and the beach at Waterside is determined in chapters 2, 4, and 5. Based on this relationship, the stratigraphic and sedimentological architecture that may result is predicted. Thirdly, where possible, ichnological (chapter 3) and sedimentological (chapter 6) relationships are semi-quantified to provide mechanisms for predicting depositional chronology and deposit morphology. Finally, relative hydraulic influences on the geomorphology and sedimentology of gravel-dominated systems is established in chapter 6. Special attention is paid to tidal influences as tides are not considered to have a significant impact on gravel-dominated coasts (Orton and Reading 1993; Reading and Collinson 1996).

Transgressive, gravel-dominated beaches reported from the rock record consist of a transgressive lag overlain by marine shales (Bourgeois and Leithold 1984; Clifton 1981; Massari and Parea 1988). In many transgressive settings this deposit type is likely to develop. However, a facies model developed from the transgressive, gravel-dominated Waterside Beach suggests that a thin lag is only one possibility, and depending on the rate of transgression, sedimentation, and tidal range, it is possible to preserve transgressive beach deposits up to 8 m thick (Fig. 4.6). The thickness of the sequence is greatly influenced by tidal regime, which in turn, controls the size and frequency of tidal channels. Where these channels debouch onto the beach, the channel is infilled with beach sediments. Rate of transgression also plays an important role. The slower

the transgression rate (which is relative and accounts for sedimentation) the thicker the preserved beach sequence. At or near the maximum transgressive shoreline, thick gravel-beach sequences can occur.

The relation between the salt marsh and the gravel beach at Waterside is important as they both exert a significant influence on the sedimentology, ichnology, and stratigraphy of the other. Within the salt marsh, it is common to observe gravel transported into the marsh by ice and by storm waves. The amount of gravel deposited in the marsh decreases away from the beach, such that the gravel content in a marsh deposit can be used to predict the proximity of the beach. Moreover, beach gravels commonly infill marsh channels where the channel is in close proximity (100 to 200 m) to the beach (Figs. 2.4 and 2.6). These washover gravels tend to develop into muddy gravel as fine-grained deposition within the marsh infills the pore spaces between clasts.

Post-glacial evolution of the marsh-beach system reveals further details regarding the preservation potential and architecture of the resultant beach deposit. Firstly, development and aggradation of the salt marsh, and the increase in size of the tidal creeks is only likely to have occurred in the past 6,500 years as a result of relative sea level rise (Fig. 5.10; Amos et al. 1991; Grant 1970; Shaw et al. 2002) and an increase in tidal range from mesotidal to megatidal (Scott and Greenberg 1983). Secondly, the main source of gravel was likely not exposed to wave erosion until approximately 3,000 years ago (Figs. 5.7 and 5.10). The beach sequence is therefore considered a recent phenomenon that thickens along the axis of the main tidal creeks (perpendicular to the depositional strike of the beach) and is thin everywhere else (Figs. 4.6, 5.3, 5.4, and 5.5).

Detailed data was collected for ichnological and sedimentological characteristics of the three systems and used, where possible, to semi-quantify relationships observed within and between deposits. Ichnologically, this was done by assessing the burrow distribution and burrowing rate of Talitrid amphipods (*Talochestia longicornis*; Fig. 3.1) within the upper foreshore and proximal backshore (Table 3.1). It was determined that to

achieve 5% bioturbtion in backshore sediments would require two consecutive seasons of colonization. Highly bioturbated backshore sediments are thus likely to occur in low wave-energy environments. Semi-quantification of sedimentological properties was done for average grain size (in phi values) versus the areal extent (size) of the intertidal zone of Waterside Beach, Alma delta, and Big Salmon River delta. The relationship derived is linear (Fig. 6.10) suggesting that for conglomeratic systems the size of a deposit is proportional to the average grain size. Moreover, for hydraulically transported sediments there is a maximum average clast size that can be transported and thus form a deposit. This appears to occur within the coarse-cobble grain-size division (-7.75 ϕ or 215 mm).

Relative contributions of river-, wave- and tidal-energy to the morphology and sedimentological character of the three systems are also assessed and the systems classified accordingly (Fig. 6.11). For Waterside Beach, Alma delta, and BSR delta, wave- and tidal-energy inputs are assumed to be similar reflecting their close proximity and orietation in a megatidal setting. Differences in morphology are therefore characterized by variable river discharge (measured by the area of the drainage basin) relative to standardized wave and tide conditions. The two deltas (Alma and BSR) are river-dominated with differing degrees of wave-modification (Figs. 6.4 and 6.11). Although wave conditions are considered to be similar at all three sites, fluvial discharge rates (and drainage-catchment areas) are not (Table 6.1). The Big Salmon River drains an area of 278 km^2, which is 1.4 times larger than the combined drainage areas of the Alma delta (200 km^2). BSR is also the coarsest-grained (Fig. 6.2), and areally the samllest of the three systems (Fig. 6.4). Consequently, the Big Salmon River delta is considered river-dominated with low to moderate wave modification and the Alma delta is classified as river-dominated with high wave modification. Waterside is the finest-grained and most expansive deposit, and is classified as a highly tide-modified, wave-dominated beach. Combined, the tidal creeks at Waterside Beach drain an area of approximately 16 km^2 (Table 6.1).

In conglomeratic systems, hydraulic processes exhibit a hierarchy where river processes are dominant, followed by waves, and finally tides. As such, gravel systems are rarely if ever classified as tide dominated (Orton and Reading 1993). In wave-dominated settings though, it is possible to observe tidal influences in both the topography of the beach and in its relationship to other depositional environments within the same coastal zone. Beaches, including Waterside Beach, can be classified by comparing tidal range to significant wave height (Masselink and Short 1993; Short 1991; Wright and Short 1984), where the topography of the beach is a result of those two factors. Waterside exhibits a topography that fits the classification of a low-tide terrace beach (Fig. 4.2). Tidal influence is greatest, however, in its control on the morphology of depositional environments associated with gravel beaches. At Waterside a salt marsh and tidal creeks back the beach. The cross-sectional area of the creeks is a function of the tidal prism, such that in megatidal settings the creeks are large. Consequently, the thickness of the beach sequence developed over the tidal-creek scour is much thicker than the surrounding deposit and is oriented perpendicular to the depositional strike of the beach (Figs. 4.2, 4.6, 5.4, and 5.5).

REFERENCES

Amos, C.L., Tee, K.T., and Zaitlin, B.A., 1991, The post-glacial evolution of Chignecto Bay, Bay of Fundy, and its modern environment of deposition, *in* Smith, D.G., Reinson, G.E., Zaitlin, B.A., and Rahmani, R.A., eds., Clastic Tidal Sedimentology: Calgary, AB, Canada, Canadian Society of Petroleum Geologists, p. 59-89.

Bourgeois, J., and Leithold, E.L., 1984, Wave-worked conglomerates - depositional processes and criteria for recognition, *in* Koster, E.H., and Steel, R.J., eds., Sedimentology of Gravels and Conglomerates: Calgary, AB, Canada, Canadian Society of Petroleum Geologists, p. 331-343.

Clifton, H.E., 1981, Progradational sequences in Miocene shoreline deposits, southeastern Caliente range, California: Journal of Sedimentary Petrology, v. 51, p. 165-184.

Grant, D.R., 1970, Recent coastal submergence of the Maritime Provinces, Canada: Canadian Journal of Earth Sciences, v. 7, p. 676-689.

Massari, F., and Parea, G.C., 1988, Progradational gravel beach sequences in a moderate- to high-energy, microtidal marine environment: Sedimentology, v. 35, p. 881-913.

Masselink, G., and Short, A.D., 1993, The effect of tidal range on beach morphodynamics and morphology: a conceptual beach model: Journal of Coastal Research, v. 9, p. 785-800.

Orton, G.J., and Reading, H.G., 1993, Variability in deltaic processes in terms of sediment supply, with particular emphasis on grain size: Sedimentology, v. 40, p. 475-512.

Reading, H.G., and Collinson, J.D., 1996, Clastic Coasts, *in* Reading, H.G., ed., Sedimentary Environments; Processes, Facies and Stratigraphy: Oxford, U.K., Blackwell Science, p. 154-231.

Scott, D.B., and Greenberg, D.A., 1983, Relative sea-level rise and tidal development in the Fundy tidal system: Canadian Journal of Earth Sciences, v. 20, p. 1554-1564.

Shaw, J., Gareau, P., and Courtney, R.C., 2002, Palaeogeography of Atlantic Canada 13-0 kyr: Quaternary Science Reviews, v. 21, p. 1861-1878.

Short, A.D., 1991, Macro-meso tidal beach morphodynamics: Journal of Coastal Research, v. 7, p. 417-436.

Wright, L.D., and Short, A.D., 1984, Morphodynamic variability of surf zones and beaches: A synthesis: Marine Geology, v. 56, p. 93-118.

APPENDIX A

Sieve and sedigraph grain-size data for Waterside Beach, Alma delta, and Big Salmon River delta. Values for mean grain size, sorting and skewness reported in the text are highlighted in bold. Mathematical moments are calculated using millimeter values and then converted to the phi scale. Graphical moments are determined from phi-scale, cumulative grain-size curves. Grain-size categories larger than -2 phi were dependent on the size of field sieves available. Sedigraph analyses are done on samples or portions of samples below fine-grained sand (where the fines comprised at least 4% of the total sample). Where values were determined for a grain-size category by sieving and sedigraph, the sedigraph value was assumed to be zero. Therefore, most sedigraph values are corrected for sand content.

Waterside grain-sze data is reported on pages 183 to 200, Alma on 201 to 206, and Big Salmon River on pages 207 to 212. Wolman values (grid sampling) are reported separately on pages 213 to 217.

Waterside Sediment Samples							MATHEMATICAL MOMENTS			
					Location		1st M	1st M	2nd M	3rd M
Sample #	Unique Sample ID	Year	Sampling Method	Analysis Method	UTM Easting	WGS84 Northing	Mean Avg size (mm)	Mean Avg size (phi)	Std Dev	Skew
								converted		
1	WS03-N1-B4	2003	Hand	Sieve			**2.266**	**-1.18**	1.32	-1.28
2	WS03-N1-C	2003	Hand	Sieve	358200	5054465	**0.440**	**1.18**	0.26	6.21
3	WS03-N1-D	2003	Hand	Sieve	358183	5054405	**0.564**	**0.83**	0.42	3.74
4	WS03-N1-E	2003	Hand	Sieve/ Sedigraph	358167	5054366	**0.261**	**1.94**	0.19	2.77
5	WS03-N1-F	2003	Hand	Sieve	358104	5054190	**0.436**	**1.20**	0.31	5.49
6	WS03-N2-A3	2003	Hand	Sieve	358589	5054388	**0.456**	**1.13**	0.19	2.33
7	WS03-N2-B3	2003	Hand	Sieve	358577	5054357	**0.405**	**1.30**	0.23	9.15
8	WS03-N2-C6	2003	Hand	Sieve	358479	5054009	**0.280**	**1.83**	0.32	6.03
9	WS03-N2-C9	2003	Hand	Sieve	358404	5053820	**0.216**	**2.21**	0.18	11.01
10	WS03-N3-A	2003	Hand	Sieve	358945	5054189	**0.425**	**1.23**	0.16	2.15
11	WS03-N3-C	2003	Hand	Sieve	358870	5054076	**0.402**	**1.32**	0.27	6.48
12	WS03-N3-D4	2003	Hand	Sieve	358803	5053979	**0.338**	**1.57**	0.31	6.14
13	WS03-N3-E4	2003	Hand	Sieve	358564	5053631	**0.338**	**1.57**	0.38	5.60
14A	[redacted]	2003	Hand	Sedigraph	359147	5054016	**0.017**	**5.87**	0.02	5.34
14B		2003	Hand	Sedigraph	359147	5054016	**0.018**	**5.82**	0.02	3.56
14C		2003	Hand	Sedigraph	359147	5054016	**0.013**	**6.24**	0.01	6.68
14D		2003	Hand	Sedigraph	359147	5054016	**0.016**	**5.93**	0.02	3.35
15A		2003	Hand	Sedigraph	359135	5054000	**0.023**	**5.47**	0.03	2.78
15B		2003	Hand	Sedigraph	359135	5054000	**0.024**	**5.37**	0.03	2.74
16		2003	Hand	Sedigraph	360243	5052824	**0.022**	**5.51**	0.03	2.78
17	WS03-N6-D	2003	Hand	Sieve	360161	5053289	**0.971**	**0.04**	0.69	1.46
18	WS03-BF-1, 1-A	2003	Hand	Sieve			**0.646**	**0.63**	0.74	2.69
19	WS03-BF-1, 1-B	2003	Hand	Sieve	358750	5054305	**0.480**	**1.06**	0.20	1.26
20	WS03-BF-2, 2-A	2003	Hand	Sieve	358540	5054420	**0.448**	**1.16**	0.17	1.64
21	WS03-BF-2, 2-B	2003	Hand	Sieve	358530	5054405	**0.418**	**1.26**	0.38	6.20
22	WS03-BF-2, 2-C	2003	Hand	Sieve			**0.917**	**0.13**	0.91	1.63
23	WS03-BF-3, 3-A	2003	Hand	Sieve	358385	5054491	**0.482**	**1.05**	0.20	2.22
24	WS03-BF-3, 3-B	2003	Hand	Sieve			**0.749**	**0.42**	0.85	2.09
25	WS03-BF-3, 3-C	2003	Hand	Sieve			**0.771**	**0.38**	0.86	2.02
26	[redacted]	2003	Hand	Sedigraph	359804	5053081	**0.023**	**5.44**	0.03	2.75
27		2003	Hand	Sedigraph	359873	5053186	**0.014**	**6.18**	0.02	1.99
28		2003	Hand	Sedigraph	359873	5053186	**0.013**	**6.23**	0.02	3.72

Sample #	GRAPHICAL MOMENTS 1st M Mean Avg Phi Size	2nd M Std Dev	3rd M Skew	GRAPHICAL PHI MEASUREMENTS 5th %	16th %	50th %	84th %	95th %	Percent Sand %	Sample Total (g)	-5.65 phi (g)	>50 mm %	-5.25 phi (g)	37.5 to 50 mm %
												-6.10		-5.45
1	-0.7	**1.61**	**-0.15**	-3.1	-2.6	-0.5	1.1	1.4	60.5	1656				
2	1.0	**0.49**	**-0.12**	-0.2	0.6	1.0	1.4	1.7	99.2	886				
3	0.7	**0.73**	**-0.30**	-0.8	-0.1	0.8	1.3	1.6	97.5	2011				
4	2.0	**1.63**	**0.61**	0.5	0.8	1.5	3.8	6.3	81.9	981				
5	1.0	**0.59**	**-0.03**	-0.3	0.6	1.0	1.5	2.1	98.7	821				
6	0.8	**0.54**	**-0.25**	-0.3	0.2	0.9	1.3	1.5	99.9	806				
7	1.0	**0.37**	**-0.09**	0.3	0.6	1.0	1.4	1.5	99.4	2216				
8	1.8	**0.61**	**-0.33**	0.4	1.1	1.9	2.3	2.5	98.6	1007				
9	2.0	**0.41**	**-0.24**	1.0	1.6	2.0	2.4	2.5	99.1	999				
10	0.9	**0.47**	**-0.16**	-0.2	0.5	0.9	1.4	1.5	100.0	1404				
11	1.1	**0.51**	**0.07**	0.1	0.7	1.0	1.5	2.1	99.2	1715				
12	1.4	**0.65**	**0.06**	0.5	0.7	1.4	2.2	2.4	98.7	1499				
13	1.5	**0.66**	**-0.08**	0.5	0.8	1.6	2.2	2.4	97.4	1242				
14A	5.7	**1.13**	**0.00**	4.1	4.9	5.9	6.5	8.9	1.9					
14B									2.4					
14C									0.8					
14D									1.3					
15A	6.2	**2.30**	**0.40**	3.5	4.1	5.6	8.9	10.9	4.8					
15B									5.0					
16	6.6	**2.55**	**0.34**	3.4	4.1	5.9	9.7	11.0	5.4					
17	0.1	**1.11**	**-0.16**	-2.2	-1.1	0.1	1.1	1.6	90.2	1849				
18	0.7	**0.84**	**-0.50**	-1.8	0.0	0.9	1.2	1.8	91.5	756				
19	0.7	**0.60**	**-0.23**	-0.3	0.0	0.8	1.3	1.5	100.0	618				
20	0.8	**0.53**	**-0.24**	-0.3	0.3	0.9	1.3	1.5	99.9	992				
21	1.0	**0.47**	**0.11**	0.4	0.6	1.0	1.5	2.1	98.0	964				
22	0.2	**1.18**	**-0.52**	-2.2	-1.3	0.6	1.2	1.5	85.3	916				
23	0.7	**0.59**	**-0.25**	-0.3	0.1	0.8	1.3	1.5	99.9	1078				
24	0.5	**0.97**	**-0.57**	-1.9	-0.5	0.9	1.3	1.5	88.6	1341				
25	0.5	**1.06**	**-0.61**	-2.1	-0.8	0.8	1.3	1.5	88.3	1403				
26	6.3	**2.39**	**0.46**	3.5	4.1	5.5	9.2	10.9	4.6					
27	7.2	**2.41**	**0.19**	3.8	4.7	6.8	10.0	11.0	1.4					
28	7.5	**2.51**	**0.12**	3.8	4.8	7.2	10.4	11.2	2.1					

Sample #	-4.65 phi (g)	25 to 37.5 mm %	-3.65 phi (g)	12.5 to 25 mm %	-3.25 phi (g)	9.5 to 12.5 mm %	-2.25 phi (g)	4.75 to 9.5 mm %	-2 phi (g)	4 to 9.5 mm %	-2 phi (g)	4 to 4.75 mm %	-1 phi (g)	2 to 4 mm %
		-4.95		-4.15		-3.45		-2.75		-2.73		-2.13	granule	-1.50
1						0	180	10.87			283	17.1	191	11.5
2					0	0	0	0			2	0.2	5	0.6
3						0		0			15	0.7	35	1.7
4						0		0				0	0.5	0.1
5					0	0	0	0			2	0.2	7	0.9
6					0	0	0	0			0	0	0	0
7						0		0				0	12.6	0.6
8						0		0				0	7.6	0.8
9						0		0				0	2.2	0.2
10						0		0				0	0	0
11						0		0			0	0	10	0.6
12						0		0				0	12.2	0.8
13						0		0				0	18.9	1.5
14A														
14B														
14C														
14D														
15A														
15B														
16														
17					0	0	3.6	0.2			47.2	2.6	121.2	6.6
18						0		0			0	0	63.9	8.4
19						0		0			0	0	0	0
20						0		0			0	0	0	0
21						0		0			0	0	19.3	2.0
22						0		0			0	0	134.3	14.7
23						0		0			0	0	0.5	0.0
24						0		0			0	0	151.9	11.3
25						0		0			0	0	163.8	11.7
26														
27														
28														

Sample #	0 phi (g)	1 to 2 mm %	1 phi (g)	0.5 to 1 mm %	2 phi (g)	0.25 to 0.5 mm %	3 phi (g)	0.125 to 0.25 mm %	4 phi (g)	0.0625 to 0.125 mm %	< 4 phi (g)	<0.0625 mm %	Sedigraph analysis f.g. sand % sample	0.125 to 0.25 mm % total
	v.c.g.	-0.50	c.g.	0.50	m.g.	1.50	f.g.	2.50	v.f.g.	3.50	mud	6.00		2.5
1	167	10.1	274	16.5	524	31.6	37	2.2	0	0		0		
2	12	1.4	88	9.9	726	81.9	53	6.0	0	0		0		
3	76	3.8	440	21.9	1329	66.1	109	5.4	7	0.3		0		
4	3.9	0.4	25	2.5	474.5	48.4	215.8	22.0	84	8.6	177	[redacted]		
5	16	1.9	69	8.4	620	75.5	103	12.5	2	0.2	2	0.2		
6	8.9	1.1	162.1	20.1	607.9	75.4	26.2	3.3	0.3	0.0	0.5	0.1		
7	5.6	0.3	121.5	5.5	1982.6	89.5	92.6	4.2	0.6	0.0	0.5	0.0		
8	19.8	2.0	25.4	2.5	182.4	18.1	751.8	74.7	13.1	1.3	6.6	0.7		
9	4.9	0.5	8.8	0.9	72.6	7.3	883.9	88.4	20.7	2.1	6.3	0.6		
10	4.3	0.3	209.6	14.9	1119.1	79.7	69.2	4.9	0.8	0.1	0.7	0.0		
11	27.6	1.6	84.3	4.9	1370.6	79.9	212.8	12.4	5.2	0.3	4	0.2		
12	22.9	1.5	39.1	2.6	751	50.1	656.4	43.8	10.1	0.7	7.5	0.5		
13	18.6	1.5	24.1	1.9	527.6	42.5	624.4	50.3	15.4	1.2	13.3	1.1		
14A														0.51
14B														0.5
14C														0.31
14D														0.2
15A														0.89
15B														0.91
16														1.1
17	276	14.9	748.5	40.5	555.2	30.0	86.3	4.7	1.9	0.1	9.5	0.5		
18	12.4	1.6	86.3	11.4	543.5	71.9	49.8	6.6	0.2	0.0	0.2	0.0		
19	3.3	0.5	178.1	28.8	406.4	65.8	29.2	4.7	0.2	0.0	0.3	0.0		
20	2.3	0.2	201.4	20.3	757.8	76.4	30	3.0	0.3	0.0	0.5	0.1		
21	0.2	0.0	33.8	3.5	791.5	82.1	118.6	12.3	0.3	0.0	0.3	0.0		
22	62.4	6.8	206.9	22.6	490.6	53.6	21.4	2.3	0.2	0.0	0.3	0.0		
23	5.6	0.5	301.2	27.9	746.3	69.2	23.6	2.2	0.6	0.1	0.6	0.1		
24	65.1	4.9	113.9	8.5	943.6	70.4	65.7	4.9	0.4	0.0	0.4	0.0		
25	84.9	6.1	89.7	6.4	1042.8	74.4	20.7	1.5	0.3	0.0	0.3	0.0		
26														0.92
27														0
28														0.41

Sample #	v.f.g. sand % sample	0.063 0.125 mm % total	c. silt % sample	0.031 0.063 mm % total	m. silt % sample	0.0156 0.031 mm % total	f. silt % sample	0.008 0.0156 mm % total	v.f. silt % sample	0.0039 0.008 mm % total	clay % sample	0.0039 0.002 mm % total
		3.5		4.5		5.5		6.5		7.5		8.5
1												
2												
3												
4			29.22	5.27	32.5	5.87	10.14	1.83	4.77	0.86	4.47	0.81
5												
6												
7												
8												
9												
10												
11												
12												
13												
14A		1.43		5.53		21.19		57.32		6.86		1.23
14B		1.92		11.2		24.72		24.72		10.39		7.97
14C		0.51		3.36		14.55		49.95		21.16		1.32
14D		1.12		10.14		22.92		33.47		12.17		5.38
15A		3.95		18.16		25.27		15.6		10.07		7.21
15B		4.06		19.88		27.18		17.24		10.04		6.59
16		4.29		17.96		20.76		14.47		8.78		8.08
17												
18												
19												
20												
21												
22												
23												
24												
25												
26		3.67		19.65		25.86		14.46		7.64		7.33
27		1.37		10.98		18.27		15.84		11.4		10.67
28		1.73		9.46		14.34		15.46		12.72		10.78

Sample #	clay % sample	0.002 0.00098 mm % total	clay % sample	0.00098 0.00049 mm % total	clay % sample	0.00049 0.00024 mm % total
		9.5		10.5		11.5
1						
2						
3						
4	3.58	0.65	3.08	0.56	9.64	1.74
5						
6						
7						
8						
9						
10						
11						
12						
13						
14A		1.94		0		4.5
14B		8.07		3.83		7.16
14C		0.71		0.81		7.63
14D		4.77		2.23		7.81
15A		7.9		3.06		8.79
15B		3.96		2.74		8.32
16		7.19		7.49		10.98
17						
18						
19						
20						
21						
22						
23						
24						
25						
26		6.52		5.6		9.27
27		10.56		9.93		10.98
28		10.17		10.07		15.26

Waterside Sediment Samples							MATHEMATICAL MOMENTS			
					Location		1st M	1st M	2nd M	3rd M
Sample #	Unique Sample ID	Year	Sampling Method	Analysis Method	UTM Easting	WGS84 Northing	Mean Avg size (mm)	Mean Avg size (phi)	Std Dev	Skew
								converted		
29	[redacted]	2003	Hand	Sedigraph	359599	5053259	**0.027**	**5.24**	0.03	2.36
30	WS03-Wbar4-F1 (sand)	2003	Hand	Sieve	359599	5053259	**0.815**	**0.30**	0.77	0.88
31	[redacted]	2003	Hand	Sedigraph	359698	5053373	**0.025**	**5.33**	0.03	2.55
32	WS03-7306 (LMC sand)	2003	Hand	Sieve	360318	5053586	**0.364**	**1.46**	0.10	1.96
33	WS03-6770 (D7, sand)	2003	Hand	Sieve	359512	5052611	**0.469**	**1.09**	0.53	3.25
34	WS03-7074 (LMC west)	2003	Hand	Sieve	358807	5053190	**0.450**	**1.15**	0.44	4.24
35	WS03-7304 (Salt Marsh)	2003	Hand	Sieve/ Sedigraph	360251	5053584	**0.143**	**2.80**	0.21	1.49
36A	[redacted]	2003	Hand	Sedigraph			**0.026**	**5.28**	0.03	2.06
36B	[redacted]	2003	Hand	Sedigraph			**0.032**	**4.96**	0.03	2.32
37A	[redacted]	2003	Hand	Sedigraph			**0.016**	**5.93**	0.02	3.21
37B	[redacted]	2003	Hand	Sedigraph			**0.019**	**5.70**	0.02	3.03
38	WS04-ST1 - 30-40 cm	2004	Hand	Sieve	358823	5054258	**0.399**	**1.32**	0.14	3.78
39	WS04-ST1 - 48-56 cm	2004	Hand	Sieve	358823	5054258	**0.409**	**1.29**	0.14	2.65
40	WS04-ST1 - 65-72 cm	2004	Hand	Sieve	358823	5054258	**0.398**	**1.33**	0.13	3.17
41	WS04-ST1 - 87-95 cm	2004	Hand	Sieve	358823	5054258	**0.404**	**1.31**	0.13	2.58
42	WS04-ST3	2004	Hand	Sieve	358416	5053865	**0.558**	**0.84**	1.82	7.64
43	WS04-ST4	2004	Hand	Sieve	358571	5054351	**7.015**	**-2.81**	11.20	3.66
44	WS04-ST4 (Upper 5 mm)	2004	Hand	Sieve	358571	5054351	**0.574**	**0.80**	0.91	7.37
45	WS04-ST5	2004	Hand	Sieve	358429	5054314	**0.379**	**1.40**	0.14	5.52
46	WS04-ST6	2004	Hand	Sieve	358029	5053996	**0.189**	**2.41**	0.21	15.38
47	WS04-ST7 (Upper 7 cm)	2004	Hand	Sieve	358463	5053716	**0.200**	**2.32**	0.13	14.61
48	WS04-ST8 (Upper 5 cm)	2004	Hand	Sieve	358759	5053907	**0.732**	**0.45**	0.96	5.46
49	WS04-ST9 (Upper 4 cm)	2004	Hand	Sieve	358463	5053716	**0.512**	**0.97**	0.76	7.85
50	WS04-ST10	2004	Hand	Sieve	358921	5053124	**2.656**	**-1.41**	2.74	3.22
51	WS04-ST15 (NFLD Ck)	2004	Hand	Sieve	358943	5053788	**8.041**	**-3.01**	8.41	4.93
52	WS04-ST17 (Upper 6 cm)	2004	Hand	Sieve	359942	5052745	**0.751**	**0.41**	1.36	7.43
53	WS04-ST20 (Upper 6 cm)	2004	Hand	Sieve	360346	5053166	**3.876**	**-1.95**	6.18	6.63
54	WS04-ST20 - 6-10 cm	2004	Hand	Sieve	360346	5053166	**15.824**	**-3.98**	19.62	2.06
55	WS04-ST23 (Upper 5 mm)	2004	Hand	Sieve	359654	5053442	**0.340**	**1.56**	0.46	7.27
56	WS04-ST25 (matrix)	2004	Hand	Grid/ Sieve	359721	5052743	**1.244**	**-0.32**	1.09	0.74
57	WS04-ST26	2004	Hand	Sieve	359814	5052967	**13.578**	**-3.76**	16.39	1.82
58	WS04-ST27 (matrix)	2004	Hand	Grid/ Sieve	360249	5052892	**1.362**	**-0.45**	1.07	0.56

Sample #	GRAPHICAL MOMENTS 1st M Mean Avg Phi Size	2nd M Std Dev	3rd M Skew	GRAPHICAL PHI MEASUREMENTS 5th %	16th %	50th %	84th %	95th %	Percent Sand %	Sample Total (g)	-5.65 phi (g)	>50 mm %	-5.25 phi (g)	37.5 to 50 mm %
												-6.10		-5.45
29	6.5	**2.82**	**0.48**	3.1	3.9	5.4	10.2	11.2	7.6					
30	1.2	**2.30**	**-0.22**	-2.9	-0.9	1.7	2.8	6.2	76.6	660				
31	6.4	**2.63**	**0.33**	3.1	3.9	5.8	9.6	11.0	7.5					
32	1.1	**0.38**	**0.21**	0.6	0.8	1.1	1.4	2.1	99.7	1208				
33	1.6	**1.01**	**-0.49**	-1.5	0.7	1.8	2.3	2.5	93.1	1565				
34	1.4	**0.87**	**-0.23**	-0.9	0.7	1.5	2.2	2.4	95.9	2596				
35	4.8	**3.47**	**0.09**	0.4	1.0	4.7	8.6	10.7	33.3	29				
36A	6.0	**2.33**	**0.52**	3.5	3.9	5.2	8.8	11.0						
36B														
37A	6.9	**2.45**	**0.34**	3.7	4.6	6.3	10.0	11.1						
37B														
38	1.0	**0.42**	**-0.11**	0.1	0.6	1.0	1.4	1.6	100.0	1196		0		0
39	1.0	**0.43**	**-0.18**	-0.1	0.6	1.0	1.3	1.5	100.0	1222		0		0
40	1.0	**0.40**	**-0.12**	0.1	0.6	1.0	1.4	1.5	100.0	1058		0		0
41	1.0	**0.43**	**-0.14**	0.0	0.6	1.0	1.4	1.5	100.0	1308		0		0
42	1.9	**0.82**	**-0.37**	-1.5	1.5	1.9	2.4	2.5	93.6	7065	0	0	0	0
43	-1.7	**2.16**	**-0.02**	-5.1	-4.1	-1.8	0.7	1.3	43.1	53628	692	1.3	951	1.77
44	1.0	**0.59**	**-0.29**	-1.1	0.5	1.0	1.4	1.5	96.1	1780		0		0
45	1.0	**0.37**	**0.19**	0.5	0.7	1.0	1.4	1.9	99.8	2583		0		0
46	1.2	**0.55**	**0.31**	0.5	0.7	1.1	1.7	2.5	95.7	3206		0		0
47	2.0	**0.48**	**0.02**	1.1	1.6	2.0	2.4	3.0	99.9	3059		0		0
48	0.6	**0.83**	**-0.36**	-1.6	-0.3	0.7	1.2	1.4	94.7	2209		0		0
49	1.8	**0.69**	**-0.04**	-0.6	0.5	1.0	1.6	2.2	97.3	8075	0	0	0	0
50	-1.1	**1.40**	**0.42**	-2.7	-2.4	-1.5	0.6	1.7	50.4	8887		0		0
51	-2.2	**2.22**	**0.33**	-4.9	-4.5	-2.8	0.6	1.3	35.4	34801	0	0	0	0
52	0.7	**0.91**	**-0.44**	-1.7	-0.2	0.9	1.4	1.7	93.4	5280	0	0	0	0
53	-1.0	**1.92**	**-0.34**	-4.6	-3.2	-0.5	0.9	1.3	66.6	9919	0	0	0	0
54	-2.9	**2.33**	**0.18**	-6.5	-5.1	-3.3	-0.3	1.0	24.5	7141	646	9.0	37	0.52
55	1.5	**0.83**	**0.30**	0.5	0.7	1.4	2.3	3.4	93.9	1999	0	0	0	0
56									75.3	1836		0		0
57	-3.0	**1.98**	**0.05**	-6.0	-5.1	-3.1	-0.9	0.2	23.4	32168	1141	3.5	2348	7.30
58									73.9	2987		0		0

Sample #	-4.65 phi (g)	25 to 37.5 mm %	-3.65 phi (g)	12.5 to 25 mm %	-3.25 phi (g)	9.5 to 12.5 mm %	-2.25 phi (g)	4.75 to 9.5 mm %	-2 phi (g)	4 to 9.5 mm %	-2 phi (g)	4 to 4.75 mm %	-1 phi (g)	2 to 4 mm %
		-4.95		-4.15		-3.45		-2.75		-2.73		-2.13	granule	-1.50
29														
30					0	0	16	2.4			30.3	4.6	37.6	5.7
31														
32					0	0	0	0			0	0	0	0
33						0	6.8	0.4			26.7	1.7	45	2.9
34					0	0	11.9	0.5			35.3	1.4	53.3	2.1
35						0	0	0			0	0	0	0
36A														
36B														
37A														
37B														
38		0		0		0		0				0	0	0
39		0		0		0		0			0	0	0	0
40		0		0	0	0	0	0			0	0	0	0
41		0		0	0	0	0	0			0	0	0	0
42	0	0	46	0.7	21	0.3	77	1.1			25	0.4	199	2.8
43	1729	3.2	4919	9.2	2501	4.7	7812	14.6			2372	4.4	9561	17.8
44		0		0.0	7	0.4	0	0			28	1.6	35	2.0
45		0		0.0	0	0	0	0			0	0	0	0
46		0		0.0	0	0	0	0			5	0.2	3	0.1
47		0		0.0		0		0				0	4	0.1
48		0		0.0	4	0.2	15	0.7			33	1.5	65	2.9
49	0	0	0	0.0	9	0.1	52	0.6			16	0.2	109	1.3
50		0	110	1.2	256	2.9	0	0			1797	20.2	2243	25.2
51	1714	4.9	6425	18.5	3168	9.1	6611	19.0			1121	3.2	3430	9.9
52	0	0	12	0.2	6	0.1	72	1.4			33	0.6	216	4.1
53	155	1.6	764	7.7	391	3.9	829	8.4			184	1.9	984	9.9
54	680	9.5	1453	20.3	498	7.0	1008	14.1			263	3.7	809	11.3
55	0	0	0	0.0	0	0	0	0			18	0.9	10	0.5
56		0		0.0	0	0	0	0			0	0	454	24.7
57	2410	7.5	4239	13.2	2579	8.0	6225	19.4			1229	3.8	4470	13.9
58		0		0.0	0	0	0	0			0	0	780	26.1

Sample #	0 phi (g)	1 to 2 mm %	1 phi (g)	0.5 to 1 mm %	2 phi (g)	0.25 to 0.5 mm %	3 phi (g)	0.125 to 0.25 mm %	4 phi (g)	0.0625 to 0.125 mm %	< 4 phi (g)	<0.0625 mm %	Sedigraph analysis f.g. sand % sample	Sedigraph analysis 0.125 to 0.25 mm % total
	v.c.g.	-0.50	c.g.	0.50	m.g.	1.50	f.g.	2.50	v.f.g.	3.50	mud	6.00		2.5
29														1.55
30	33.9	5.1	40.2	6.1	105.2	15.9	277.1	42.0	49	7.4	70.8	10.7		
31														1.63
32	0.7	0.1	37.7	3.1	1024.9	84.8	139.5	11.5	1.6	0.1	4	0.3		
33	54.8	3.5	50.7	3.2	335.6	21.4	981.1	62.7	35.3	2.3	29.1	1.9		
34	44.9	1.7	48.9	1.9	1152.9	44.4	1228	47.3	15.3	0.6	5.4	0.2		
35	0	0	1.555	5.3	6.621	22.7	21	[redacted]					1.47	1.06
36A														0.51
36B														1.32
37A														0.39
37B														0.52
38	6	0.5	91	7.6	1039	86.9	56	4.7	4	0.3	0	0		
39	3	0.2	131	10.7	1031	84.4	53	4.3	4	0.3	0	0		
40	3	0.3	86	8.1	912	86.2	53	5.0	4	0.4	0	0		
41	2	0.2	128	9.8	1117	85.4	58	4.4	3	0.2	0	0		
42	228	3.2	6	0.1	344	4.9	5853	82.8	178	2.5	88	1.2		
43	6742	12.6	6299	11.7	9380	17.5	632	1.2	38	0.1	0	0		
44	47	2.6	95	5.3	1503	84.4	62	3.5	3	0.2	0	0		
45	25	1.0	61	2.4	2282	88.3	204	7.9	7	0.3	4	0.2		
46	5	0.2	27	0.8	100	3.1	2456	76.6	479	14.9	131	4.1		
47	5	0.2	7	0.2	231	7.6	2527	82.6	285	9.3	0	0		
48	75	3.4	699	31.6	1295	58.6	23	1.0	0	0	0	0		
49	235	2.9	817	10.1	5469	67.7	1311	16.2	24	0.3	33	0.4		
50	1912	21.5	1093	12.3	925	10.4	492	5.5	59	0.7	0	0		
51	2472	7.1	3639	10.5	5604	16.1	565	1.6	52	0.1	0	0		
52	329	6.2	562	10.6	3711	70.3	321	6.1	6	0.1	12	0.2		
53	1731	17.5	2434	24.5	2331	23.5	111	1.1	1	0.0	4	0.0		
54	533	7.5	466	6.5	748	10.5	0	0	0	0	0	0		
55	12	0.6	23	1.2	1055	52.8	681	34.1	106	5.3	93	4.7		
56	318	17.3	245	13.3	601	32.7	165	9.0	53	2.9	0	0		
57	3822	11.9	3234	10.1	453	1.4	18	0.1	0	0.0	0	0		
58	704	23.6	461	15.4	787	26.3	69	2.3	186	6.2	0	0		

Sample #	v.f.g. sand % sample	0.063 0.125 mm % total	c. silt % sample	0.031 0.063 mm % total	m. silt % sample	0.0156 0.031 mm % total	f. silt % sample	0.008 0.0156 mm % total	v.f. silt % sample	0.0039 0.008 mm % total	clay % sample	0.0039 0.002 mm % total
		3.5		4.5		5.5		6.5		7.5		8.5
29		6.01		23.83		20.62		10.67		6.22		6.11
30												
31		5.82		20.1		18.78		13.27		9.08		8.37
32												
33												
34												
35	5.88	4.23	19.31	13.90	18.26	13.14	13.96	10.05	9.65	6.95	8.6	6.19
36A		3.96		26.63		27.85		11.89		6.3		5.69
36B		6.19		31.27		29.95		13.2		6.9		4.37
37A		1.97		11.75		22.01		17.77		10.76		7.6
37B		2.7		14.35		24.01		19.23		12.27		8.32
38												
39												
40												
41												
42												
43												
44												
45												
46												
47												
48												
49												
50												
51												
52												
53												
54												
55												
56												
57												
58												

Sample #	clay % sample	0.002 0.00098 mm % total	clay % sample	0.00098 0.00049 mm % total	clay % sample	0.00049 0.00024 mm % total
		9.5		10.5		11.5
29		5.39		4.87		16.27
30						
31		6.22		6.12		12.2
32						
33						
34						
35	7.45	5.36	6.19	4.46	10.7	7.70
36A		4.27		3.76		9.65
36B		3.05		1.42		3.65
37A		7.9		8.39		11.85
37B		6.13		4.37		8.63
38						
39						
40						
41						
42						
43						
44						
45						
46						
47						
48						
49						
50						
51						
52						
53						
54						
55						
56						
57						
58						

Waterside Sediment Samples							MATHEMATICAL MOMENTS			
Sample #	Unique Sample ID	Year	Sampling Method	Analysis Method	Location UTM Easting	WGS84 Northing	1st M Mean Avg size (mm)	1st M Mean Avg size (phi) converted	2nd M Std Dev	3rd M Skew
59	WS04-ST28 (Upper 5 cm)	2004	Hand	Sieve	359455	5052914	**2.762**	**-1.47**	6.84	0.35
60	WS04-ST29	2004	Hand	Sieve	359773	5053117	**12.534**	**-3.65**	6.93	5.95
61	WS04-ST31 (West bar)	2004	Hand	Sieve	359509	5053282	**10.978**	**-3.46**	14.55	3.11
62	WS04-ST32 (East bar)	2004	Hand	Sieve	360043	5052836	**9.804**	**-3.29**	12.70	3.51
63	WS04-ST33	2004	Hand	Sieve	360433	5052486	**0.330**	**1.60**	0.21	6.50
64	WS04-ST34	2004	Hand	Sieve	360103	5051998	**1.080**	**-0.11**	2.96	4.89
65	WS04-THSS1	2004	Hand	Sieve	360498	5052434	**0.332**	**1.59**	0.27	8.86
66	WS04-THSS2	2004	Hand	Sieve	360595	5052536	**0.365**	**1.45**	0.18	11.28
67	GS05-WS1-Bulk	2005	Grab	Sieve/ Sedigraph	357643	5053734	**0.015**	**6.09**	0.05	13.52
68	GS05-WS2-Bulk	2005	Grab	Sieve/ Sedigraph	357492	5053311	**0.145**	**2.79**	0.42	12.67
69	GS05-WS3-Bulk	2005	Grab	Sieve/ Sedigraph	358104	5052585	**0.110**	**3.19**	0.23	16.91
70	GS05-WS4-Bulk	2005	Grab	Sieve/ Sedigraph	358284	5052377	**0.199**	**2.33**	0.67	8.47
71	GS05-WS5-Bulk	2005	Grab	Sieve/ Sedigraph	358564	5052152	**0.896**	**0.16**	2.82	4.72
72	GS05-WS6-Bulk	2005	Grab	Sieve/ Sedigraph	358752	5052433	**3.668**	**-1.87**	7.17	1.55
73	GS05-WS7-Bulk	2005	Grab	Sieve/ Sedigraph	358886	5052614	**0.143**	**2.80**	0.20	25.70
74	GS05-WS8-Bulk	2005	Grab	Sieve/ Sedigraph	359073	5052758	**0.128**	**2.96**	0.19	20.30
75	GS05-WS9-Bulk	2005	Grab	Sieve/ Sedigraph	359348	5052416	**0.120**	**3.06**	0.10	8.84
76	GS05-WS10-Bulk	2005	Grab	Sieve	359574	5052266	**0.226**	**2.14**	0.19	20.65
77	GS05-WS11-Bulk	2005	Grab	Sieve	359697	5052343	**0.941**	**0.09**	1.68	5.10
78	GS05-WS12-Bulk	2005	Grab	Sieve/ Sedigraph	359429	5052108	**0.026**	**5.29**	0.03	1.90
79	GS05-WS15-Bulk	2005	Grab	Sieve/ Sedigraph	359749	5051631	**0.029**	**5.12**	0.04	2.41
80	GS05-WS17-Bulk	2005	Grab	Sieve/ Sedigraph	359574	5051401	**0.242**	**2.05**	0.79	7.19
81	GS05-WS18-Bulk	2005	Grab	Sieve/ Sedigraph	359340	5051662	**0.125**	**3.00**	0.46	12.23
82	GS05-WS19-Bulk	2005	Grab	Sieve/ Sedigraph	358851	5052037	**0.160**	**2.64**	0.31	16.09
83	GS05-WS20-Bulk	2005	Grab	Sieve/ Sedigraph	358377	5052531	**0.252**	**1.99**	0.73	7.22
84	GS05-WS21-Bulk	2005	Grab	Sieve/ Sedigraph	358503	5052612	**0.026**	**5.28**	0.03	2.56
85	GS05-WS22-Bulk	2005	Grab	Sieve	358863	5053004	**0.219**	**2.19**	0.25	21.66
86	GS05-WS23-Bulk	2005	Grab	Sieve/ Sedigraph	358436	5053497	**0.058**	**4.10**	0.04	3.22
87	GS05-WS24-Bulk	2005	Grab	Sieve/ Sedigraph	358172	5053189	**0.870**	**0.20**	3.23	4.82
88	GS05-WS25-Bulk	2005	Grab	Sieve/ Sedigraph	357744	5053953	**0.021**	**5.55**	0.10	14.36

Sample #	GRAPHICAL MOMENTS 1st M Mean Avg Phi Size	2nd M Std Dev	3rd M Skew	GRAPHICAL PHI MEASUREMENTS 5th %	16th %	50th %	84th %	95th %	Percent Sand %	Sample Total (g)	-5.65 phi (g)	>50 mm %	-5.25 phi (g)	37.5 to 50 mm %
												-6.10		-5.45
59	0.0	**1.84**	**-0.48**	-4.0	-2.0	0.6	1.4	2.4	72.8	6149	0	0	124	2.02
60	-3.7	**0.82**	**-0.15**	-5.0	-4.7	-3.6	-2.9	-2.5	0.0	7351	0	0	0	0
61	-2.8	**1.90**	**0.12**	-5.4	-4.7	-2.9	-0.7	0.6	25.6	31056	1037	3.3	452	1.46
62	-2.2	**2.38**	**0.28**	-5.3	-4.7	-2.8	0.8	1.4	34.7	22695	495	2.2	249	1.10
63	1.4	**0.64**	**0.18**	0.5	0.7	1.3	2.1	2.4	99.0	4322	0	0	0	0
64	1.2	**1.10**	**-0.18**	-2.8	0.6	1.1	1.8	2.3	91.3	4213	0	0	0	0
65	1.4	**0.64**	**0.19**	0.5	0.7	1.3	2.1	2.4	98.3	1676	0	0	0	0
66	1.1	**0.45**	**0.18**	0.5	0.7	1.1	1.5	2.2	99.3	1243	0	0	0	0
67	7.5	**2.47**	**0.09**	3.9	4.9	7.3	10.4	11.2	1.7	71	0	0	0	0
68	4.4	**3.09**	**0.48**	1.0	1.7	3.5	8.2	10.8	49.8	634	0	0	0	0
69	4.6	**3.04**	**0.43**	1.3	1.8	3.8	8.3	10.8	45.5	574	0	0	0	0
70	4.3	**3.01**	**0.49**	0.8	1.7	3.3	7.8	10.6	49.7	1035	0	0	0	0
71	3.7	**3.79**	**0.18**	-2.9	0.4	3.1	7.4	10.6	43.3	609	0	0	0	0
72	2.7	**5.41**	**-0.26**	-4.7	-4.2	4.2	8.0	10.8	13.1	166	0	0	0	0
73	2.5	**0.94**	**0.31**	1.6	1.8	2.5	3.4	5.2	87.7	814	0	0	0	0
74	3.1	**1.80**	**0.37**	1.6	1.8	3.0	4.4	9.2	66.5	746	0	0	0	0
75	3.1	**1.99**	**0.61**	1.6	1.8	2.6	4.9	9.7	66.4	333	0	0	0	0
76	1.8	**0.62**	**-0.11**	0.7	1.3	1.9	2.4	2.9	97.3	701	0	0	0	0
77	0.5	**1.26**	**-0.44**	-2.5	-0.7	0.9	1.5	2.2	89.6	2483	0	0	0	0
78	10.0	**2.63**	**0.34**	3.1	3.8	5.7	9.5	11.0	8.3	44	0	0	0	0
79	6.6	**2.80**	**0.16**	2.5	3.8	6.2	9.8	11.1	11.6	61	0	0	0	0
80	3.8	**2.94**	**0.66**	0.7	1.7	2.5	7.4	10.7	55.6	768	0	0	0	0
81	4.8	**3.04**	**0.34**	1.4	1.9	4.2	8.4	10.8	37.6	460	0	0	0	0
82	3.5	**2.52**	**0.71**	0.8	1.7	2.3	6.4	9.7	60.7	690	0	0	0	0
83	3.6	**2.84**	**0.47**	0.2	1.4	2.8	6.5	10.6	54.6	588	0	0	0	0
84	6.4	**2.61**	**0.26**	2.9	3.9	5.9	9.4	11.0	8.7	73	0	0	0	0
85	1.9	**0.57**	**-0.07**	0.8	1.5	2.0	2.4	3.0	98.1	683	0	0	0	0
86	3.9	**1.53**	**0.30**	2.5	3.0	3.9	4.8	9.6	28.2	251	0	0	0	0
87	3.5	**3.04**	**0.01**	-2.8	1.0	3.3	6.3	8.5	45.6	459	0	0	0	0
88	7.6	**3.02**	**0.32**	3.7	4.6	6.8	11.5	12.2	2.9	48	0	0	0	0

Sample #	-4.65 phi (g)	25 to 37.5 mm %	-3.65 phi (g)	12.5 to 25 mm %	-3.25 phi (g)	9.5 to 12.5 mm %	-2.25 phi (g)	4.75 to 9.5 mm %	-2 phi (g)	4 to 9.5 mm %	-2 phi (g)	4 to 4.75 mm %	-1 phi (g)	2 to 4 mm %
		-4.95		-4.15		-3.45		-2.75		-2.73		-2.13	granule	-1.50
59	0	0	162	2.6	87	1.4	391	6.4			134	2.2	587	9.5
60	399	5.4	2308	31.4	1280	17.4	2762	37.6			602	8.2	0	0
61	1765	5.7	5016	16.2	2291	7.4	6077	19.6			1331	4.3	5089	16.4
62	1823	8.0	3115	13.7	1754	7.7	4108	18.1			827	3.6	2445	10.8
63	0	0	0	0.0	0	0	0	0			0	0	10	0.2
64	0	0	87	2.1	32	0.8	105	2.5			19	0.5	111	2.6
65	0	0	0	0.0	0	0	0	0			2.41	0.1	6.85	0.4
66	0	0	0	0.0	0	0	0	0			0.56	0.0	2.33	0.2
67	0	0	0	0	0	0			0	0			0	0.0
68	0	0	0	0	0	0			1.9	0.3			2.1	0.3
69	0	0	0	0	0	0			0.3	0.1			1	0.2
70	0	0	0	0	0	0			9.0	0.9			7	0.7
71	0	0	9	1.5	10	1.6			15.1	2.5			22.1	3.6
72	0	0	29.1	17.5	3.4	2.0			3.0	1.8			0.2	0.1
73	0	0	0	0	0	0			0.5	0.1			0.6	0.1
74	0	0	0	0	0	0			0.3	0.0			0.8	0.1
75	0	0	0	0	0	0			0	0			0.1	0.0
76	0	0	0	0	0	0			0.3	0.0			0.6	0.1
77	0	0	5.8	0.2	10	0.4			83.2	3.4			152	6.1
78	0	0	0	0	0	0			0	0			0	0.0
79	0	0	0	0	0	0			0	0			0	0.0
80	0	0	0	0	0	0			9.2	1.2			7.1	0.9
81	0	0	0	0	0	0			1.7	0.4			1.5	0.3
82	0	0	0	0	0	0			1.1	0.2			0.7	0.1
83	0	0	0	0	0	0			5.4	0.9			6.5	1.1
84	0	0	0	0	0	0			0	0			0	0.0
85	0	0	0	0	0	0			0.8	0.1			0.4	0.1
86	0	0	0	0	0	0			0	0			0	0.0
87	0	0	12.1	2.6	3.4	0.7			8.4	1.8			3.9	0.9
88	0	0	0	0	0	0			0	0			0	0.0

Sample #	0 phi (g)	1 to 2 mm %	1 phi (g)	0.5 to 1 mm %	2 phi (g)	0.25 to 0.5 mm %	3 phi (g)	0.125 to 0.25 mm %	4 phi (g)	0.0625 to 0.125 mm %	< 4 phi (g)	<0.0625 mm %	Sedigraph analysis f.g. sand % sample	0.125 to 0.25 mm % total
	v.c.g.	-0.50	c.g.	0.50	m.g.	1.50	f.g.	2.50	v.f.g.	3.50	mud	6.00		2.5
59	527	8.6	751	12.2	2561	41.6	560	9.1	81	1.3	185	3.0		
60	0	0	0	0	0	0	0	0	0	0	0	0		
61	3851	12.4	2468	7.9	1521	4.9	108	0.3	16	0.1	33	0.1		
62	1421	6.3	1883	8.3	3652	16.1	296	1.3	628	2.8	0	0		
63	34	0.8	148	3.4	2509	58.1	1556	36.0	30	0.7	35	0.8		
64	104	2.5	81	1.9	2682	63.7	963	22.9	18	0.4	12	0.3		
65	11.99	0.7	27	1.6	1002	59.8	582	34.7	24	1.5	20	1.2		
66	4.86	0.4	25	2.0	1029	82.7	172	13.9	3	0.3	6	0.5		
67	0	0	0.27	0.4	0	0	0	0	70.7					
68	2	0.3	2.2	0.3	44.8	7.1	223	35.2	358					
69	0.8	0.1	2	0.3	30.1	5.2	178.8	31.1	361					
70	4.9	0.5	6.3	0.6	80.3	7.8	356.7	34.5	571					
71	20.4	3.4	22	3.6	42	6.9	141	23.2	327					
72	0.2	0.1	0.3	0.2	0.7	0.4	5.1	3.1	124					
73	0.5	0.1	0.9	0.1	12.4	1.5	397.7	48.9	302	37.1	99.4			
74	1.3	0.2	3	0.3	18	2.4	304	40.7	419					
75	0.1	0.0	0	0.1	5	1.4	154	46.2	174					
76	1.2	0.2	2.7	0.4	140.9	20.1	506.6	72.3	30.5	4.4	17.8	2.5		
77	190.2	7.7	308	12.4	1390.6	56.0	327.6	13.2	9.3	0.4	6.3	0.3		
78	0	0	0	0	0	0	0.3	0.7	44					
79	0	0	0	0	0	0	3	4.7	58					
80	7.1	0.9	7.5	1.0	45.1	5.9	307.1	40.0	385					
81	1.6	0.3	2	0.4	19	4.0	119	25.9	316					
82	1.2	0.2	5.4	0.8	79.4	11.5	311.1	45.1	291					
83	9.3	1.6	10.9	1.9	69.3	11.8	173.6	29.5	313					
84	0	0	0	0	0	0	1.6	2.2	71.4					
85	0.6	0.1	1	0.1	111	16.2	508	74.4	50	7.3	12	1.7		
86	0	0	0.1	0.0	0.3	0.1	11	4.4	239					
87	7	1.5	15.9	3.5	47.6	10.4	91.6	20.0	269					
88	0.2	0.4	0	0	0	0	0.1	0.2	47.4					

Sample #	v.f.g. sand % sample	0.063 0.125 mm % total	c. silt % sample	0.031 0.063 mm % total	m. silt % sample	0.0156 0.031 mm % total	f. silt % sample	0.008 0.0156 mm % total	v.f. silt % sample	0.0039 0.008 mm % total	clay % sample	0.0039 0.002 mm % total
		3.5		4.5		5.5		6.5		7.5		8.5
59												
60												
61												
62												
63												
64												
65												
66												
67	1.35	1.34	7.71	7.68	16.88	16.82	15.21	15.15	10.83	10.79	10.10	10.06
68	12.20	6.89	20.70	11.68	11.50	6.49	10.51	5.93	10.19	5.75	9.86	5.57
69	13.80	8.68	23.52	14.80	13.85	8.71	9.45	5.95	8.24	5.18	7.80	4.91
70	11.60	6.40	23.43	12.92	13.53	7.46	10.33	5.70	9.05	4.99	8.84	4.88
71	11.70	6.29	25.95	13.95	15.92	8.56	9.35	5.03	8.02	4.31	7.57	4.07
72	12.5	9.34	29.85	22.31	17.78	13.29	9.7	7.25	5.93	4.43	5.6	4.18
73			41.84	5.11	22.14	2.70	9.56	1.17	5.59	0.68	3.26	0.40
74	40.60	22.81	34.41	19.33	6.72	3.78	3.48	1.96	2.20	1.24	2.09	1.17
75	35.80	18.72	31.08	16.25	7.26	3.80	4.84	2.53	4.11	2.15	3.63	1.90
76												
77												
78	7.62	7.57	24.01	23.85	15.87	15.76	10.96	10.88	9.5	9.43	9.08	9.02
79	7.2	6.86	17.58	16.75	14.35	13.67	11.76	11.20	11.54	10.99	10.14	9.66
80	15.60	7.82	22.74	11.39	12.73	6.38	10.23	5.13	7.94	3.98	6.75	3.38
81	10.10	6.93	23.17	15.91	16.67	11.44	10.90	7.48	9.01	6.18	8.07	5.54
82	7.60	3.21	23.58	9.95	18.64	7.87	12.67	5.35	9.78	4.13	8.14	3.44
83	18.50	9.85	31.54	16.79	13.24	7.05	6.73	3.58	5.61	2.99	5.05	2.69
84	6.7	6.55	19.88	19.44	16.62	16.26	13.35	13.06	11.42	11.17	9.28	9.08
85												
86	24.83	23.70	55.29	52.78	9.10	8.69	1.48	1.41	0.79	0.75	0.79	0.75
87	17.52	10.26	24.10	14.12	12.71	7.45	9.53	5.58	6.57	3.85	5.37	3.15
88	2.27	2.26	11.55	11.48	19.17	19.05	14.02	13.93	9.59	9.53	9.48	9.42

Sample #	clay % sample	0.002 0.00098 mm % total	clay % sample	0.00098 0.00049 mm % total	clay % sample	0.00049 0.00024 mm % total
		9.5		10.5		11.5
59						
60						
61						
62						
63						
64						
65						
66						
67	11.77	11.73	11.46	11.42	14.69	14.63
68	7.45	4.21	5.04	2.84	12.60	7.11
69	6.81	4.28	5.49	3.45	10.99	6.91
70	6.82	3.76	6.60	3.64	9.80	5.41
71	6.35	3.41	5.12	2.75	10.02	5.39
72	4.74	3.54	4.63	3.46	9.27	6.93
73	3.15	0.38	2.80	0.34	11.66	1.42
74	2.20	1.24	1.85	1.04	6.49	3.65
75	3.02	1.58	3.02	1.58	7.26	3.80
76						
77						
78	6.68	6.63	6.16	6.12	10.12	10.05
79	8.63	8.22	6.8	6.48	11.97	11.40
80	6.53	3.27	5.55	2.78	11.97	6.00
81	6.60	4.53	4.61	3.16	10.90	7.48
82	6.80	2.87	4.53	1.91	8.24	3.48
83	4.71	2.51	4.49	2.39	10.10	5.38
84	6.73	6.58	6.32	6.18	9.68	9.47
85						
86	2.37	2.26	1.78	1.70	3.56	3.40
87	6.02	3.53	4.38	2.57	13.80	8.08
88	8.76	8.70	8.66	8.61	16.49	16.39

Alma and BSR Sediment Samples							MATHEMATICAL MOMENTS			
					Location		1st M	1st M	2nd M	3rd M
Sample #	Unique Sample ID	Year	Sampling Method	Analysis Method	UTM Easting	WGS84 Northing	Mean Avg size (mm)	Mean Avg size (phi)	Std Dev	Skew
ALMA								converted		
1	AL04-ST1 (matrix)	2004	Hand	Grid/ Sieve	348539	5051459	**1.288**	**-0.37**	0.99	0.80
2	AL04-ST2 (Upper 2 cm)	2004	Hand	Sieve	348932	5051248	**0.608**	**0.72**	0.68	2.05
3	AL04-ST3	2004	Hand	Sieve	349223	5051138	**7.312**	**-2.87**	9.89	3.83
4	AL04-ST4 (matrix)	2004	Hand	Grid/ Sieve	349056	5051028	**1.157**	**-0.21**	1.00	0.87
5	AL04-ST5 (matrix)	2004	Hand	Grid/ Sieve	348125	5051170	**0.866**	**0.21**	0.83	1.70
6	AL04-ST11 (matrix)	2004	Hand	Grid/ Sieve	348533	5050729	**0.912**	**0.13**	1.02	1.13
7	AL04-ST13 (Upper 3 cm)	2004	Hand	Sieve	348314	5051213	**0.287**	**1.80**	0.22	3.09
8	AL04-ST17 (Upper 3 cm)	2004	Hand	Sieve	349133	5050832	**1.867**	**-0.90**	2.40	4.60
9	AL04-ST18 (matrix)	2004	Hand	Grid/ Sieve	348921	5050907	**1.295**	**-0.37**	0.99	0.70
10	AL04-ST19 (matrix)	2004	Hand	Grid/ Sieve	348696	5051018	**0.648**	**0.63**	0.71	2.31
11	AL04-ST20 (matrix)	2004	Hand	Grid/ Sieve	348624	5050595	**1.195**	**-0.26**	1.09	0.72
12	AL04-ST21 (Upper 2 cm)	2004	Hand	Sieve	348206	5050537	**0.428**	**1.23**	0.25	6.14
13	AL04-ST22-S2	2004	Hand	Sieve	348558	5051106	**5.362**	**-2.42**	6.58	3.66
14	AL04-ST23-S1 (matrix)	2004	Hand	Grid/ Sieve	347952	5050610	**0.862**	**0.21**	0.58	1.07
15	[redacted]	2004	Hand	Sedigraph	348143	5050995	**0.045**	**4.47**	0.02	0.67
16		2004	Hand	Sedigraph	348524	5051145	**0.028**	**5.16**	0.02	0.83
17		2004	Hand	Sedigraph	348161	5051611	**0.038**	**4.72**	0.03	1.18
18		2004	Hand	Sedigraph	348416	5051005	**0.026**	**5.27**	0.03	2.00
19		2004	Hand	Sedigraph	348377	5051185	**0.032**	**4.99**	0.02	0.64
20		2004	Hand	Sedigraph	349177	5051197	**0.022**	**5.49**	0.02	0.99
21	GS05-AL1-Bulk	2005	Grab	Sieve	348234	5049978	**1.502**	**-0.59**	3.14	3.51
22	GS05-AL4-Bulk	2005	Grab	Sieve	348289	5049720	**0.443**	**1.18**	1.99	4.90
23	GS05-AL5-Bulk	2005	Grab	Sieve	349481	5050891	**0.228**	**2.14**	0.19	16.15
24	GS05-AL6-Bulk	2005	Grab	Sieve	349716	5051122	**0.146**	**2.77**	0.10	16.78
25	GS05-AL7-Bulk	2005	Grab	Sieve	349404	5051160	**19.859**	**-4.31**	22.80	0.60
26	GS05-AL8-Bulk	2005	Grab	Sieve	349039	5050203	**2.095**	**-1.07**	6.33	11.90
27	GS05-AL9-Bulk	2005	Grab	Sieve	348907	5050378	**1.114**	**-0.16**	3.59	3.42

Sample #	GRAPHICAL MOMENTS 1st M Mean Avg Phi Size	2nd M Std Dev	3rd M Skew	GRAPHICAL PHI MEASUREMENTS 5th %	16th %	50th %	84th %	95th %	Percent Sand %	Sample Total (g)	-5.65 phi (g)	>50 mm %	-5.25 phi (g)	37.5 to 50 mm %
ALMA												-6.10		-5.45
1									78.7	951				
2	1.2	**1.47**	**-0.46**	-1.78	-0.46	1.72	2.40	3.22	90.2	3435				
3	-2.0	**1.99**	**-0.16**	-5.06	-4.36	-1.73	-0.01	0.89	44.1	29139	221	0.8	312	1.1
4									81.2	1704				
5									89.6	3307				
6									80.2	1459				
7	1.6	**0.89**	**-0.07**	0.13	0.78	1.71	2.41	3.35	96.2	3258				
8	-0.3	**1.73**	**0.10**	-3.15	-1.82	-0.40	1.38	2.97	75.6	5822				
9									77.9	1721				
10									91.2	1697				
11									77.3	1805				
12	1.0	**0.52**	**-0.01**	-0.17	0.63	0.99	1.41	1.94	99.0	4011				
13	-1.8	**1.74**	**-0.10**	-4.68	-3.66	-1.66	0.03	0.71	45.5	14936	0	0	59	0.4
14									93.5	1636				
15	4.3	**1.50**	**0.54**	2.9	3.7	4.1	5.0	10.6	11.7					
16	5.7	**2.25**	**0.59**	3.6	3.9	4.9	8.4	11.1	4.1					
17	4.9	**1.98**	**0.63**	3.0	3.7	4.3	6.8	10.9	10.0					
18	6.0	**2.34**	**0.50**	3.5	3.9	5.2	8.8	10.9	4.7					
19	5.3	**1.94**	**0.67**	3.5	4.0	4.6	7.3	10.9	4.6					
20	6.1	**2.32**	**0.52**	3.6	4.1	5.3	8.9	11.0	1.6					
21	-0.5	**1.95**	**0.06**	-3.4	-2.4	-0.5	1.3	3.3	71.7	3548	0	0.00	0	0.00
22	2.7	**2.31**	**0.32**	-2.8	1.5	2.1	4.6	7.4	91.0	915	0	0.00	0	0.00
23	1.9	**0.88**	**0.04**	0.6	1.0	1.9	2.9	3.3	96.4	841	0	0.00	0	0.00
24	2.5	**0.65**	**0.17**	1.6	1.8	2.4	3.2	3.5	94.9	623	0	0.00	0	0.00
25	-2.2	**3.29**	**-0.29**	-6.8	-6.3	-1.2	1.0	2.9	52.2	1283	293.9	22.92	0	0.00
26									83.3	1816	0	0.00	0	0.00
27	0.6	**2.32**	**-0.54**	-3.4	-2.4	1.7	2.7	3.4	76.0	988	0	0.00	0	0.00

Sample #	-4.65 phi (g)	25 to 37.5 mm %	-3.65 phi (g)	12.5 to 25 mm %	-3.25 phi (g)	9.5 to 12.5 mm %	-2.25 phi (g)	4.75 to 9.5 mm %	-2 phi (g)	4 to 9.5 mm %	-2 phi (g)	4 to 4.75 mm %	-1 phi (g)	2 to 4 mm %
ALMA		-4.95		-4.15		-3.45		-2.75		-2.73		-2.13	granule	-1.50
1											0.0	0.0	203.0	21.3
2							0	0			81.0	2.4	161.0	4.7
3	1175	4.0	4028	13.8	1445	5.0	3512	12.1			974.0	3.3	4549.0	15.6
4											0.0	0.0	320.0	18.8
5											0.0	0.0	345.0	10.4
6											0.0	0.0	223.2	15.3
7											0.0	0.0	0.0	0.0
8	0	0	61	1.0	108	1.9	303	5.2			98.0	1.7	742.0	12.7
9											0.0	0.0	356.7	20.7
10											0.0	0.0	105.0	6.2
11											0.0	0.0	409.0	22.7
12							0	0			8.0	0.2	19.0	0.5
13	167	1.1	1525	10.2	914	6.1	2343	15.7			545.0	3.6	2562.0	17.2
14											0.0	0.0	34.1	2.1
15														
16														
17														
18														
19														
20														
21	0	0.00	52.3	1.47	79	2.23			335.1	9.45			435.5	12.3
22	0	0.00	2.5	0.27	7.9	0.86			40.4	4.41			32.0	3.5
23	0	0.00	0	0.00	0	0.00			0.3	0.04			0.6	0.1
24	0	0.00	0	0.00	0	0.00			0.0	0.00			0.4	0.1
25	121.5	9.47	31	2.42	9.9	0.77			43.2	3.37			87.3	6.8
26	53.1	2.92	64.3	3.54	32.3	1.78			84.0	4.62			69.6	3.8
27	0	0.00	21	2.12	27.1	2.74			87.3	8.83			56.9	5.8

Sample #	0 phi (g)	1 to 2 mm %	1 phi (g)	0.5 to 1 mm %	2 phi (g)	0.25 to 0.5 mm %	3 phi (g)	0.125 to 0.25 mm %	4 phi (g)	0.0625 to 0.125 mm %	< 4 phi (g)	<0.0625 mm %
ALMA	v.c.g.	-0.50	c.g.	0.50	m.g.	1.50	f.g.	2.50	v.f.g.	3.50	mud	6.00
1	224.0	23.6	256.0	26.9	212.0	22.3	34.0	3.6	22.0	2.3	0.0	0.0
2	289.0	8.4	430.0	12.5	397.0	11.6	1707.0	49.7	276.0	8.0	94.0	2.7
3	5764.0	19.8	5078.0	17.4	1682.0	5.8	89.0	0.3	251.0	0.9	59.0	0.2
4	370.0	21.7	438.0	25.7	243.0	14.3	69.0	4.0	264.0	15.5	0.0	0.0
5	468.0	14.2	617.0	18.7	1725.0	52.2	31.0	0.9	121.0	3.7	0.0	0.0
6	258.5	17.7	187.4	12.8	130.2	8.9	295.8	20.3	298.4	20.5	65.4	4.5
7	54.0	1.7	173.0	5.3	1066.0	32.7	1592.0	48.9	249.0	7,6	124.0	3.8
8	1416.0	24.3	1750.0	30.1	466.0	8.0	424.0	7.3	346.0	5.9	108.0	1.9
9	473.3	27.5	457.7	26.6	211.0	12.3	73.1	4.2	125.8	7.3	23.1	1.3
10	150.1	8.8	286.6	16.9	802.1	47.3	145.7	8.6	163.6	9.6	43.6	2.6
11	358.0	19.8	339.0	18.8	216.0	12.0	140.0	7.8	343.0	19.0	0.0	0.0
12	54.0	1.3	359.0	9.0	3237.0	80.7	307.0	7.7	14.0	0.3	13.0	0.3
13	2845.0	19.0	3041.0	20.4	871.0	5.8	13.0	0.1	20.0	0.1	31.0	0.2
14	468.1	28.6	612.8	37.5	342.8	21.0	63.2	3.9	42.2	2.6	72.7	4.4
15												
16												
17												
18												
19												
20												
21	882.5	24.9	876.8	24.7	380.0	10.7	72.4	2.0	333.5	9.4	100.4	2.8
22	21.8	2.4	13.6	1.5	29.0	3.2	528.0	57.7	239.9	[redacted]		
23	1.2	0.1	6.7	0.8	255.4	30.4	373.3	44.4	174.3	20.7	29.2	3.5
24	0.6	0.1	0.4	0.1	1.4	0.2	344.3	55.3	244.3	39.2	31.3	5.0
25	158.4	12.4	251.8	19.6	163.8	12.8	29.0	2.3	67.1	5.2	25.6	2.0
26	65.1	3.6	62.3	3.4	85.6	4.7	824.4	45.4	475.7	[redacted]		
27	40.1	4.1	50.1	5.1	155.2	15.7	366.6	37.1	139.3	14.1	44.8	4.5

Sample #	0.125 to 0.25 mm % total	v.f.g. sand % sample	0.063 0.125 mm % total	c. silt % sample	0.031 0.063 mm % total	m. silt % sample	0.0156 0.031 mm % total	f. silt % sample	0.008 0.0156 mm % total	v.f. silt % sample	0.0039 0.008 mm % total
ALMA	2.5		3.5		4.5		5.5		6.5		7.5
1											
2											
3											
4											
5											
6											
7											
8											
9											
10											
11											
12											
13											
14											
15	0.10		11.65		64.56		14.51		2.17		0.89
16	0.00		4.10		34.07		27.55		9.46		4.63
17	0.50		9.47		48.06		19.74		5.48		2.69
18	0.51		4.20		27.90		24.41		12.72		7.38
19	0.00		4.61		41.80		27.25		8.09		2.77
20	0.00		1.61		23.66		32.02		12.59		7.25
21											
22		16.67	4.37	23.67	6.21	10.4	2.73	10.29	2.70	8.5	2.23
23											
24											
25											
26											
27											

Sample #	clay % sample	0.0039 0.002 mm % total	clay % sample	0.002 0.00098 mm % total	clay % sample	0.00098 0.00049 mm % total	clay % sample	0.00049 0.00024 mm % total
ALMA		8.5		9.5		10.5		11.5
1								
2								
3								
4								
5								
6								
7								
8								
9								
10								
11								
12								
13								
14								
15		0.49		0.2		0		5.43
16		4.84		3.26		1.05		11.04
17		1.40		1.60		2.39		8.67
18		5.54		4.92		3.79		8.62
19		2.56		2.05		2.56		8.30
20		5.34		4.43		2.92		10.17
21								
22	7.72	2.02	6.26	1.64	4.59	1.20	12.3	3.22
23								
24								
25								
26								
27								

Alma and BSR Sediment Samples							MATHEMATICAL MOMENTS			
Sample #	Unique Sample ID	Year	Sampling Method	Analysis Method	Location UTM Easting	WGS84 Northing	1st M Mean Avg size (mm)	1st M Mean Avg size (phi) converted	2nd M Std Dev	3rd M Skew
BIG SALMON RIVER										
28	BSR04-ST2 (matrix)	2004	Hand	Grid/ Sieve	311941	5032100	**1.313**	**-0.39**	1.03	0.63
29	BSR04-ST3 (matrix)	2004	Hand	Grid/ Sieve	312083	5032302	**1.509**	**-0.59**	1.03	0.41
30	BSR04-ST6 (matrix)	2004	Hand	Grid/ Sieve	312070	5031966	**2.176**	**-1.12**	0.99	-0.68
31	BSR04-ST8 (matrix)	2004	Hand	Grid/ Sieve	312270	5032284	**2.016**	**-1.01**	1.05	-0.43
32	BSR04-ST11 (matrix)	2004	Hand	Grid/ Sieve	312517	5031903	**1.726**	**-0.79**	1.08	-0.01
33	BSR04-ST13 (matrix)	2004	Hand	Grid/ Sieve	312611	5032130	**0.292**	**1.77**	0.69	3.35
34	BSR04-ST15 (matrix)	2004	Hand	Grid/ Sieve	312362	5031798	**1.409**	**-0.49**	1.04	0.45
35	[redacted]	2004	Hand	Sedigraph	311992	5032344	**0.035**	**4.82**	0.02	1.74
36		2004	Hand	Sedigraph	311992	5032344	**0.023**	**5.44**	0.02	1.81
37		2004	Hand	Sedigraph	311992	5032344	**0.010**	**6.70**	0.01	2.86
38		2004	Hand	Sedigraph	311796	5031973	**0.019**	**5.70**	0.02	2.89
39		2004	Hand	Sedigraph	312189	5032233	**0.019**	**5.71**	0.02	1.13
40		2004	Hand	Sedigraph	312170	5032000	**0.024**	**5.38**	0.02	0.96
41		2004	Hand	Sedigraph	312329	5032011	**0.022**	**5.48**	0.02	2.24
42		2004	Hand	Sieve	312627	5032260	**0.027**	**5.22**	0.02	2.72
43		2004	Hand	Sieve	312611	5032130	**0.022**	**5.50**	0.02	2.43

Sample #	GRAPHICAL MOMENTS 1st M Mean Avg Phi Size	2nd M Std Dev	3rd M Skew	GRAPHICAL PHI MEASUREMENTS 5th %	16th %	50th %	84th %	95th %	Percent Sand %	Sample Total (g)	-5.65 phi (g)	>50 mm %	-5.25 phi (g)	37.5 to 50 mm %
BSR												-6.10		-5.45
28									0.0	1480		0		0
29									0.0	1787		0		0
30									0.0	1334		0		0
31									0.0	1399		0		0
32									60.2	1445		0		0
33									0.0	578		0		0
34									67.8	932		0		0
35	4.7	**1.42**	**0.40**	3.2	3.7	4.5	5.8	9.2	6.6					
36	5.5	**1.81**	**0.38**	3.7	4.1	5.2	7.1	10.6	1.8					
37	7.8	**2.37**	**0.21**	4.3	5.4	7.3	10.7	11.2	0.7					
38	6.6	**2.41**	**0.61**	3.8	4.5	5.4	9.7	11.1	1.0					
39	6.5	**2.50**	**0.49**	3.7	4.3	5.6	9.8	11.1	1.3					
40	6.1	**2.37**	**0.57**	3.6	4.0	5.2	9.0	11.0	2.3					
41	6.3	**2.45**	**0.52**	3.6	4.1	5.4	9.4	11.1	2.8					
42	5.2	**1.70**	**0.42**	3.6	4.1	5.0	6.5	10.9	2.6					
43	6.2	**2.32**	**0.52**	3.6	4.2	5.3	9.0	11.0	2.2					

Sample #	-4.65 phi (g)	25 to 37.5 mm %	-3.65 phi (g)	12.5 to 25 mm %	-3.25 phi (g)	9.5 to 12.5 mm %	-2.25 phi (g)	4.75 to 9.5 mm %	-2 phi (g)	4 to 9.5 mm %	-2 phi (g)	4 to 4.75 mm %	-1 phi (g)	2 to 4 mm %
BSR		-4.95		-4.15		-3.45		-2.75		-2.73		-2.13	granule	-1.50
28		0		0	0	0	0	0			0	0	339.1	22.9
29		0		0	0	0	0	0			0	0	506.6	28.3
30		0		0	0	0	0	0			0	0	739.6	55.4
31		0		0	0	0	0	0			0	0	692.8	49.5
32		0		0	0	0	0	0			0	0	536.4	37.1
33		0		0	0	0	0	0			0	0	31.6	5.5
34		0		0	0	0	0	0			0	0	235.6	25.3
35														
36														
37														
38														
39														
40														
41														
42														
43														

Sample #	0 phi (g)	1 to 2 mm %	1 phi (g)	0.5 to 1 mm %	2 phi (g)	0.25 to 0.5 mm %	3 phi (g)	0.125 to 0.25 mm %	4 phi (g)	0.0625 to 0.125 mm %	< 4 phi (g)	<0.0625 mm %
BSR	v.c.g.	-0.50	c.g.	0.50	m.g.	1.50	f.g.	2.50	v.f.g.	3.50	mud	6.00
28	367.7	24.8	385.8	26.1	178.9	12.1	17.9	1.2	140.5	9.5	50.4	3.4
29	513.1	28.7	410.9	23.0	232.8	13.0	32.6	1.8	41.8	2.3	49.4	2.8
30	404.4	30.3	90.2	6.8	12.9	1.0	6.3	0.5	29.1	2.2	51.4	3.9
31	403.7	28.9	151.6	10.8	44.9	3.2	13.0	0.9	22.4	1.6	70.7	5.1
32	456.4	31.6	219.7	15.2	53.3	3.7	15.4	1.1	124.7	8.6	38.7	2.7
33	14.9	2.6	6.8	1.2	7.7	1.3	39.3	6.8	358.1	62.0	119.1	20.6
34	269.7	28.9	223.5	24.0	64.5	6.9	14.8	1.6	59.2	6.4	64.7	6.9
35												
36												
37												
38												
39												
40												
41												
42												
43												

Sample #	0.125 to 0.25 mm % total	v.f.g. sand % sample	0.063 0.125 mm % total	c. silt % sample	0.031 0.063 mm % total	m. silt % sample	0.0156 0.031 mm % total	f. silt % sample	0.008 0.0156 mm % total	v.f. silt % sample	0.0039 0.008 mm % total
BSR	2.5		3.5		4.5		5.5		6.5		7.5
28											
29											
30											
31											
32											
33											
34											
35	0.50		6.09		42.81		31.84		9.18		2.79
36	0.10		1.67		20.19		37.76		19.87		7.74
37	0.00		0.70		5.32		11.35		18.07		18.77
38	0.31		0.72		14.40		38.17		14.30		5.86
39	0.00		1.25		19.77		27.58		11.97		7.80
40	0.00		2.26		26.08		33.57		10.68		4.83
41	0.41		2.36		22.92		28.16		10.79		7.81
42	0.51		2.13		24.26		46.70		10.86		2.74
43	0.40		1.81		21.25		31.52		12.59		7.45

Sample #	clay % sample	0.0039 0.002 mm % total	clay % sample	0.002 0.00098 mm % total	clay % sample	0.00098 0.00049 mm % total	clay % sample	0.00049 0.00024 mm % total
BSR		8.5		9.5		10.5		11.5
28								
29								
30								
31								
32								
33								
34								
35		1.20		0.90		0.10		5.09
36		2.30		2.09		1.57		6.80
37		12.45		8.63		5.62		19.08
38		4.63		4.57		4.22		13.17
39		6.76		7.39		5.52		11.97
40		4.11		4.72		2.77		10.99
41		6.78		5.45		3.91		11.82
42		1.62		2.54		0.71		8.43
43		6.44		5.04		3.93		9.97

Wolman tests 2004					MATHEMATICAL MOMENTS (PHI)				
Station #	Location	Location Easting	UTM Northing	# of clasts	1st Moment Average Phi size Mean	2nd Moment Standard Deviation Phi size	3rd Moment Skewness Phi Size	1st Moment Average Phi size mm	Converted to Phi
Waterside					0.00				
25	WS04-ST25	359721	5052743	119	-4.19	5.09	1.11	**50.14**	**-5.65**
25	WS04-ST25 (unimodal)	359721	5052743	119	-4.19	5.09	1.11	**54.40**	**-5.77**
27	WS04-ST27	360249	5052892	126	-4.73	5.43	1.13	**71.74**	**-6.16**
Alma									
1	AL04-ST1	348539	5051439	96	-4.95	5.49	1.08	**61.83**	**-5.95**
4	AL04-ST4	349056	5051018	108	-3.45	4.63	1.29	**31.23**	**-4.96**
5	AL04-ST5	348125	5051170	115	-4.85	6.05	0.96	**96.08**	**-6.59**
5	AL04-ST5 (unimodal)	348125	5051170	115	-4.85	6.05	0.96	**105.40**	**-6.72**
11	AL04-ST11	348533	5050729	114	-2.88	5.01	1.38	**23.49**	**-4.55**
11	AL04-ST11 (unimodal)	348533	5050729	114	-2.88	5.01	1.38	**26.40**	**-4.72**
18	AL04-ST18	348921	5050907	118	-3.15	4.02	1.57	**20.77**	**-4.38**
19	AL04-ST19	348696	5051018	114	-3.69	5.48	1.14	**36.65**	**-5.20**
19	AL04-ST19 (unimodal)	348696	5051018	114	-3.69	5.48	1.14	**42.15**	**-5.40**
20	AL04-ST20	348624	5050595	116	-4.30	5.44	1.33	**35.94**	**-5.17**
23	AL04-ST23	347952	5050610	115	-3.91	5.32	1.21	**62.16**	**-5.96**
23	AL04-ST23 (unimodal)	347952	5050610	115	-3.91	5.32	1.21	**78.05**	**-6.29**
Big Salmon River									
2	BSR04-ST2	311941	5032100	117	-4.09	5.04	1.53	**38.42**	**-5.26**
3	BSR04-ST3	312083	5032302	107	-4.09	4.63	1.51	**37.91**	**-5.24**
6	BSR04-ST6	312070	5031966	117	-3.76	3.84	2.34	**33.02**	**-5.05**
8	BSR04-ST8	312270	5032284	115	-6.42	6.57	1.33	**193.51**	**-7.60**
11	BSR04-ST11	312517	5031903	112	-3.94	4.51	1.72	**42.71**	**-5.42**
13	BSR04-ST13	312611	5032130	113	-2.70	6.86	1.00	**34.93**	**-5.13**
13	BSR04-ST13 (unimodal)	312611	5032130	113	-2.70	6.86	1.00	**47.86**	**-5.58**
15	BSR04-ST15	312362	5031798	116	-5.07	5.96	1.56	**65.04**	**-6.02**

Station #	GRAPHICAL MOMENTS			GRAPHICAL ANALYSIS								
	Average Phi size Mean	Standard Deviation Phi size	Skewness Phi Size	5th %	16th %	50th %	84th %	95th %	-9 phi 512 to #	1024mm % -9.50	-8 phi 256 to #	512mm % -8.50
Waterside												
25	-4.96	**2.52**	**0.51**	-7.5	-7.1	-5.7	-2.1	1.0	0	0.0	0	0.0
25	-5.48	**1.86**	**0.39**	-7.5	-7.1	-5.9	-3.5	-1.2	0	0.0	0	0.0
27	-5.58	**2.41**	**0.32**	-8.3	-7.8	-5.9	-3.1	0.0	0	0.0	0	0.0
Alma												
1	-5.63	**1.89**	**0.32**	-8.0	-7.3	-6.0	-3.6	-1.6	0	0.0	0	0.0
4	-4.23	**2.44**	**0.40**	-7.1	-6.3	-4.8	-1.6	1.1	0	0.0	0	0.0
5	-5.69	**2.79**	**0.53**	-8.5	-8.0	-6.5	-2.6	1.0	1	0.9	5	4.3
5	-6.20	**2.17**	**0.43**	-8.6	-8.0	-6.7	-3.8	-1.3	1	0.9	5	4.3
11	-3.64	**2.80**	**0.54**	-6.5	-6.0	-4.6	-0.4	2.7	0	0.0	0	0.0
11	-4.48	**1.82**	**0.36**	-6.5	-6.1	-4.8	-2.6	-0.2	0	0.0	0	0.0
18	-3.98	**1.93**	**0.33**	-6.4	-5.6	-4.3	-2.0	0.4	0	0.0	0	0.0
19	-4.01	**2.84**	**0.54**	-7.3	-6.5	-5.2	-0.4	1.4	0	0.0	0	0.0
19	-5.27	**1.67**	**0.31**	-7.3	-6.6	-5.5	-3.7	-1.1	0	0.0	0	0.0
20	-5.11	**1.65**	**0.40**	-7.1	-6.4	-5.4	-3.5	-0.9	0	0.0	0	0.0
23	-4.60	**3.05**	**0.43**	-8.2	-7.4	-5.6	-0.8	0.9	0	0.0	1	0.9
23	-5.90	**1.79**	**0.28**	-8.3	-7.6	-6.3	-3.8	-2.8	0	0.0	1	0.9
Big Salmon River												
2	-4.84	**1.76**	**0.10**	-7.4	-6.5	-4.9	-3.2	-1.3	0	0.0	1	0.9
3	-4.87	**1.80**	**0.25**	-7.3	-6.6	-5.2	-2.9	-1.5	0	0.0	0	0.0
6	-4.53	**1.89**	**-0.05**	-7.3	-6.6	-4.4	-2.7	-1.3	0	0.0	0	0.0
8	-6.89	**2.24**	**0.33**	-9.8	-9.0	-7.4	-4.3	-2.8	8	7.0	20	17.4
11	-4.76	**2.12**	**0.15**	-7.6	-6.9	-4.9	-2.5	-0.8	0	0.0	0	0.0
13	-2.83	**4.17**	**0.57**	-7.3	-6.8	-4.8	3.1	4.0	0	0.0	0	0.0
13	-5.49	**1.74**	**0.37**	-7.3	-7.0	-5.8	-3.7	-1.2	0	0.0	0	0.0
15	-5.78	**1.66**	**0.13**	-8.2	-7.3	-5.8	-4.2	-2.3	0	0.0	2	1.7

Station #	-7 phi 128 to #	256mm % -7.50	-6 phi 64 to #	128mm % -6.50	-5 phi 32-64mm #	% -5.50	-4 phi 16 to #	32 mm % -4.50	-3 phi 8 to #	16 mm % -3.50	-2 phi 4-8mm #	% -2.50	matrix <4mm #	<-2 phi %
Waterside														
25	5	4.2	32	26.9	28	23.5	17	14.3	10	8.4	6	5.0	21	17.6
25	5	4.2	32	26.9	28	23.5	17	14.3	10	8.4	6	5.0	21	17.6
27	27	21.4	20	15.9	27	21.4	19	15.1	10	7.9	7	5.6	16	12.7
Alma														
1	10	10.4	24	25.0	26	27.1	12	12.5	10	10.4	8	8.3	6	6.3
4	1	0.9	12	11.1	25	23.1	23	21.3	16	14.8	10	9.3	21	19.4
5	23	20.0	30	26.1	14	12.2	11	9.6	6	5.2	7	6.1	18	15.7
5	23	20.0	30	26.1	14	12.2	11	9.6	6	5.2	7	6.1	18	15.7
11	0	0.0	5	4.4	26	22.8	28	24.6	15	13.2	12	10.5	28	24.6
11	0	0.0	5	4.4	26	22.8	28	24.6	15	13.2	12	10.5	28	24.6
18	0	0.0	4	3.4	17	14.4	32	27.1	32	27.1	12	10.2	21	17.8
19	2	1.8	16	14.0	31	27.2	23	20.2	14	12.3	6	5.3	22	19.3
19	2	1.8	16	14.0	31	27.2	23	20.2	14	12.3	6	5.3	22	19.3
20	0	0.0	13	11.2	43	37.1	24	20.7	18	15.5	9	7.8	9	7.8
23	16	13.9	25	21.7	17	14.8	12	10.4	8	7.0	12	10.4	24	20.9
23	16	13.9	25	21.7	17	14.8	12	10.4	8	7.0	12	10.4	24	20.9
Big Salmon River														
2	4	3.4	13	11.1	19	16.2	34	29.1	23	19.7	13	11.1	10	8.5
3	2	1.9	16	15.0	28	26.2	22	20.6	14	13.1	13	12.1	12	11.2
6	2	1.7	18	15.4	18	15.4	17	14.5	28	23.9	18	15.4	16	13.7
8	27	23.5	27	23.5	8	7.0	5	4.3	7	6.1	10	8.7	3	2.6
11	6	5.4	20	17.9	18	16.1	20	17.9	26	23.2	4	3.6	18	16.1
13	0	0.0	25	22.1	22	19.5	13	11.5	12	10.6	4	3.5	37	32.7
13	0	0.0	25	22.1	22	19.5	13	11.5	12	10.6	4	3.5	37	32.7
15	12	10.3	22	19.0	33	28.4	24	20.7	15	12.9	2	1.7	6	5.2

Sieve Analysis

Station #	Matrix Total weight %	Matrix Avg Phi Size	Matrix Avg size mm	matrix 2-4mm #	-1 phi % -1.50	matrix 1-2 mm (g)	0 phi % -0.50	matrix 0.5-1 mm (g)	+1 phi % 0.50	matrix 0.25-0.5 mm (g)	+2 phi % 1.50
Waterside											
25	1836.0	**0.43**	**1.24**	454	24.7	318	17.3	245	13.3	601	32.7
25	1836.0	**0.43**	**1.24**	454	24.7	318	17.3	245	13.3	601	32.7
27	2987.0	**0.24**	**1.36**	780	26.1	704	23.6	461	15.4	787	26.3
Alma											
1	951.0	**0.20**	**1.29**	203	21.3	224	23.6	256	26.9	212	22.3
4	1704.0	**0.60**	**1.16**	320	18.8	370	21.7	438	25.7	243	14.3
5	3307.0	**0.80**	**0.87**	345	10.4	468	14.2	617	18.7	1725	52.2
5	3307.0	**0.80**	**0.87**	345	10.4	468	14.2	617	18.7	1725	52.2
11	1458.9	**1.37**	**0.91**	223.2	15.3	258.5	17.7	187.4	12.8	130.2	8.9
11	1458.9	**1.37**	**0.91**	223.2	15.3	258.5	17.7	187.4	12.8	130.2	8.9
18	1720.7	**0.31**	**1.30**	356.7	20.7	473.3	27.5	457.7	26.6	211	12.3
19	1696.7	**1.36**	**0.65**	105	6.2	150.1	8.8	286.6	16.9	802.1	47.3
19	1696.7	**1.36**	**0.65**	105	6.2	150.1	8.8	286.6	16.9	802.1	47.3
20	1805.0	**0.69**	**1.20**	409	22.7	358	19.8	339	18.8	216	12.0
23	1635.9	**0.78**	**0.86**	34.1	2.1	468.1	28.6	612.8	37.5	342.8	21.0
23	1635.9	**0.78**	**0.86**	34.1	2.1	468.1	28.6	612.8	37.5	342.8	21.0
Big Salmon River											
2	1480.3	**0.41**	**1.31**	339.1	22.9	367.7	24.8	385.8	26.1	178.9	12.1
3	1787.2	**0.03**	**1.51**	506.6	28.3	513.1	28.7	410.9	23.0	232.8	13.0
6	1333.9	**-0.62**	**2.18**	739.6	55.4	404.4	30.3	90.2	6.8	12.9	1.0
8	1399.1	**-0.40**	**2.02**	692.8	49.5	403.7	28.9	151.6	10.8	44.9	3.2
11	1444.6	**-0.09**	**1.73**	536.4	37.1	456.4	31.6	219.7	15.2	53.3	3.7
13	577.5	**3.51**	**0.29**	31.6	5.5	14.9	2.6	6.8	1.2	7.7	1.3
13	577.5	**3.51**	**0.29**	31.6	5.5	14.9	2.6	6.8	1.2	7.7	1.3
15	932.0	**0.38**	**1.41**	235.6	25.3	269.7	28.9	223.5	24.0	64.5	6.9

Station #	matrix 0.125-0.25 mm (g)	+3 phi % 2.50	matrix 0.0625 to (g)	+4 phi 0.125mm % 3.50	matrix mud (g)	<+4 phi <0.0625 mm % 6.00
Waterside						
25	165	9.0	53	2.9	0	0
25	165	9.0	53	2.9	0	0
27	69	2.3	186	6.2	0	0
Alma						
1	34	3.6	22	2.3	0	0
4	69	4.0	264	15.5	0	0
5	31	0.9	121	3.7	0	0
5	31	0.9	121	3.7	0	0
11	295.8	20.3	298.4	20.5	65.4	4.5
11	295.8	20.3	298.4	20.5	65.4	4.5
18	73.1	4.2	125.8	7.3	23.1	1.3
19	145.7	8.6	163.6	9.6	43.6	2.6
19	145.7	8.6	163.6	9.6	43.6	2.6
20	140	7.8	343	19.0	0	0
23	63.2	3.9	42.2	2.6	72.7	4.4
23	63.2	3.9	42.2	2.6	72.7	4.4
Big Salmon River						
2	17.9	1.2	140.5	9.5	50.4	3.4
3	32.6	1.8	41.8	2.3	49.4	2.8
6	6.3	0.5	29.1	2.2	51.4	3.9
8	13	0.9	22.4	1.6	70.7	5.1
11	15.4	1.1	124.7	8.6	38.7	2.7
13	39.3	6.8	358.1	62.0	119.1	20.6
13	39.3	6.8	358.1	62.0	119.1	20.6
15	14.8	1.6	59.2	6.4	64.7	6.9

APPENDIX B

Total Organic Carbon data for Waterside Beach, Alma delta, and Big Salmon River delta. Values were determined using Loss-On-Ignition (LOI). Samples were first dried for 24 hours at 105° C and crushed with mortar and pestle. LOI analysis involved heating samples at 550° C for 4 hours. Waterside TOC data is reported on pages 219 to 222, Alma on 222 and 223, and Big Salmon River on page 223.

Total Organic Carbon					PRE-LOI			POST_LOI		
Sample #	Location	Year	Easting	Northing	Crucible weight (g)	Sediment & Crucible (g)	Sediment Weight (g)	Sediment & Crucible (g)	Sediment Weight (g)	TOC %
WATERSIDE										
1	GS05-WS1-Surface	2005	357643	5053734	12.643	16.523	3.880	16.32	3.675	**5.28**
2	GS05-WS1-Bulk	2005	357643	5053734	7.866	11.886	4.020	11.68	3.814	**5.12**
3	GS05-WS2-Surface	2005	357492	5053311	10.238	14.623	4.385	14.54	4.306	**1.80**
4	GS05-WS3-Surface	2005	358104	5052585	10.260	14.125	3.865	14.00	3.742	**3.18**
5	GS05-WS4-Surface	2005	358284	5052377	13.334	17.525	4.191	17.43	4.093	**2.34**
6	GS05-WS5-Surface	2005	358564	5052152	13.146	17.025	3.879	16.94	3.794	**2.19**
7	GS05-WS6-Surface	2005	358752	5052433	11.944	16.004	4.060	15.80	3.858	**4.98**
8	GS05-WS6-Bulk	2005	358752	5052433	10.376	17.244	6.868	17.03	6.652	**3.15**
9	GS05-WS10-Surface	2005	359574	5052266	8.052	17.911	9.859	17.79	9.741	**1.20**
10	GS05-WS12-Bulk	2005	359429	5052108	10.368	14.056	3.688	13.93	3.564	**3.36**
11	GS05-WS15-Surface	2005	359749	5051631	11.237	15.090	3.853	14.99	3.75	**2.67**
12	GS05-WS15-Bulk	2005	359749	5051631	10.296	14.075	3.779	13.95	3.653	**3.33**
13	GS05-WS17-Surface	2005	359574	5051401	11.123	16.424	5.301	16.33	5.205	**1.81**
14	GS05-WS18-Surface	2005	359340	5051662	11.278	14.818	3.540	14.75	3.471	**1.95**
15	GS05-WS18-Bulk	2005	359340	5051662	11.978	16.029	4.051	15.88	3.906	**3.58**
16	GS05-WS19-Surface	2005	358851	5052037	11.948	18.183	6.235	18.07	6.119	**1.86**
17	GS05-WS20-Surface	2005	358377	5052531	13.474	17.475	4.001	17.40	3.925	**1.90**
18	GS05-WS21-Surface	2005	358503	5052612	10.743	14.891	4.148	14.75	4.006	**3.42**
19	GS05-WS21-Bulk	2005	358503	5052612	7.985	12.129	4.144	12.00	4.01	**3.23**
20	GS05-WS22-Surface	2005	358863	5053004	10.879	19.477	8.598	19.38	8.504	**1.09**
21	GS05-WS23-Surface	2005	358436	5053497	14.499	20.045	5.546	19.96	5.456	**1.62**
22	GS05-WS24-Surface	2005	358172	5053189	13.383	17.075	3.692	16.99	3.603	**2.41**
23	GS05-WS25-Surface	2005	357744	5053953	10.408	14.407	3.999	14.14	3.732	**6.68**
24	GS05-WS25-Bulk	2005	357744	5053953	13.154	16.968	3.814	16.73	3.575	**6.27**

Total Organic Carbon					PRE-LOI			POST_LOI		
Sample #	Location	Year	Easting	Northing	Crucible weight (g)	Sediment & Crucible (g)	Sediment Weight (g)	Sediment & Crucible (g)	Sediment Weight (g)	TOC %
25	WS04-ST3-S1	2004	358416	5053865	10.405	14.357	3.952	14.25	3.845	**2.71**
26	WS04-ST3-S2	2004	358416	5053865	12.644	16.351	3.707	16.295	3.651	**1.51**
27	WS04-ST6-TOC1	2004	358029	5053996	13.236	16.859	3.623	16.797	3.561	**1.71**
28	WS04-ST6-TOC2	2004	358029	5053996	12.37	16.152	3.782	16.085	3.715	**1.77**
29	WS04-ST7-TOC3	2004	358463	5053716	9.609	13.288	3.679	13.234	3.625	**1.47**
30	WS04-ST8-TOC4	2004	358759	5053907	10.326	14.273	3.947	14.216	3.89	**1.44**
31	WS04-ST9-TOC5	2004	358651	5053543	13.475	17.348	3.873	17.311	3.836	**0.96**
32	WS04-ST10-TOC1	2004	358921	5053124	11.985	15.885	3.9	15.817	3.832	**1.74**
33	WS04-ST17-TOC1	2004	359942	5052745	12.455	16.012	3.557	15.987	3.532	**0.70**
34	WS04-ST18-TOC2	2004	359837	5052963	13.581	17.563	3.982	17.431	3.85	**3.31**
35	WS04-ST22-TOC1	2004	359815	5053281	13.154	17.012	3.858	16.898	3.744	**2.95**
36	WS04-ST23-TOC1	2004	359654	5053442	12.447	16.216	3.769	16.139	3.692	**2.04**
37	WS04-ST24-TOC2	2004	359740	5053269	10.474	14.296	3.822	14.198	3.724	**2.56**
38	WS04-ST28-TOC1	2004	359455	5052914	13.384	17.371	3.987	17.328	3.944	**1.08**
39	WS04-ST29-TOC2	2004	359773	5053117	12.141	15.698	3.557	15.584	3.443	**3.20**
40	WS04-ST29-TOC3	2004	359773	5053117	11.68	15.531	3.851	15.438	3.758	**2.41**
41	WS04-ST30-TOC1	2004	359858	5053686	11.934	15.535	3.601	15.433	3.499	**2.83**
42	WS04-ST30-TOC2	2004	359858	5053686	12.871	16.863	3.992	16.703	3.832	**4.01**
43	WS04-ST42-TOC2	2004	359796	5053755	11.016	14.721	3.705	14.284	3.268	**11.79**
44	WS04-ST43-TOC1	2004	360502	5053477	11.942	15.905	3.963	15.72	3.778	**4.67**
45	WS-N1-B6	2003	358208	5054515	10.410	13.566	3.156	13.535	3.125	**0.98**
46	Wbar2-H4	2003	359873	5053186	12.215	15.56	3.345	15.435	3.22	**3.74**
47	WS-7304-7557-3619	2003	360251	5053584	13.43	16.839	3.409	16.757	3.327	**2.41**
48	WS-Wbar4-F1	2003	359599	5053259	11.38	14.632	3.252	14.566	3.186	**2.03**
49	WS-Wbar4-F4	2003	359698	5053373	11.343	13.88	2.537	13.806	2.463	**2.92**

Total Organic Carbon					PRE-LOI			POST_LOI		
Sample #	Location	Year	Easting	Northing	Crucible weight (g)	Sediment & Crucible (g)	Sediment Weight (g)	Sediment & Crucible (g)	Sediment Weight (g)	TOC %
50	WS-N1-C	2003	358200	5054465	11.934	15.663	3.729	15.622	3.688	1.10
51	WS-N2-C6	2003	358479	5054009	13.474	16.738	3.264	16.692	3.218	1.41
52	WS-N2-B6	2003	358558	5054298	12.954	16.673	3.719	16.64	3.686	0.89
53	Wbar2-H1	2003	359873	5053186	13.483	16.965	3.482	16.842	3.359	3.53
54	WS-N5-B2	2003	360407	5053050	11.808	15.681	3.873	15.636	3.828	1.16
55	WS-N1-A	2003	358215	5054558	11.685	15.544	3.859	15.524	3.839	0.52
56	WS-N2-B2	2003	358579	5054368	11.281	15.318	4.037	15.289	4.008	0.72
57	WS-N2-C9	2003	358404	5053820	13.428	17.086	3.658	17.04	3.612	1.26
58	WS-N1-D	2003	358183	5054405	11.262	14.929	3.667	14.895	3.633	0.93
59	WS-N6-D	2003	360120 ?	5051438 ?	12.648	16.123	3.475	16.104	3.456	0.55
60	WS-N3-D4	2003	358803	5053979	12.452	16.187	3.735	16.152	3.7	0.94
61	WS-N3-E4	2003	358564	5053631	13.629	17.284	3.655	17.244	3.615	1.09
62	WS-N3-C	2003	358870	5054076	13.158	16.366	3.208	16.336	3.178	0.94
63	WS-6770-8109-3616	2003	359512	5052611	13.671	17.213	3.542	17.174	3.503	1.10
64	FA1(iii) - Ocp 3 (F5)	2003			12.448	15.695	3.247	15.613	3.165	2.53
65	FA3(i) - b/w ocp 2&4 (F4)	2003			13.222	16.488	3.266	16.392	3.17	2.94
66	WS-N4-B5 (F3)	2003	359135	5054000	11.946	15.182	3.236	15.097	3.151	2.63
67	WS-N4-B3 (F1)	2003	359147	5054016	12.842	16.195	3.353	15.996	3.154	5.93
68	WS-N4-E2	2003	358944	5053733	12.419	16.088	3.669	16.05	3.631	1.04
69	WS-N5-B3	2003	360387	5053027	11.949	15.421	3.472	15.351	3.402	2.02
70	WS-N5-E4	2003	360200	5052757	12.14	15.818	3.678	15.983	3.843	-4.49
71	WS-N1-E	2003	358167	5054366	12.63	16.346	3.716			
72	WS-N1-F	2003	358104	5054190	10.887	14.822	3.935	14.786	3.899	0.91
73	WS-N1-E	2003	358167	5054366	11.018	14.406	3.388	14.315	3.297	2.69
74	WS-N5-E2	2003	360243	5052824	12.071	15.483	3.412	15.382	3.311	2.96

Total Organic Carbon					PRE-LOI			POST_LOI		
Sample #	Location	Year	Easting	Northing	Crucible weight (g)	Sediment & Crucible (g)	Sediment Weight (g)	Sediment & Crucible (g)	Sediment Weight (g)	TOC %
75	Wbar2-F3	2003	359804	5053081	11.674	15.01	3.336	14.904	3.23	**3.18**
76	WS-N1-E (f, vf, & M)	2003	358167	5054366	10.779	14.064	3.285	13.981	3.202	**2.53**
77	WS-Wbar4-F1 (vf, f, & M)	2003	359599	5053259	12.871	16.452	3.581	16.398	3.527	**1.51**
78	WS-N4-B5 (F3)	2003	359135	5054000	11.942	15.492	3.55	15.392	3.45	**2.82**
79	WS-N4-B3 (F1)	2003	359147	5054016	12.841	16.159	3.318	15.93	3.089	**6.90**
80	WS-N5-E4	2003	360200	5052757	12.138	15.645	3.507	15.601	3.463	**1.25**
81	WS-N1-E	2003	358167	5054366	12.629	16.344	3.715	16.292	3.663	**1.40**
82	WS-N1-F	2003	358104	5054190	10.883	14.835	3.952	14.796	3.913	**0.99**
83	WS-N1-E (Mud)	2003	358167	5054366	10.776	14.564	3.788	14.458	3.682	**2.80**
84	WS-Wbar4-F1 (Mud)	2003	359599	5053259	12.868	16.274	3.406	16.206	3.338	**2.00**
85	Wbar2-F3	2003	359804	5053081	11.674	15.235	3.561	15.111	3.437	**3.48**
ALMA										
86	GS05-AL1-Surface	2005	348234	5049978	12.630	20.365	7.735	20.25	7.624	**1.44**
87	GS05-AL4-Surface	2005	348289	5049720	12.601	19.743	7.142	19.62	7.021	**1.69**
88	GS05-AL5-Surface	2005	349481	5050891	12.458	20.553	8.095	20.45	7.993	**1.26**
89	GS05-AL6-Surface	2005	349716	5051122	13.580	21.065	7.485	20.97	7.391	**1.26**
90	GS05-AL7-Surface	2005	349404	5051160	11.604	19.714	8.110	19.61	8.001	**1.34**
91	GS05-AL8-Surface	2005	349039	5050203	12.139	19.591	7.452	19.48	7.343	**1.46**
92	AL04-ST2-TOC1	2004	348932	5051248	12.84	16.77	3.930	16.696	3.856	**1.88**
93	AL04-ST6-TOC1	2004	348143	5050995	13.671	17.357	3.686	17.294	3.623	**1.71**
94	AL04-ST7-TOC2	2004	348524	5051145	12.092	15.782	3.69	15.667	3.575	**3.12**
95	AL04-ST8-TOC1	2004	348161	5051611	11.86	15.437	3.577	15.387	3.527	**1.40**
96	ALO4-ST9-TOC2	2004	348416	5051005	11.608	15.579	3.971	15.439	3.831	**3.53**
97	AL04-ST15-TOC1	2004	348922	5051292	13.201	17.042	3.841	16.977	3.776	**1.69**
98	AL04-ST16-TOC3	2004	349177	5051197	11.95	15.809	3.859	15.679	3.729	**3.37**

Total Organic Carbon					PRE-LOI			POST_LOI		
Sample #	Location	Year	Easting	Northing	Crucible weight (g)	Sediment & Crucible (g)	Sediment Weight (g)	Sediment & Crucible (g)	Sediment Weight (g)	TOC %
99	AL04-ST10-TOC3	2004	348377	5051185	12.605	16.359	3.754	16.265	3.66	**2.50**
100	AL04-ST17-TOC3	2004	349133	5050832	11.28	14.817	3.537	14.766	3.486	**1.44**
101	AL04-ST20-TOC1	2004	348624	5050595	11.921	15.776	3.855	15.709	3.788	**1.74**
102	ALU-9464-1226-3714	2003	349464	5051226	13.841	17.197	3.356	17.143	3.302	**1.61**
103	ALU-8288-1226-3715	2003	348288	5051226	12.254	15.933	3.679	15.883	3.629	**1.36**
BIG SALMON RIVER										
104	BSR04-ST1-TOC1	2004	311992	5032344	13.183	16.741	3.558	16.703	3.52	**1.07**
105	BSR04-ST1-A2-TOC1	2004	311992	5032344	13.626	17.426	3.8	17.382	3.756	**1.16**
106	BSR04-ST1-B2-TOC2	2004	311992	5032344	11.26	15.12	3.86	15.001	3.741	**3.08**
107	BSR04-ST5-TOC1	2004	311796	5031973	12.63	16.278	3.648	16.14	3.51	**3.78**
108	BSR04-ST7-TOC2	2004	312189	5032233	11.765	15.474	3.709	15.294	3.529	**4.85**
109	BSR04-ST9-TOC1	2004	312170	5032000	12.602	16.525	3.923	16.378	3.776	**3.75**
110	BSR04-ST10-TOC2	2004	312329	5032011	12.982	16.745	3.763	16.596	3.614	**3.96**
111	BSR04-ST12-TOC1	2004	312627	5032260	14.499	18.14	3.641	18.033	3.534	**2.94**
112	BSR04-ST13-TOC2	2004	312611	5032130	12.423	16.183	3.76	16.045	3.622	**3.67**